FUNCTIONAL ANALYSIS OF CELL WALL-RELATED BARLEY GLYCOSYLTRANSFERASES

Submitted by

Naser Farrokhi, B. Sc., M. Sc.

A thesis submitted in fulfillment of the requirements
for the degree of Doctor of Philosophy

Discipline of Plant and Pest Sciences
School of Agriculture and Wine
Faculty of Sciences
University of Adelaide, Waite Campus
Glen Osmond, SA, 5064
Australia

June 2005

Printed on acid-free paper.

STATEMENT OF AUTHORSHIP

This work contains no material that has been accepted for the award of any other degree or diploma in any university or other tertiary institution. This thesis does not contain any material previously published or written by another person, except where due reference has been made in the text.

I give consent to this copy of my thesis, when deposited in the University Library, being available for loan and photocopying.

Naser Farrokhi

June 2005

TABLE OF CONTENTS

ACKNOWLEDGMENTS

I am grateful to the Ministry of Science, Research and Technology of Iran for their sponsorship towards a Ph.D degree and to my principal supervisor Professor Geoffrey Fincher for the extra funding that supported this research from the Grains, Research and Development Corporation grant. I would also like to thank him for his guidance, patience, inspiration and invaluable discussions throughout the project. I also wish to thank my co-supervisors Professor Peter Langridge, Dr. Rachel Burton and Dr. Qisen Zhang. Peter as the CEO of the Australian Centre for Plant Functional Genomics (ACPFG) has provided a vibrant environment for research and development through the course of my project. Rachel enthusiastically taught me many skills in molecular biology and showed that good science is achieved by hard work and determined effort. Qisen has shared an extensive knowledge and experience in biochemistry and I enjoyed our long discussions about different aspects of science and technology.

I thank Dr. Andrew Harvey and Dr. David Gibeaut for guidance in bioinformatic aspects of the work and earlier discussions that we had about the progression of the project. I would like to thank Dr. Neil Shirley for his contribution in quantitative analyses of the transcripts. I thank Dr. Sarah Wilson for performing the electron microscopy and immunolocalisation. Thanks to Dr. Sergiy Lopato and Ms. Natalia Bazanova for their contribution and providing various materials during investigating protein-protein interaction. I thank Mr. Jelle Lahnstein for protein purification and amino acid sequencing. I would like to express my appreciation to Dr. Keith Gatford for his friendship, expert opinions and assistance in dsRNAi gene silencing. I thank Mrs. Margaret Pallotta for her assistance with genetic mapping. I am grateful to Dr. Brendon King for his assistance during the BAC library screening. I am thankful to Dr. Christina Lunde for moss transformation. I would like to thank Ms. Sally Richards and Ms. Margaret Cargill for their help in editing my thesis.

I would also like to thank many others without whose collaboration, generosity and advice the work presented in this thesis would not have been possible. I would therefore like to thank Maria Hrmova, Ute Baumann, Robert Lee, Simon Rutten, Michael Schober Jacinda Rethus, Vanessa Richardson, Damian Drew, Jan Nield, Andrew Jacobs, David Harris, Bronwyn Norton, Lisa Incoll, Roma Hardy, Ann Marshal, Nuredin Habili, Bianca Kuchel and Nicola Featherstone. I would also like to thank my Iranian friends in Adelaide for their support and kindness. I thank the Maros family (Kathleen and Michael) for being good Australian friends to my family and voluntarily teaching us the Aussies' slang.

I would like to thank all my family especially my step mother "Faezeh" and my father "Nosratollah" for their encouragement and support. Finally, I would like to express my great appreciation to my wife "Mandana" for her patience, understanding and love.

PUBLICATIONS

Refereed papers

Burton, RA., **Farrokhi, N.,** Bacic, A., and Fincher, GB., (2005) Plant cell wall polysaccharide biosynthesis: real progress in the identification of participating genes. *Planta*, **221:** 309-312

Farrokhi, N., Burton, RA., Brownfield, L., Hrmova, M., Wilson, SM., Bacic, A., and Fincher, GB., (2005) Plant cell wall biosynthesis: genetic, biochemical and functional genomics approaches to the identification of key genes. In press (*Plant Biotechnology Journal*)

Conference proceedings

7th International Congress of Plant Molecular Biology, 2003, Barcelona, Spain

Farrokhi, N., Burton, R.A., Shirley, N.J., Gatford, K., and Fincher, G.B.
"Functional analysis of barley (*Hordeum vulgare*) glycosyltransferases with focus on family GT34"

X Cell wall meeting, 2004, Sorento, Italy

Fincher, G.B., Burton, R.A., Medhurst, A., Harvey, A.J., **Farrokhi, N.,** Newbigin, E.J., Doblin, M., Shirley, N.J., Stone, B.A., Wilson, S., and Bacic, A.
"Biosynthesis of (1,3;1,4)-β-D-Glucans and arabinoxylans in cereals, presented by Prof. Fincher"

COMBIO, 2004, Perth, Australia

Farrokhi, N., Burton, R.A., Zhang, Q., and Fincher, G.B.
"Barley Glycosyltransferases"

Genomics in Barrossa, 2004, Adelaide, Australia

Farrokhi, N., Baumann, U., and Fincher, G.B.
"Cell Wall-Related Biosynthetic Glycosyltransferases in Rice"

ABBREVIATIONS

Acces.	Accession number
°C	Degrees centigrade
2-ME	2-mercaptoethanol
3D	3-dimentional
Approx.	Approximately
AD	Activation domain
BSA	Bovine serum albumin
CaMV	Cauliflower mosaic virus
cDNA	Complementary DNA
Ci/mmol	Curies per millimole
Cm	Centimeter
CPM	Count per minute
CTAB	Cetylmethylammonium bromide
d	Days
Da	Dalton
DES	*Drosophila* expression system
DMSO	Dimethy sulfoxide
DNA	Deoxyribunucleic acid
dNTP	Deoxynucleotide triphosphate
dsRNA	Double stranded RNA
DTT	Dithiothreitol
E. coli	*Escherichia coli*
EDTA	Ethylene diamine tetraacetic acid
EGTA	Ethylenebis (oxyethylenenitrio) tetraacetic acid
EST	Expressed sequence tag
g	Gram
Gal4	Yeast transcriptional activator protein
GFP	Green fluorescent protein
GTE	Glucose Tris EDTA
GUS	Glucuronidase synthase
h	Hours
HEPES	(N-[2-hydroxyethyl]piperazidine-N'-[2-ethanesulphonic acid])
HPLC	High-performance liquid chromatography
HvGlyT	Barley glycosyltransferase
IgG	Immunoglobulin G
IPTG	Isopropylthiogalactosidase
Kb	Kilo base pair
Kcal/mol	Kilo calorie per molar
KDa	Kilo Dalton
KPa	Kilo Pascal
KV	Kilo volt
l	Litre
LB	Luria-Bertani (liquid broth)
M	Molar
mA	Milli amperage
Mb	Mega base
µF	Micro Faraday
mg	Milligram
mg/ml	Milligram per milli liter
µg	Micrograms
µg/µl	Micrograms per micro liter
µg/ml	Micrograms per milli liter
µl	Micro liter
ml	Milliliter
ml/min	Milliliter per minute
MSA	Multiple sequence alignment
mM	Milli molar
mSec	Milli seconds
min	Minutes

mRNA	Messenger RNA
NF	Normalisation factor
ng	Nanograms
Ni-NTA	Nickel-nitrilotriacetic acid
nm	Nanometers
OD	Optical density
Ω	Ohom
PBS	Phosphate-buffered saline
PCR	Polymerase chain reaction
pg	picograms
pH	Potential of Hydrogen
pI	Isoelectric point
PIPES	Piperazine-N,N′-bis(2-ethanesulfonic acid)
psi	Pound per square inch
PVP	Polyvinyl pyrilidone
RACE	Randomly amplified cDNA ends
RNA	Ribonucleic acid
RNAi	RNA interference
rpm	Revolutions per minute
RT-PCR	Reverse transcriptase PCR
s	Sedimentation coefficient
SDS	Sodium dodecyl sulphate
SDS-PAGE	SDS-polyacrylamide gel electrophoresis
Sec	Seconds
TB	Tris buffered saline
T-DNA	Transfer DNA
TEMED	N,N,N',N'-Tetramethylethylenediamine
T_m	Melting temperature
TMH	Transmembrane helix
Tris	Hydroxymethyl amino methane
UDP	Uridine diphosphate
V	Voltage
Vol	Volume
v/v	Volume for volume
w/v	Weight for volume
×	times
×g	Units of relative centrifugal force
X-Gal	5-Bromo-4-chloro-3-indolyl-β-D-galactopyranoside

ABSTRACT

Glycosyltransferases (GTs) are enzymes involved in the formation of glycosidic linkages by transferring sugar molecules from donor molecules, usually nucleoside diphospho-sugars, to specific acceptor molecules. GTs have been classified into more than 70 families of which *Arabidopsis* has been represented in 40 (http://afmb.cnrs-mrs.fr/CAZY/; Campbell *et al.*, 1997; Coutinho *et al.*, 2003). GTs catalyse the biosynthesis of many di-, oligo-, and poly-saccharides, and the glycosylation of other macromolecules (Zhong and Ye, 2003). Biosynthesis of the plant cell wall requires the involvement of a variety of GTs synthesising the main chain of polysaccharides in an iterative manner; these enzymes are referred to as polysaccharide synthases. The enzymes that transfer sugar moieties to these backbones in a single event are also known as "glycosyltransferases", but in a more limited context. While the chemical structures of most wall polysaccharides have been defined in detail, the enzymes involved in their synthesis remain largely unidentified. A major contributing factor to our poor understanding of the GTs has been that many of the enzymes are large, membrane-bound proteins that have resisted extensive biochemical efforts for their purification in an active form. Nevertheless, emerging molecular technologies have enhanced our ability to discover the functional specificity of GTs in wall polysaccharide synthesis. This knowledge will be used to enhance the cell wall structure for agroindustrial processes such as paper and pulping, food quality and texture, malting and brewing, bioethanol production, dietary fibre and ruminant digestibility *via* plant breeding. The potential involvement of barley GT34 and GT47 family members in cell wall biosynthesis is investigated in this thesis.

Four near full-length and one partial-length cDNAs of barley glycosyltransferases were isolated using molecular techniques. Four of these GTs belong to family GT34, designated *HvGlyT1*, *HvGlyT2*, *HvGlyT3* and *HvGlyT5*, and one belongs to family GT47, designated *HvGlyT4*. Detailed analyses of protein sequences were performed to

investigate the presence of motifs, secondary structures, the presence of transmembrane helices (TMH) and their post-translational modification sites. Homology searches and multiple sequence alignments indicated that HvGlyT1, HvGlyT2 and HvGlyT3 were putative α-xylosyltransferases, HvGlyT4 was a putative pectin glucuronosyltransferase, and possibly HvGlyT5 was an α-galactosyltransferase.

Transcript profiles of the barley GTs were established in a range of barley tissues using both the real-time PCR and a barley microarray. The relative abundance of transcripts in different tissues and the coordinate expression of individual barley GTs with other genes also provided clues to their function. HvGlyT1 might be a xylosyltransferase involved in the biosynthesis of xylogalacturonan in root tip exudates. *HvGlyT3* is highly transcribed in all barley tissues studied in this project with a tendency for higher amounts in dividing and elongating cells. The abundance of this transcript may suggest its involvement in the biosynthesis of an abundant cell wall polysaccharide, such as glucuronoarabinoxylans. Based on the evidence available, it was speculated that HvGlyT3 may be an α-arabinosyltransferase but unequivocal evidence was not obtained.

HvGlyT4 mRNA is also highly abundant, particularly in mature tissues. Transcript data was not helpful in proposing a function for HvGlyT4, because it is highly homologous to a previously characterised rhamnogalacturonan II glucuronosyltransferase (Iwai *et al.*, 2002), and a similar function is possible in barley. *HvGlyT5* is a grain-specific gene, which increases during early endosperm development and disappears in the later stages of grain development. The low transcript levels correlate to the limited amount of galactoglucomannan, 2% of cell wall polysaccharides of a barley grain (Fincher, 1992), which might suggest an α-galactosyltransferase function for this protein. Again the evidence for these conclusions was indirect.

The possibility of interaction of glycosyltransferases with other enzymes involved in cell wall biosynthesis and remodeling, including glycan synthases, sugar nucleotide interconverters and glycosyl hydrolases, convinced us to investigate protein-protein

interactions *via* yeast two-hybrid screening. Thus, amongst the isolated barley GTs, *HvGlyT3* and *HvGlyT4*, and an enzyme involved in generating the UDP-arabinose pool in the cell, barley UDP-xylose epimerase (HVUXEP), were used as bait to explore two previously made wheat early developing grain and endosperm cDNA libraries. HvGlyT3 showed a true interaction with an unknown protein and with a serine carboxypeptidase. Although the unknown protein was evaluated for its physiochemical properties and for the presence of diagnostic motifs, nominating a function was not possible. Furthermore, establishing a functional relationship between HvGlyT3 and serine carboxypeptidase was also not possible at this stage.

The cDNA fragments of barley GTs, with and without TMHs, were expressed heterologously in a range of systems, including *E. coli*, mammalian cells, moss and insect cells. All expressed proteins in *E. coli* appeared in the insoluble fraction, even when induction conditions were changed or cells were co-transformed with a helper vector to overcome the codon bias problem. Mammalian cells and moss failed to express any protein. While using baculovirus technology, insect cells produced recombinant proteins as an insoluble fraction. Efforts were made to recover these fractions to perform enzyme assay. The assay results were not reproducible and the amount of radioactivity incorporated was not high enough compared with the negative controls to allow us to confidently conclude that the apparent activity was real.

Finally, dRNAi silencing technology was used to silence barley members of family GT34. Three constructs were made; a family-specific construct based on the conserved region of three barley GTs, *HvGlyT2* and *HvGlyT3*. The generic construct was derived from *HvGlyT1*. The constructs were delivered to 5 d old immature barley embryos using particle bombardment. The transcript levels were measured and compared with the tissues obtained from 5 d old immature barley embryos bombarded with empty vector. Although up-regulation of transcripts was sometimes observed in some tissues, transcript levels were usually down-regulated. The tissues were studied for any obvious phenotypic changes and the barley tissues bombarded with *HvGlyT3* construct showed a hairy root

tip phenotype. Sections prepared from these roots showed bigger cortical cells, which suggested weakening of the cell wall. In addition the dividing walls in the sub-epidermal layer were not present. Scanning electron micrographs of the coleoptiles obtained from the same embryo showed a drastic effect on elongating cells. These cells were damaged and stress fractures were visible. Although the data suggested the involvement of HvGlyT3 in cell wall biosynthesis, detailed cell wall analysis could not be carried out as a result of the low frequency of the phenotype.

During the course of this project, a polyclonal antibody was developed against barley HvGlyT4. The HvGlyT4-specific antibody recognised both the antigen and the entire protein extracted from barley tissues. This antibody was used to investigate the cellular location of HvGlyT4, which appeared to be mostly in the Golgi apparatus, with a minor amount of binding to the plasma membrane.

CHAPTER 1

GENERAL INTRODUCTION

The overall aim of the work presented in this thesis was to isolate and characterise cDNAs encoding family GT34 and GT47 cell wall-related glycosyltransferases from barley. Primary walls of plants are composed of cellulose microfibrils embedded in a matrix of polysaccharides including pectins, xyloglucans, heteroxylans and heteromannans (Carpita and Gibeaut, 1993). Smaller amounts of protein, phenolic acids and glycoproteins are present in the walls of most plants, callose is detectable in some walls, and lignin is often found after secondary thickening. Barley (*Hordeum vulgare* L.) cell wall polysaccharides share common features with other members of the grass family (Poaceae), where the cellulosic microfibrils are embedded in a matrix phase having (1→3,1→4)-β-D-glucans and arabinoxylans as major components, with lesser amounts of xyloglucans and pectins compared with walls of many dicots (Fincher, 1975, 1992; Hrmova and Fincher, 2002). Enzymes involved in synthesising these polysaccharides are broadly known as glycosyltransferases, but here a distinction is made between enzymes that are responsible for the iterative incorporation of glycosyl residues into the glycan backbone of wall polysaccharides, which are referred to as glycan synthases, and enzymes that add single glycosyl substituents to the backbone polysaccharide, which are referred to as glycosyltransferases. For example, during arabinoxylan biosynthesis the enzyme that synthesises the backbone of the polysaccharide is referred to as a xylan synthase, while the enzyme that adds arabinosyl substituents to the xylan backbone is called an arabinosyltransferase.

In this project, attention was focused on glycosyltransferases that are involved in the biosynthesis of the matrix phase polysaccharides, and on defining the specific function of cloned glycosyltransferase cDNAs from barley. In the following sections, barley cell wall composition, the enzymes involved in cell wall biosynthesis and some of the techniques that were used to address the functional analysis of putative glycosyltransferases are introduced.

1.1 PLANT CELL WALL COMPOSITION

1.1.1 Introduction

Plant cell walls maintain cell shape against interior turgor pressure and exterior mechanical forces, and delineate the ultimate shape of the cell in a given tissue (Hayashi, 1989; Carpita and Gibeaut, 1993; Reiter, 1998). Wall structure changes throughout cell development. Primary walls are laid down on the cell plate just after cell division and during cell development the walls expand. Following the cessation of cell expansion, secondary cell walls are deposited in many cells, depending on their function. Lignin, the second most abundant biomolecule in nature, is found where secondary walls are present. Lignin increases the strength and decreases the permeability of walls to water and other organic or inorganic molecules (Carpita and McCann, 2000).

Primary cell walls have been divided into type I and type II according to the relative abundance of xyloglucan (XG) and glucuronoarabinoxylans (GAXs) (Carpita and Gibeaut, 1993; Faik *et al.*, 2000). The non-cellulosic polysaccharides of type I walls, which are found in all dicots and in the non-graminaceaus monocots, are mainly composed of xyloglucan and pectin (Figure 1.1). In contrast, the major matrix phase glycans in type II walls are GAXs and (1→3,1→4)-β-D-glucans, with lower levels of pectic polysaccharides and xyloglucans (Carpita and Gibeaut, 1993; Brett and Waldron, 1996; Carpita and McCann, 2000; Willats *et al.*, 2001). Walls of the Poaceae are particularly rich in (1→3,1→4)-β-D-glucan (Fincher, 1992; Smith and Harris, 1999), and contain relatively low amounts of pectic polysaccharides and mannans (Smith and Harris, 1999; Willats *et al.*, 2001). In addition to polysaccharides, there are low levels of proteins in the matrix phase of the cell wall. The proteins in walls have both structural and enzymic roles (Table 1.1). Structural proteins may form another network to interlace with the microfibrillar and matrix phases polysaccharides (Fincher, 1992), and include glycine-rich proteins, proline-rich proteins and hydroxyproline-rich glycoproteins. Wall-bound enzymes (for

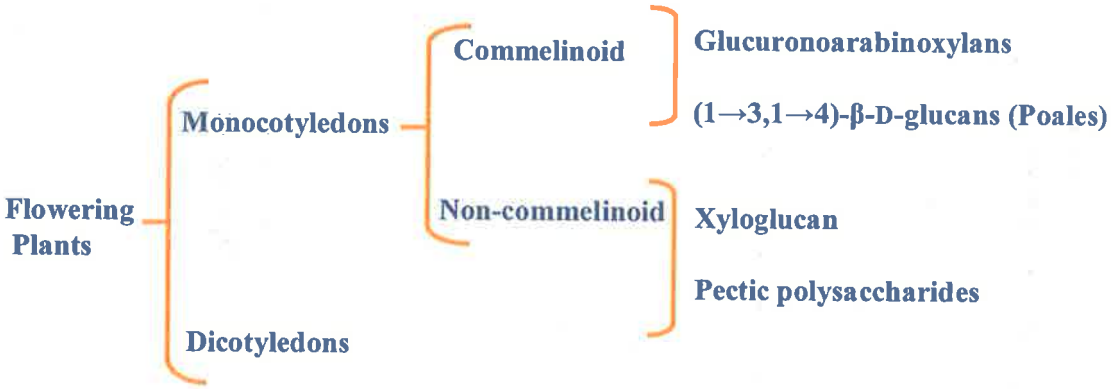

Figure 1.1 Comparison of the major non-cellulosic cell wall polysaccharides of flowering plants. Monocotyledons are divided into two groups, Commelinoid and non-Commelinoid, based on the composition of major non-cellulosic cell wall polysaccharides. Not all commelinoid monocots have (1→3,1→4)-β-D-glucans; only the Poales (grasses and related families) have this polysaccharide (Smith and Harris, 1999).

Structural proteins	Hydroxyproline rich glycoprotein
	Proline rich proteins
	Glycine rich proteins
Enzymic proteins	Peroxidase
	Invertase
	Cellulase
	Acid phosphatase
	Pectinase
	Pectin methylesterase
	Malate dehydrogenase
	Exoglucanase
	Endo (1→4)- β-D-glucanase
	Endo (1→3)- β-D-glucanase
	Endo-transglycosylase
	Xylanase
	Laccase
	Germin oxidase
	Others

Table 1.1 Structural and enzymic proteins of cell wall (Brett and Waldron, 1996; Lane, 2000; Huttermann *et al.*, 2001; Collins *et al.*, 2005)

examples refer to Table 1.1) participate in cell wall changes, remodelling and turnover during wall development and elongation (MacGregor and Fincher, 1993; Brett and Waldron, 1996; Carpita and McCann, 2000). Expansins are particularly important wall-associated proteins (McQueen-Mason *et al.*, 1992; Cosgrove *et al.*, 2002) and have been implicated in the acid growth phenomenon of walls in elongating cells. Two classes of expansins, α-expansin and β-expansin, have been distinguished and are believed to participate in wall loosening during growth (Cosgrove *et al.*, 2002). The proteins have been purified and assayed for their ability to 'loosen' associations between cellulose molecules and other wall polysaccharides *in vitro*, but they have no known enzymic activity. It has been suggested that the two classes of expansins function in essentially the same manner, but perhaps target different polysaccharides in the cell wall (Cosgrove *et al.*, 2002).

Other minor components in the cell wall include minerals, particularly silicates, and in certain tissues suberin, cutin, waxes, and aromatic substances (MacGregor and Fincher, 1993; Carpita and McCann, 2000). Aromatic substances can be found in the nonlignified primary cell walls of the Commelinoids and Chenopodiaceae. Aromatics are largely hydroxycinnamic acids such as ferulic acid and *p*-coumaric acid, and may form a large network through interconnection of GAXs in grasses (Brett and Waldron, 1996). Furthermore, hydoxycinnamic acids linked to polysaccharides may act as primers or start points for lignin polymerisation in secondary cell walls (Fincher, 1992; Carpita and McCann, 2000).

1.1.2 Barley cell wall polysaccharides

Barley is a member of the Poaceae family and shares similar wall characteristics with the other members of this family. The compositions of wall polysaccharides from selected tissues of barley are shown in Table 1.2. In barley grain, arabinoxylan and (1→3,1→4)-β-D-glucans are the principal wall polysaccharides, but they differ in proportion between aleurone and endosperm walls. The low level of cellulose and the absence of lignin in endosperm walls facilitate rapid enzymic degradation of the walls during germination (Fincher, 1992). In vegetative tissues the dominant poly-

saccharide is cellulose (Table 1.2). The structures and properties of the major cell wall polysaccharides are described below.

1.1.2.1.1 Cellulose

Cellulose is an unbranched chain of (1→4)-β-D-glucosyl residues. Each chain has a degree of polymerisation (DP) of up to 6,000 and 14,000 in primary and secondary walls, respectively (Fincher and Stone, 2004). The chains adhere to each other by hydrogen bonds and van der Waal's interactions to produce the so-called micro-fibrillar structure (Srisodsuk *et al.*, 1998). About three dozen chains of (1→4)-β-D-glucopyranose are arranged in highly ordered parallel crystalline arrays to make paracrystalline fibres (3 nm in primary walls and 5-10 nm in secondary walls) that are visible under the electron microscope (Jarvis, 2003; Fincher and Stone, 2004). This well-ordered structure in crystalline cellulose may lose its pattern in places where interactions are weaker, especially on the surface of the microfibrils. In addition to microfibrillar associations, cellulose microfibrils may interact with other matrix polysaccharides present in the wall (Fincher and Stone, 2004). These inter- and intra-molecular forces produce a water insoluble cellulosic network that shapes the ultrastructure of the walls.

1.1.2.1.2 Arabinoxylans (AXs) and glucuronoarabinoxylans (GAXs)

AXs and GAXs, also known as heteroxylans or pentosans, are abundant polysaccharides of graminaceaus monocots. Their abundance differs between tissue types (for example see Table 2.1) and is affected by both genotypic and environmental factors (Fincher and Stone, 2004). Both AXs and GAXs are unbranched polymers of (1→4)-β-D-xylosyl residues with substituents of α-L-arabinosyl (Ara*f*) residues attached mostly to the C(O)3, sometimes to C(O)2 and occasionally to both C(O)3 and C(O)2 (Perlin, 1951; Voragen *et al.*, 1987; Vietor *et al.*, 1994; Smith and Harris, 1999). Ara*f* substitution of the xylan backbone is irregular, differs across species and depends on wall type and the developmental stage of the wall (Carpita, 1996; Fincher and Stone, 2004). For example, walls of lignified vegetative tissues contain high Xyl*p*:Ara*f* ratios, while walls of the aleurone layer and

Tissue	Major Polysaccharide Components	References
Aleurone (mature grain)	71% arabinoxylan 26% (1→3,1→4)-β-D-glucans 2% cellulose 2% glucomannan 1% (1→3)-β-glucan	(Bacic and Stone, 1981) (Bacic and Stone, 1981)
Starchy Endosperm (mature grain)	75% (1→3,1→4)-β-D-glucans 20% arabinoxylan 2% cellulose 2% glucomannan	(Fincher, 1975) (Ballance and Manners, 1978)
Coleoptile (4 days)	36% cellulose 33% arabinoxylan 10% (1→3,1→4)-β-D-glucans 10% xyloglucan 10% pectin	(D.M. Gibeaut and G.B. Fincher, unpublished)
Stems (4th internode)	65% cellulose 28% hetroxylan 5% (1→3,1→4)-β-D-glucans	(Wilkie, 1979) (Kokubo *et al.*, 1989)
Young leaves (top 2 cm, dark grown)	63% cellulose 16% (1→3,1→4)-β-D-glucans 5% pectin ? xyloglucan	(Sakurai and Masuda, 1978)

Table 1.2 Composition of cell wall polysaccharides from barley (after Fincher, 1992)

starchy endosperm have lower Xyl*p*:Ara*f* ratios (Fincher and Stone, 2004). Furthermore, it has been shown that the dividing and elongating cells contain highly substituted GAXs, while less highly substituted GAXs are found in non-dividing cells (Gibeaut and Carpita, 1991; Carpita, 1996; Gibeaut *et al.*, 2005). This suggests that the chemical structures of GAXs are being altered during plant growth and development through the removal of arabinosyl units (Lee *et al.*, 2001). Glucuronosyl residues (GlcA*p*) and their 4-O-methyl ethers, attached to C(O)2 of the Xyl*p* unit, and other minor glycosyl residues are also present in GAXs (MacGregor and Fincher, 1993). Hydroxycinnamic acids, such as ferulic acid (FA) and *p*-coumaric acid, are also present. Feruloyl esters reside at C(O)5 of Ara*f* in the heteroxylans (Fincher and Stone, 2004). Amongst these phenolic acids, FA plays important roles in establishing cross-links between AX chains and also between lignin and AXs in lignified cell walls (Lapierre *et al.*, 2001; Fincher and Stone, 2004). *In vitro*, cross linked AX chains can form thermo-reversible gels at high concentration, *via* either non-covalent interactions or dimerisation of feruloyl units (Fincher and Stone, 2004). FA has autofluorescence properties that can be used to investigate the presence or absence of heteroxylans in cell walls, and also to indicate the level of substitution of Ara*f* with FA (Gubler and Ashford, 1985; Wende and Fry, 1997). Cellulose microfibrils may also interact with less highly substituted heteroxylans *via* hydrogen bonding (Fincher and Stone, 2004).

Sedimentation velocity techniques (Podrazky, 1964) and gel filtration chromatography (Bathgate *et al.*, 1974; Forrest, 1977) have been used to estimate the average molecular weight of cereal heteroxylans. Degrees of polymerisation (DP) of 500-38,000 have been obtained, and these correspond to molecular sizes between 65 $\times 10^3$ and 5 $\times 10^6$ (Fincher and Stone, 2004). As opposed to the glucosyl residues in cellulose, where two hydrogen bonds form between adjacent glucosyl residues (O2′-H-O6′ and O5′-H-O3′), xylosyl residues in unsubstituted heteroxylans can only establish one inter-residue hydrogen bond (O5′-H-O3′). As a result, AX chains are structurally more flexible than cellulose (Fincher and Stone, 2004). AXs form aqueous solutions of high viscosity, as a result of their asymmetrical conformation, high DP and the arrangement of their Ara*f* substituents (Fincher, 1992; MacGregor and Fincher, 1993; Fincher and Stone, 2004).

1.1.2.1.3 (1→3,1→4)-β-D-Glucans

(1→3,1→4)-β-D-Glucans are cereal- and grass-specific homopolymers, which provide important physiological properties for the matrix phase of primary walls, including water holding capacity, porosity and elasticity (Ramesh and Tharanathan, 2003). The (1→3,1→4)-β-D-glucans appear in most tissues (Table 1.2.) and accumulate during cell expansion; they often disappear during cell maturation (Carpita, 1996). Starchy endosperm walls from barley are particularly rich in (1→3,1→4)-β-D-glucans in comparison with other tissues (Fincher, 1992), as are the walls from oat and rye (Fincher and Stone, 2004). A structurally related (1→3,1→4)-β-D-glucan, known as lichenin, is found in the Iceland moss lichen (*Cetraria islandica*).

The average molecular mass of cereal (1→3,1→4)-β-D-Glucans is species-specific and ranges between 48×10^3 (DP approx. 300) and 3×10^6 (DP approx. 1850). The (1→3,1→4)-β-D-glucans can be water-soluble (pH 7.0 at 40°C) and water-insoluble, depending on their DP, their fine structure and the degree of inter- and intra-molecular association in the wall (Fincher and Stone, 2004). Despite this classification, water extractability of (1→3,1→4)-β-D-glucans is temperature dependent and it has been shown that almost all of the (1→3,1→4)-β-D-glucan is extracted from walls of barley endosperm at 100°C (Ballance and Manners, 1978; Ahluwalia and Fry, 1986). Regardless of water extractability, (1→3,1→4)-β-D-glucans are comprised of linear, unbranched chains of β-D-glucosyl residues linked by either (1→3)- or (1→4)-linkages. The dominant structure of (1→3,1→4)-β-D-glucans contains a series of cellotriosyl ($G4G4G_{Red}$), and sometimes cellotetraosyl ($G4G4G4G_{Red}$) units connected to each other *via* single (1→3)-β-D-linkages (Hrmova and Fincher, 2001). Therefore, (1→4)-linkages are more frequent (up to 2.6 fold) than (1→3)-linkages. There is no regularity in linkage arrangements and their ratios are fairly constant within species. The number of repeating units of (1→4)-β-D-linkages can also be different from the dominant form, where up to 10% of the chain may contain more than four adjacent (1→4)-linked-β-D-glucosyl residues (Fincher and Stone, 2004). The ratio of these two linkage types within (1→3,1→4)-β-D-glucan molecules affect physiochemical properties, such as viscosity, gelation, and melting temperature. The

presence of (1→3)-linkages within (1→3,1→4)-β-D-glucans results in molecular "kinks" that ultimately makes them more soluble than cellulose molecules (Fincher and Stone, 2004).

1.1.2.1.4 Xyloglucan (XG)

XG has a backbone of cellulose-like (1→4)-β-D-glucan with (1→6)-α-D-xylosyl substituents and is generally water-soluble. There are two other major substitution patterns in which (1→2)-β-D-galactosyl residues bind to the xylosyl residues and a (1→2)-α-D-fucosyl residue is bound to the galactosyl residue (Figure 1.2). Many other types of XGs with different substitution patterns are found, and are usually species- and tissue-specific (O'Neill and York, 2003). Fry *et al.* (1993) proposed a nomenclature of XGs for which an example is shown in Figure 1.2. Type II walls have less xyloglucan in comparison to Type I walls (Gibeaut and Carpita, 1994). The grass XGs are less substituted with xylosyl residues, contain few galactosyl residues, and have few or no fucosyl residues. The (1→4)-β-D-glucan backbone therefore contains stretches of β-D-glucosyl residues (Brett and Waldron, 1996; O'Neill and York, 2003). XGs have a DP of 600-700, which corresponds to a molecule mass of about 1×10^6 and form associations with cellulose microfibrils *via* hydrogen bonds to establish a cellulose/xyloglucan network (Vincken *et al.*, 1995; Fincher and Stone, 2004). It has been suggested that binding to cellulose depends on XG fine structure and molecular weight (Lima *et al.*, 2004). For example, lower degrees of substitution will increase the self-association capacity of XGs and will promote binding of XG to cellulose (Lima *et al.*, 2004).

1.1.2.1.5 Glucomannan

Another glycan in walls of the Poaceae is glucomannan, which exists in small amounts that bind tightly to cellulose microfibrils. Glucomannans are mostly found in aleurone and starchy endosperm cells of barley (Table 1.2). Glucomannans (Figure 1.2) typically have DPs ranging from less than 100 to several thousand, and consist of backbone of (1→4)-β-D-mannosyl residues interspersed with (1→4)-β-D-glucosyl residues; sometimes the mannosyl residues are substituted with (1→6)-α-D-galactosyl residues (Elbein, 1969; Brett and Waldron, 1996; Fincher and Stone, 2004). The

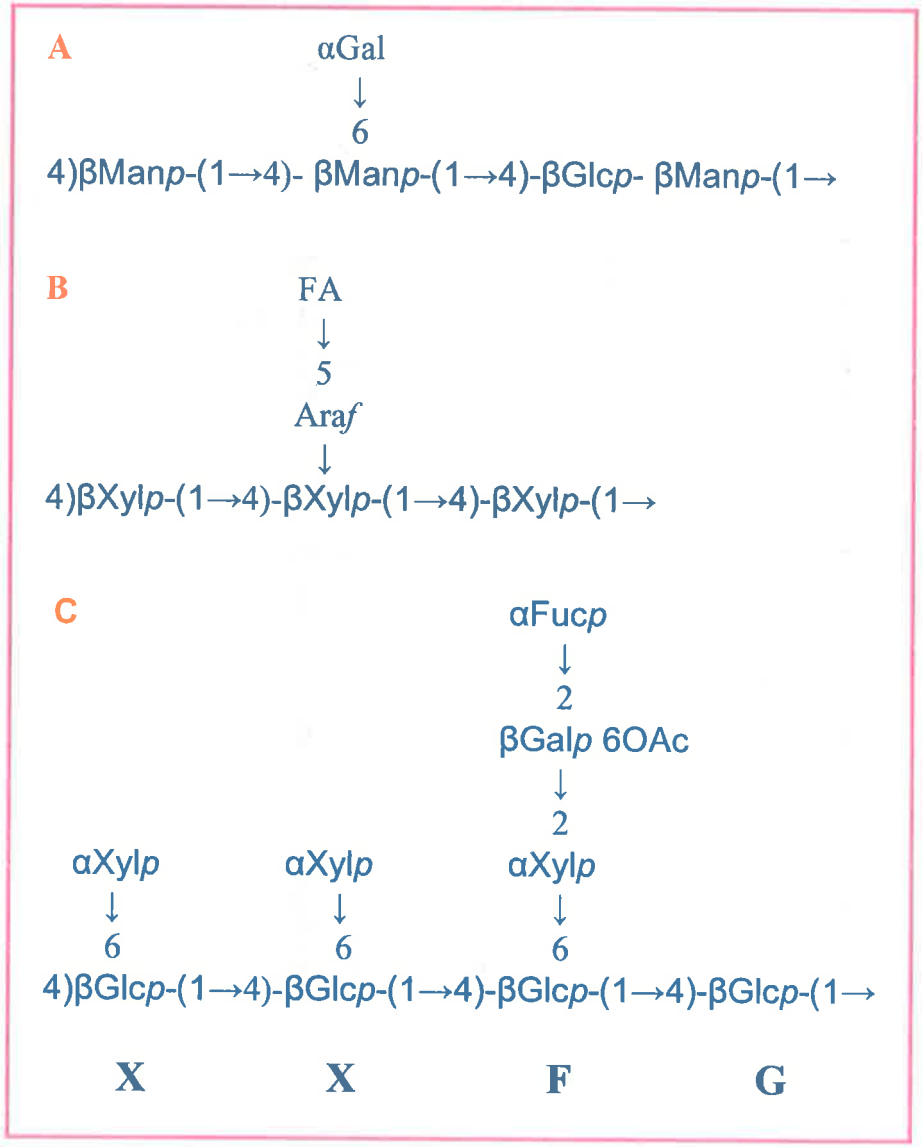

Figure 1.2 Structural features of three non-cellulosic polysaccharides.

A: glucomannans, **B**: arabinoxylans, FA is a ferulic acid residue on C(O)5 of Ara*f* and the xylopyranosyl backbone is substituted with arabinosyl residues at C(O)3, C(O)2 or both, **C**: common structure of xyloglucan, G = an unsubstituted glucopyranosyl (Glc*p*) residue, X = a Glc*p* substituted with α-D-xylopyronosyl (Xyl*p*) residue, F = a Glc*p* residue bearing a trisaccharide (α-L-Fuc*p*-(1→2)-β-D-Gal*p*-(1→2)-α-D-Xyl*p*) at O6, L = a Glc*p* residue bearing a disaccharide (β-D-Gal*p*-(1→2)-α-D-Xyl*p*) at O6 (not shown), S = a Glc*p* residue bearing an O5 acetylated disaccharide (α-Ara*f*-(1→2)-α-D-Xyl*p*) at O6 (not shown). Fuc*p* = fucopyronosyl residue, Gal*p* = galactopyranosyl residue, Man*p* = mannopyranosyl residue, and 6OAc = acetylation of galactopyronosyl residue at O6.

mannosyl residues are generally more abundant than glucosyl residues, and account for about 70% of the polysaccharide (Fincher and Stone, 2004).

1.1.2.1.6 Pectic polysaccharides

Pectin is a polysaccharide rich in polygalacturonic acid. In all plants except the Poales, pectin is one of the most abundant polysaccharides found in the matrix phase of primary cell walls and middle lamellae (Smith and Harris, 1999). There are two major types of pectic polysaccharides that have different branching patterns; homogalacturonan (HGA) and highly substituted rhamnogalacturonan (RG) (Willats *et al.*, 2001).

Homogalacturonan is a linear chain of (1→4)-α-D-galacturonic acid residues (Willats *et al.*, 2001). This linear homopolymer is sometimes substituted with xylosyl residues at C(O)-3 and apiosyl residues at C(O)-2 or C(O)-3 to form xylogalacturonan and apiogalacturonan. The negatively charged galacturonic acid (GalA) residues of HGA interact with Ca^{2+}, and this interaction promotes gelation through formation of Ca^{2+}-bridges between unesterified galacturonosyl units on adjacent chains (Willats *et al.*, 2001).

The RG component of pectic polysaccharides is found in two forms, RG I and RG II. RG I consists of repeating disaccharide units of (1→2)-α-L-rhamnosyl-(1→4)-α-D-galacturonic acid and is believed to be covalently linked to HGA (Willats *et al.*, 2001). RG I also contains side chains of arabinan, galactan and arabinogalactan I. The arabinan is a homopolymer of (1→5)-α-L-arabinosyl residues, the galactan is a polymer of (1→4)-β-D-galactosyl residues, and type I arabinogalactan has the (1→4)-β-D-galactan structure with non-reducing arabinosyl substituents on C(O)3 (Carpita and Gibeaut, 1993; Mohnen, 1999; Willats *et al.*, 2001). RG II has a backbone of HGA with different glycosyl substituents, including apiose, aceric acid and 2-keto-3-deoxy-D-manno-octulosonic acid (KDO) (Vidal *et al.*, 2000; Willats *et al.*, 2001). The apiosyl residues from two RG II domains are usually cross-linked through a borate molecule (Kobayashi *et al.*, 1996; O'Neill *et al.*, 2004). Type II arabino-galactan is another side chain found on pectic polysaccharides (Willats *et al.*, 2001).

1.1.2.1.7 Type II arabinogalactan

Arabinogalactan II consists of a backbone of (1→3)-β-D-galactosyl residues with side chains of (1→6)-β-D-galactosyl residues and non-reducing terminal (1→3)-α-L-arabinosyl and rhamnosyl residues (Gaspar *et al.*, 2001; Willats *et al.*, 2001). Arabinogalactans are covalently bound to hydroxyproline residues of proteins, to form arabinogalactan proteins (AGPs). AGPs are termed proteoglycans since they are heavily glycosylated with arabinogalactan II and other glycosyl residues (Gaspar *et al.*, 2001), and exist in a wide array of chemical forms. They are not generally considered a cell wall component, but may be bound to cellular membranes or secreted into the periplasmic space (Bacic *et al.*, 1996).

1.2 PLANT GLYCOSYLTRANSFERASES

1.2.1 Introduction

The biosynthesis of the wall polysaccharides described in the previous sections involves two quite distinct processes, namely the synthesis of the backbone through the activity of glycan synthases, and the addition of glycosyl substituents to the backbone chain by the action of glycosyltransferases (Perrin *et al.*, 2001). The polysaccharides that are secreted into the wall may undergo further modifications within the wall (Fry, 1995). Glycosyltransferases (GTs), as their name implies, are enzymes that transfer a sugar moiety to an acceptor molecule to form a glycosidic linkage. The glycosyl residue is usually obtained from an activated diphospho-nucleotide sugar in either the UDP- or GDP- form (Kleene and Berger, 1993; Breton and Imberty, 1999). Acceptor molecules in plants include cell wall polysaccharides, glycoproteins, glycolipids, hormones and flavonoids (Keegstra and Raikhel, 2001).

GTs are among the largest groups of enzymes found, and can be classified into families based on sequence similarities, the existence of certain motifs, hydrophobic cluster analysis (HCA) and their catalytic specificity (Campbell *et al.*, 1997; Imberty *et al.*, 1999; Ross *et al.*, 2001; Rosen *et al.*, 2004). In general, homology among and

within GT families is low, which makes the definition of function based on sequence similarity very difficult (Breton and Imberty, 1999). Further, high sequence identity in GTs does not always allow an exclusive function of the gene to be deduced. Henrissat and colleagues have taken sequence homology, an *E* value of less than –3 over at least 100 amino acids, and hydrophobicity cluster analysis (HCA)-based approaches (Campbell *et al.*, 1997) to classify the GTs into more than 70 families (http://afmb.cnrs-mrs.fr/CAZY/-20/6/2004). It is expected that members of each family share a conserved three dimensional (3D) structure (Coutinho *et al.*, 2003).

Examination of the amino acid sequences of GT families has revealed the presence of a consensus motif, DxD, also termed the U motif, in 71% of all GTs (Coutinho *et al.*, 2003). The U motif usually appears after a hydrophobic cluster of amino acid residues predicted to be a β-strand (Breton *et al.*, 1998; Breton and Imberty, 1999; Imberty *et al.*, 1999). Several studies, involving site-directed mutagenesis of aspartate residues of the DxD motif (Busch *et al.*, 1998; Hagen *et al.*, 1999; Malissard *et al.*, 2002) and photoaffinity labelling using azido-UDP sugars (Busch *et al.*, 1998), suggest a crucial role for this motif in sugar nucleotide binding. Through crystallography of some GTs it has been shown that the DxD motif is located at the bottom of the catalytic pocket, where it participates in coordination of the divalent cation associated with the activated sugar nucleotide (Busch *et al.*, 1998; Breton and Imberty, 1999; Gastinel *et al.*, 2001; Persson *et al.*, 2001). A demonstrated exception to divalent cation binding by DxD motif is a bovine β4 galactosyltransferase (Gastinel *et al.*, 1999). This enzyme contains a DVD motif, which is in contact with the nucleotide substrate through water-mediated hydrogen binding, rather than through the divalent cation. Furthermore, it has been shown that some GTs have more than one U motif, but not all are bound to the metal cofactor or involved in catalytic activity of the enzyme (Persson *et al.*, 2001). It is worth mentioning that the presence of DxD motif does not necessarily mean that a protein sequence is a glycosyltransferase. A search in SwissProt (version 40; 119,805 entries) was revealed that 51% of all sequences contain this signature and that 69% of glycosyl hydrolases also have a DxD motif in their sequence (Coutinho *et al.*, 2003). In addition to this consensus motif, DxD, there might be other amino acid signatures present. These

motifs are more likely to be family-specific and can be determined either *via* multiple alignment of sequences within a certain family (Iwai *et al.*, 2002) or through solving the crystal structure of a specific GT (Charnock and Davies, 1999).

Catalytic specificity, which encompasses the type of activated sugar nucleotide, the type of glycosyl residue that the enzyme transfers and the type of linkage formed, is a useful means of classification of GTs. Because most GTs catalyse specific reactions, there are a large number of glycosyltransferases in any organism. Despite this fact, the biochemical activity of only a small number of plant GTs has been demonstrated so far (Keegstra and Raikhel, 2001). The reason why the functions and identities of many GTs have remained elusive is partly due to difficulties in the heterologous expression of cDNAs and partly due to difficulties in identifying the correct substrates for the expressed enzyme (Zhang *et al.*, 2003). The *Arabidopsis* genome sequence reveals that about 1.6% of the genome is made up of genes that encode glycosyltransferases (Egelund *et al.*, 2004). This value accounts for 415 genes from 38 GT families, compared to approximately 200 in the human genome (Breton *et al.*, 2001; Scheible and Pauly, 2004). One of the reasons why plants have so many GTs is believed to be for the synthesis of the cell wall (Coutinho *et al.*, 2003). The structures and functions of GTs known to be involved in cell wall polysaccharide biosynthesis are discussed in the following sections.

1.2.2 Classes of plant cell wall-related glycosyltransferases

Plant cell wall polysaccharides are composed of nine abundant glycosyl residues (glucosyl, galactosyl, mannosyl, xylosyl, arabinosyl, fucosyl, rhamnosyl, galacturonosyl, and galacturonosyl residues), together with other minor sugars such as apiose and aceric acid (Carpita and Gibeaut, 1993; Brett and Waldron, 1996). The glycosyl residues can be linked through a variety of different linkage types involving different carbon atoms and with different anomeric configurations. Therefore the biosynthesis of the many wall polysaccharides and their assembly requires multiple GTs to fulfil these requirements (Perrin *et al.*, 2001). Wall-related GTs are generally

membrane-bound enzymes. These GTs are divided into type I and type II membrane proteins, depending on their structure (Gibeaut, 2000).

1.2.2.1 Type I integral membrane GTs

Integral membrane enzymes involved in wall synthesis include the glycan synthases, or repetitive glycosyltransferases (Perrin *et al.*, 2001; Vergara and Carpita, 2001; Bonetta *et al.*, 2002). These enzymes are found in the plasma membrane and in the Golgi membrane, and contain numerous transmembrane helices (TMH). They are believed to be involved in the biosynthesis of homopolysaccharides such as cellulose, and possibly (1→3)-β-D-glucans and (1→3,1→4)-β-D-glucans (Gibeaut, 2000; Saxena and Brown, 2000; Richmond and Somerville, 2001; Bonetta *et al.*, 2002). The other putative function for integral membrane proteins is the synthesis of the backbones of matrix phase heteropolysaccharides, including xyloglucans, arabinoxylans, and glucomannans (Perrin, 2001; Vergara and Carpita, 2001; Dhugga *et al.*, 2004).

Cellulose synthases (CesA), cellulose synthase like enzymes (Csl) and (1→3)-β-D-glucan synthases (GSL) are integral membrane proteins; the first two belong to family GT2 and the last is classified in family GT48. These enzymes are large proteins, with about 1000 and 2000 amino acid residues in the GT2 and GT48 enzymes, respectively (Saxena and Brown, 2000; Richmond and Somerville, 2001; Jacobs *et al.*, 2003). The putative catalytic site of integral membrane proteins is oriented toward the cytosol (Gibeaut, 2000; Saxena and Brown, 2000). The CesA/Csl enzymes contain 3-6 TMH towards the COOH-terminus and 1-2 TMH towards the NH_2-terminus (Figure 1.3). They share a common DDDQxxRW motif, which is believed to be involved in sugar binding and catalytic activity of the enzyme (Richmond and Somerville, 2001; Bonetta *et al.*, 2002). The CesAs have two putative zinc finger domains, also known as LIM-like or RING-like domains, located at the cytosolic NH_2-terminus of the protein, and these might be involved in protein-protein interactions (Saxena and Brown, 2000; Vergara and Carpita, 2001; Reiter, 2002). The Csl proteins generally lack this domain (Dhugga, 2001). Plant CesA proteins have two specific conserved

(CRP) and highly variable (HVR) insertions that differentiate them from their bacteria homologues (Delmer, 1999; Saxena and Brown, 2000; Doblin *et al.*, 2002). Amino acid sequence homology studies have shown that orthologues of CesA/Csl proteins are more similar to each other than to their paralogues, implying that gene duplications occurred before division into different classes in the plant kingdom (Saxena and Brown, 2000; Doblin *et al.*, 2002; Burton *et al.*, 2004). Analysis of some plant genomes has shown the presence of gene families for both *CesA* (10 in *Arabidopsis*, 12 in rice and maize, and at least eight in barley) and *Csl* genes (eight groups, *CslA-CslH*) (Richmond, 2000; Richmond and Somerville, 2000; Hazen *et al.*, 2002; Burton *et al.*, 2004). Investigation of map locations for *CesA* genes show that they are scattered across the genome in *Arabidopsis* and barley (Saxena and Brown, 2000; Burton *et al.*, 2004). Genes encoding the CesA and Csl families have 10-14 and 3-9 exons, respectively (Saxena and Brown, 2000).

Cellulose synthases are located at the plasma membrane in structures known as rosette terminal complexes, as shown by freeze fracture electron microscopy and antibody labelling (Kimura *et al.*, 1999; Saxena and Brown, 2000; Perrin *et al.*, 2001; Doblin *et al.*, 2002). Isolation of an active cellulose synthase has been difficult to achieve for a number of reasons, including instability of the rosette structure during cell rupture for protein extraction, and the dominant activity of callose synthase in tissue extracts (Feingold *et al.*, 1958; Doblin *et al.*, 2002; Lai-Kee-Him *et al.*, 2002). The only convincing example of significant cellulose synthase activity *in vitro* was demonstrated in microsomal fractions of blackberry cell suspension culture by Lai-Kee-Him *et al.* (2002). Heterologous expression of cotton *CesA1*, having the conserved motif, showed UDP-Glc binding activity but no catalytic activity (Pear *et al.*, 1996).

Although attempts to measure the biochemical activity of CesA proteins *in vitro* have met with little success, the use of reverse genetics *via* mutant analysis and gene silencing has produced information that has allowed functions to be assigned to plant *CesAs*, including their involvement in the biosynthesis of cellulose microfibrils (Pear *et al.*, 1996; Arioli *et al.*, 1998; Burton *et al.*, 2000; Doblin *et al.*, 2002). Complementation of cellulose synthase in *Arabidopsis* mutants suggested that a

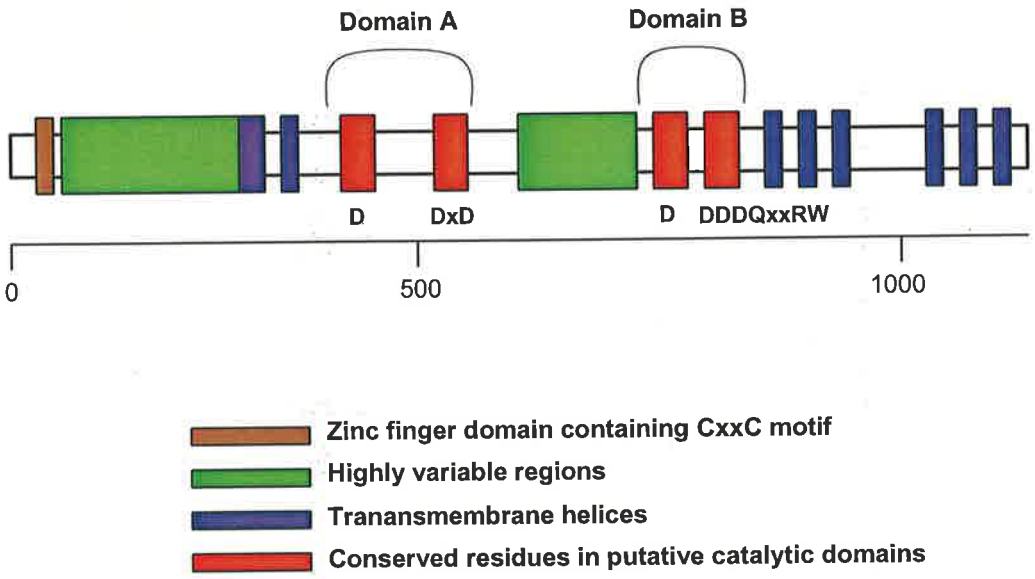

Figure 1.3 Schematic representation of a plant CesA protein. The domains are depicted in different colors. Domains A and B are oriented towards the cytosol (Richmond, 2000).

number of *CesAs* are required to synthesise cellulose, and therefore members of the gene family are not functionally redundant (Taylor *et al.*, 2000; Perrin, 2001). Detailed transcript analysis showed that certain *CesA* genes are co-ordinately regulated, suggesting different functions for each set of genes (Vergara and Carpita, 2001; Doblin *et al.*, 2002; Burton *et al.*, 2004). Mutant and transcript analysis suggested that *CesA* genes form two functional groups, each of which has three different *CesAs*. The encoded proteins might interact as subunits of rosettes (Eckardt, 2003; Burton *et al.*, 2004). Mutant analysis in *Arabidopsis* revealed that group I and group II CesAs are responsible for the biosynthesis of cellulose in primary and secondary cell walls, respectively (Eckardt, 2003).

Searches of expressed sequence tagged (EST) sequences of family GT2 genes revealed the presence of other sequences that are less similar to the *CesA* gene families, and this other group was named cellulose synthase like (Csl) (Richmond and Somerville, 2000). The *Csl* genes that can be divided into eight subfamilies, designated *CslA*, *CslB*, *CslC*, *CslC*, *CslD*, *CslE*, *CslF*, *CslG* and *CslH*, each of which contains multiple genes (Hazen *et al.*, 2002; Goubet *et al.*, 2003). Another subfamily, designated *CslJ*, has also identified in certain cereals (RA Burton, AJ Harvey, NJ Shirley and GB Fincher, unpublished data). In *Arabidopsis* there are 29 known Csl genes and in rice about 37 (Hazen *et al.*, 2002; Somerville *et al.*, 2004). The Csl enzymes might be involved in backbone synthesis of polysaccharides having (1→4)-β-linkages (Perrin *et al.*, 2001; Vergara and Carpita, 2001; Goubet *et al.*, 2003). Although little is known about Csl function, some information has been obtained from mutant analysis using T-DNA insertion and transposon tagged lines (Doblin *et al.*, 2001; Favery *et al.*, 2001; Wang *et al.*, 2001; Goubet *et al.*, 2003). Goubet *et al.* (2003) demonstrated the involvement of AtCslA7 in synthesis of a polysaccharide important in pollen tube growth and embryogenesis *via* analysis of its transposon mutant line. It has been shown that a CslA gene from guar (*Cyamopsis tetragonoloba*),encodes a (1→4)-β-mannan synthase (Dhugga *et al.*, 2004). This result was quickly confirmed by Liepman (2005), who expressed *Arabidopsis CslA* genes heterologously in Drosophila S2 cells. The recombinant CslA proteins produced (1→4)-β-D-mannans or (1→4)-β-D-glucomannans when incubated *in vitro* with GDP-mannose and GDP-glucose (Liepman *et al.*, 2005).

In summary, type I integral membrane proteins that are involved in cell wall biosynthesis are enzymes with several transmembrane helices and have been classified in family GT2. These enzymes are likely to be involved in iterative biosynthesis of the backbone of wall polysaccharides. The *CesA* genes are clearly involved in the synthesis of cellulose (Pear *et al.*, 1996; Burton *et al.*, 2004). *In vitro* synthesis of cellulose has shown that complexes of enzymes containing some of the CesA proteins are required for cellulose polymerisation and microfibril assembly (Lai-Kee-Him *et al.*, 2002). Based on transcript analysis of *CesA* genes and mutant analysis, a model has been proposed for the biosynthesis of cellulose in plants (Doblin *et al.*, 2002; Tanaka *et al.*, 2003; Taylor *et al.*, 2003; Burton *et al.*, 2004). In this model two complexes of CesA proteins each containing three proteins, work together to synthesise primary and secondary wall cellulose. In contrast, the *Csl* genes appear to encode enzymes involved in synthesising the backbones of non-cellulosic wall polysaccharides (Dhugga *et al.*, 2004).

1.2.2.2 Type II membrane GTs

Type II GTs are believed to be largely bound to Golgi membranes (Roth, 1991; Rabouille *et al.*, 1995). They have a single TMH with at least twenty amino acids, which spans the membrane and functions as an anchor, together with a short cytosolic NH_2-terminus, an extended luminal hydrophilic stem region and a globular catalytic domain within the lumen of the Golgi, towards the COOH-terminus of the protein (Kleene and Berger, 1993; Breton and Imberty, 1999; Gibeaut, 2000; Keegstra and Raikhel, 2001; Perrin *et al.*, 2001; Sterling *et al.*, 2001; Pagny *et al.*, 2003). The relative ease with which this group of GTs can be dissociated in an active form from membranes with mild detergents has enabled some progress on their characterisation through classical biochemical routes (Edwards *et al.*, 1999). In Figure 1.4 the predicted structure of both type I and Type II GTs are been shown. Deletion studies have shown that removal of amino acids from the COOH-terminus leads to malfunction of the enzyme (Xu *et al.*, 1996; Pagny *et al.*, 2003). Confocal and electron microscopy of a series of NH_2-terminally truncated, GFP-tagged AtXylT

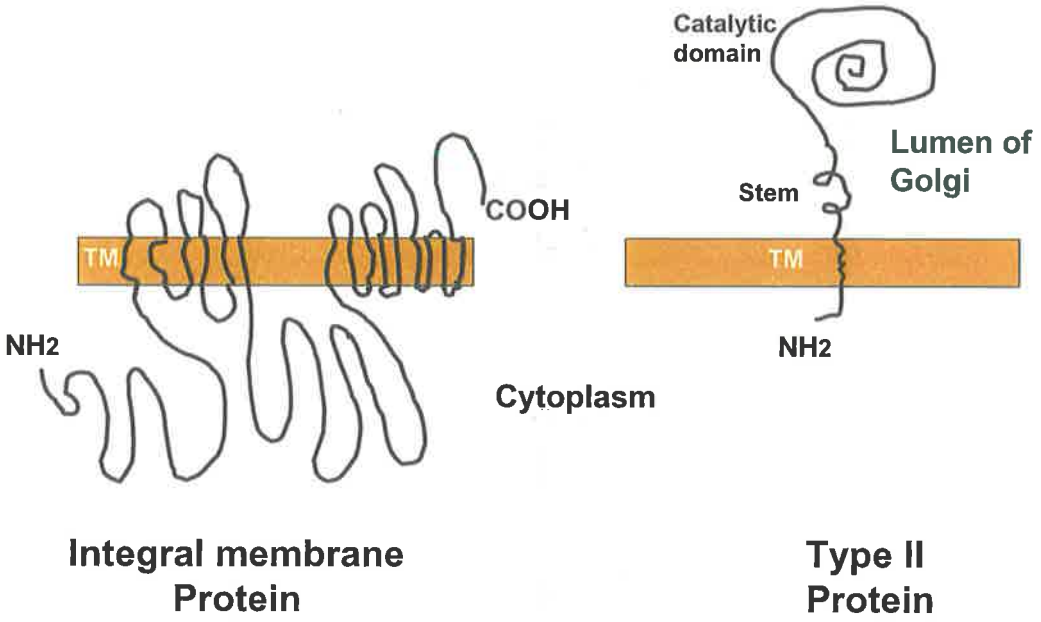

Figure 1.4 Comparison between type I and type II glycosyltransferases. Type I GTs have several transmembrane helices (TMH), compared with one in type II enzymes. The Type II GTs usually reside on the Golgi membrane with the catalytic domain oriented towards the lumen of Golgi and a short NH_2-terminal sequence in the cytosol. In contrast, the catalytic domain(s) of type I GTs seem to be located in the cytosol. In general, Type I GTs are comparatively larger in size.

proteins in tobacco cells revealed that the TMH and the cytosolic NH_2-terminal sequence are necessary to locate the enzyme in the medial Golgi cisternae. In addition, mutant analysis showed that the stem region and more specifically the proline-rich region of the stem near the catalytic site is essential for enzyme activity (Pagny *et al.*, 2003).

Whether the TMH is necessary for function when the enzyme is expressed heterologously is not clear. In some expressed GTs, activity is obtained only when the TMH has been removed (Edwards *et al.*, 1999). However, in other cases the TMH plays a crucial role (Faik *et al.*, 2002). It seems that the strategy of choice to express GTs and to investigate enzyme activity would be the expression of both full length and truncated versions of the gene. In attempts to assign a function to *Arabidopsis* gene family members of GT34 (eight GTs) and GT37 (ten GTs), only one from each family showed activity following heterologous expression of the genes (Perrin *et al.*, 1999; Faik *et al.*, 2002). The identification of the exogenous acceptors for measuring enzyme activity is one of the problems in biochemical assays (Edwards *et al.*, 1999). Given that only a limited number of the glycosyltransferases have been characterised, these will be discussed individually in the sections below.

Galacturonosyltransferase (GT8)

Two allelic mutants (*qua1-1* and *qua1-2*) of *Arabidopsis* showed a dwarfed and weak cell adhesion phenotype (Bouton *et al.*, 2002). Analysis of wall composition showed a 25% reduction in galacturonic acid (GalA) content. The reduction in GalA, but not in neutral sugars, was similar to a related mutant (*Quasimodo1*) of pectin biosynthesis, and the reduction of HGA in mutant compared to the wild type was further confirmed with the HGA-specific antibodies JIM5 and JIM7. The *QUA1* gene is a putative α-D-galacturonosyltransferase, but its protein product has not been characterised biochemically (Bouton *et al.*, 2002).

Galactosyltransferase (GT34)

Edwards *et al.* (1999) purified and partially sequenced a 51 kDa putative galactomannan (1→6)-α-D-galactosyltransferase (GMGT) protein from fenugreek (*Trigonella foenum-graecum*). The peptide sequence was used to isolate a cDNA

clone from developing endosperm. A truncated cDNA clone (*GMGT*) lacking the TMH was expressed in yeast (*Pichia pastoris*) and the expressed protein showed galactomannan galactosyltransferase activity (Edwards *et al.*, 1999). Overexpression of *GMGT* in tobacco resulted in an increase in galactosylation of the mannan backbone by 25% from the T1 to the T2 generation (Reid *et al.*, 2003). Following the isolation of *GMGT* from fenugreek, an orthologue of this gene was isolated from *Lotus japonicum* (Edwards *et al.*, 2004). Post transcriptional gene silencing of *GMGT* showed an increase in Man/Gal ratio from 1.2 to 6, suggesting down-regulation of the galactosyltransferase activity in developing *L. japonicum* endosperm (Edwards *et al.*, 2004).

Xylosyltransferase (GT34)

Faik *et al.* (2002) used the fenugreek galactosyltransferase (GalT) peptide sequence to find the orthologous gene in *Arabidopsis*. Database searches revealed eight genes with significant sequence similarity to the fenugreek gene (Keegstra and Raikhel, 2001). The cDNAs of all eight *Arabidopsis* genes were isolated and expressed in *Pichia* to investigate the biochemical activity of the gene products (Faik *et al.*, 2002). One of the putative genes showed α-D-xylosyltransferase (*XylT*) activity on cello-oligosaccharides. The truncated version of *AtXylT*, unlike the fenugreek *GalT*, was not active following the heterologous expression (Faik *et al.*, 2002). In the same study a pea homologue was isolated from detergent-washed microsomes and showed α-xylosyltransferase activity. The *PsXylT* catalysed the transfer of xylose from UDP-xylose onto cello-oligosaccharides bigger than DP5, unlike *AtXylT* which also used cellotetraose as its acceptor (Faik *et al.*, 2002).

Fucosyltransferase (GT37)

A fucosyltransferase (FUT) enzyme was originally purified from pea epicotyls and partial amino acid sequences of the active 63 kDa protein were generated (Perrin *et al.*, 1999). The pea fucosyltransferase was isolated from pea microsomes, solubilised with detergent and purified on a GDP-hexanolamine-agarose followed by gel filtration (Faik *et al.*, 2000). The peptide sequences from the purified enzyme were used to design degenerate primers for PCR amplification of a partial cDNA sequence,

and the 5′- and 3′- ends of the transcript were subsequently identified using 5′- and 3′- RACE. The cDNA has been cloned and named *PsFUT1*. Biochemical characterisation was carried out using the native protein, which showed that the active form is an oligomer with a higher molecular weight (~250 kDa) than predicted from the cDNA. PsFUT1 catalyses the last step of pea cell wall xyloglucan synthesis by transferring fucose from GDP-fucose to either XXFG or XLFG (Figure 1.2) through a (1→2)-α linkage.

The peptide sequence of the pea enzyme was subsequently used to isolate an *Arabidopsis* orthologue (*AtFUT1*), which was later cloned and characterised by expression in mammalian COS cells (Perrin *et al.*, 1999). *AtFUT1* has little sequence similarity with known mammalian fucosyltransferases (*FUT*), and it is grouped in a separate family, GT37 (Keegstra and Raikhel, 2001). *PsFUT1* cDNA has 62.3% identity with *AtFUT1* and the enzymes share common short sequence motifs (Perrin *et al.*, 1999; Faik *et al.*, 2000; Keegstra and Raikhel, 2001). It has been shown that *mur2*, a deletion mutant of *AtFUT1* on chromosome 2 of *Arabidopsis*, decreases xyloglucan fucosylation by 98% (Reiter *et al.*, 1997; Keegstra and Raikhel, 2001; Vanzin *et al.*, 2002).

Glucuronosyltransferase (GT47)

A *Nicotiana plumbaginifolia* T-DNA insertion mutant, *nolac-H18* (non-organogenic callus with loosely attached cells), was isolated by Iwai *et al.* (2002). The gene was named *NpGUT1* (glucuronosyltransferase1) because of its sequence similarities with animal orthologues (Iwai *et al.*, 2002). Overexpression of *NpGUT1* in mutant lines complemented the mutant phenotype. Gene silencing of *NpGUT1* in normal *N. tabacum* resulted in the formation of crumbled shoots (Iwai *et al.*, 2002). Cell wall compositional analysis of normal and *nolac-H18* calli supported a β-D-glucuronosyltransferase function for *NpGUT1*. *NpGUT1* is believed to be involved in transferring glucuronic acid (GlcA) to type II rhamnogalacturonan in pectin. Iwai *et al.* (2002) also showed that the lack of GlcA in the mutants, and ultimately in pectin RG II, affects the formation of borate cross-links. The enzyme has a long amino acid signature that is similar to its orthologues in plants and animals (Iwai *et al.*, 2002), which suggests it is related evolutionally across the kingdoms.

Galactosyltransferase (GT47)

In a similar approach, the gene responsible for the *Arabidopsis* mutant (*mur3*) was positionally cloned and isolated (Madson *et al.*, 2003). Cell wall analyses of *mur3* plants showed a 50% reduction in fucose content in XG (Reiter *et al.*, 1997). Detailed studies on *mur3* cell walls revealed that a galactosyl residue is missing from a specific xylosyl residue of xyloglucan (Figure 1.2), which ultimately means there would be no fucose in this structure. Further to the loss of the galactosyl residue, the addition of a galactosyl residue to another xylosyl residue is increased (Madson *et al.*, 2003). The lack of the galactosyl residue suggested that *mur3* encodes a xyloglucan β-D-galactosyltransferase. The *mur3* gene was identified to be in a region of 290 kbp on the *Arabidopsis* genome and a hydropathy plot was used to search for a protein with single TMH at its NH_2-termnius of all the coding regions located in the region. The search resulted in the identification of a single candidate gene encoding a 619 amino acid protein with a predicted TMH located at amino acids 32 to 54. Later in the study the isolated cDNA clone was heterologously expressed in *Pichia* to confirm galactosyltransferase (GalT) activity. Extracts from yeast expressing the GalT enzyme showed an approximate 25-fold increase in the incorporation of radiolabelled galactosyl residues into ethanol-insoluble acceptor molecule, compared with a negative control yeast bearing an empty plasmid vector. The result was further verified by enzymatic digestion of the radioactively labelled xyloglucan product with endo-(1→4)-β-D-glucanase, followed by separation of digested materials by HPAEC (Madson *et al.*, 2003). The enzyme is believed to transfer a galactosyl residue to a specific xylosyl residue, suggesting narrow substrate specificity. Etiolated *mur3* hypocotyls were examined for rigidity by measuring tensile parameters, and showed mechanically weakened walls as a result of the missing fucogalactosyl residues (Ryden *et al.*, 2003). Further studies on tensile strength showed galactosylation of the side chains of xyloglucan is more important than fucosylation for the maintenance of wall strength (Pena *et al.*, 2004). Li *et al.* (2004) analysed 10 coding regions homologous to *mur3* in *Arabidopsis*. They found two T-DNA insertion lines, *AtGT13* and *AtGT18*, in which Gal contents in leaf walls were lowered by 10.3% and 13.5%, respectively, suggesting that these two genes also encode wall-related galactosyltransferases (Li *et al.*, 2004).

Family	Examples	Type of Linkage	Reference
GT8	Pectic polysaccharide galacturonosyltransferase	α-D-GalAT	(Bouton *et al.*, 2002)
GT34	Galactomannan galactosyltransferase	(1→6)-α-D-GalT	(Edwards *et al.*, 1999; Edwards *et al.*, 2004)
	Xyloglucan xylosyltransferase	(1→6)-α-D-XylT	(Faik *et al.*, 2002)
GT37	Xyloglucan fucosyltransferase	(1-2)-α-L-FuT	(Perrin *et al.*, 1999; Faik *et al.*, 2000)
GT47	Xyloglucan galactosyltransferase	(1→2)-β-D-GalT	(Madson *et al.*, 2003; Li *et al.*, 2004)
	RG II glucuronosyltransferase	(1→4)-β-D-GlcAT	(Iwai *et al.*, 2002)

Table 1.3 Characterised type II cell wall biosynthetic glycosyltransferases, their family and the type of linkage that they catalyse.

1.3 IDENTIFICATION AND FUNCTIONAL ANALYSIS OF CANDIDATE GENES FOR TYPE II GTS IN BARLEY (*HORDEUM VULGARE* L.)

As discussed earlier, plant cell walls are a complex of macromolecules with polysaccharides as major components. Each polysaccharide is composed of one or more types of sugar residues that are chemically linked by particular glycosidic linkages. Hundreds of wall glycosyltransferases may be required to build the wide array of wall polysaccharides (Scheible and Pauly, 2004). For example, the biosynthesis of pectic polysaccharides requires at least 46 GTs (Willats *et al.*, 2001).

Despite the fact that much is known about the composition and structure of the plant cell wall, only a handful of biosynthetic *GT* genes have been characterised (Turner *et al.*, 1998; Edwards *et al.*, 1999; Perrin *et al.*, 1999; Kuroyama and Tsumuraya, 2001; Peugnet *et al.*, 2001; Li *et al.*, 2003; Nunan and Scheller, 2003; Dhugga *et al.*, 2004). As discussed above, inherent biochemical difficulties in isolation and purification of these enzymes, coupled with the complexity of the relevant enzymatic assays, are contributing causes to the slow progress in isolating the related genes. In biochemical approaches, the relative abundance of a certain polysaccharide in a particular species is important, for example galactomannan is relatively abundant in the endosperm of legumes (Edwards *et al.*, 1999; Reid *et al.*, 2003) and xyloglucan is the main matrix phase polysaccharide in dicot walls (Perrin *et al.*, 1999; Faik *et al.*, 2000; Faik *et al.*, 2002; Madson *et al.*, 2003). Knowing that a certain tissue contains an abundant polysaccharide assists in unravelling the likely functions of the GTs *via* biochemical assays and correlating enzyme activity with the abundant polysaccharide. The isolation of wall biosynthetic enzymes begins with laborious biochemical protein purification steps, such as microsomal membrane preparation and fractionation *via* sucrose density gradient centrifugation, fraction concentration and detection of enzymes using SDS-PAGE, Western analysis and activity measurement. The isolated peptide is subjected to peptide sequencing, and sequences can be used to isolate the gene sequence or cDNA clone (Perrin *et al.*, 2001).

The completed genome sequences of *Arabidopsis* (*Arabidopsis* Genome Initiative, 2000) and rice (Goff *et al.*, 2002; Yu *et al.*, 2002), extensive EST databases, detailed genetic map of cereals, expanding QTL data and well-characterised mutant libraries have now opened up several genetic approaches for the isolation and characterisation of GT genes from barley. The development of bioinformatics tools has been of great assistance in gene discovery, and in identifying protein structure and function. Another approach to identifying candidate genes is transcript profiling in particular tissues and correlation of transcript abundance with cell wall composition.

When the candidate gene(s) has been identified, functional analysis can be carried out in several ways, including direct expression in heterologous systems and measurement of enzyme activity, and/for gain-of-function and loss-of-function assays. Isolated cDNAs can be cloned in plasmid vectors under the control of a strong promoter and used in transformation of host organisms to produce milligrams amount of protein. The heterologously expressed protein can be purified *via* affinity techniques and used in biochemical assays. In gain-of-function assays, the candidate gene is either expressed in an organism lacking similar enzyme activity, for example expression of (1→3,1→4)-β-D-glucan synthase in a host organism such as *Arabidopsis* or yeast where no synthesis of (1→3,1→4)-β-D-glucan normally occurs, or overexpressed in the plant to demonstrate extra enzyme activity. In the wall biosynthesis context, the latter approach would lead to increasing relative abundance of a certain sugar or polysaccharide, which can be determined by cell wall compositional analysis (Dhugga *et al.*, 2004). In loss-of-function assays, the candidate gene is silenced, either *via* mutation or post-transcriptional gene silencing techniques. In the context of wall biosynthesis, one expects to see phenotypic changes in walls such as wall weakening or compositional change(s), after the gene has been inactivated. Use of the previously mentioned methods reveals the function of the gene directly or indirectly. In the following sections the bioinformatic tools, which are necessary in the initial stages of gene isolation and later in the classification of the isolated genes are discussed, together with available procedures for the functional analysis of candidate genes, with examples related to the cell wall biosynthesis.

1.3.1 Bioinformatic tools

Relatively time-consuming, low throughput procedures of gene cloning involve a forward genetic approach from protein purification, peptide sequence analysis and the screening of gene or cDNA libraries using probes based on the amino acid sequences. Another option is the analysis of available sequences from a range of organisms through homology, motif and structure searches within and among genomes (Perrin *et al.*, 2001). This is known as comparative genome analysis, and might reveal the homologue of a gene or a protein of interest. A variety of gene isolation methods that follow this principle has been described in the literature, such as phage and BAC library screening (Grunstein and Hogness, 1975; Benton and Davis, 1977) and/or PCR based techniques (Frohman *et al.*, 1988; Siebert *et al.*, 1995).

Homology searching can be carried out in several ways, including pairwise/multiple sequence alignments, phylogenetic classification and sequence search methods. However, sequence similarity does not always indicate a biological relationship (homology) or conservation of gene function (Xu *et al.*, 2000). To execute pairwise/multiple sequence alignments, a variety of matrices and algorithms have been developed based on mutation/insertion rates and gaps found in databases. The most widely used pairwise sequence alignment tool is BLAST (The Basic Local Alignment Search Tool). Although a BLAST search is comparatively fast and provides an expectation value for an alignment, it may be less sensitive compared with other tools, such as those that are highly sensitive in detection of short sequences (Altschul *et al.*, 1997; Xu *et al.*, 2000). Multiple sequence alignment is the basis for classification, phylogenetic construction, motif detection and identification of functionally important regions. The most popular programmes for multiple sequence alignments are CLUSTAL (Thompson *et al.*, 1994; Chenna *et al.*, 2003) and PILEUP (Needleman and Wunsch, 1970), which align sequences in a progressive manner (Feng and Doolittle, 1987). Progressive alignment starts with pairwise alignment to find similar scores and continues to align all the sequences together (Xu *et al.*, 2000).

Based on multiple sequence alignment, glycosyltransferases have been classified into more than 70 families (Campbell *et al.*, 1997). The search tool Pfam (Bateman *et al.*, 1999) has been used to build multiple sequence alignments of glycosyltransferase families using a profile called the Hidden Markov Model (HMM). HMM searches for remotely homologous sequences within databases on the basis of multiple sequence alignment (Eddy, 1996; Xu *et al.*, 2000). The HMM method has been used to classify 47 GT families into four super-families, namely GTS-A, -B, -C, and -D (Kikuchi *et al.*, 2003). Identification of super-families helps to unravel the evolutionary relationships between prokaryotes and eukaryotes, to reveal the different steps of the protein glycosylation pathway, to predict the locations of particular enzymes belonging to a particular superfamily in a cellular organelle, and finally to find functionally important motifs (Kikuchi *et al.*, 2003).

Phylogenetic classification is another representation of multiple sequence alignment. Instead of looking at the sequences and their similarities in terms of the presence or absence of a particular amino acid or base sequence, a tree-shape structure represents the same criteria as genetic distances (Xu *et al.*, 2000). Phylogenetic classification is a useful method to demonstrate the differences between gene families within or between species. Richmond and Somerwhille (2001) established a web site (http://cellwall.stanford.edu/) to illustrate the relatedness of *CesA*, *CSL* and *GSL* genes (Perrin *et al.*, 2001). Multiple sequence alignment is also useful to find short conserved sequences. Amino acid sequence motifs are usually important with respect to their involvement in protein function and can be used to find other functionally related proteins (Perrin *et al.*, 2001). Motif searches in wall GTs showed the presence of different and specific motifs for each family, as discussed earlier.

In addition to phylogenetic classifications and multiple sequence alignments, there are other ways to demonstrate relatedness of protein sequences, through similarities in secondary and three dimensional structures (Gibeaut, 2000). Here, the focus is on techniques that consider the secondary structure, since no crystal structure of plant cell wall related GTs has been solved so far. Hydrophobic cluster analysis (HCA) (Geremia *et al.*, 1996; Callebaut *et al.*, 1997; Breton *et al.*, 1998; Gibeaut, 2000) and topology illustrations of proteins to predict TMH(s) (Gibeaut, 2000) are among the

frequently used techniques to explain secondary structures of GTs. HCA is a helical representation of amino acid sequence that has been used to find motifs and their location, and to identify α-helices and β-strands in the structure of a given protein (Callebaut *et al.*, 1997). In studies of GTs, HCA profiles (using the drawHCA site: http://www.lmcp.jussieu.fr/~soyer/www-hca/hca-seq.html) from various members of a family have been compared to find particular motifs (Breton *et al.*, 1998; Gibeaut, 2000). Hydropathy scales, designated for amino acids, have also been used in the prediction of the number and location of TMHs, and thus topology (Xu *et al.*, 2000). There are specialised tools to predict the topology of a protein and among them TMHMM (http://www.cbs.dtu.dk/services/TMHMM/) (Sonnhammer *et al.*, 1998), which locates TMH(s) on the basis of the hidden Markov model, is popular (Gibeaut, 2000). Thus, HCA and TMHMM are invaluable tools for finding important motifs and distinguishing type I and II glycosyltransferases (Gibeaut, 2000).

The bioinformatics tools mentioned above are being used routinely by molecular biologists or protein chemists to find candidate genes and study their structure, to unravel the structure of the encoded proteins and to predict functions. In the next section other functional genomics techniques that are necessary for gene discovery and assignment of a specific function to an isolated gene are discussed.

1.3.2 Transcript analysis

Understanding the temporal and spatial expression patterns of genes in order to correlate these patterns with developmental stages of cells and/or tissues provides an important basis for functional analysis of unknown genes (Ruan *et al.*, 1998). For example, during coleoptile growth, elongation and senescence, considerable quantities of polysaccharides are deposited in the cell wall (Inouhe *et al.*, 1997). Transcript analysis can monitor the up-regulation of genes during this period to predict and correlate the abundant transcripts with the polysaccharide composition of the wall. It should be noted that transcript levels are not always representative of protein levels or enzyme activity (Donson *et al.*, 2002; Holtorf *et al.*, 2002), because post-translational modifications are often a requirement for activity (Gygi *et al.*, 1999; Dhugga *et al.*,

2004). Nevertheless, a great deal of attention has been focused on developing novel techniques to estimate transcript levels in whole plants, tissues and cells (Figure 1.5). These methods started with techniques that analysed one gene at a time, such as Northern analysis and *in situ* hybridisation (Donson *et al.*, 2002). The necessity to understand the whole picture of different steps of gene regulation, and to do parallel expression analysis of large number of genes, shifted attention towards the establishment of high throughput systems such as analysis of expressed sequence tagged (EST) sequence databases, massively parallel signature sequencing (MPSS), cDNA-amplified fragment length polymorphism (cDNA-AFLP), cDNA and oligonucleotide arrays and *in-silico* analysis of microarrays (Figure 1.5).

In the context of wall biosynthesis, the study of co-ordinately expressed genes appears to be crucial in gene discovery. Table 1.4 lists useful websites for plant transcript analysis. For example, by looking at the transcriptome of a tissue we may find an unknown glycosyltransferase gene and a candidate xylan synthase gene with similar expression patterns. If the two transcripts increase at the same time as the content of arabinoxylan is increased in a particular tissue this would identify the GT as a candidate for an arabinosyltransferase involved in the biosynthesis of arabinoxylans. Pear *et al.* (1996) isolated two *CesA* genes (*CelA1* and *CelA2*) through sequencing a cotton fibre cDNA library, the place where the synthesis of all other cell wall biosynthetic enzymes related to the primary wall cease and secondary wall synthesis begins. In a similar approach aimed at discovering a mannan synthase (ManS), 15,000 ESTs obtained from guar seed 25 days after flowering, the time at which highest levels of mannan synthase activity are detected, were searched for any *CesA* or *Csl* gene homologues (Dhugga *et al.*, 2004). The search located 15 ESTs matching the query, from which 10 overlapping ESTs were used to assemble a full-length cDNA similar to the CslA family. The ManS activity was detected through overexpression of the isolated cDNA in embryogenic soybean suspension-culture cells, which do not normally express any ManS (Dhugga *et al.*, 2004).

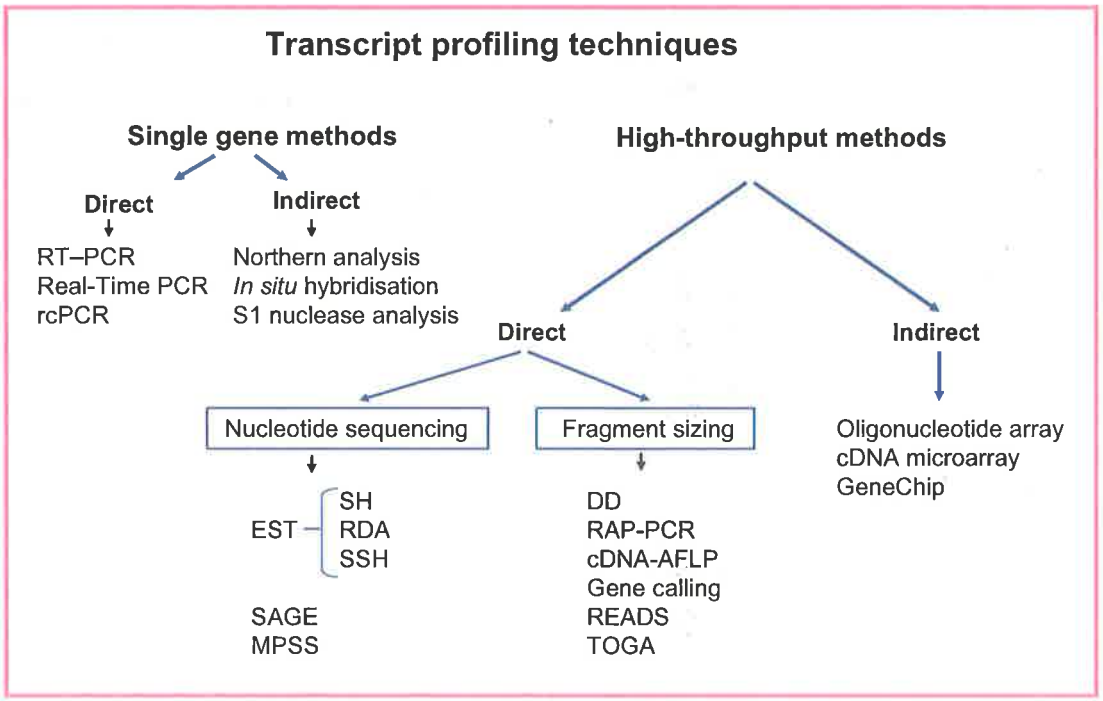

Figure 1.5 Transcript profiling techniques (single gene and high-throughput methods). Single gene transcript analysis techniques are sensitive but time consuming. Real-Time PCR provides relatively accurate estimates of mRNA levels. In contrast, high-throughput methods evaluate large numbers of genes at one time, with low sensitivity. These techniques are relatively expensive and require complicated laboratory facilities, including laboratory information management system (LIMS), automation, data management and mining systems, and optimised normalisation systems. Transcript levels can be analysed either directly *via* nucleotide sequencing or fragment sizing or indirectly through nucleic acid hybridisation of mRNA or cDNA fragments (Donson *et al.*, 2002). RT-PCR = reverse transcriptase polymerase chain reaction, EST = expressed sequence tag, SH = subtractive hybridisation (Sargent, 1987), RDA = representational difference analysis (Hubank and Schatz, 1994), SSH = subtractive subtraction hybridisation (Diatchenko *et al.*, 1996), SAGE = serial analysis of gene expression (Velculescu *et al.*, 1995), MPSS = massively parallel signature sequencing (Brenner *et al.*, 2000), rcPCR = real competitive PCR (Ding and Cantor, 2003), DD = differential display (Liang and Pardee, 1992), RAP-PCR = RNA arbitrarily primed PCR (Welsh *et al.*, 1992), cDNA AFLP = cDNA-amplified fragment length polymorphism (Vos *et al.*, 1995), Gene calling (Shimkets *et al.*, 1999), READS = restriction enzyme-digested cDNAs (Prashar and Weissman, 1996), TOGA = total gene expression analysis (Sutcliffe *et al.*, 2000), GeneChip (Lipshutz *et al.*, 1999).

Resource	Website
Grain Genes	http://wheat.pw.usda.gov/index.shtml
Rice Genome Project	http://rgp.dna.affrc.go.jp/
The *Arabidopsis* Information Resource (TAIR)	http://www.arabidopsis.org
Rice transcriptional database	http://microarray.rice.dna.affrc.go.jp
Affymetrix	http://www.affymetrix.com/products/arabidopsis
TIGR	http://tigrblast.tigr.org/tgi/
Triticeae database	http://wheat.pw.usda.gov/ggpages/ITMI/
HarvEST	http://harvest.ucr.edu
Maize genetics and genome database	http://www.maizegdb.org/
EBI: The ArrayExpress database	http://www.ebi.ac.uk/arrayexpress/
TIGR Arabidopsis arrays	http://atarrays.tigr.org
GARNet	http://www.york.ac.uk/res/garnet/may.htm
Project 2010	http://www.arabidopsis.org/info/2010_projects/comp_proj/AFGC/RevisedAFGC/site2L.htm

Table 1.4 Websites relevant to plant transcript analysis

The above achievements were accomplished where a single type of polysaccharide was the dominant component of the wall. However in situations where many polysaccharides are present, gene discovery remains a challenge and techniques other than transcript analysis need to be considered.

1.3.3 Heterologous expression

As mentioned earlier, the purification of native GTs *via* biochemical means is a laborious procedure, particularly for membrane-bound proteins. In addition, the quantity of purified protein is not always enough to allow extensive functional analysis. Recombinant DNA techniques through which the gene of interest is cloned into a specialised vector for protein expression in heterologous systems are becoming popular to investigate unknown gene function. The isolated gene or cDNA, either full or partial length, is cloned in a plasmid vector for protein expression and purification. An expression plasmid vector usually has a strong inducible promoter to enhance protein expression. Once the protein is expressed heterologously in a certain system, it has to be purified, usually *via* an affinity tag. The most commonly used tag is a stretch of six histidine (6 His-) residues, which has a strong affinity towards either a nickel or a cobalt resin (Hochuli *et al.*, 1987). The expressed protein can be purified from other proteins present in the cell homogenate by affinity chromatography. It is possible to add the tag either at the NH_2- or COOH-terminus of the expressed protein, or to put it at both ends. However, in isolated cases the high background of endogenous protein becomes problematic where the His-tag is hidden and purification of soluble protein becomes difficult.

Although expression in *Escherichia coli* (*E. coli*) has the benefit of being fast and simple, bacterial systems lack the eukaryotic post-translational machinery (Bencurova *et al.*, 2003). In most cases, post translational modifications are necessary to produce a soluble and active eukaryotic protein. For example, Pagny *et al.* (2003) demonstrated the importance of N-glycosylation of GTs, both through a series of *Arabidopsis* (1→2)-β-xylosyltransferase (*XylT*) mutants and the use of tunicamycin, an antibiotic that blocks the first step of the glycoprotein glycosylation reaction. The

results showed that N-glycosylation is necessary to form a properly folded, active and stable protein. This result may provide a clue as to why heterologously expressed eukaryotic proteins in *E. coli* are often inactive.

There are several eukaryotic heterologous expression systems, including insect, yeast, various mammalian cells and other eukaryotic cells. These systems might be expected to effect post-translational modifications of the type found in higher plants. Insect and mammalian systems usually direct high expression levels of the exogenous protein but require sophisticated laboratory tools (Bencurova *et al.*, 2003). A heterologous expression system in mammalian COS cells led to the production of an active *Arabidopsis* xyloglucan fucosyltransferase (Perrin *et al.*, 1999). Yeast (*Pichia pastoris*) has been used to express soluble and properly folded glycosyltransferase proteins more frequently than the other systems (Bencurova *et al.*, 2003). A fenugreek galactomannan galactosyltransferase (GalT) (Edwards *et al.*, 1999), an *Arabidopsis* xyloglucan xylosyltransferase (Faik *et al.*, 2002), and an *Arabidopsis* galactosyltransferase (Madson *et al.*, 2003) were expressed in *Pichia*, all of which resulted in biochemically active proteins. Thus, if a heterologous expression system that allows the synthesis of an active protein can be identified for the candidate gene, this procedure will provide strong, direct evidence for the function of the gene.

1.3.4 Loss-of-function

Where direct heterologous expression systems are not available, several research groups have used loss-of-function, reverse genetics approaches. Chemically induced mutations (Henikoff and Comai, 2003), insertional mutagenesis and post-transcriptional gene silencing (Waterhouse and Helliwell, 2003) are amongst the commonly used loss-of-function techniques. Insertional mutagenesis can be established either by randomly transferred DNA (T-DNA) (Parinov *et al.*, 1999; Speulman *et al.*, 1999) or by transposon tagging (Krysan *et al.*, 1999; Young *et al.*, 2001). In post-transcriptional gene silencing, the gene of interest can be partly or completely inactivated by targeting its mRNA, through delivery of a double stranded RNA to the target plant cell or tissue, either transiently or through stable integration

(Waterhouse and Helliwell, 2003). Sometimes, degradation of the transcript leads to alteration of phenotype (Burton *et al.*, 2000), which can be a useful way to demonstrate the gene function.

Chemically induced mutants. Chemical mutagens such as ethylmethanesulfonate (EMS) can produce single nucleotide changes in plants through alkylation of guanine molecules, which then pair with T instead of C (Henikoff and Comai, 2003). The base substitution not only creates gene knockouts but also generates an allelic series of a gene, which may provide valuable information about protein function (Henikoff *et al.*, 2004). To screen chemically induced point mutations, high throughput systems have been developed. Targeting Induced Local Lesions IN Genomes (TILLING) allows the detection of allelic mutations by PCR amplification of pooled DNA samples of chemical mutants, followed by denaturing high performance liquid chromatography (DHPLC) to detect mismatches in DNA heteroduplexes (McCallum *et al.*, 2000; Henikoff and Comai, 2003; Till *et al.*, 2003; Henikoff *et al.*, 2004). More recently an alternative type of TILLING was developed, based on enzymatic mismatch cleavage, and this method speeds up the screening procedure (Henikoff *et al.*, 2004). In this new approach amplified PCR products are incubated with *CEL* I (a type of S1 endonuclease), which cleaves the 3' end of the mismatches and generates a loop in heteroduplexes between mutant DNA and wild type, followed by electrophoresis and image analysis of differentially double end-labelled amplicons (Henikoff *et al.*, 2004). TILLING can be utilised effectively in detecting mutants of glycosyltransferases where obvious phenotypes are not found.

Insertional mutagenesis. Insertional mutagenesis is a functional analysis tool to randomly silence genes of interest, but must be followed by screening for mutants involving the candidate gene. Since screening of chemically induced mutants sometimes requires sophisticated tools, transposon tagged and T-DNA insertion lines are easier to use. In these lines a known sequence, usually about 12.8 Kbp in length (http://signal.salk.edu/), is integrated into the genome and inhibits the function of the so-called "tagged" gene. The gene with the insertion can be identified simply by PCR amplification from the known inserted DNA. T-DNA insertion mutants are generated *via Agrobacterium*-mediated transformation. To demonstrate the preference of T-

DNA integration into the genome, a comparison was carried out between rice and *Arabidopsis*. The result showed that T-DNA integration in *Arabidopsis* is rather random compared to rice, where insertions were biased towards functional genes rather than heterochromatins (Barakat *et al.*, 2000). Considering that the cereal genome is mostly (75-90%) composed of gene free sequences (Barakat *et al.*, 1997), the use of T-DNA insertion lines generated by *Agrobacterium* is an efficient way to study gene function in rice (Murray *et al.*, 2004). Examples of the use of T-DNA insertion lines to elucidate the function of wall biosynthetic enzymes were described earlier in this chapter (Bonetta *et al.*, 2002; Bouton *et al.*, 2002; Iwai *et al.*, 2002; Perrin *et al.*, 2003; Li *et al.*, 2004). T-DNA insertions are stable through multiple generations following integration into the genome (Krysan *et al.*, 1999). In contrast, transposon lines may change through jumping from one gene to another, specifically where members of a gene family are arranged in tandem along a chromosome (Krysan *et al.*, 1999). Table 1.5 provides some useful websites for available mutants for candidate genes.

Post-transcriptional gene silencing (PTGS). PTGS can be carried out in a number of ways but the method of choice in plants is double-stranded RNA interference (dsRNAi) (Fire *et al.*, 1998). In this technique a plasmid vector with a strong promoter is used to drive expression of a sense DNA fragment with its reverse fragment (antisense) connected to it by an intron region (Wesley *et al.*, 2001). The plasmid is transformed into the plant to incorporate the dsRNAi construct into the genome, either transiently or stably (Jacobs *et al.*, 2003). The inserted gene is transcribed in the host plant to produce a double stranded RNA (dsRNA). Double stranded RNA activates a surveillance or sequence-specific degradation system which specifically degrades both the dsRNA and plant homologous mRNA (Waterhouse *et al.*, 1998). More details and a pictorial illustration of how the system works are provided in Chapter 6. Although RNAi is a powerful tool in PTGS, there are some limitations in the use of this technology, including efficient DNA delivery and potential side effects (Scherer and Rossi, 2003).

The RNAi plasmid vector is delivered into target plants by particle bombardment or *Agrobacterium*. In particle bombardment, the plasmid is coated on beads of heavy

metals such as gold and tungsten, and using the pressure of an inert gas, usually helium, the coated particles are transferred into the plant tissues. In contrast, in *Agrobacterium*-mediated transformation, the RNAi plasmid is transferred into the bacteria, and plants are subsequently infected with bacteria for transfer of the dsRNAi construct into the plant genome (Leemans *et al.*, 1981). Both techniques have been used successfully in barley (Wan and Lemaux, 1994; Tingay *et al.*, 1997). In general, *Agrobacterium*-mediated transformation delivers several advantages in comparison to microprojectile bombardment (Murray *et al.*, 2004). Defined transgene integration, low transgene copy number, low frequency of insert rearrangement (Murray *et al.*, 2004) and integration into euchromatin (Barakat *et al.*, 2000) are some of the advantages of *Agrobacterium*-mediated transformation. Despite the low frequency of transformation in cereals, *Agrobacterium* will infect cereals and transfer DNA into the host genome, although it is more efficient in some genotypes than others (Tingay *et al.*, 1997; Wang *et al.*, 2001; Murray *et al.*, 2004).

One important consideration for dsRNAi gene silencing is its potential for unwanted side effects. For instance, in a study to silence cellulose synthase genes, Burton *et al.* (2000) demonstrated the compensation of cellulose reduction by increased pectic polysaccharide synthesis. Another factor which needs to be considered is how to silence individual members of a gene family. Many plant genes are members of multi-gene families. Members of the family will share common regions but differ in other variable regions, such as 3' untranslated regions (3'UTR). Therefore, to silence an entire gene family the plasmid vector has to include a conserved region of all genes. To specifically silence an individual gene member, highly variable regions have to be targeted.

In forward genetics, one looks for the gene sequence that effects a mutant phenotype, as opposed to reverse genetics in which the information about the sequence of the gene is available and analysis of the resulting phenotype is important (Krysan *et al.*, 1999). The wealth of sequence information often facilitates the application of reverse

Resource	Website
Gramene	http://www.gramene.org/rice_mutant/Mutant_Search1.html
Gabi-Kat	http://www.mpiz-koeln.mpg.de/GABI-Kat/
GarNet project	http://atidb.cshl.org/
Riken	http://pfgweb.gsc.riken.go.jp/projects/acds.html
Wisconsin knock-out project	http://www.biotech.wisc.edu/Arabidopsis/
Agrikola	http://www.agrikola.org/
Salk Institute	http://signal.salk.edu/cgi-bin/tdnaexpress
Oryzabase	http://www.grs.nig.ac.jp/rice/oryzabase/top/top.jsp
ABRC (transposon lines)	http://www.arabidopsis.org/abrc/catalog/transposon_individ_5.html

Table 1.5 Websites relevant to plant T-DNA insertion, transposons and activation tagged lines.

genetics in comparison with forward genetics, and therefore provides powerful tools to indirectly resolve the function of a gene. These techniques show their strength when there is no biochemical assay available to analyse the function of a candidate gene. Furthermore, some proteins are only active in a complex of proteins and direct functional investigation would not be straightforward. Despite the power of loss-of-function approaches, these techniques suffer from some downsides. As discussed earlier, inactivating a gene that is a member of multi-gene family may not produce a noticeable phenotype, but on the other hand inactivation of all members of the gene family may be lethal (Perrin *et al.*, 2001). For instance, silencing of 86% of the predicted *Caenorhabditis elegans* genes (19,427 genes) resulted in only 10% (1,722 genes) of the mutants showing a phenotype (Kamath *et al.*, 2003).

1.3.5 Gain-of-Function

To resolve possible downsides that stem from the loss-of-function assays, a small number of gain-of-function systems have been developed in plants (Zhang, 2003; Tani *et al.*, 2004). These systems are based on three common methods: complementation of yeast knockout mutant phenotypes, overexpression of a gene in a place or time where is not normally expressed, and activation T-DNA tagging using four tandem repeats of a strong promoter's enhancer elements (Bassham and Raikhel, 2000; Zhang, 2003; Tani *et al.*, 2004).

Yeast mutant complementation studies using plant genes are a useful way of identifying the involvement of proteins in a particular biochemical activity, where the direct functional analysis has proven to be difficult. However, interpretation of results from yeast may not always be valid and might require confirmation in plants, especially when the compartmentalisation of the gene product is necessary to define its specific function (Bassham and Raikhel, 2000).

Overexpression of genes can be a useful tool for functional analysis, either through introducing a gene into different hosts or through complementation of mutant

phenotypes (Iwai *et al.*, 2002; Madson *et al.*, 2003; Perrin *et al.*, 2003). Moreover, complementation of a mutant sometimes generates new phenotypes (Wada *et al.*, 1997) and leads to an understanding of gene function. For example, overexpression of *AtFUT1* in an *Arabidopsis Atfut1* mutant (lacking fucose in xyloglucan) recovered the fucosylation of xyloglucan and also showed a higher amount of O-acetylation of galactosyl residue, suggesting fucosylated xyloglucan is a requirement for the activity of at least one O-acetyltransferase (Perrin *et al.*, 2003).

Activation T-DNA tagging is another form of gain-of-function analysis. Instead of introducing the gene of interest to the plant, expression of the endogenous gene is enhanced following the introduction of a T-DNA containing enhancer elements and strong promoters (Tani *et al.*, 2004). Enhancer activation tagging has been shown to be a successful technique in the functional analysis of genes in both *Arabidopsis* and rice (Weigel *et al.*, 2000; Jeong *et al.*, 2002) and results have proven to be an accurate reflection of natural gene function (Tani *et al.*, 2004). Activation tagging not only enhances the expression of genes, but also sometimes generates mutant lines through insertional mutagenesis by T-DNA integration, which can be useful in functional analysis (Tani *et al.*, 2004). Activation tagging has some disadvantages, including the fact that not all genes are activated (Tani *et al.*, 2004), instability of tag-activated alleles (Weigel *et al.*, 2000; Tani *et al.*, 2004), activation of only a subset of adjacent genes, probably because of promoter preference (Ohtsuki *et al.*, 1998), and tissue specificity of some enhancer sequences (Benfey *et al.*, 1990; Weigel *et al.*, 2000).

1.4 OBJECTIVES

The overall aim of this project was to isolate barley cell wall glycosyltransferase genes on the basis of sequence homology with the homologous sequences available in databases. A key additional objective was to assign functions to the isolated glycosyltransferase genes in terms of donor and acceptor molecule specificity and the linkages which they generate. At the commencement of the project, the only GT sequence available was that of the fenugreek galactomannan galactosyltransferase (Edwards *et al.*, 1999). As the project progressed, other GT sequences were released into the public databases and were linked by functional analysis to other cell wall related GTs (Faik *et al.*, 2002; Iwai *et al.*, 2002). The isolation and characterisation of the isolated cDNA clones are discussed in Chapter 2. Another aim of this project was to undertake detailed transcript analyses of the isolated cDNA clones to address the function of each GT in relation to known alterations in cell wall composition during the developmental stages of a range of tissues. Transcript analyses of isolated genes are presented in Chapter 3. To reveal putative protein-protein interactions, yeast two-hybrid screening was performed, as outlined in Chapter 4. Chapters 5 and 6 address the functional analysis of isolated cDNA clones through heterologously expressed proteins and transiently induced gene silencing. General discussions about the steps undertaken towards functional analysis of barley cell wall-related GTs, and future directions of this research are presented in Chapter 7.

CHAPTER 2 ISOLATION AND CHARACTERISATION OF cDNAs ENCODING BARLEY GLYCOSYLTRANSFERASES

2.1 INTRODUCTION

In this Chapter, experiments are described that led to the isolation of cDNAs encoding barley glycosyltransferases. Although a key target cDNA was that encoding an α-arabinosyltransferase, it was decided initially to isolate a wide range of candidate genes for barley glycosyltransferases. More specifically, three near full-length cDNAs encoding family GT34 glycosyltransferases from barley were isolated; these were designated *HvGlyT1* to *HvGlyT3*. In addition, a partial cDNA encoding another family GT34 glycosyltransferase, designated *HvGlyT5*, was isolated and characterised. Finally, a near full-length cDNA, designated *HvGlyT4*, encoding a family GT47 glycosyltransferase was also isolated. The numbering of the *HvGlyT* genes reflects the order in which they were isolated.

The overall strategy for the isolation of the *HvGlyT1-HvGlyT4* cDNAs was based on searching barley EST databases for cDNA sequences that were similar to the fenugreek (1→6)-α-galactosyltransferase cDNA sequence (Edwards *et al.,* 1999) for *HvGlyT1-HvGlyT3*, and to the *Nicotiana plumbaginifolia* glucuronosyltransferase cDNA described by Iwai *et al.* (2002) for the *HvGlyT4* cDNA. The EST sequences were used to design PCR primers for the amplification of cDNA fragments from RNA preparations, but subsequent screening of cDNA libraries with a *HvGlyT1* probe failed to identify full-length cDNAs. Thus, genomic walking was used to generate full-length sequences for the *HvGlyT1*, *HvGlyT2*, *HvGlyT3* and *HvGlyT4* genes, and near-full length cDNAs were later amplified from RNA preparations by PCR. In the case of the partial *HvGlyT5* cDNA, the gene sequence was detected on the Affymetrix barley DNA microarray chip (Close *et al.,* 2004) and the cDNA was isolated by PCR from RNA preparations. Following the determination of the nucleotide sequences of the *HvGlyT1-5* cDNAs, the sequences were used to investigate the corresponding gene families in barley, through EST database analysis, and the positions of the genes on the barley genome were mapped to the chromosome level using wheat-barley addition lines (Islam *et al.,* 1981). The *HvGlyT5* gene was polymorphic when examined in a number of barley varieties, and could therefore be incorporated into high density genetic maps (Barr *et al.,* 2003; Karakousis *et al.,* 2003). The deduced

amino acid sequences of the proteins encoded by the *HvGlyT* genes were analysed for the presence of sequence similarities with published plant cell wall-related glycosyltransferases, for hydrophobicity and transmembrane helices, for catalytic and substrate binding motifs, and for secondary structural elements.

In later Chapters, experiments are described in which the five cDNAs were used in detailed transcript analyses and in which attempts were made to define the substrate specificities of the encoded enzymes.

2.2 MATERIAL AND METHODS

2.2.1 Materials

Barley bacterial artificial chromosome (BAC) library filters were purchased from the Clemson University Genomic Institute (USA). Polymerase Chain Reaction (PCR) primers were designed using the Netprimer programme available at the following web address (http://www.premierbiosoft.com/netprimer/netprlaunch/netprlaunch.html) and were synthesised by Geneworks (Adelaide, SA, Australia). MicroSpin^{TM}S-200 HR columns, Megaprime DNA labelling system, Sephadex G-50, positively charged nylon transfer membrane (Hybond-N^{+}), CM Sepharose CL-6B and [α-^{32}P]-dCTP were supplied by Amersham Life Sciences (Buckinghamshire, UK). The DNA-free^{TM} kit for removal of DNA from RNA preparations was from Ambion Inc. (Austin, TX, USA). NitroPure nitrocellulose gridded membranes were obtained from Osmonics (Minnetonka, MN, USA). Chromatography 3MM Whatman filter paper was purchased from Whatman International Ltd (Maidstone, Kent, UK). Gene Pulser cuvettes (0.1cm electrode) were from BioRad (CA, USA). Big Dye reagents (versions 2 and 3) were purchased from Applied Biosystems (Foster City, CA, USA). The pGEM-T Easy vector system I kit was provided by Promega (Madison, WI, USA). The Thermoscript II cDNA synthesis kit, 1 Kb Plus DNA Ladder, λ DNA *Hin*dIII Fragments, TRIZOL reagent, Elongase reagents and T4 DNA Ligase were purchased from Invitrogen (Carlsbad, CA, USA). Taq DNA polymerase was purchased from Gibco-BRL (Rockville, MD, USA). X-gal, IPTG, ampicillin, dextran blue, orange G, dimethyl sulfoxide (DMSO), RNase A, ethidium bromide, Ficoll, PVP, PVPP, sarkosyl, glycerol, salmon sperm DNA, DTT, EDTA, HEPES, PIPES, spermidine, bromophenol blue, Tris[hydroxymethyl] amino methane (Tris), dextran sulphate and chloramphenicol were purchased from SIGMA-Aldrich (St Louis, MO, USA). Fuji medical X-ray film was supplied by Fuji Photo Film Co. (Tokyo, Japan). The Nucleospin extraction kit was from Macherey-Nagel (Duren, Germany). Bacto-yeast extract, bacto tryptone, agarose and agar were obtained from Becton Dickinson (Sparks, MD, USA). Restriction enzymes and bovine serum albumin (BSA) were

from New England Biolabs (Beverly, MA, USA). Dextran sulphate was obtained from Progen Industries Limited (Melbourne, Vic, Australia). The dNTPs were from Fisherbiotech (West Perth, WA, Australia). Magnesium chloride, sodium chloride, ethanol, chloroform, dimethylformamide, glucose, isoamyl alcohol, PEG_{8000}, sodium acetate, sodium citrate, glycerol, potassium acetate and SDS were from Merck Pty Ltd (Kilsyth, VIC, Australia). Magnesium acetate and xylene cyanol were bought from Ajax Chemicals (Auburn, NSW, Australia). Klenow DNA polymerase I was purchased from Roche Applied Science (Castle Hill, NSW, Australia). Glycogen (molecular biology grade) was obtained from Boehringer Mannheim (Mannheim, Germany). Phenol (special grade) was from Novachem Pty Ltd (South Yarra, VIC, Australia). The serum gel (silica matrix) tubes were from Sarstedt (SA, Australia). All PCRs were performed in a PTC-100 Peltier Thermal Cycler (MJ Research), which was purchased from GeneWorks (Adelaide, SA, Australia).

2.2.2 Total RNA isolation and cDNA synthesis

Barley grain (50 g of cv. Sloop) was imbibed in 1 litre of aerated water for 24 h at 20°C. Imbibed grains were sown on moist vermiculite and covered with extra vermiculite. The seedlings were grown under a 25/18°C day/night regime with a 12-13 h day. Barley tissue (50-100 mg) was hand-ground with a plastic pestle in an Eppendorf tube containing 500 µl TRIZOL and another 500 µl TRIZOL was added to bring the total volume up to 1 ml. The homogenate was allowed to stand at room temperature for 5 min. Chloroform (200 µl) was added and the mixture hand shaken vigorously for 15 sec, followed by incubation at room temperature for another 3 min. The solution was centrifuged at 4°C at 12,000 ×g for 15 min to separate the phases. After phase separation, the upper aqueous phase containing total RNA was removed carefully to avoid any contamination with interface material and transferred into a clean 1.5 ml Eppendorf tube. Isopropanol (500 µl) was added and, after incubation for 10 min at room temperature, total RNA was precipitated at 4°C at 12,000 ×g for 10 min. The supernatant was removed with care and the pellet washed with 75% (v/v) ethanol (1 ml) at 4°C and recovered by centrifugation at 7,500 ×g for 5 min. The pellet was air-dried for approx. 5 min after removing all the supernatant and

resuspended in 30 µl sterile water. The RNA extract was subjected to DNase I treatment using the DNA-free™ kit to remove any contaminating DNA. DNase I buffer (10 ×, 3 µl) and DNase I (2 units, 1 µl) were added to the RNA extract and the reaction allowed to stand at 37°C for 30 min. DNase Inactivation Reagent (5 µl) was added and mixed thoroughly. The mixture was incubated for 2 min with mixing at 1 min intervals. The slurry was pelleted at 10,000 ×g and the clean aqueous layer, containing the total RNA, transferred to a clean tube. The quality of the RNA was confirmed by agarose gel electrophoresis at 100 V on 1% or 1.6% (w/v) agarose gels in 1 × TAE buffer (40 mM Tris-acetate buffer, pH 8.0, containing 1 mM EDTA) containing 0.1 µg/ml ethidium bromide. The bands of ribosomal RNA (28S and 18S), transfer RNA and the faint background smear of messenger RNA were observed under ultraviolet light. The quantity of RNA was measured at 260 nm and the ratio of 260 to 280 nm was used as an indication of RNA quality.

First strand cDNA was synthesised from RNA extracted from a range of barley tissues using the Thermoscript II RT-PCR kit according to the manufacturer's instructions. Total RNA (2 µg), 50 mM oligo-(dT) primer (1 µl) and 10 mM dNTP mix (1 µl) were added to an Eppendorf tube and the volume adjusted to 10 µl using sterile water. The mixture was incubated at 65°C for 5 min, followed by immediate incubation on ice to allow annealing of the oligo-(dT) to the RNA template. An aliquot of a master reverse transcriptase (RT) mix (10 µl including 2 µl 10 × first strand buffer, 4 µl 25 mM $MgCl_2$, 2 µl 0.1M DTT, 1 µl RNaseOUT and 1 µl of 50 units RT) was added to the reaction, which was incubated at 42°C for 1 h. The reaction was terminated by incubation at 70°C for 15 min.

2.2.3 RT-PCR

RT-PCR was carried out on a range of barley tissue cDNAs. PCR was performed in 25 µl reactions containing 1 µl of each cDNA, 2.5 µl 10 × PCR buffer (containing 500 mM KCl, 100 µM Tris-HCl, pH 9.0, 10% v/v Triton X-100), 1.5 µl 25 mM $MgCl_2$, 1 µl 5 mM dNTPs, 1 µl 34 ng/µl of both the forward and reverse primers and 0.5 µl Taq DNA polymerase. PCR tubes were set up with or without 10% DMSO and the

total volume of the PCR brought up to 25 µl using sterile water. The PCR was started with an initial denaturation at 94°C for 5 min, followed by 35 cycles of [94°C: 30 sec; 55°C (or the lowest T_m of the primer pair): 30 sec; 72°C: 30 sec], followed by 72°C for 5 min. PCR products were separated on 2% agarose gels containing 0.1 mg/ml ethidium bromide.

2.2.4 3'-RACE-PCR

In order to isolate the missing 3'-end of barley cDNAs, nested gene-specific primers in the sense direction (5'→3') were designed on the basis of available sequences from partial ESTs. These primers were used in conjunction with TRACE (5'GACTCGAGTCGAC ATCGATTTTTTTTTTTTTTTT3') for the first round PCR and RACE3' (5'GAC TCGAGTCGACATCG3') for the second nested round of PCR. The TRACE primer contains $(dT)_{17}$, which binds to the poly(A) tail at the 3'-end of the messenger RNA molecule (Frohman *et al.*, 1988). PCR was performed containing 2.5 µl 10 × PCR buffer; 1.5 µl 25 mM $MgCl_2$; 1 µl 5 mM dNTP; 1 µl 34 ng/µl of each of the primers; 1 µl Taq DNA polymerase with 1 µl cDNA template for the first round PCR and 1 µl of a 1:100 dilution of the first round PCR product as template for the second round. PCR amplification was started with 94°C for 5 min as the initial denaturation; and 35 cycles of [94°C: 30 sec; 48-53°C annealing temperature based on the T_m of the gene-specific primers: 30 sec; 72°C: 1 min/1 kb]; 72°C for 5 min followed by incubation at 4°C. The amplified products from the second round PCR were separated by agarose gel electrophoresis and DNA bands were observed under ultraviolet light. When a proof-reading polymerase was required, Elongase was used. In these cases, 5 µl of each buffer A and B (provided by the manufacturer), 2 µl 5 mM dNTPs, 1 µl 34 ng/µl of each of the primers, 2 µl DNA template, 2 µl Elongase (for sizes less than 2 kb) and 32 µl MilliQ water were added to a total of 50 µl. The PCR protocol in this case started with 1 min at 94°C as the initial denaturation, followed by 35 cycles [94°C: 30 min; lowest T_m of the primer set as the annealing temperature: 30 sec; 68°C: 1 min], and a final incubation at 4°C.

2.2.5 Bacterial growth and preparation of electrocompetent cells

A single colony of *E. coli* (DH5α, XL1Blue, or BL21) was grown overnight in Luria-Bertani medium (LB: 1% w/v bacto-tryptone, 0.5 w/v bacto-yeast extract, 1% w/v NaCl, pH 7.0) at 37˚C. The following day, 20 ml culture was added to 500 ml LB and cells were grown at 37˚C until the cell suspension reached an optical density of 0.68 at 600 nm. Cells were pelleted at 5000 ×g for 10 min at 4ºC, followed by resuspension in 200 ml ice-cold sterile water. The centrifugation and resuspension steps in ice-cold water were repeated twice in 40 ml and 10 ml, respectively. The pellet was resuspended in 10 ml 10% (v/v) ice-cold glycerol and centrifuged at 5000 ×g for 10 min. Finally, the cells were resuspended in 3 ml 10% (v/v) ice cold glycerol, aliquoted out at 40 µl/tube and snap frozen in liquid nitrogen. The frozen cells were stored at -80˚C for use in the electroporation procedure.

2.2.6 DNA ligation into pGEM-T Easy and electroporation of plasmid DNA

Some DNA Taq polymerases add a single adenosine to the 3′-end of PCR products (Clark, 1988; Graham and Newton, 1997), which facilitates the cloning of an amplified fragment into a vector with a single overhanging thymidine, such as pGEM-T Easy. The ligation of amplified DNA fragments was carried out using the pGEM-T Easy vector system I kit as follows: 2 µl amplified DNA fragment, 5 µl 2 × ligase buffer, 1 µl 1:5 dilution of plasmid vector, 0.5 µl 500 units/µl T4 DNA ligase and 1.5 µl sterile water were mixed together and incubated overnight at 16˚C. The following day, the reaction mixture was precipitated with butanol (10 µl ligation reaction, 40 µl sterile water and 0.5 ml butanol), followed by a 75% (v/v) ethanol (0.5 ml) wash to remove the residual salt. The plasmid pellet was dried and resuspended in 10 µl sterile water. To transfer the re-ligated plasmid into *E. coli*, 2 µl cleaned ligation mixture was added to a 40 µl aliquot of electrocompetent cells in a pre-chilled 0.1 cm Gene Pulser Cuvette. A Gene Pulser apparatus was set at 25 µF with the pulse controller at 200 Ω to provide a 4-5 msec pulse to the cuvette in a pre-chilled safety chamber at 1.8 KV. The cuvette was removed immediately and 0.3 ml LB added. After gentle resuspension of the cells, the suspension was transferred to a clean

Eppendorf tube and incubated for 1 h at 37˚C. The cells were plated on LB agar medium (20-25 ml/plate) containing 4 mg/ml X-gal in dimethylformamide, 0.17 mM IPTG and 5 mg/ml ampicillin. The multiple cloning site of the pGEM-T Easy vector has been engineered into the lacZ operon. The intact operon produces a blue colour in the presence of 40 mM IPTG and 20 mg/ml XGal. Therefore, insertion of a fragment disrupts the activity of the operon and results in a white colony. White colonies were selected and grown in LB medium with 0.1 mg/ml ampicillin.

2.2.7 Isolation of plasmid DNA and restriction enzyme digestion

Transformed *E. coli* cells were grown in LB at 37˚C overnight in a rotary shaker. The following day, 2 ml culture was centrifuged and the supernatant removed. The pellet was resuspended in GTE buffer (25 mM Tris-HCl buffer, pH 8.0, containing 50 mM filter sterilised glucose and 10 mM EDTA) on a vortex mixer and placed on ice. A freshly prepared solution of 0.2 ml 1% SDS and 0.2 M NaOH (0.2 ml) was added to the resuspended cells. The tube containing the mixture was turned gently and allowed to stand on ice for 2 min. A 0.15 ml aliquot of 3 M potassium acetate (pH 4.8) was added and the tube inverted to form a white precipitate, followed by incubation at -20˚C for 10 min. To separate the white precipitate of cellular debris, the solution was centrifuged at 13,200 rpm for 15 min. The supernatant was removed into a clean tube and plasmid DNA was precipitated with 1 ml absolute ethanol on ice for 5 min followed by centrifugation at 13,200 rpm for 10 min. The supernatant was removed and the pellet washed with 0.2 ml 70% (v/v) ethanol by centrifugation at 13,200 rpm for 2 min. The pellet was dried and resuspended in 30 µl TE40 (10 mM Tris-HCl buffer, pH 8.0, containing 1 mM EDTA and 40 µg/ml RNase A). To examine the size of the insert, the plasmid was digested using an appropriate restriction enzyme with a site located in the multiple cloning site of the plasmid, usually *Eco*RI, which is found both 3' and 5' of the insertion site, to release the cloned fragment. The restriction enzyme digest of plasmid DNA (5 µl) was carried out in a tube containing 2 µl digest buffer, 2 µl 10 × BSA, 0.5 µl of 10 units/µl restriction endonuclease and 10.5 µl sterile water at 37˚C for 2 h. The plasmid and excised DNA fragment were separated

by agarose gel electrophoresis in the presence of 0.1 mg/ml ethidium bromide, followed by observation under UV light.

2.2.8 DNA sequencing and sequence analysis

After confirmation of insert size, the fragment was sequenced using the chain termination method of Sanger *et al.* (1977). Plasmid DNA, isolated as described in section 2.2.8, was separated from salts using Sepharose Cl-6B. The sequencing reaction was carried out using two pGEM-T Easy specific primers, T7 (5'TGTAATA CGACTCACTATAGGGCGA3') and SP6 (5'ATTTAGGTGACACTATAGAATACT 3'), which are located at either end of the polylinker. The sequencing reaction included 4 µl ABI PRISM Big Dye Terminators (version 2 or 3) reaction mixture, 3 µl plasmid DNA as the template, 3.2 pmol primer and 11 µl sterile water. The PCR protocol was as follows: 96°C for 30 sec for initial denaturation and 25 cycles of [96°C for 10 sec; 50°C for 5 sec; 60°C for 4 min]. Freshly diluted 75% (v/v) isopropanol (80 µl) was added to the sequencing reactions, left for 15 min at room temperature and the mixture was centrifuged at 13,200 rpm for 20 min. The pellet was washed a second time with the same solution (150 µl) by centrifugation at 13,200 rpm for 5 min, dried under vacuum and sent to the Institute of Medical and Veterinary Science (IMVS, Adelaide, SA, Australia) for sequencing on an ABI 3700 DNA analyser.

Data from sequencing reactions were viewed using Chromas software (version 2.23). Sequence alignments and database searches were carried out using the NCBI web site (http://www.ncbi.nlm.nih.gov/BLAST/) and the ANGIS suite of programmes (http://www1.angis.org.au/pbin/WebANGIS). Codon usage, motif searches and detection of transmembrane helices (TMH) were performed *via* the molecular biology tools web site (http://www.molbiol.net). Transmembrane helices were predicted using either TMHMM (http://www.cbs.dtu.dk/services/TMHMM/) or PSORT II (http://psort.nibb.ac.jp/form.html). Furthermore, a Kyte-Doolittle hydropathy plot (available at http://kr. expasy.org/cgi-bin/protscale.pl) was generated to predict the TMH (scores higher than + 1.6 in a window of 19 amino acids) and also the surface regions

of the protein molecules (peaks below the mid line). Hydrophobic cluster analysis (HCA) (http://www.lmcp. jussieu.fr/~soyer /www-hca/hca-file.html) was used to align the predicted secondary structures and conserved motifs of each enzyme family. Physical and biochemical properties of the proteins were predicted using the Protparam program (http://au.expasy.org/tools/protparam.html). Secondary structure of protein molecules were predicted using PSIPRED (Jones, 1999; McGuffin *et al.*, 2000) software (http://bioinf.cs.ucl.ac.uk/psipred/psiform.html) and the predicted structures were edited using Adobe Illustrator version 10.0.3. Clustal W (http://clustalw.genome.jp/) was used for multiple sequence alignment. Genomatix software (available at http://www.genomatix.de/cgi-bin/dialign/dialign.pl) was used for multiple sequence alignment and for calculating the percentage identity between sequences. The TCoffee program (available at http://igs-server.cnrs-mrs.fr/Tcoffee /tcoffee.cgi /index.cgi) was used for multiple sequence alignment and the drawing of phylogenetic trees (Poirot *et al.,* 2004). Genedoc software (downloadable from http://www.psc.edu /biomed/genedoc/) was used to edit the multiple sequence alignments. TreeView software was used to open the phylogenetic trees generated with the TCoffee program. SignalP V2.0.b2 (http://www.cbs.dtu.dk/services/ signalP-2.0/) was used to predict the signal peptide cleavage sites within the protein molecules.

Almost all Golgi glycosyltransferases are cleaved at either end or near to the end of the TMH, to release the soluble form (Young, 2004). This soluble form acts either as a soluble enzyme or is degraded during normal cellular protein turnover (Young, 2004). The TMH hydrophobic region has sequence characteristics that resemble regions of NH_2-terminal signal peptides of proteins that are targeted to the endoplasmic reticulum. In the latter case the following sub-regions of the signal peptide can be detected. Moving from the NH_2-terminus of the signal peptide towards the cleavage point, a common structure of amino acid residues is found. This contains a positively charged NH_2-terminal region, followed by a hydrophobic h-region and a neutral but polar COOH-terminal region. Another important requirement for accurate cleavage is the presence of a small and neutral amino acid residue at positions -3 and -1 from the cleavage site (von Heijne, 1983, 1985). Given that the TMH of some barley glycosyltransferases is located close to the NH_2-terminus of the enzyme, it was

important to distinguish, as far as possible, between a TMH sequence and a signal peptide sequence. As mentioned previously, TMHs were predicted using TMHMM or PSORT II and Kyte-Doolittle hydropathy plot. Prediction of signal peptide cleavage sites was carried out in the SignalP 3.0 server available at http://www.cbs.dtu.dk/services/SignalP/ (Nielsen *et al.*, 1997; Nielsen and Krogh, 1998; Bendtsen *et al.*, 2004).

2.2.9 Genomic DNA isolation from barley leaf tissue

A 7 d old barley leaf (1 g) was ground in liquid nitrogen to a fine powder with a mortar and pestle. The powder was allowed to thaw at room temperature for 5 min. DNA extraction buffer (2.25 ml) [1% w/v Sarkosyl, 100 mM Tris-HCl, 100 mM NaCl, 10 mM EDTA, 2% w/v PVPP with a final pH of 8.5] was added to the powder and the mixture homogenised for 1 min. The homogenate was transferred to a 10 ml plastic tube and 2.25 ml phenol/chloroform/isoamyl alcohol (25:24:1) was added. The solution was hand-mixed before the homogenate was further mixed on an orbital rotor for 10 min at room temperature. The phases were separated by centrifugation at 5,000 rpm for 10 min at 4°C. The supernatant was transferred to a silica matrix tube, another 2.25 ml of equilibrated phenol added and the solution mixed on an orbital rotor for 5 min. Phase separation was carried out by centrifugation at 5000 rpm for 10 min at 4°C and the supernatant transferred to a clean 10 ml tube. Sodium acetate (200 µl, 3 M, pH 4.8) and 2 ml isopropanol were added to the supernatant. The solution was mixed gently to precipitate the DNA. DNA was spooled out with a glass Pasteur pipette and transferred to a 2 ml Eppendorf tube containing 1 ml 70% (v/v) ethanol. The DNA was precipitated for 2 min at 13,200 rpm and the supernatant was removed. TE40 (175 µl) was added to the DNA pellet and DNA was resuspended on an orbital mixer at 4°C overnight.

2.2.10 Southern blot analysis

Barley genomic DNA or BAC clone DNA (10-15 µg) was digested with various restriction enzymes, in a reaction containing 7.5 µl 10 × digestion buffer (1 M Tris-HCl buffer, pH 7.5, containing 5 M potassium acetate, 1 M magnesium acetate, 0.1 M spermidine, 0.1 M DTT) and 5 µl 10 units/µl restriction enzyme (2.5 µl was added at the beginning of the digestion and 2.5 µl added after 2.5 h) in a total volume of 25 µl. The digest was incubated at 37°C for 5 h. A 1% agarose gel (1 × 20 × 20 cm) was prepared and poured into a levelled gel tray. The digested DNA reactions were loaded into the wells after adding 5 µl 6 × gel-loading buffer (0.25% w/v bromophenol blue, 0.25% w/v xylene cyanol FF and 30% v/v glycerol). A 20 µl aliquot of 1 Kb Plus DNA Ladder was loaded into a separate well. Electrophoresis of the digested DNA was performed at 35 V and 31 mA for more than 16 h, or until the upper dye had progressed to about 4.5 cm from the wells. The gel was stained with 0.5-1 mM ethidium bromide for 20 min on a shaker and rinsed with Milli-Q^{TM} water. The gel was observed under UV light and photographed. A sponge soaked in 0.4 M NaOH was placed in a plastic tray, a 3MM Whatman filter was placed on the sponge, and a screen (overhead transparency) was positioned on the sponge/filter paper set-up. The gel, previously soaked in 0.4 M NaOH, was placed upside-down on top of this. A nitrocellulose membrane soaked in 0.4 M NaOH was placed on the gel, followed by a sheet of Whatman paper soaked in the same buffer. A stack of paper towels (10 cm) was placed on top of the Whatman paper. Care was taken to avoid trapping air bubbles in any of the layers. The tray was filled with 0.4 M NaOH and the DNA allowed to transfer to the membrane overnight. The blot was dismantled, the membrane rinsed in 100 ml 2 × SSC (0.3 M NaCl in 30 mM sodium citrate buffer, pH 7.0) for 1 min and dried on Whatman paper.

2.2.11 Screening of a barley BAC library

A barley BAC library has been constructed for the barley cultivar Morex. Genomic fragments ranging between 30-195 kb are inserted into the *Hin*dIII site of pBeloBAC11, a low copy number vector of 7.5 kb, which is flanked with T7 and Sp6

promoters (Kim *et al.,* 1996). The library can be purchased from Clemson University Genomics Institute (CGUI). Two selectable markers in the vector, lacZ for recombinant selection and chloramphenicol for transformant selection, facilitate the cloning procedures. The library contains 313,344 clones (816 × 384-well plates) with an average insert size of 106 kb. The clones were robotically arrayed on 17 gridded filters in a 4 × 4 double-spotted pattern. Each filter carries 18,432 clones. If the barley genome size is assumed to be about 5,000 Mb, these 17 filters provide about 6.64 haploid genome equivalents (Yu *et al.,* 2000).

Out of the 17 filters, 9 were screened as described in section 2.2.14. Screening of these nine membranes provides more than 3.5 haploid genome equivalents and allowed a more than 90% probability of obtaining any specific sequence of interest. Addresses of BAC clones (positions on the filter) appearing as duplicate spots after screening with the radiolabelled probe were identified based on the BAC manual (http://www.genome.clemson.edu/).

2.2.12 Preparation of [α-^{32}P]-dCTP radiolabelled probes for BAC screening

Radioactively labelled DNA probes were synthesised by random priming (Feinberg and Vogelstein, 1983). Random nanomer primers (6 µl 0.1 mg/ml) were annealed to the DNA (20 ng) template by boiling the reaction mixture for 3 min and chilling immediately on ice for 5 min. Labelling buffer (10 µl 0.5 M HEPES, pH 6.6, 125 mM Tris-HCl, pH 8.0, 12.5 mM DTT, 12.5 mM $MgCl_2$, 1.0 mg/ml BSA) was added to the reaction, which was transferred into a 2 ml Eppendorf tube containing 3 µl deoxycytidine-5′-[α-^{32}P]-triphosphate. Sterile water was added to bring the total reaction volume to 24 µl. Klenow DNA polymerase I (1.0 unit) was added and the reaction incubated at room temperature overnight. Labelled DNA was separated from unincorporated [α-^{32}P]-dCTP by fractionation on a prepacked MicroSpin^{TM}S-200 HR column after adding 120 µl TEN solution (0.1 M NaCl, 1.0 mM EDTA, 10 mM Tris-HCl buffer, pH 7.2) according to instructions provided by the manufacturer. The labelled DNA probe was boiled for 5 min and added to the hybridisation buffer.

2.2.13 Preparation of [α-^{32}P]-dCTP radiolabelled probes

A Megaprime DNA labelling kit was used to prepare the radiolabelled probe from DNA fragments excised from plasmid preparations and gel purified PCR-amplified DNA fragments. An aliquot of clean DNA (3 µl) and random primers (5 µl) in a 33 µl volume was denatured by boiling for 5 min and chilled on ice for 5 min for primer annealing. Labelling buffer (10 µl) was added to the chilled mixture, followed by the addition of 2 µl 1.0 unit/µl Klenow DNA polymerase and 5 µl [α-^{32}P]-dCTP. The reaction was incubated at 37°C for 30 min to incorporate the radiolabelled dCTP. A Sephadex G-50 gel filtration column was prepared in a 1.0 ml syringe to separate the radiolabelled probe from unincorporated nucleotides. This column was washed and kept wet with 1 × TE buffer (10 mM Tris-HCl buffer, pH 8.0, containing 1 mM EDTA). Fractionation dye (50 µl containing 1.5% w/v dextran blue and 0.5% w/v orange G in 1 × TE buffer) was added to the probe reaction and loaded onto the column. During elution with 1 × TE buffer, the blue fraction was collected as the purified probe, boiled for 5 min and added to the hybridisation buffer.

2.2.14 DNA hybridisation and autoradiography

The membranes containing either genomic DNA or BAC clones were pre-hybridised/hybridised in a 10 ml solution containing 3.0 ml of 5 × HSB (0.1 M PIPES buffer, pH 6.8, containing 25 mM EDTA, 3.0 M NaCl), 2.0 ml 50 × Denhardt's (2.0% w/v BSA, 2.0% w/v Ficoll 400, 2.0% w/v PVP), 3.0 ml 25% (w/v) dextran sulphate, 1.8 ml MilliQ^{TM} water and 200 µl 10 mg/ml denatured salmon sperm. Membranes were placed in the hybridisation bottle and pre-hybridised initially for 10 min at 95°C, followed by 5 h at 65°C. The buffer was replaced by fresh hybridisation solution, the labelled DNA was added and the membrane incubated overnight at 65°C. The probe was removed and the hybridised membranes were washed, first in 2 × SSC, 0.1% w/v SDS at room temperature for 5 min (three times) and twice for 10 min in 0.2 × SSC, 0.1% w/v SDS at 65°C. Subsequent washes were undertaken until the membrane signal strength fell to 10-15 counts/second. Filters were dried, wrapped with Saran

wrap and exposed to X-ray film against an intensifying screen at -80˚C for a minimum of 3-5 days. Radioactive ink was used to orient the membrane.

2.2.15 Colony screening of the barley BAC clones

Hybridising BAC clones were obtained from CGUI as stab cultures. These were subcultured in duplicate onto gridded nitrocellulose membranes supported on LB agarose containing 25 µg/ml chloramphenicol and grown at 37˚C overnight. The gridded membranes were peeled from the LB agarose plates containing 25 µg/ml chloramphenicol and placed on a plate containing 10% w/v SDS for 3 min with the colony side up. The membrane was placed successively onto plates containing denaturing solution (0.5 M NaOH, 1.5 M NaCl) and neutralising solution (1.5 M NaCl in 0.5 M Tris-HCl buffer, pH 7.4) for 10 min each. The membranes were transferred into 2 × SSC, allowed to stand for 5 min and cleaned with a tissue in order to remove as much cellular debris as possible. The membranes were dried on a paper towel and sandwiched between two sheets of dry 3MM Whatman paper. The DNA was fixed to the membrane by baking the membrane for 1-2 h at 80ºC in a vacuum oven. These membranes were hybridised as described in section 2.2.14.

2.2.16 Isolation of BAC plasmid DNA

Each positively hybridising colony identified after screening was grown overnight in LB medium containing 25 µg/ml chloramphenicol in a rotary shaker at 37˚C. Each culture (2 ml) was pelleted by centrifugation for 1 min. The supernatant was discarded and the pellet was resuspended in 200 µl GTE buffer. Freshly prepared 0.2 M NaOH/1% (w/v) SDS (300 µl) was added and gently mixed by inversion and left on ice for 2 min. The mixture was neutralised by adding 300 µl 3 M potassium acetate (pH 4.8), mixed gently by inversion and left at -20ºC for 10 min. The cellular debris was removed by centrifugation for 10 min at room temperature and the supernatant transferred to a clean tube. Phenol-chloroform-isoamyl alcohol (25:24:1) (600 µl) was added to the supernatant and the mixture rotated for 15 min at room

temperature, followed by centrifugation for 1 min. The aqueous phase was extracted again with 400 µl chloroform. The mixture was hand-shaken for 30 sec and centrifuged for 1 min to separate the phases. The aqueous phase was transferred to a clean 1.5 ml tube. The DNA was precipitated by adding an equal volume of 100% (v/v) isopropanol and immediately centrifuged for 10 min at room temperature. The supernatant was discarded and the DNA pellet was washed with 500 µl 70% (v/v) ethanol. After centrifugation for 5 min, the pellet was dried under vacuum. The DNA pellet was dissolved in 32 µl Milli-Q^{TM} H_2O. DNA was precipitated by first adding 8 µl 4 M NaCl and 40 µl autoclaved 13% (w/v) PEG_{8000}. After thoroughly mixing the tube contents, the DNA was pelleted by centrifugation at 4°C for 25 min. The supernatant was removed carefully and the pellet centrifuged for 5 min after adding 500 µl 70% (v/v) ethanol. The pellet was air-dried and resuspended in 20 µl TE40. DNA was stored at -20°C prior to analysis.

Isolated BAC plasmid DNA (2 µl) was subjected to electrophoresis on a 1% TAE agarose gel to determine the approximate amount of DNA to be digested with *Hin*dIII. Based on ethidium bromide binding, 8 µl purified BAC DNA was digested with *Hin*dIII to release the insert from the BAC vector. A Southern transfer was carried out on twelve BAC clones.

2.2.17 PCR based genomic walking

Based on the method of Siebert *et al.* (1995), 2.5 µg aliquots of BAC DNA, prepared as described in section 2.2.16, were digested overnight with ten enzymes that produce blunt ends, namely *Dra*I, *Eco*RV, *Msc*I, *Nae*I, *Pml*I, *Pvu*II, *Sma*I, *Ssp*I, *Stu*I and *Sca*I. The restriction digests were extracted with phenol: chloroform: isoamyl alcohol (25:24:1) by rotating for 15 min on an orbital rotor followed by centrifugation for 1 min. The upper phase was transferred to a clean tube and extracted with chloroform by vigorous shaking for 30 sec followed by centrifugation for 1 min. The upper phase was transferred to a clean tube and 250 µl 95% (v/v) ethanol containing 0.1 vol 3 M sodium acetate and 1 µl 20 µg/ml glycogen was added. The mixture was shaken gently and DNA pelleted by centrifugation for 15 min at 4°C. The DNA pellet was

washed with 70% (v/v) ethanol, centrifuged for 5 min, and dried under vacuum. The pellet was redissolved in 20 µl TE.

Two adaptors, adaptor 1: 5'CTAATACGACTCACTATAGGGCTCGAGCGGCCG CCCGGGCAGGT3' and adaptor 2: 5'ACCTGCCC-H_2N3' were synthesised. Adaptor 2 has an amine group (NH_2) on the 3′-end, which suppresses concatenation. Thus, adaptor 2 binds to adaptor 1, but not to itself. An adaptor mix reaction was set up to anneal the two adaptors together. This contained 41.2 µM adaptor 1 (24.3 µl), 91.4 µM adaptor 2 (10.9 µl), 5 µl of 10 × ligase buffer and 9.8 µl MilliQ^{TM} H_2O. The mixture was heated at 90°C for 10 min and left overnight at room temperature to allow hybridisation of the two adaptors. A reaction was set up with 10 µl digested BAC clone DNA, 5 µl annealed adaptor mix, 2 µl 10 × ligase buffer, 1 µl MilliQ^{TM} H_2O and 2 µl of 1 unit/µl T_4 DNA ligase, in order to ligate the adaptor to the blunt ends of the digested BAC DNA. The adaptor ligation reactions were mixed gently and incubated at 16°C overnight. The following day, ligation reactions were heat-inactivated at 70°C for 5 min. The reactions were cooled and diluted 10-fold using 180 µl TE.

The diluted adaptor ligation reaction (2 µl) was used in the first round PCR, which contained 2.5 µl 10 × PCR buffer, 1.5 µl $MgCl_2$, 1 µl 5 mM dNTPs, 1 µl 34 ng/µl adaptor primer 1 (AP_1: 5'GGATCCTAATACGACTCACTATAGGG3'), 1 µl 34 ng/µl 1st gene-specific primer, 0.5 µl Taq DNA polymerase and 15.5 µl Milli-Q^{TM} H_2O. Adaptor primers are the primers that anneal to the ligated adaptor to amplify the target sequence. The PCR was carried out either in two or three steps. In the two-step PCR, the reaction started with an initial denaturation for 1 min at 94˚C, followed by 35 cycles of [94˚C for 30 sec; 64˚C for 6 min]. In the three-step PCR, the T_m values of the primers were used as the annealing temperature, with an initial start at 94˚C for 5 min. This was followed by 35 cycles of [94˚C for 30 sec; lowest T_m of the gene-specific primers for 30 sec; 72˚C for 2 min] and finally, 72˚C for 5 min. The PCR products were diluted 100-fold and 1 µl was used in a second round PCR. The same conditions and cycle parameters were applied using the nested adaptor primer (AP_2: 5'AATAGGGCTCGAGCGGC3') and the second gene-specific primer. PCR products

were separated on an agarose gel, fragments of interest excised from the gel and further purified using a Nucleospin extract kit. The purified PCR products were cloned into the pGEM-T Easy vector to further characterise by DNA sequencing.

2.2.18 Genetic mapping

Barley genomic DNA was extracted from 16 barley cultivars (Galleon, Haruna Nijo, Chebec, Harrington, Clipper, Sahara, Alexis, WI 2875-1, Sloop, Halcyon, Arapiles, Franklin, WI 2585, Amagi Nijo, VB 9524, ND 11231-12), a range of doubled haploid mapping populations and wheat-barley addition lines (Chinese Spring with an extra chromosome from the barley variety Betzes) (Islam *et al.*, 1981) by Mrs. Margaret Pallotta (Australian Centre for Plant Functional Genomics, University of Adelaide, Australia). The genomic DNA was digested with restriction endonucleases and transferred onto nitrocellulose membranes by Southern blot. Probes were prepared as described in section 2.2.13 and used to detect polymorphisms amongst the parents of the mapping populations. If the parents were found to be polymorphic, the double haploid lines produced from these parents were probed with the same probes to locate the gene. Map Manager QTX version 0.29 was used to score the presence or absence of the bands in the population (Manly *et al.*, 2001). In cases where no polymorphism was observed amongst parental lines, wheat-barley addition lines were used to locate each glycosyltransferase to a specific chromosome.

2.2.19 In silico analyses of GT34 and GT47 in Arabidopsis thaliana and rice (Oryza sativa)

The isolated barley cDNA clones were used as queries to search the rice protein dataset available at (http://www.tigr.org/tdb/e2k1/osa1/pseudo_molecules/info.shtml) and the *Arabidopsis* protein dataset available in the BAC end sequence database (http://www.tigr.org/tdb/e2k1/ath1/abe/bac_end_search.shtml). Protein-protein BLAST searches (Altschul *et al.*, 1997) were performed against the rice and *Arabidopsis* protein dataset with an initial E-value cut off of e^{-10} to retrieve rice and *Arabidopsis*

homologues. These sequences were reused against the rice and *Arabidopsis* datasets to ensure that distant family members were not missed. ClustalW was used to confirm the relatedness of retrieved versus original sequences. Aberrant length sequences were re-examined for possible incorrect predictions. The numbers of homologues within each family were identified. I would like to acknowledge the help of Dr. Ute Baumann (Australian Centre for Plant Function Genomics, Adelaide, Australia) in this aspect of the work.

2.3 RESULTS

2.3.1 Isolation and characterisation of four cDNA clones encoding barley homologues of family GT34 glycosyltransferases

2.3.1.1 Isolation and characterisation of *HvGlyT1*

A partial-length barley EST clone (805 bp) containing a poly (A) tail (accession number: HW105I09V) was identified using the fenugreek galactosyltransferase sequence (*TfGalT*) as a query to search the NCBI EST database. The EST showed approximately 40% identity at the nucleotide level to the 3′-end of *TfGalT*. This sequence was used as the basis for primer design in order to PCR amplify a probe fragment. Attempts to isolate a full-length barley glycosyltransferase through screening a barley seedling cDNA library with the probe and performing 5′ RACE-PCR were both unsuccessful.

The sequence of the original EST was used as a template to amplify a 147 bp fragment in the 3′UTR using two gene-specific primers, GalTUTR5' and GalTUTR3' (Figure 2.3). The amplified fragment was used to generate a radiolabelled probe as described in section 2.2.12. Nine barley BAC membranes were screened with the probe by Dr. Brendon King (University of Adelaide, SA, Australia). Genuine spots hybridising in a duplicate pattern were addressed and clones of each were obtained from CGUI as stab cultures. Twelve putative BACs (presented in Table 2.1) were digested with the *Hin*dIII restriction enzyme to excise the insert from the vector (pBeloBAC11, 7.5KB, section 2.2.11). Southern fingerprint analysis was performed on the BACs using the same probe (Figure 2.1). Southern analysis indicated four potential glycosyltransferase clones: BAC clones number 370P12 (1), 42121 (10) and 48L22 (12) all contained the same size band, but BAC clone number 42122 (9) showed a different hybridisation pattern. The latter BAC clone was used for further analysis, because in addition to containing the conserved band it also contained a

larger hybridising fragment, increasing the chance of retrieving the full-length barley glycosyltransferase gene and thus cDNA at a later date. BAC clones number 406C3 (2) and 406M11 (7) were degraded. Two lanes were empty of any hybridising bands except for a faint vector band, corresponding to numbers 624D16 (4) and 270J5 (11). The other BAC clones contained hybridising fragments bigger than the size of the vector.

BAC clone number 42112 (9) was used to make a library for genomic walking with the restriction enzymes outlined in section 2.2.17. The first round PCR was carried out using the gene-specific primer GTAS2 (Figures 2.2 and 2.3) and AP1. A second round of PCR was performed using a nested gene-specific primer GTAS3 (Figures 2.2 and 2.3) and AP2; bands were excised, cloned into pGEM-T Easy and sequenced. One fragment of 425 bp overlapped the original EST by 235 bp. A further walk was performed using GTAS6 (1^{st} round gene-specific primer) and AP1 and GTAS7 (2^{nd} round gene-specific primer) and AP2 (Figures 2.2 and 2.3), which produced a 235 bp fragment containing a 50 bp overlap with the previously obtained fragment. The cDNA fragments were assembled into a contig of 1465 bp. The steps involved in retrieving *HvGlyT1* are presented in Figure 2.2. Analysis of the contig using TMHMM predicted a TMH of 22 amino acids that started 12 amino acid residues from the NH_2-terminus, as observed in typical type II glycosyltransferases (Figure 2.3). This information and the presence of a methionine at the beginning of the sequence suggested that the sequence obtained from BAC walking represented a near full-length barley glycosyltransferase, which was called *HvGlyT1*.

A near full-length *HvGlyT1*cDNA was subsequently obtained by nested PCR using 1 day-old root cDNA as a template, with Elongase and NFS1 and NFAS1 as the first round primers, and NFS2 and NFAS2 as the second round gene-specific primers (Figures 2.2 and 2.3). The near full-length cDNA and deduced protein sequence of the *HvGlyT1* gene were generated using the Map program in the ANGIS suite of programmes and is shown in Figure 2.3. *HvGlyT1* encodes a protein of 424 amino acids with a predicted molecular weight and isoelectric point (pI) of 48 kDa and 6.21, respectively. Predicted glycosylation sites for HvGlyT1 are shown in Figure 2.4. The predicted secondary structure for HvGlyT1 using the PSIPRED program is shown in

Number	BAC Clone Number
1	370P12
2	406C3
3	592J7
4	624D16
5	355H19
6	667A7
7	406M11
8	334022
9	42122
10	42121
11	27035
12	48L22

Table 2.1 Twelve BAC clones identified by colony screening using a *HvGlyT1* probe.

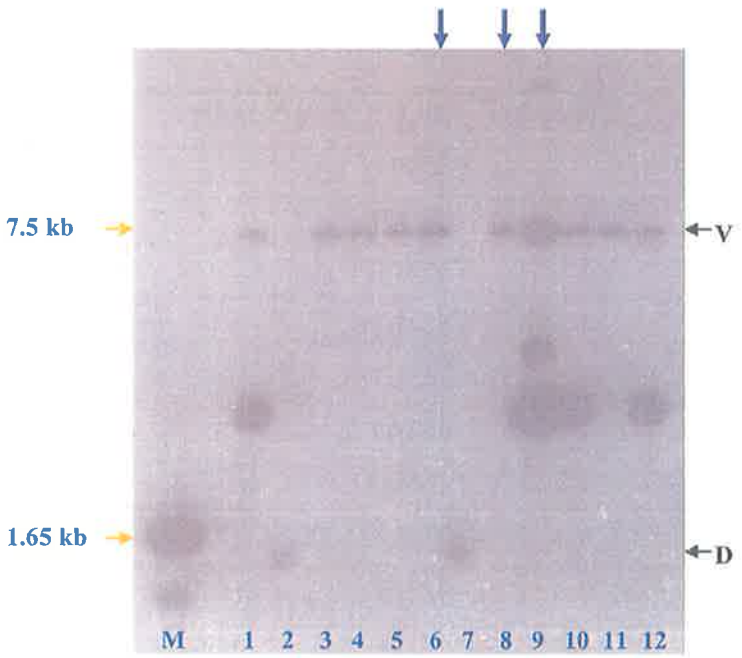

Figure 2.1 Southern fingerprint of twelve BAC clones digested with *Hind*III and probed with a small 3'UTR fragment of a barley glycosyltransferase. Numbers and corresponding BACs are listed in table 2.2. The blue arrows indicate the lanes containing bands larger in size than the vector band. M=size marker, V=vector band, D=degraded BAC clone.

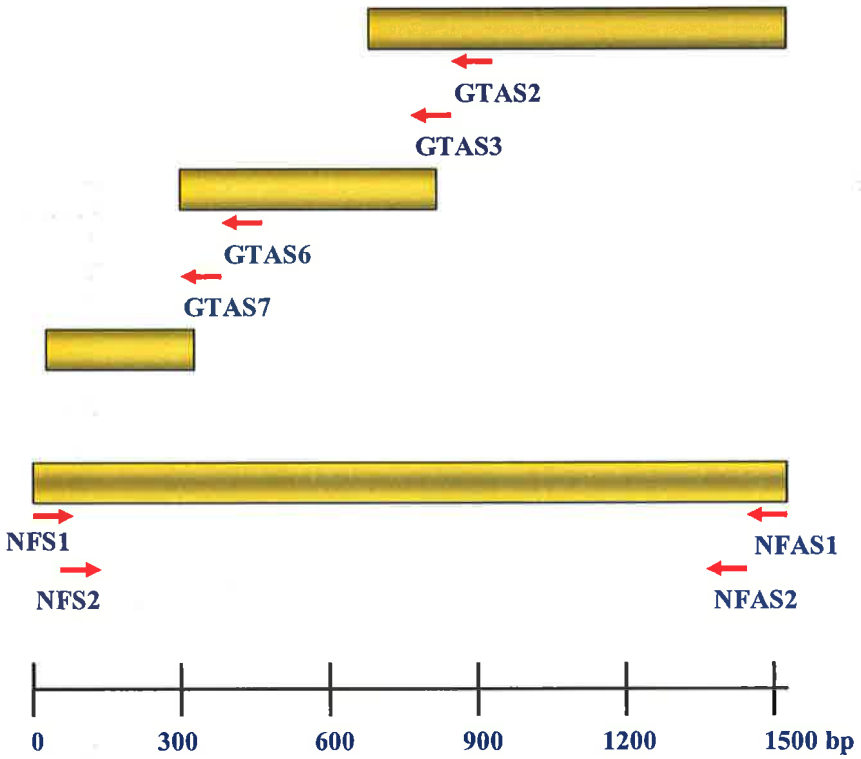

Figure 2.2 Schematic representation of the cloning steps of *HvGlyT1* via genomic walking. Primers that were used in the genomic walking and to retrieve the near full-length *HvGlyT1* are shown. The steps involved in the cloning of the *HvGlyT1* cDNA are described in the text.

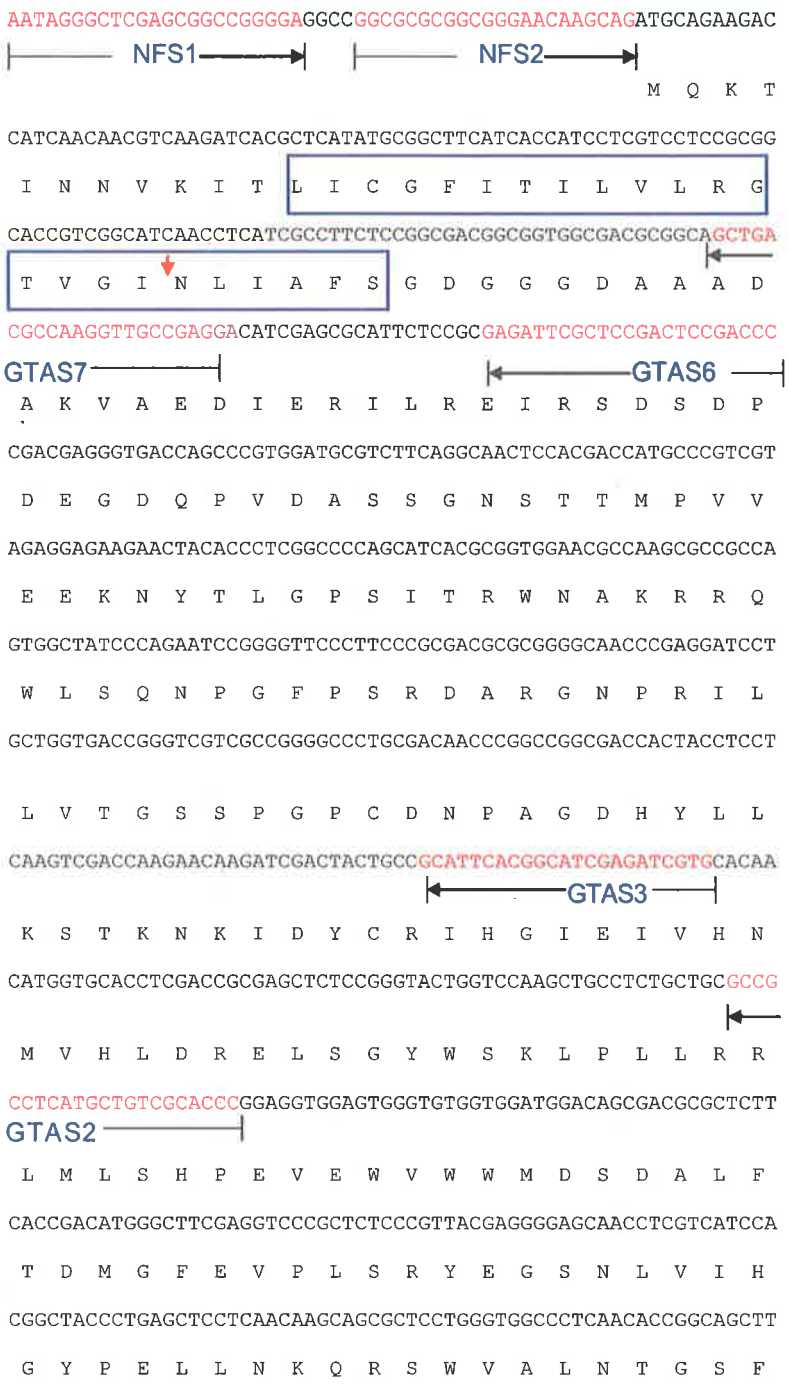
AATAGGGCTCGAGCGGCCGGGGAGGCCGGCGCGCGGCGGGAACAAGCAGATGCAGAAGAC
NFS1
NFS2
M Q K T
CATCAACAACGTCAAGATCACGCTCATATGCGGCTTCATCACCATCCTCGTCCTCCGCGG
I N N V K I T L I C G F I T I L V L R G
CACCGTCGGCATCAACCTCATCGCCTTCTCCGGCGACGGCGGTGGCGACGCGGCAGCTGA
T V G I N L I A F S G D G G G D A A A D
CGCCAAGGTTGCCGAGGACATCGAGCGCATTCTCCGCGAGATTCGCTCCGACTCCGACCC
GTAS7
GTAS6
A K V A E D I E R I L R E I R S D S D P
CGACGAGGGTGACCAGCCCGTGGATGCGTCTTCAGGCAACTCCACGACCATGCCCGTCGT
D E G D Q P V D A S S G N S T T M P V V
AGAGGAGAAGAACTACACCCTCGGCCCCAGCATCACGCGGTGGAACGCCAAGCGCCGCCA
E E K N Y T L G P S I T R W N A K R R Q
GTGGCTATCCCAGAATCCGGGGTTCCCTTCCCGCGACGCGCGGGGCAACCCGAGGATCCT
W L S Q N P G F P S R D A R G N P R I L
GCTGGTGACCGGGTCGTCGCCGGGGCCCTGCGACAACCCGGCCGGCGACCACTACCTCCT
L V T G S S P G P C D N P A G D H Y L L
CAAGTCGACCAAGAACAAGATCGACTACTGCCGCATTCACGGCATCGAGATCGTGCACAA
GTAS3
K S T K N K I D Y C R I H G I E I V H N
CATGGTGCACCTCGACCGCGAGCTCTCCGGGTACTGGTCCAAGCTGCCTCTGCTGCGCCG
M V H L D R E L S G Y W S K L P L L R R
CCTCATGCTGTCGCACCCGGAGGTGGAGTGGGTGTGGTGGATGGACAGCGACGCGCTCTT
GTAS2
L M L S H P E V E W V W W M D S D A L F
CACCGACATGGGCTTCGAGGTCCCGCTCTCCCGTTACGAGGGGAGCAACCTCGTCATCCA
T D M G F E V P L S R Y E G S N L V I H
CGGCTACCCTGAGCTCCTCAACAAGCAGCGCTCCTGGGTGGCCCTCAACACCGGCAGCTT
G Y P E L L N K Q R S W V A L N T G S F

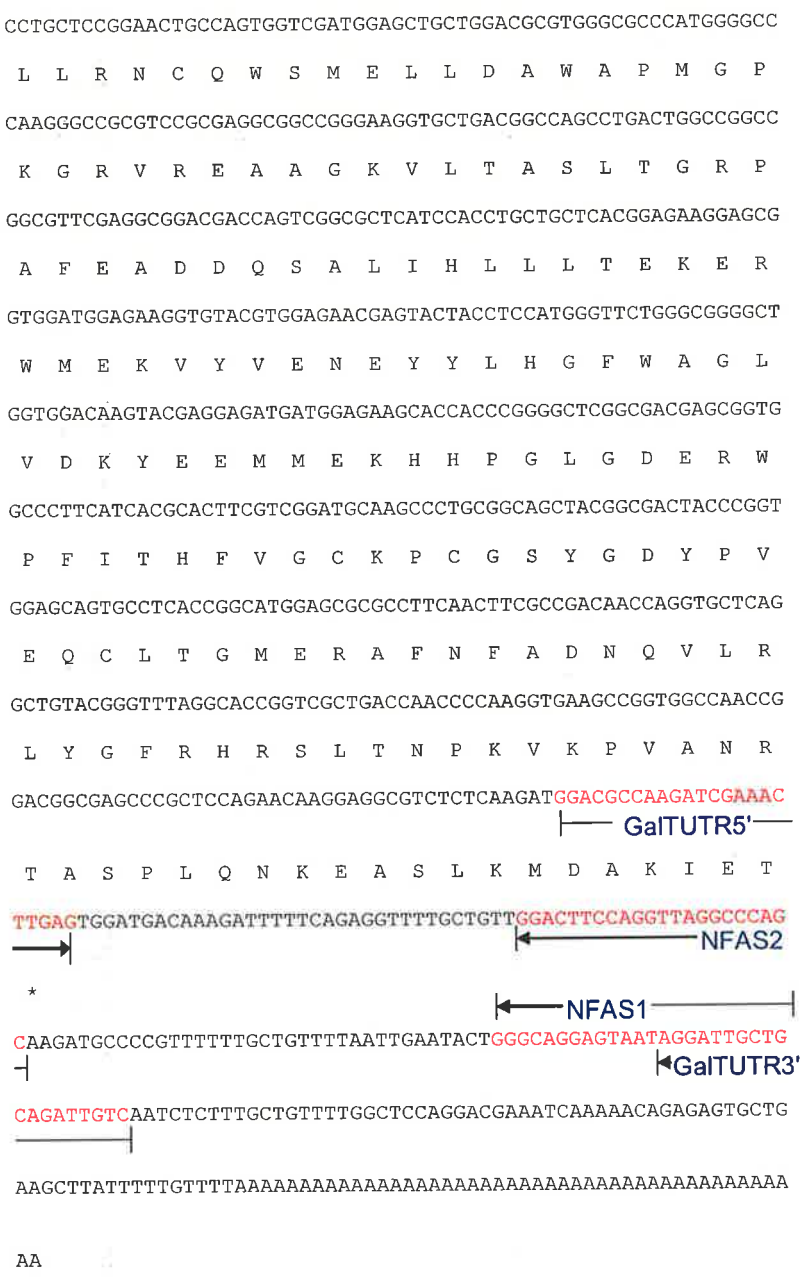

Figure 2.3 The nucleotide and deduced amino acid sequence of *HvGlyT1*. The predicted TMH is enclosed in a blue box. The predicted signal peptide cleavage site is shown by a red arrow in the -7 position at the end of the TMH. The primers which were used to isolate the *HvGlyT1* cDNA and to make a probe for screening the BAC library are highlighted in red and arrows indicate their orientations.

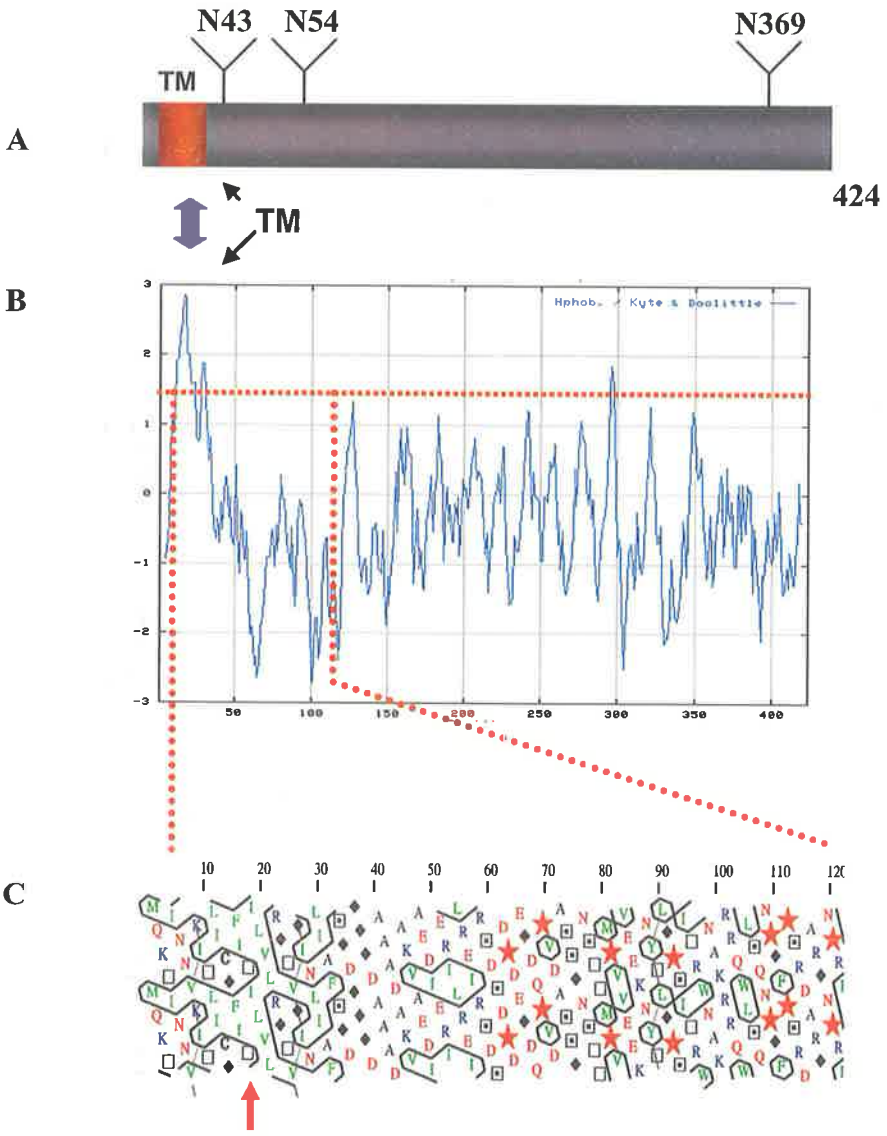

Figure 2.4 Secondary structural prediction of the HvGlyT1 sequence. **A**: Schematic representation of the HvGlyT1 protein, showing predicted putative glycosylation sites and the TMH. **B**: Hydropathy plot using the Kyte-Doolittle scale to predict the TMH. Y axis = probability of occurrence of TMH and X axis = number of amino acids. **C**: Hydrophobic cluster analysis of TMH and putative stem region. The TMH, indicated with a red arrow, contains a number of very hydrophobic amino acids. In the HCA profile, star = proline, diamond = glycine, square with a point = serine, empty square = threonine. Horizontal and vertical boxes represent α-helices and β-strands, respectively.

Figure 2.5. A comparison of the sequences obtained from BAC walking and the cDNA shows that this gene is unlikely to contain any introns.

2.3.1.2 Isolation and characterisation of *HvGlyT2* and *HvGlyT3*

Based on sequence information from *HvGlyT1* and other known plant members of family GT34 glycosyltransferases, the EST database was searched for other barley glycosyltransferase homologues. The ESTs obtained were used to construct a number of contigs using ContigExpress software, which is part of Vector NTI, Suite 7.0 (Maryland, USA). Originally, three contigs were built and named Groups I, II and III. Later, sequence analysis revealed that Groups I and III represented isoforms of a single enzyme. Group II corresponded to *HvGlyT2* whilst groups I and III corresponded to *HvGlyT3*.

The gene-specific primers for *HvGlyT2*: FGII1 (1st round PCR), FGII2 (2nd round PCR) and for *HvGlyT3*; FGI1 (1st round PCR: 5'GAGAACCCCGTCGGCGACCA C3'), FGI2 (2nd round PCR: 5'CCACGGCCTCGAATCTTCTAC3') were designed and used in conjunction with 3' RACE-PCR specific primers; TRACE (1st round PCR primer) and RACE3' (2nd round PCR primer) to retrieve fragments containing the poly (A) tail. These gene-specific primers above were based on a single pass sequence of the EST and, in this case, did not completely match the correct sequence obtained at a later date. Two total RNA samples from 4 d old coleoptiles and 1 d old roots were used as the template for these PCRs. Here, instead of using the oligo-(dT) primer for cDNA synthesis, TRACE was used. Both cDNA templates produced sharp PCR bands, which were excised from the gel and cloned into the pGEM-T Easy for sequencing (Figure 2.6). This revealed that the 3′ end of fragments corresponding to the *HvGlyT2* and *HvGlyT3* sequences both contained a poly (A) tail and a stop codon. To increase the chance of obtaining the 5′ ends of the clones, different cDNA libraries were used as the PCR templates but the attempts were not successful. Therefore, genomic walking (Section 2.2.17) was used to find the 5′ sequences of *HvGlyT2* and *HvGlyT3*. DNA was extracted from barley (cv. Sloop) and digested with fourteen

Figure 2.5 Secondary structural element prediction of HvGlyT1 using the PsiPred algorithm. The numbers indicate the amino acids in the primary structure of the protein. The red line illustrates the presence of the catalytic binding motif in a loop after a hydrophobic β-strand.

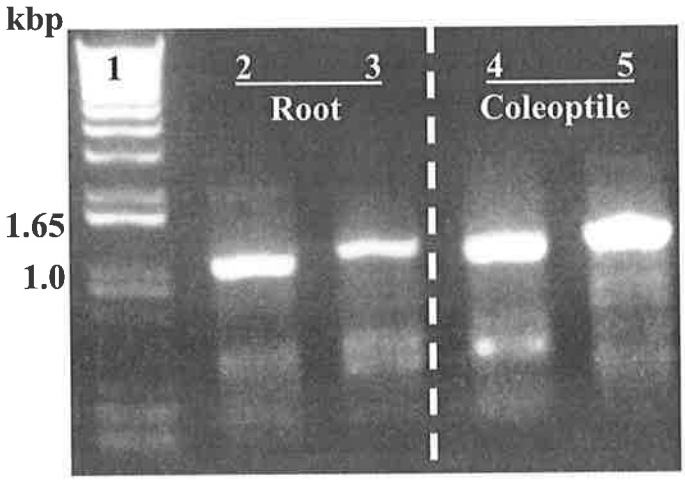

Figure 2.6 Second round of 3′ RACE-PCR. Lane 1 = DNA size marker, Lanes 2 and 3 = PCR fragments amplified from root cDNA for *HvGlyT2* and *HvGlyT3*, respectively. Lanes 4 and 5 = PCR fragments amplified from coleoptile cDNA for *HvGlyT2* and *HvGlyT3* respectively. The broken line indicates that some lanes have been removed from the original photo.

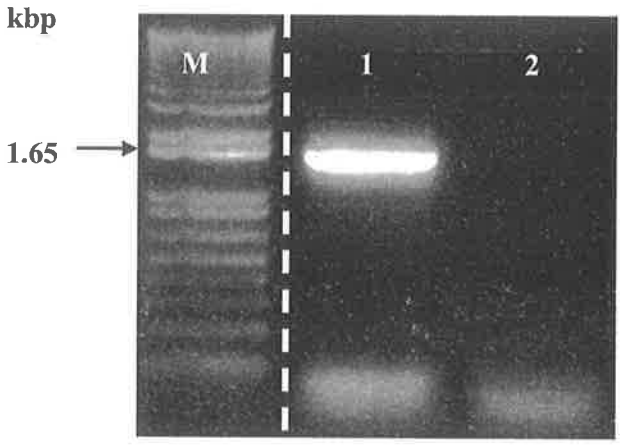

Figure 2.7 Second round PCR amplification of *HvGlyT2*. Root cDNA was used as the PCR template. Lane 1 = PCR amplified fragment of *HvGlyT2* from a root cDNA population, Lane 2 = negative control containing MilliQ™ water as the template, M = DNA size marker. Broken line indicates that some lanes have been removed from the original photo.

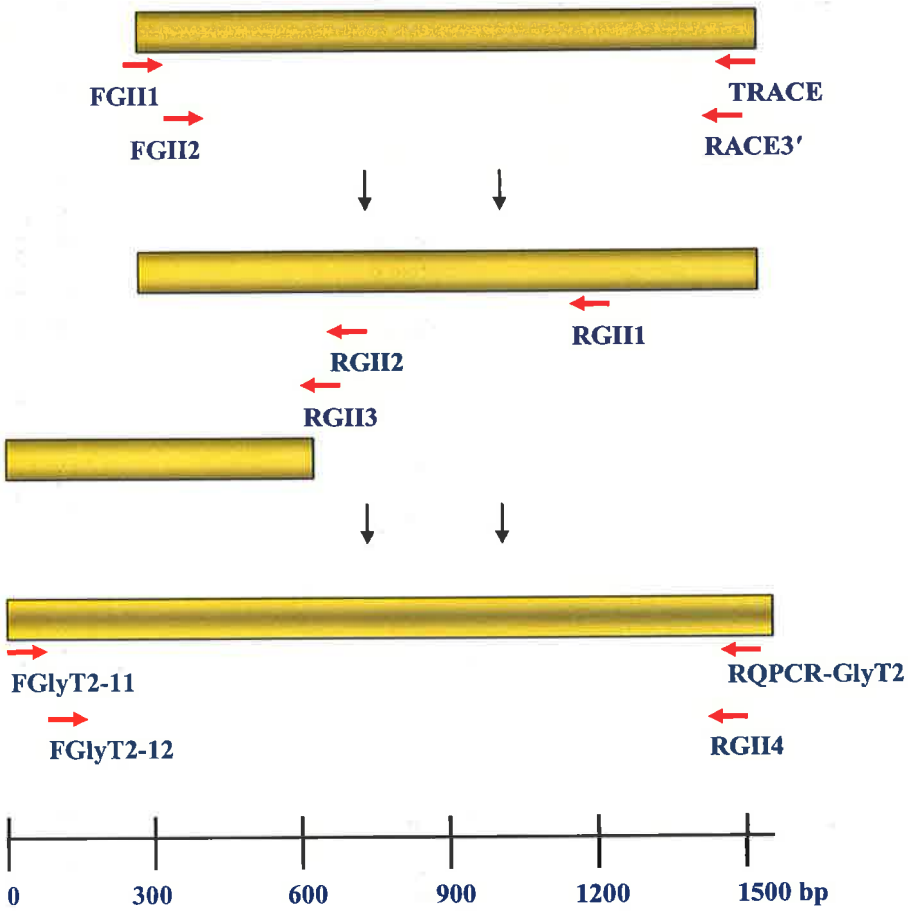

Figure 2.8 Schematic representation of the cloning steps of *HvGlyT2* *via* genomic walking. Primers that were used in the genomic walking and to retrieve the near full-length *HvGlyT2* are shown. The steps involved in the cloning of the *HvGlyT2* cDNA are described in the text. FGII1 and FGII2 were designed based on an EST sequence and they do not completely match the actual cDNA sequence.

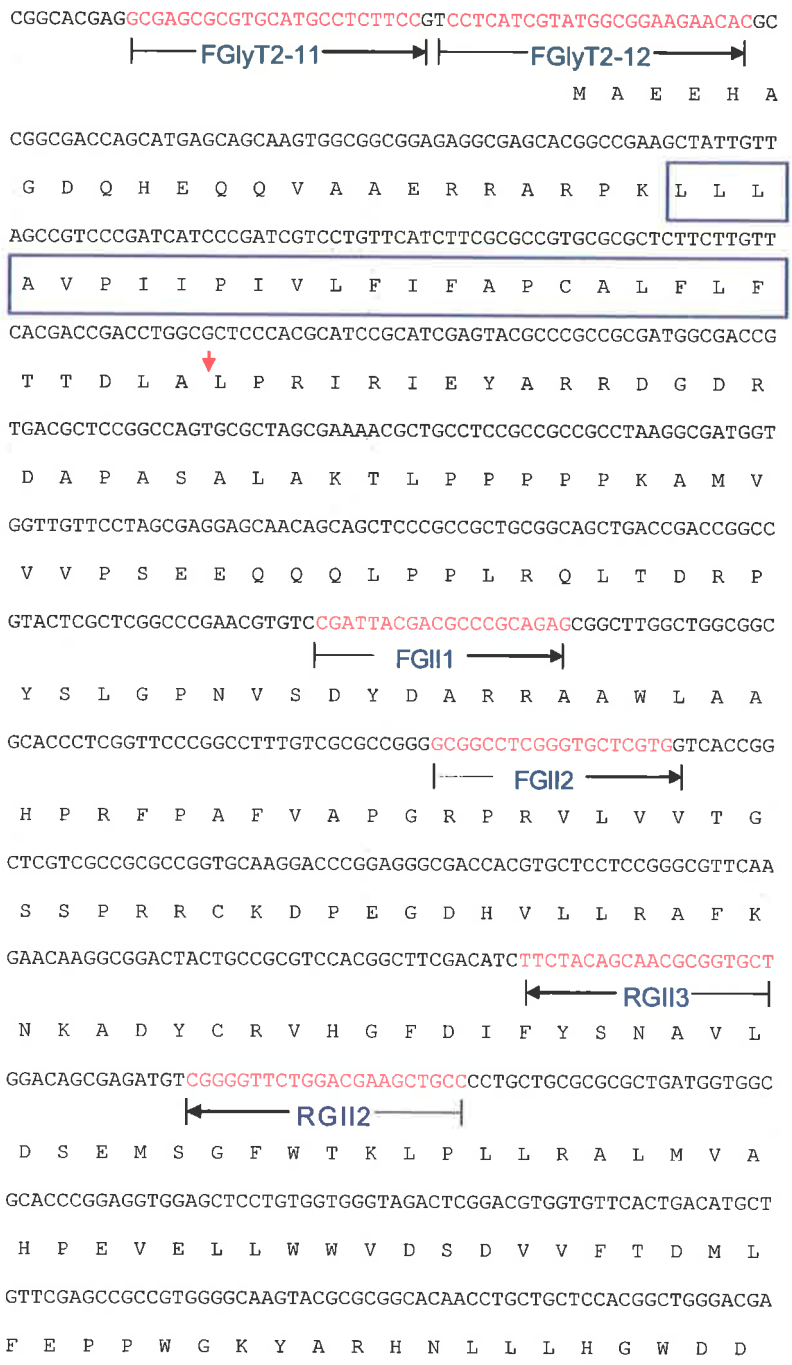
CGGCACGAGGCGAGCGCGTGCATGCCTCTTCCGTCCTCATCGTATGGCGGAAGAACACGC
FGlyT2-11
FGlyT2-12
M A E E H A
CGGCGACCAGCATGAGCAGCAAGTGGCGGCGGAGAGGCGAGCACGGCCGAAGCTATTGTT
G D Q H E Q Q V A A E R R A R P K L L L
AGCCGTCCCGATCATCCCGATCGTCCTGTTCATCTTCGCGCCGTGCGCGCTCTTCTTGTT
A V P I I P I V L F I F A P C A L F L F
CACGACCGACCTGGCGCTCCCACGCATCCGCATCGAGTACGCCCGCCGCGATGGCGACCG
T T D L A L P R I R I E Y A R R D G D R
TGACGCTCCGGCCAGTGCGCTAGCGAAAACGCTGCCTCCGCCGCCGCCTAAGGCGATGGT
D A P A S A L A K T L P P P P P K A M V
GGTTGTTCCTAGCGAGGAGCAACAGCAGCTCCCGCCGCTGCGGCAGCTGACCGACCGGCC
V V P S E E Q Q Q L P P L R Q L T D R P
GTACTCGCTCGGCCCGAACGTGTCCGATTACGACGCCCGCAGAGCGGCTTGGCTGGCGGC
FGII1
Y S L G P N V S D Y D A R R A A W L A A
GCACCCTCGGTTCCCGGCCTTTGTCGCGCCGGGGCGGCCTCGGGTGCTCGTGGTCACCGG
FGII2
H P R F P A F V A P G R P R V L V V T G
CTCGTCGCCGCGCCGGTGCAAGGACCCGGAGGGCGACCACGTGCTCCTCCGGGCGTTCAA
S S P R R C K D P E G D H V L L R A F K
GAACAAGGCGGACTACTGCCGCGTCCACGGCTTCGACATCTTCTACAGCAACGCGGTGCT
RGII3
N K A D Y C R V H G F D I F Y S N A V L
GGACAGCGAGATGTCGGGGTTCTGGACGAAGCTGCCCCTGCTGCGCGCGCTGATGGTGGC
RGII2
D S E M S G F W T K L P L L R A L M V A
GCACCCGGAGGTGGAGCTCCTGTGGTGGGTAGACTCGGACGTGGTGTTCACTGACATGCT
H P E V E L L W W V D S D V V F T D M L
GTTCGAGCCGCCGTGGGGCAAGTACGCGCGGCACAACCTGCTGCTCCACGGCTGGGACGA
F E P P W G K Y A R H N L L L H G W D D

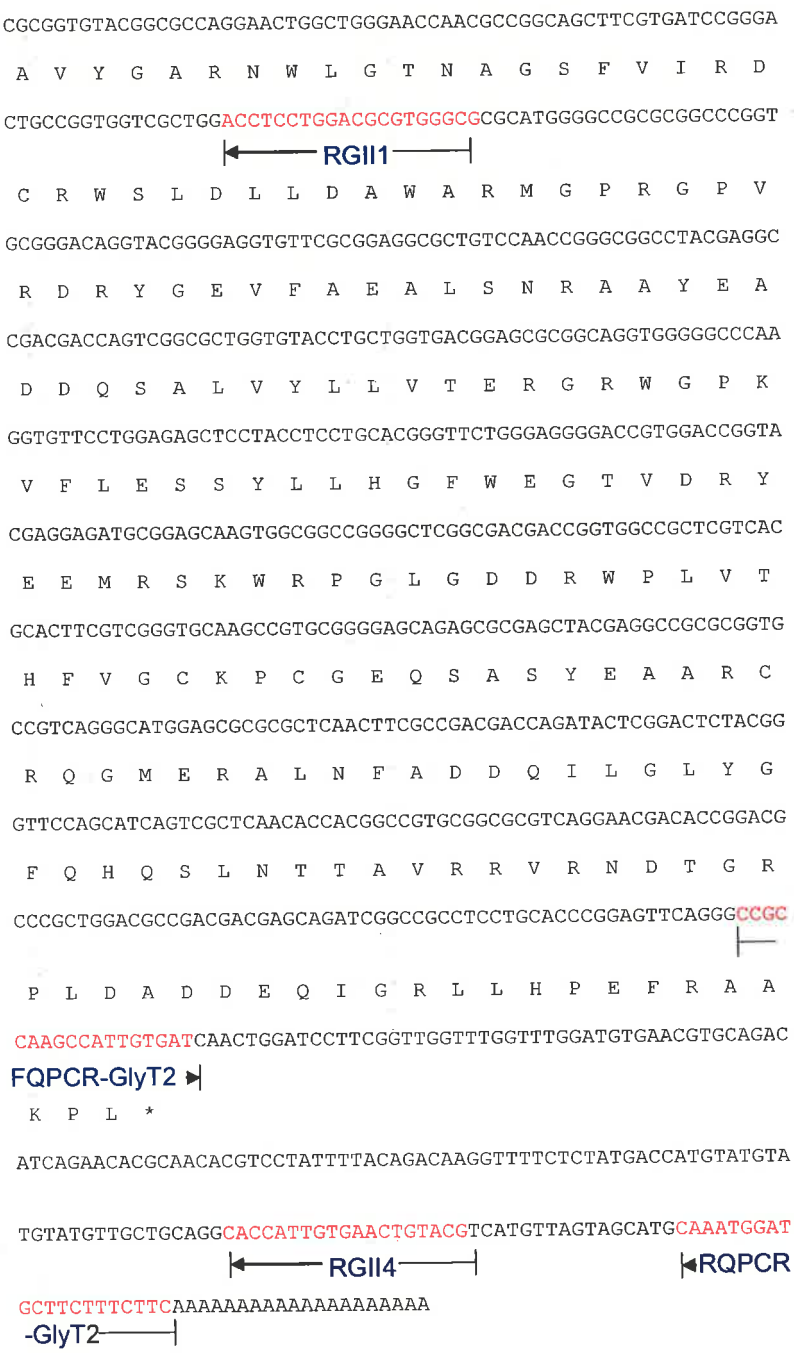

Figure 2.9 The nucleotide and deduced amino acid sequence of *HvGlyT2*. The primers that were used in the cDNA isolation procedure are shown in red and arrows indicate their orientations. The predicted 22 amino acid TMH is enclosed in a blue box. The predicted signal peptide cleavage site is shown by a red arrow at +5 position from the end of the TMH.

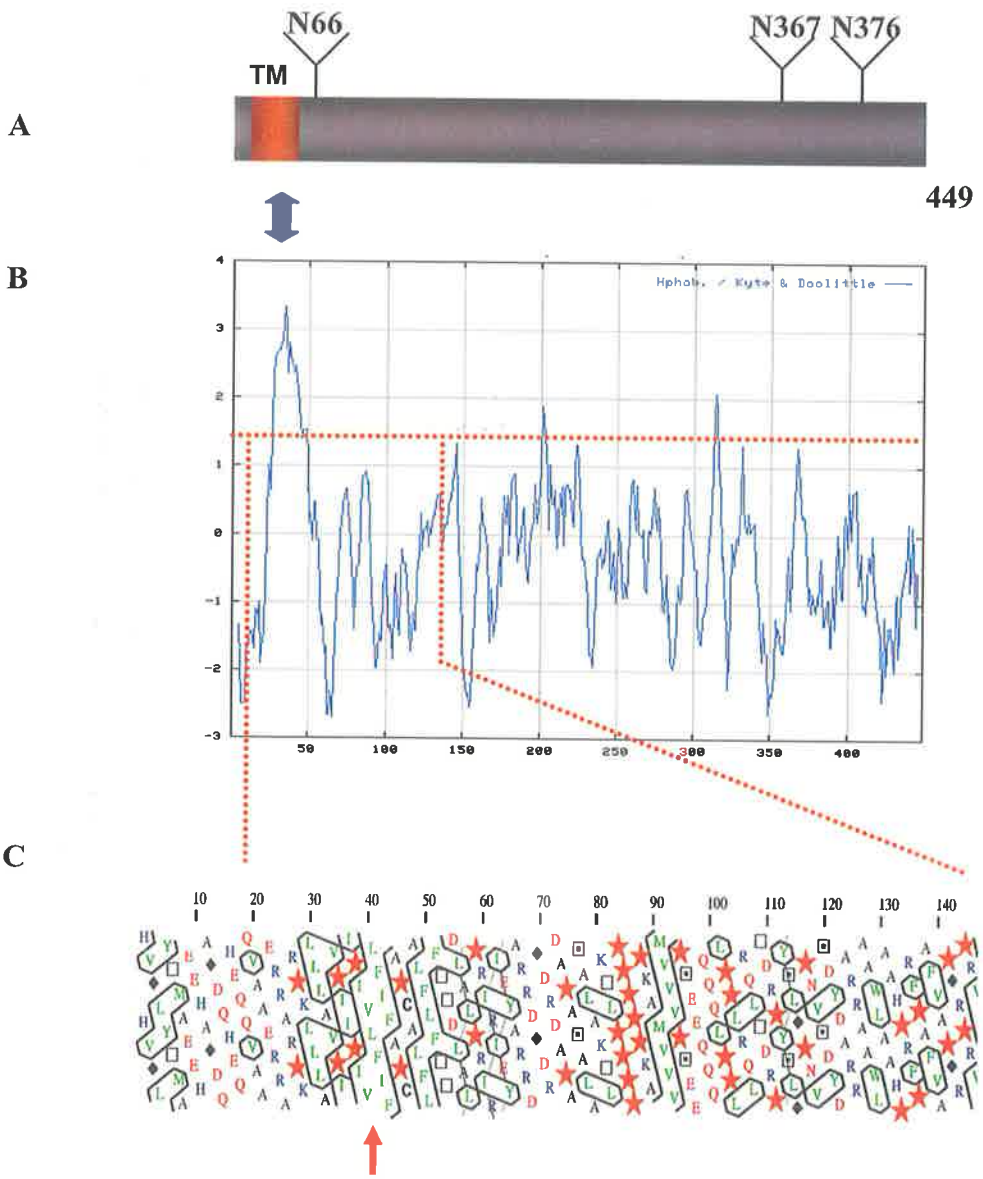

Figure 2.10 Secondary structural prediction of HvGlyT2. **A**: Schematic representation of HvGlyT2, showing predicted putative glycosylation sites and the TMH. **B**: Hydropathy plot using the Kyte-Doolittle scale to predict the TMH. Y axis = probability of occurrence of TMH and X axis = number of amino acids. **C**: Hydrophobic cluster analysis of the TMH and putative stem region, which contains a high number of proline residues, marked by stars. The TMH, indicated with a red arrow, contains a number of very hydrophobic amino acids. Diamond = glycine, square with a point = serine, empty square = threonine. Horizontal and vertical boxes represent α-helices and β-strands, respectively.

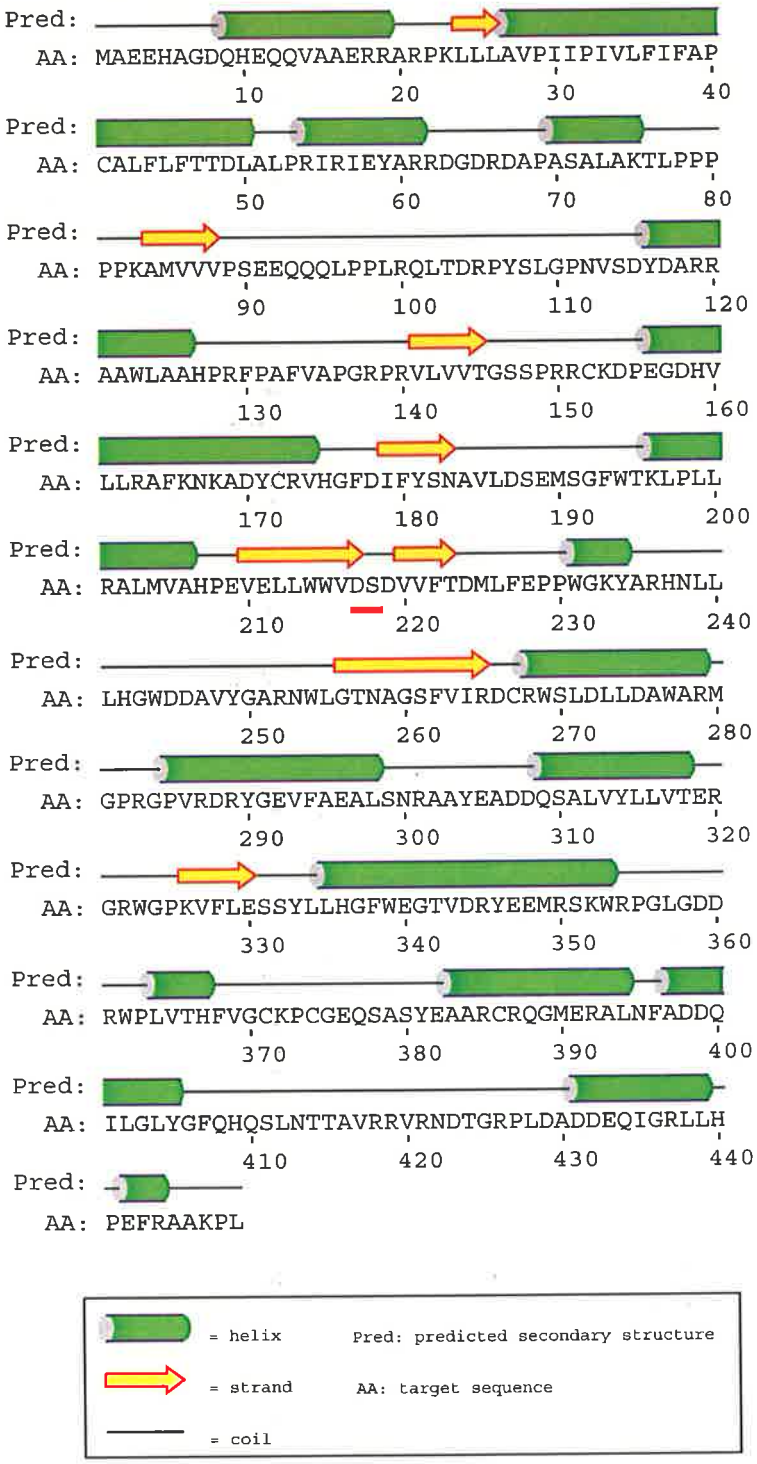

Figure 2.11 Secondary structural element prediction of HvGlyT2 using the PsiPred algorithm. The numbers indicate amino acids in the primary structure of the protein. The red line illustrates the presence of the catalytic binding motif in a loop after a hydrophobic β-strand.

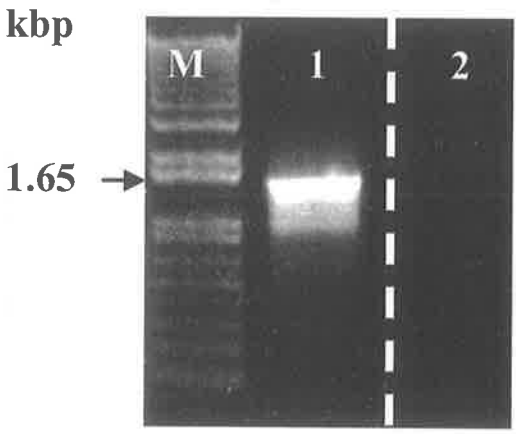

Figure 2.12 Second round PCR amplification of *HvGlyT3*. Coleoptile cDNA was used as a PCR template (Lane 1) and yielded a product smaller than 1.65 kb. Lane 2 = negative control containing MilliQ™ water as the template. M is the DNA size marker. The broken line indicates that some lanes have been removed from the original photo.

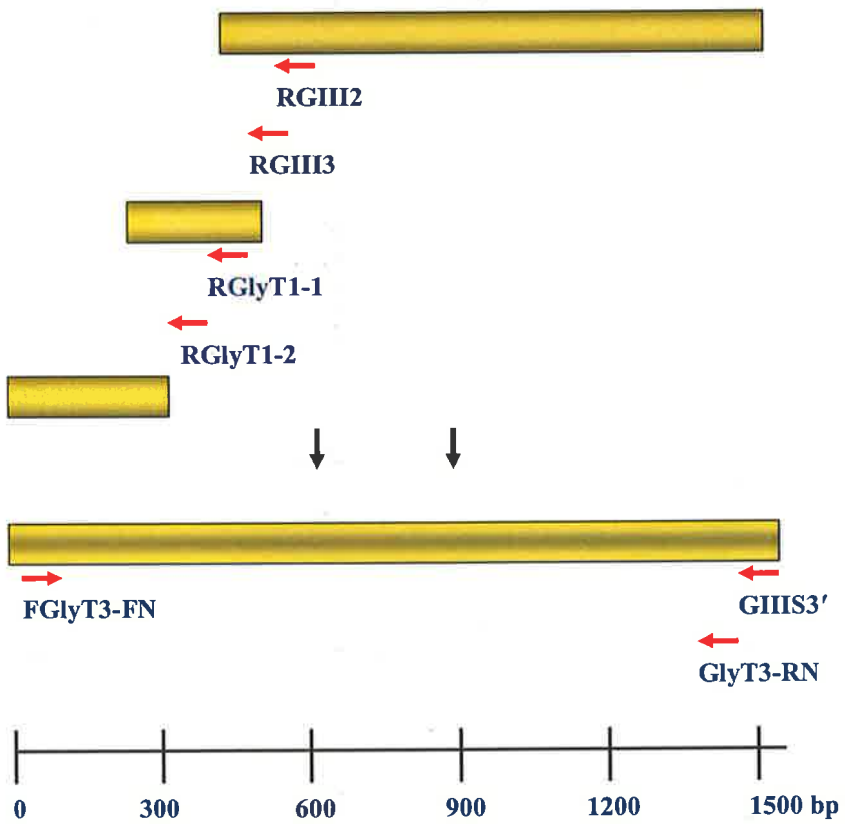

Figure 2.13 Schematic representation of the cloning steps of *HvGlyT3* via genomic walking. Primers that were used in the genomic walking and to retrieve the near full-length *HvGlyT3* are shown. The steps involved in the cloning of the *HvGlyT3* cDNA are described in the text.

restriction endonucleases that create blunt ends (*Bsr*BI, *Bst*Z17I, *Dra*I, *Eco*RV, *Hin*cII, *Hpa*I, *Msc*I, *Nae*I, *Pml*I, *Pvu*II, *Sma*I, *Ssp*I, *Stu*I, *Sca*I) and the libraries were constructed as described in section 2.2.16. For both *HvGlyT2* and *HvGlyT3*, a number of PCRs were carried out using gene-specific primers [*HvGlyT2*: RGII1, RGII2, and RGII3, Figure 2.9; *HvGlyT3*: RGIII2, RGIII3,RGlyT1-1, RGlyT1-2, Figure 2.14] in conjunction with adaptor-specific primers (AP1 and AP2) in order to genome walk until the near full-length sequences of *HvGlyT2* and *HvGlyT3* were obtained. The primer sequences and a schematic representation of the cloning steps are shown in Figures 2.8 and 2.9 for *HvGlyT2* and Figures 2.13 and 2.14 for *HvGlyT3*.

The near full-length *HvGlyT2* cDNA clone was 1347 bp long (Figure 2.9) and was obtained by nested PCR amplification of a root cDNA population using the primers FGlyT2-11 and RQPCR-GlyT2 in the 1st- and FGlyT2-12 and RGII4 in the 2nd round PCR (Figure 2.7). A semi-nested PCR approach (primers for 1st round PCR: GlyT3-FN, GIII S3′ and for 2nd round PCR: GlyT3-FN, GlyT3-RN) was used to isolate the near full-length *HvGlyT3* using a coleoptile cDNA population (Figure 2.12). These were excised from the gel and cloned into the pGEM-T Easy vector. The nucleotide sequence, primers and deduced amino acid sequence are shown in Figures 2.9 and 2.14 for *HvGlyT2* and *HvGlyT3*, respectively.

HvGlyT2 and *HvGlyT3* encode proteins of 449 and 456 amino acids respectively with predicted molecular weights (MW) and isoelectric points (pI) of 50 kDa/6.65 and 51 kDa/6.54. Figures 2.10 and 2.15 illustrate the putative glycosylation sites and presence of a TMH for HvGlyT2 and HvGlyT3, respectively. These Figures also demonstrate the structure of a relatively proline rich region that is known as a stem. The predicted secondary structure for HvGlyT2 and HvGlyT3 are shown in Figures 2.11 and 2.16, respectively.

2.3.1.3 Codon usage of some family GT34 barley glycosyltransferases

Codon usage analysis revealed that the barley glycosyltransferases, which belong to family GT34, contained a higher GC content at the wobble base position, similar to a

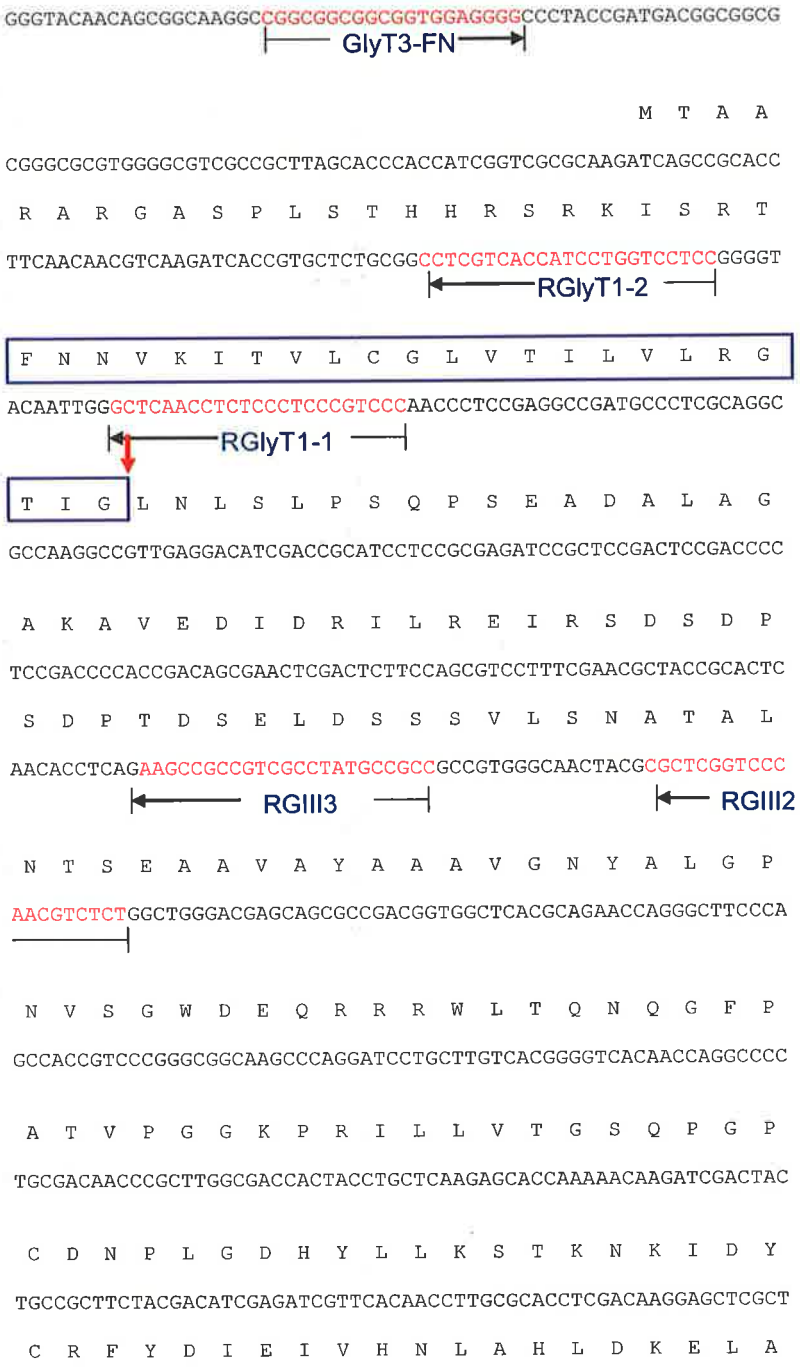
GGGTACAACAGCGGCAAGGCCGGCGGCGGCGGTGGAGGGGCCCTACCGATGACGGCGGCG
GlyT3-FN
M T A A
CGGGCGCGTGGGGCGTCGCCGCTTAGCACCCACCATCGGTCGCGCAAGATCAGCCGCACC
R A R G A S P L S T H H R S R K I S R T
TTCAACAACGTCAAGATCACCGTGCTCTGCGGCCTCGTCACCATCCTGGTCCTCCGGGGT
RGlyT1-2
F N N V K I T V L C G L V T I L V L R G
ACAATTGGGCTCAACCTCTCCCTCCCGTCCCAACCCTCCGAGGCCGATGCCCTCGCAGGC
RGlyT1-1
T I G L N L S L P S Q P S E A D A L A G
GCCAAGGCCGTTGAGGACATCGACCGCATCCTCCGCGAGATCCGCTCCGACTCCGACCCC
A K A V E D I D R I L R E I R S D S D P
TCCGACCCCACCGACAGCGAACTCGACTCTTCCAGCGTCCTTTCGAACGCTACCGCACTC
S D P T D S E L D S S S V L S N A T A L
AACACCTCAGAAGCCGCCGTCGCCTATGCCGCCGCCGTGGGCAACTACGCGCTCGGTCCC
RGIII3
RGIII2
N T S E A A V A Y A A A V G N Y A L G P
AACGTCTCTGGCTGGGACGAGCAGCGCCGACGGTGGCTCACGCAGAACCAGGGCTTCCCA
N V S G W D E Q R R R W L T Q N Q G F P
GCCACCGTCCCGGGCGGCAAGCCCAGGATCCTGCTTGTCACGGGGTCACAACCAGGCCCC
A T V P G G K P R I L L V T G S Q P G P
TGCGACAACCCGCTTGGCGACCACTACCTGCTCAAGAGCACCAAAAACAAGATCGACTAC
C D N P L G D H Y L L K S T K N K I D Y
TGCCGCTTCTACGACATCGAGATCGTTCACAACCTTGCGCACCTCGACAAGGAGCTCGCT
C R F Y D I E I V H N L A H L D K E L A

```
GGTTACTGGGCCAAGCTGCCGCTGCTCCGCCGACTTATGCTCTCCCACCCGGAGGTCGAG
  G  Y  W  A  K  L  P  L  L  R  R  L  M  L  S  H  P  E  V  E
TGGATCTGGTGGATGGACAGCGACGCCCTATTCACCGACATGGCCTTTGAGCTGCCCCTC
 W  I  W  W  M  D  S  D  A  L  F  T  D  M  A  F  E  L  P  L
TCGCGCTATGACAACCATAACCTCATCATCCACGGGTATCAGGATCTCCTCGTTGAGAAG
 S  R  Y  D  N  H  N  L  I  I  H  G  Y  Q  D  L  L  V  E  K
CACTCTTGGATCGCGCTCAACACCGGCAGCTTCCTCTTCCGGAACTGCCAGTGGTCGCTC
 H  S  W  I  A  L  N  T  G  S  F  L  F  R  N  C  Q  W  S  L
GATCTTCTCGATGCATGGGCTCCTATGGGGCCGAAGGGCTTCATCCGCGAGGAAGCCGGG
 D  L  L  D  A  W  A  P  M  G  P  K  G  F  I  R  E  E  A  G
AAGATACTCACCGCATACCTCAAGGGTCGCCCAGCATTCGAGGCTGACGACCAGTCTGCG
 K  I  L  T  A  Y  L  K  G  R  P  A  F  E  A  D  D  Q  S  A
CTGATATACCTCTTGCTCTCGCAGAAGGAGAAGTGGATGGACAAGGTGTATATAGAGAAT
 L  I  Y  L  L  L  S  Q  K  E  K  W  M  D  K  V  Y  I  E  N
TCATACTACTTGCATGGTTTCTGGGCTGGATTGGTGGACAAGTGCGAGGAGATGATGGAG
 S  Y  Y  L  H  G  F  W  A  G  L  V  D  K  C  E  E  M  M  E
AACCACCATCCAGGGCTTGGGGATGAGCGGTGGCCATTTGTGACACACTTTGTCGGGTGC
 N  H  H  P  G  L  G  D  E  R  W  P  F  V  T  H  F  V  G  C
AAGCCATGCGGAAGCTATGGTGATTATCCAGTTGACCGGTGTCTCAAGAGTATGGAGAGA
 K  P  C  G  S  Y  G  D  Y  P  V  D  R  C  L  K  S  M  E  R
GCATTTAATTTTGCCGATAACCAGGTGCTACGCCTGTATGGTTTCGCACACAAGGGGCTG
 A  F  N  F  A  D  N  Q  V  L  R  L  Y  G  F  A  H  K  G  L
GAAAGCCCCAAGATCAAGAGGATCAGGAGTCAGACCACAAAGCCAATTAATGACAAGGAG
 E  S  P  K  I  K  R  I  R  S  Q  T  T  K  P  I  N  D  K  E
AACCTTGATGTGAAGGCCAAGATGCCGACCACTTCTTGAAGCTACTGAAGATAAGGCAAT
 N  L  D  V  K  A  K  M  P  T  T  S

AGCATTGGTCTCTTCAAGGTCAGCTTTTTGTCACTTGGTTGCTGTTCTAGTTTCTACTAT
```

GlyT3-RN

Figure 2.14 The nucleotide and deduced amino acid sequence of *HvGlyT3*. The predicted 22 amino acid TMH is enclosed in a blue box. The predicted signal peptide cleavage site is shown by a red arrow just at the end of the TMH. The primers which were used for cloning steps are highlighted in red and arrows indicate their orientations.

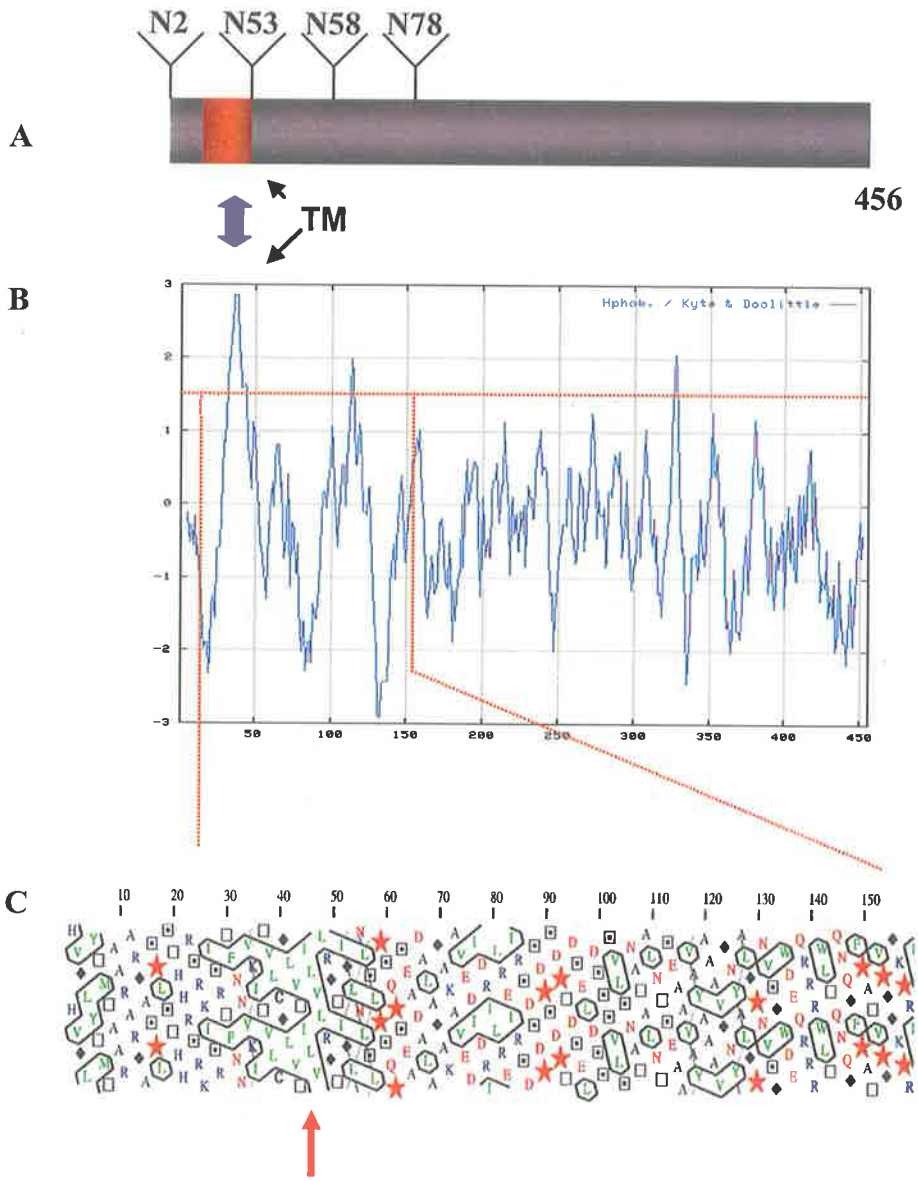

Figure 2.15 Secondary structural prediction of HvGlyT3. **A**: Schematic representation of the HvGlyT3 protein, showing predicted putative glycosylation sites and the TMH. **B**: Hydropathy plot using the Kyte-Doolittle scale to predict the TMH. Y axis = probability of occurrence of TMH and X axis = number of amino acids. **C**: Hydrophobic cluster analysis of the TMH and putative stem region where proline residues are marked by stars. The TMH, indicated with a red arrow, contains a number of very hydrophobic amino acids. Diamond = glycine, square with a point = serine, empty square = threonine. Horizontal and vertical boxes represent α-helices and β-strands, respectively.

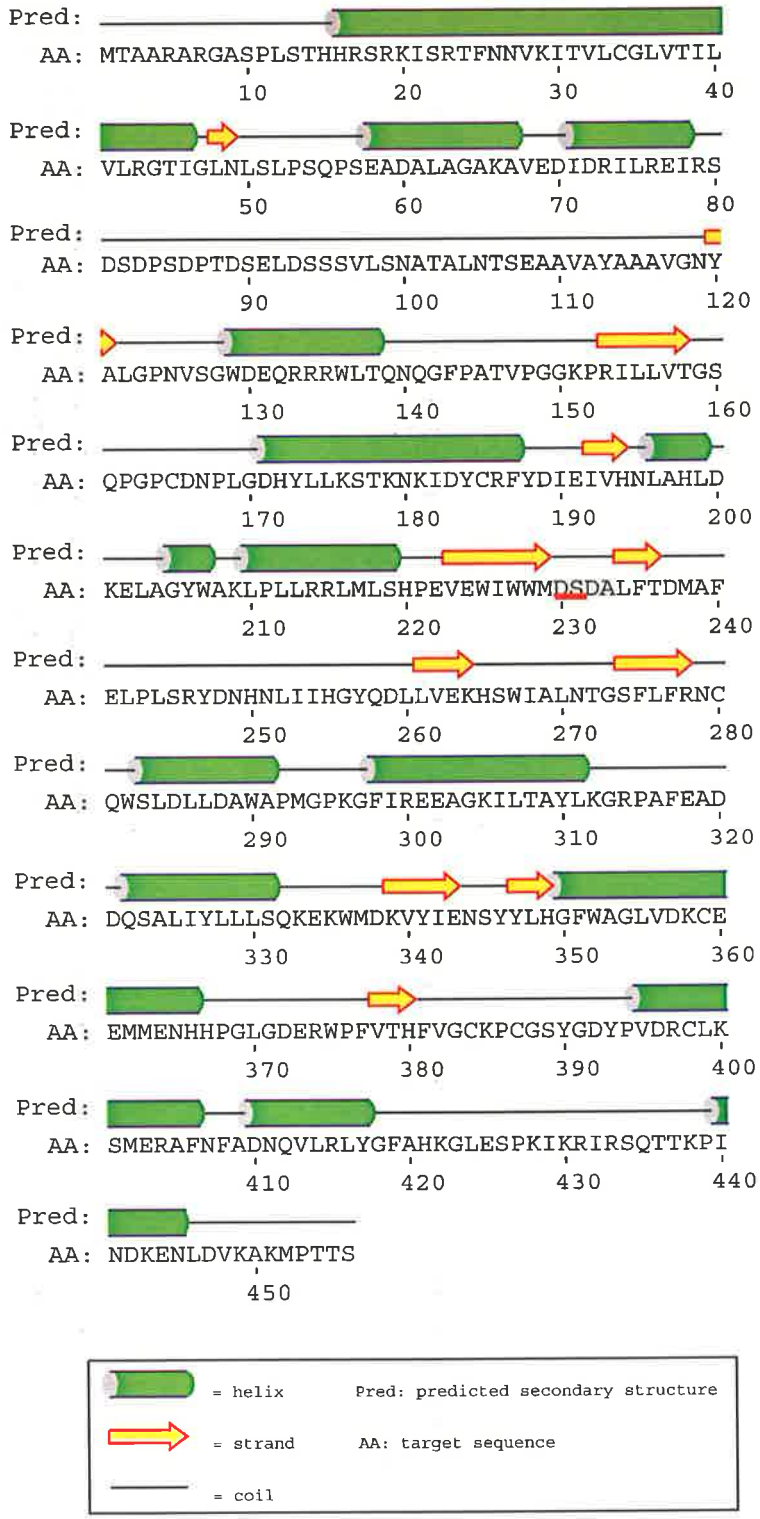

Figure 2.16 Secondary structural element prediction of HvGlyT3 using the PsiPred algorithm. The numbers indicate the amino acids in the primary structure of the protein. The red line illustrates the presence of a catalytic binding motif in a loop after a hydrophobic β-strand.

other monocot genes. *HvGlyT1*, *HvGlyT2* and *HvGlyT3* contained 94%, 92% and 78% of G or C in the third position of codons, respectively.

2.3.1.4 Isolation of partial-length *HvGlyT5*

A search for other family GT34 members in the barley EST databases and on the barley Affymetrix chip, revealed the presence of one other member (accession number: BI957062), designated *HvGlyT5*. A partial-length *HvGlyT5* was isolated from barley coleoptile cDNA population *via* 3′ RACE-PCR using CON1-1 (Figure 2.18) and TRACE in the 1st round PCR and CON1-2 (Figure 2.18) and RACE3′ primers in the 2nd round PCR as described in section 2.2.4 (Figure 2.17). The partial-length *HvGlyT5* cDNA containing a poly (A) tail is shown in Figure 2.18.

2.3.2 Multiple sequence alignment and the presence of gene families in GT34

Rice and *Arabidopsis* sequences, belonging to family GT34 glycosyltransferases, were retrieved as described in section 2.2.19 and used in a multiple sequence alignment (MSA), together with the barley homologues isolated in this work (Figure 2.19). The MSA was carried out using the TCoffee web site on the near full-length sequences, which showed more than 35% identity at the amino acid level, and further edited using Genedoc software. Since HvGlyT5 and an *Arabidopsis* sequence (accession No. At4g38310.1) were not near full-length, they were not included in the MSA. Figure 2.19 shows the presence of seven members in both *Arabidopsis* and rice, including an *Arabidopsis* xyloglucan (1→6)-α-xylosyltransferase (accession number At3g62720), and other functionally characterised members of family GT34 (fenugreek and *Lotus japonicum* galactomannan (1→6)-α-galactosyltransferase). The MSA shows the presence of conserved motifs within family GT34 and also the presence of a putative divalent cation-binding motif (DxD). Sequences similar to fenugreek and *Lotus japonicum* galactomannan (1→6)-α-galactosyltransferase contain an extra sequence of about 50 amino acid residues that differentiates them from the rest of the sequences (Figure 2.19). The sequence data were used to generate

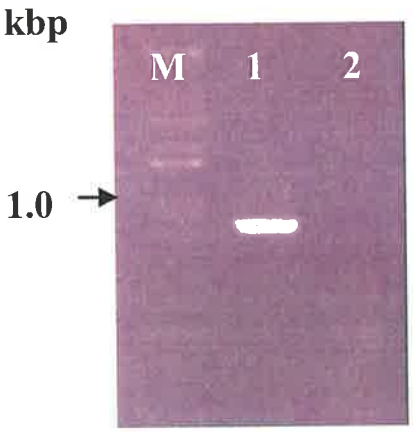

Figure 2.17 Second round of 3'RACE-PCR amplification of *HvGlyT5*. M = DNA size marker, Lane 1 = partial-length *HvGlyT5*, Lane 2 = negative control containing MilliQ™ water.

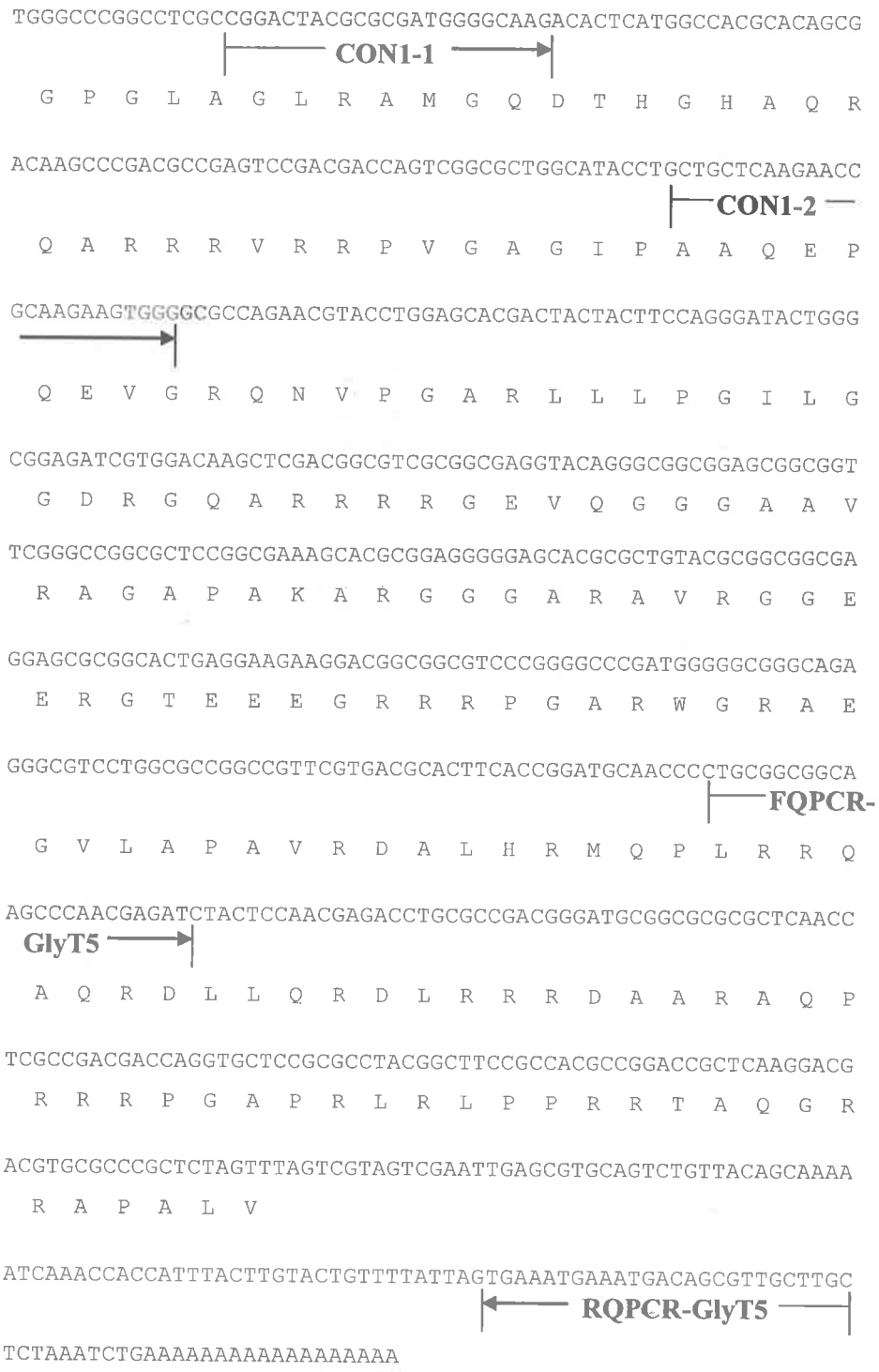

Figure 2.18 Partial-length nucleotide and amino acid sequences of *HvGlyT5*. The primers which were used for fragment isolation are highlighted in red and arrows indicate their orientations.

a phylogenetic tree with the TCoffee program, which is presented using the TreeView software (Figure 2.20). The phylogenetic tree tentatively categorises the plant members of family GT34 glycosyltransferases into seven groups, designated A-G. Groups B and D contain the functionally characterised members of this family but none of the barley members described here group with them; this suggests a distinct functional role for the barley proteins.

2.3.3 Protein analysis of isolated barley members of family GT34

All the barley glycosyltransferases characterised here that contain a start codon were predicted to contain a short TMH (22 amino acid residues) near the NH_2-terminus of the sequence. The TMH probably traverses the Golgi membrane. In all cases, the TMH was predicted using TMHMM and shown on a hydropathy plot using the Kyte-Doolitle scale (Figures 2.3, 2.10, 2.15). Hydrophobic cluster analysis (HCA) of the stem region, a stretch of hydrophilic amino acids that is located between the predicted catalytic domain and the TMH, showed a proline rich area (Figures 2.3, 2.10, 2.15). The HCA patterns of barley glycosyltransferases and the two previously characterised members of family GT34 were compared and the plot depicted nearly identical β-strands and α-helices amongst different members (Figure 2.21). Glycosylation sites, important in the activity of glycosyltransferases, were predicted using the Protparm program (Figures 2.3, 2.10 and 2.15). The percent identity between barley GlyTs and other functionally defined members of family GT34 is shown in Table 2.2.

2.3.4 Isolation and characterisation of a cDNA clone encoding a barley homologue of family GT47glycosyltransferases

A search was carried out to find barley homologues of the *N. plumbaginifolia* glucuronosyltransferase (*NpGUT1*) (Iwai *et al.*, 2002) in the public databases. The resultant EST sequences were assembled and four contiguous sequences were originally designated GUT1, GUT2, GUT3 and GUT4, using the ContigExpress

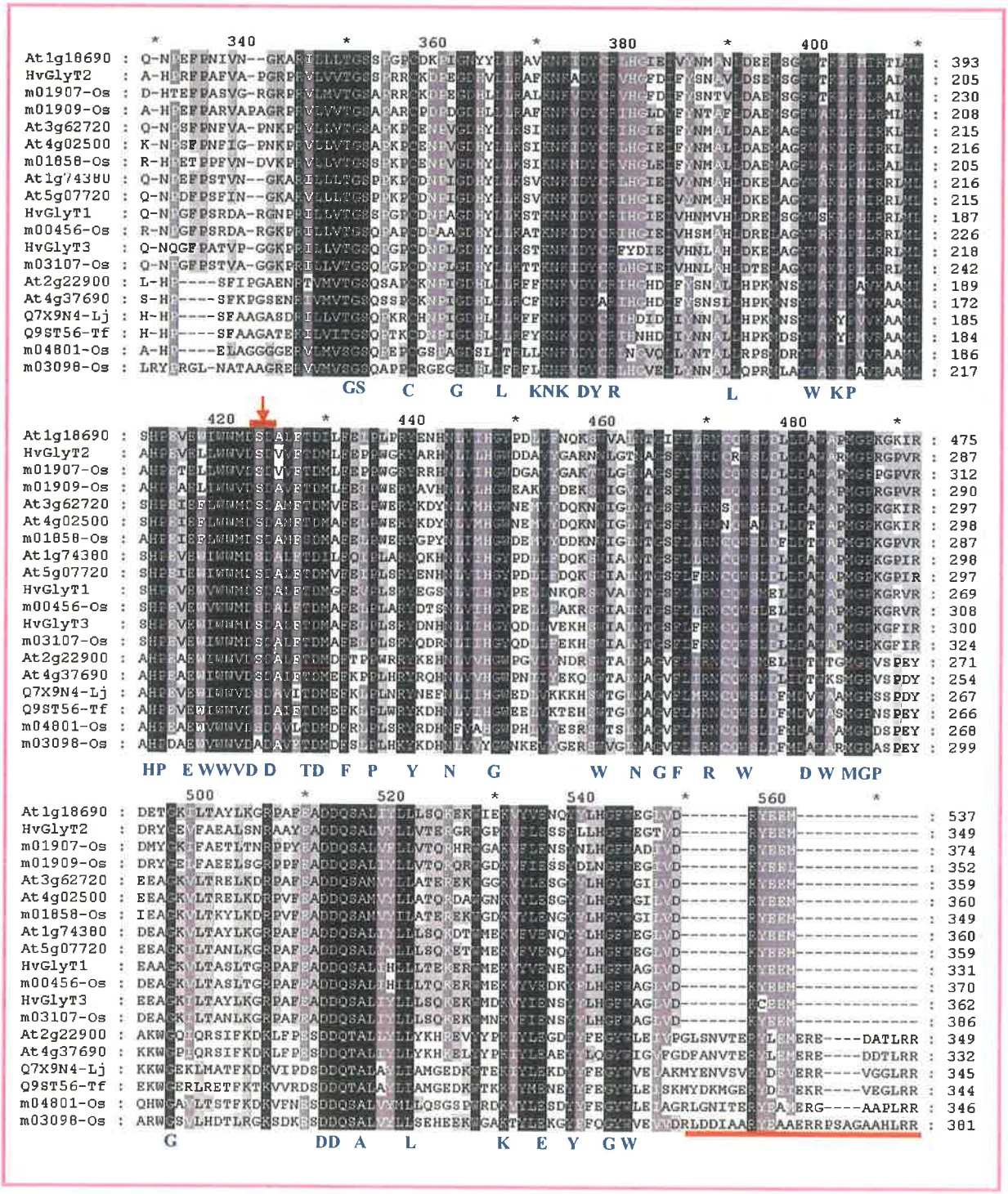

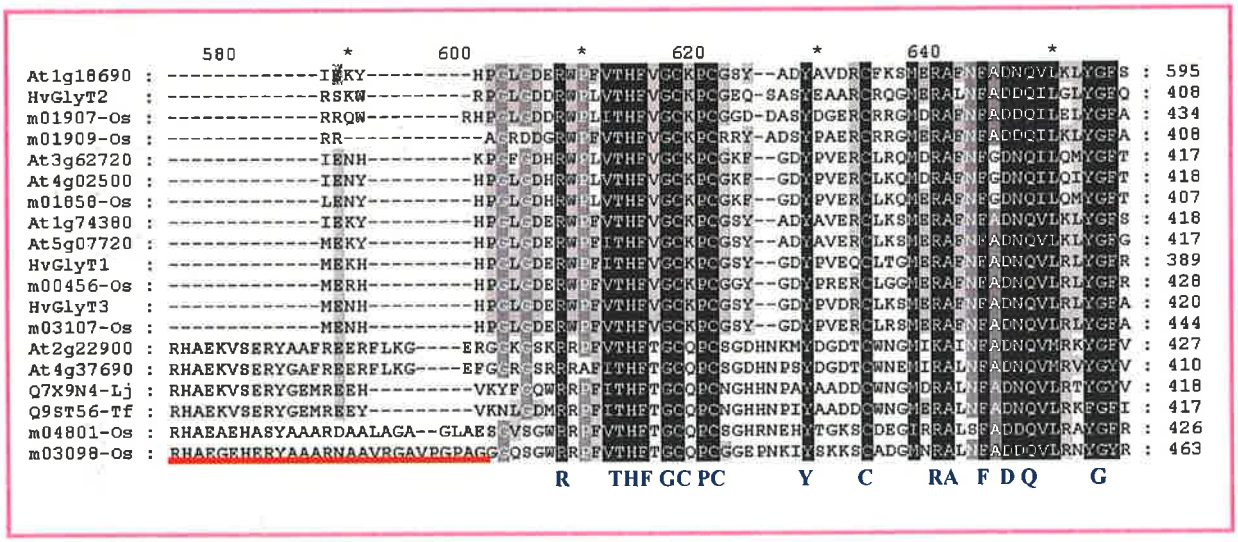

Figure 2.19 Partial multiple sequence alignment of plant family members of GT34. The sequences starting with At are derived from *Arabidopsis*. The sequences that end with Os, Tf and Lj correspond to rice (*Oryza sativa*), fenugreek (*Trigonella foenum*) and *Lotus japonicum*, respectively. The red arrow indicates the position of the DxD motif. Sequences similar to α-(1→6)-galactomannan galactosyltransferase contain extra amino acids, which differentiate them from the rest of the sequences (underlined in red).

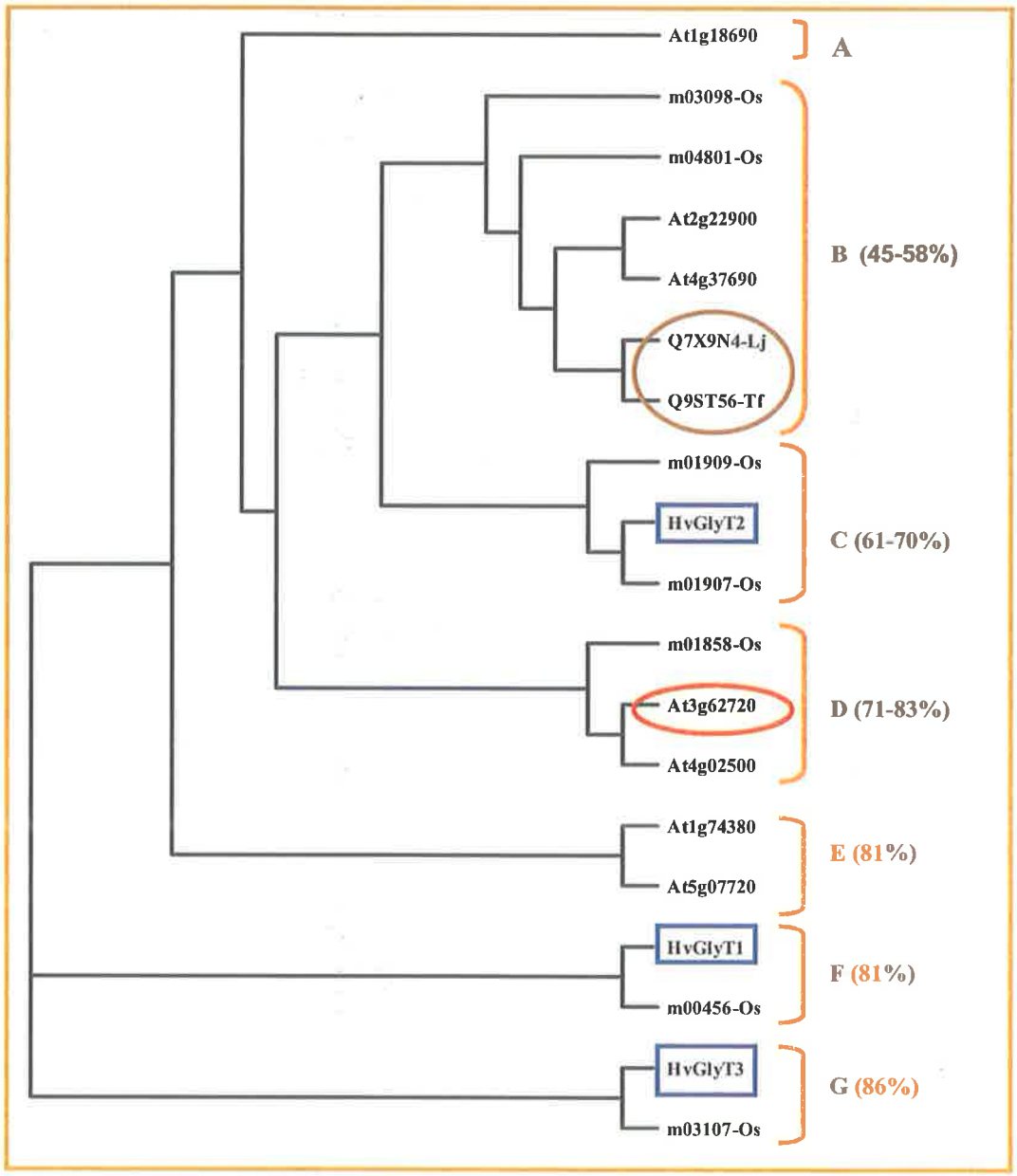

Figure 2.20 Phylogenetic tree of the glycosyltransferases in family GT34. The sequences are tentatively divided into seven groups A-G. Fenugreek and Lotus α-(1→6) galactomannan galactosyltransferases are in group B as indicated by a brown circle. *Arabidopsis* α-(1→6) xyloglucan xylosyltransferase is in group D as indicated with an red circle. The barley clones are shown in blue boxes. *Arabidopsis* sequences start with At. The sequences that end with Os, Tf and Lj are from rice (*Oryza sativa*), fenugreek (*Trigonella foenum*) and *Lotus japonicum*, respectively. The numbers on the right represent the range of percentage amino acid sequence identity within each group. HvGlyT5 and a partial *Arabidopsis* sequence (At4g38310.1) were excluded from the tree.

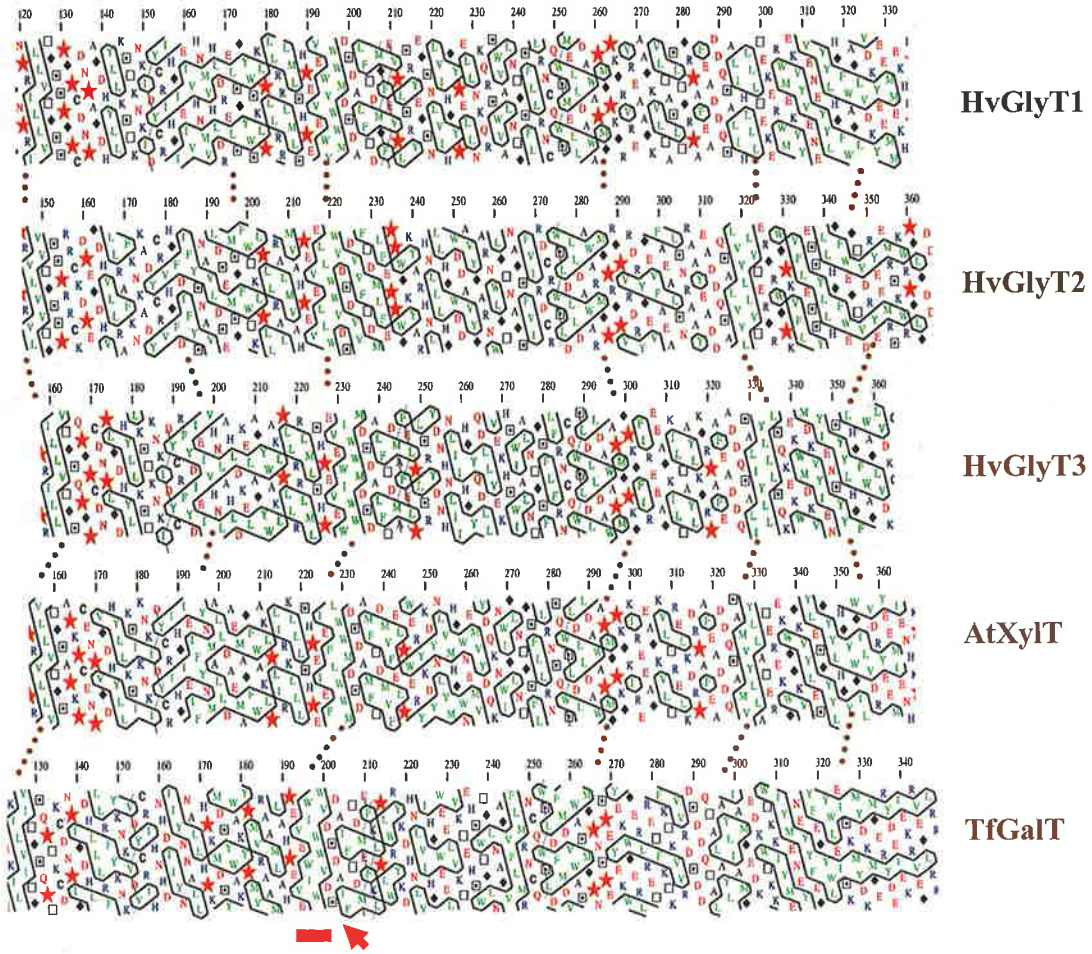

Figure 2.21 Hydrophobic cluster analysis of partial barley glycosyltransferases and functionally defined members of family GT34. The figure illustrates the conserved secondary structure of the peptides in the same family. The numbers indicate amino acids in the primary structure of the proteins. The dotted brown lines connecting the profiles illustrate a highly similar pattern of β-strands and α-helices between the secondary structures of these sequences. The dark red line indicates the presence of a hydrophobic cluster just prior to the DxD motif, indicated by a red arrow. Star = proline, diamond = glycine, square with a point = serine, empty square = threonine. Horizontal and vertical boxes represent α-helices and β-strands, respectively.

	HvGlyT1	HvGlyT2	HvGlyT3	AtXylT	TfGalT
HvGlyT1	-	-	-	-	-
HvGlyT2	45.6	-	-	-	-
HvGlyT3	70.7	43.4	-	-	-
AtXylT	54.7	49.8	55.5	-	-
TfGalT	40.9	41	41	22.2	-

Table 2.2 Comparison of barley glycosyltransferase amino acid sequences with known plant members of family GT34. Comparisons are given in percent sequence identity. AtXylT = *Arabidopsis* xyloglucan (1→6)-α-xylosyltransferase, TfGalT = *Trigonella foenum* galactomannan (1→6)-α-galactosyltransferase.

software. The differences amongst these contigs were very low, and the design of gene-specific PCR primers for each of them was difficult. Based on a region containing a few differing bases, a pair of primers (GUT1 and GUT2) were designed. The primers were used in conjunction with the 3'RACE-PCR primers. The PCR produced two bands of different sizes, which were cloned and sequenced. The products corresponded to two of the contigs, namely GUT1 and GUT3. Sequence alignment with *NpGUT1* (Iwai *et al.*, 2002) showed that barley GUT1 contained the putative start codon. An attempt was therefore made to isolate a near full-length GUT1 cDNA. Two antisense primers (GUTAS3 and GUTAS4, Figure 2.22), in conjunction with AP1 and AP2 primers, were used to obtain the 5' end of the sequence *via* PCR-based genomic walking (Section 2.2.17). A fragment of 610 bp, which covered the putative start codon and part of the promoter region, was recovered. Two sense primers (GUT1S and GUT2S, Figure 2.22), in conjunction with 3' RACE-PCR primers, were used to clone a near full-length barley homologue of *NpGUT1* from a root cDNA library. The barley near full-length cDNA clone was named *HvGlyT4*. The nucleotide sequence and deduced amino acid sequence of *HvGlyT4* are shown in Figure 2.22. *HvGlyT4* encodes a protein with a predicted mass of approximately 41 kDa, with a pI of 7.65.

2.3.5 Multiple sequence alignment and the presence of gene families in GT47

Rice and *Arabidopsis* sequences, homologous to family GT47 glycosyltransferases, were retrieved as described in section 2.2.19. The number of sequences in *Arabidopsis* and rice homologous to the *N. plumbaginifolia* glucuronosyltransferase were two and six, respectively. All showed more than 70% sequence identity at the amino acid level. The other homologous sequences were showed 33% sequence identity or less, which were ignored and considered to have different biological role. These highly homologous sequences were used in a MSA together with the barley homologue, a sequence from *N. tabacum* and the functionally characterised *N. plumbaginifolia* glucuronosyltransferase (Figure 2.24). The MSA showed a conserved long amino acid motif that is probably involved in catalytic activity of the enzymes (underlined in red in Figure 2.24). The sequence data were used to generate

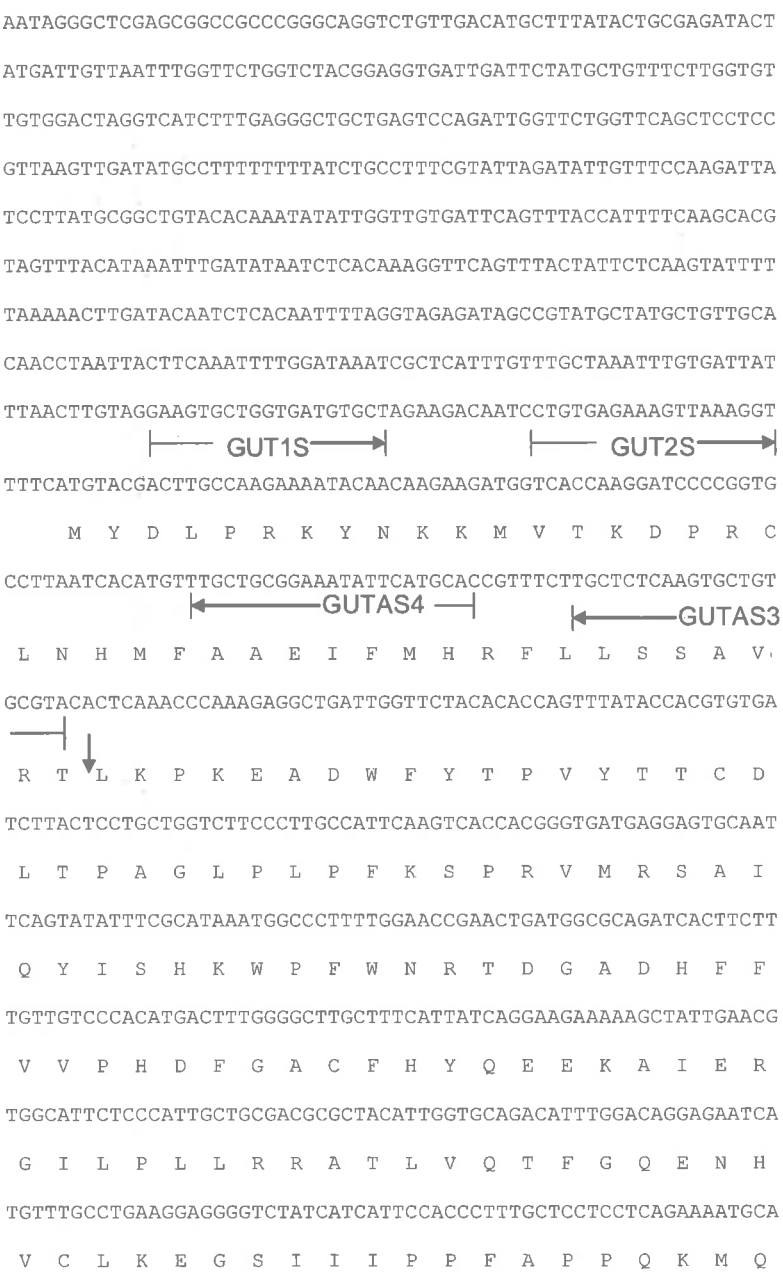
AATAGGGCTCGAGCGGCCGCCCGGGCAGGTCTGTTGACATGCTTTATACTGCGAGATACT
ATGATTGTTAATTTGGTTCTGGTCTACGGAGGTGATTGATTCTATGCTGTTTCTTGGTGT
TGTGGACTAGGTCATCTTTGAGGGCTGCTGAGTCCAGATTGGTTCTGGTTCAGCTCCTCC
GTTAAGTTGATATGCCTTTTTTTTATCTGCCTTTCGTATTAGATATTGTTTCCAAGATTA
TCCTTATGCGGCTGTACACAAATATATTGGTTGTGATTCAGTTTACCATTTTCAAGCACG
TAGTTTACATAAATTTGATATAATCTCACAAAGGTTCAGTTTACTATTCTCAAGTATTTT
TAAAAACTTGATACAATCTCACAATTTTAGGTAGAGATAGCCGTATGCTATGCTGTTGCA
CAACCTAATTACTTCAAATTTTGGATAAATCGCTCATTTGTTTGCTAAATTTGTGATTAT
TTAACTTGTAGGAAGTGCTGGTGATGTGCTAGAAGACAATCCTGTGAGAAAGTTAAAGGT
GUT1S
GUT2S
TTTCATGTACGACTTGCCAAGAAAATACAACAAGAAGATGGTCACCAAGGATCCCCGGTG
M Y D L P R K Y N K K M V T K D P R C
CCTTAATCACATGTTTGCTGCGGAAATATTCATGCACCGTTTCTTGCTCTCAAGTGCTGT
GUTAS4
GUTAS3
L N H M F A A E I F M H R F L L S S A V
GCGTACACTCAAACCCAAAGAGGCTGATTGGTTCTACACACCAGTTTATACCACGTGTGA
R T L K P K E A D W F Y T P V Y T T C D
TCTTACTCCTGCTGGTCTTCCCTTGCCATTCAAGTCACCACGGGTGATGAGGAGTGCAAT
L T P A G L P L P F K S P R V M R S A I
TCAGTATATTTCGCATAAATGGCCCTTTTGGAACCGAACTGATGGCGCAGATCACTTCTT
Q Y I S H K W P F W N R T D G A D H F F
TGTTGTCCCACATGACTTTGGGGCTTGCTTTCATTATCAGGAAGAAAAAGCTATTGAACG
V V P H D F G A C F H Y Q E E K A I E R
TGGCATTCTCCCATTGCTGCGACGCGCTACATTGGTGCAGACATTTGGACAGGAGAATCA
G I L P L L R R A T L V Q T F G Q E N H
TGTTTGCCTGAAGGAGGGGTCTATCATCATTCCACCCTTTGCTCCTCCTCAGAAAATGCA
V C L K E G S I I I P P F A P P Q K M Q

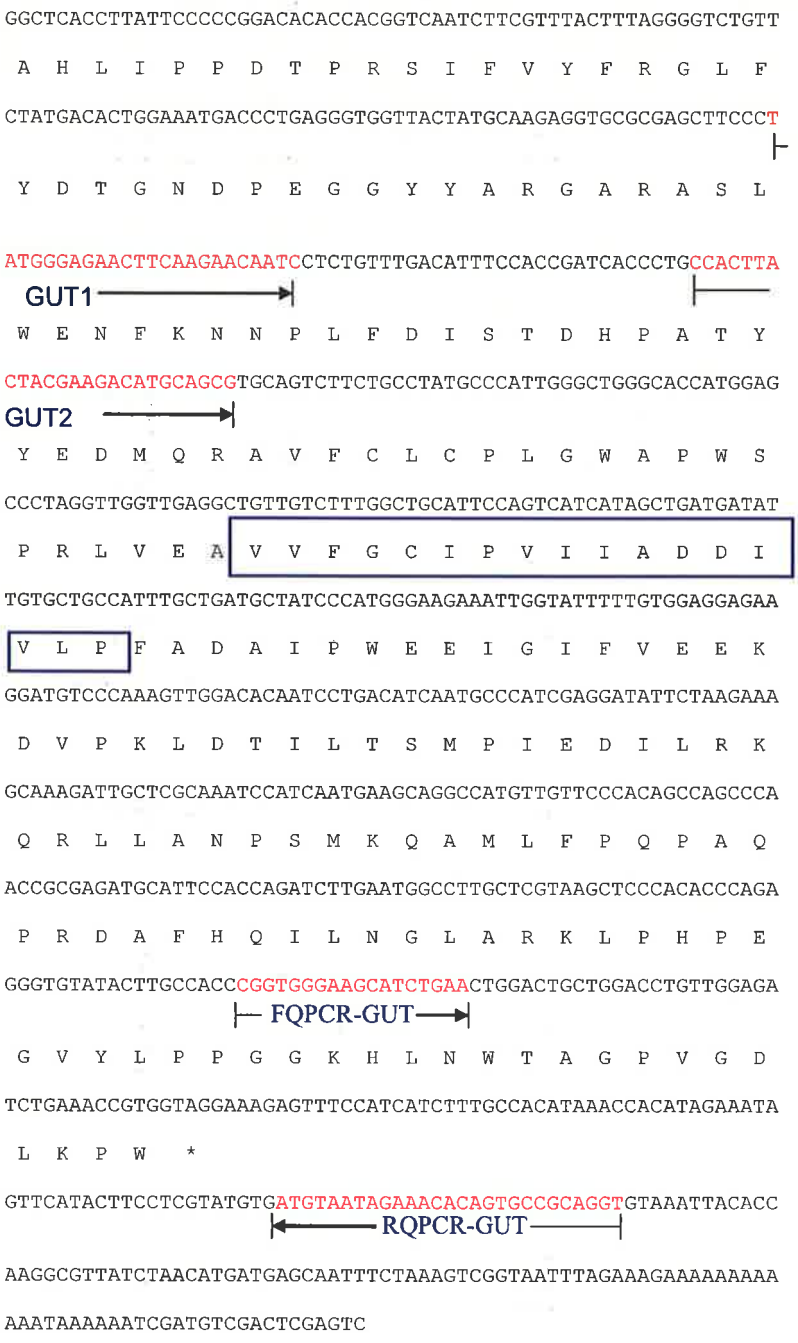

Figure 2.22 The nucleotide and deduced amino acid sequence of *HvGlyT4*. The predicted 17 amino acid highly hydrophobic cluster is enclosed in a blue box between amino acid numbers 245-261. The predicted signal peptide cleavage site is shown by a red arrow. The primers which were used to isolate the HvGlyT4 cDNA are highlighted in red and arrows indicate their orientations.

a phylogenetic tree using the TCoffee program, which presented using the TreeView software (Figure 2.25). The tree illustrated the tentative presence of four groups A-D, and group B was further separated into subgroups I-II.

2.3.6 Protein analysis of HvGlyT4

SignalP V2.0.b2 was used to predict a signal peptide cleavage site, which is indicated by a red arrow in Figure 2.22. The positions of two predicted glycosylation sites in the structure of HvGlyT4 are shown in Figure 2.23. A hydropathy plot and PSORT II were used to predict a TMH in HvGlyT4; the result showed that HvGlyT4 contained a very hydrophobic region near the COOH-terminus, which indicates a different topology to type II transferases (Figure 2.23). Thus, HvGlyT4 is most likely to be a peripheral rather than an integral membrane protein. Figure 2.26 shows the secondary structure of HvGlyT4, predicted using the PSIPRED programme. Furthermore, HCA (Figure 2.27) was used to compare the secondary structure of HvGlyT4 with the *N. plumbaginifolia* glucuronosyltransferase. The HCA showed almost identical β-strands and α-helices between the two sequences.

2.3.7 Genetic mapping

The 3′UTR sequences of *HvGlyT1* (primers: GalTUTR5′ and GalTUTR3′, Figure 2.3), *HvGlyT2* (primers: FQPCR-GlyT2 and RQPCR-GlyT2, Figure 2.9), *HvGlyT3* (primers: FGlyT1A-QPCR and RGlyT1A-QPCR, Figure 2.14), *HvGlyT4* (primers: FQPCR-GUT and RQPCR-GUT, Figure 2.22) and *HvGlyT5* (primers: FQPCR-GlyT5 and RQPCR-GlyT5, Figure 2.18) were PCR amplified. The PCR fragments were sequenced as described in section 2.2.8 and radioactive probes were prepared as described in section 2.2.13. *HvGlyT1*, *HvGlyT2*, *HvGlyT3* and *HvGlyT4* probes failed to detect any polymorphism amongst the sixteen barley parental lines and these genes could not be located on the detailed barley genetic map. However, wheat-barley

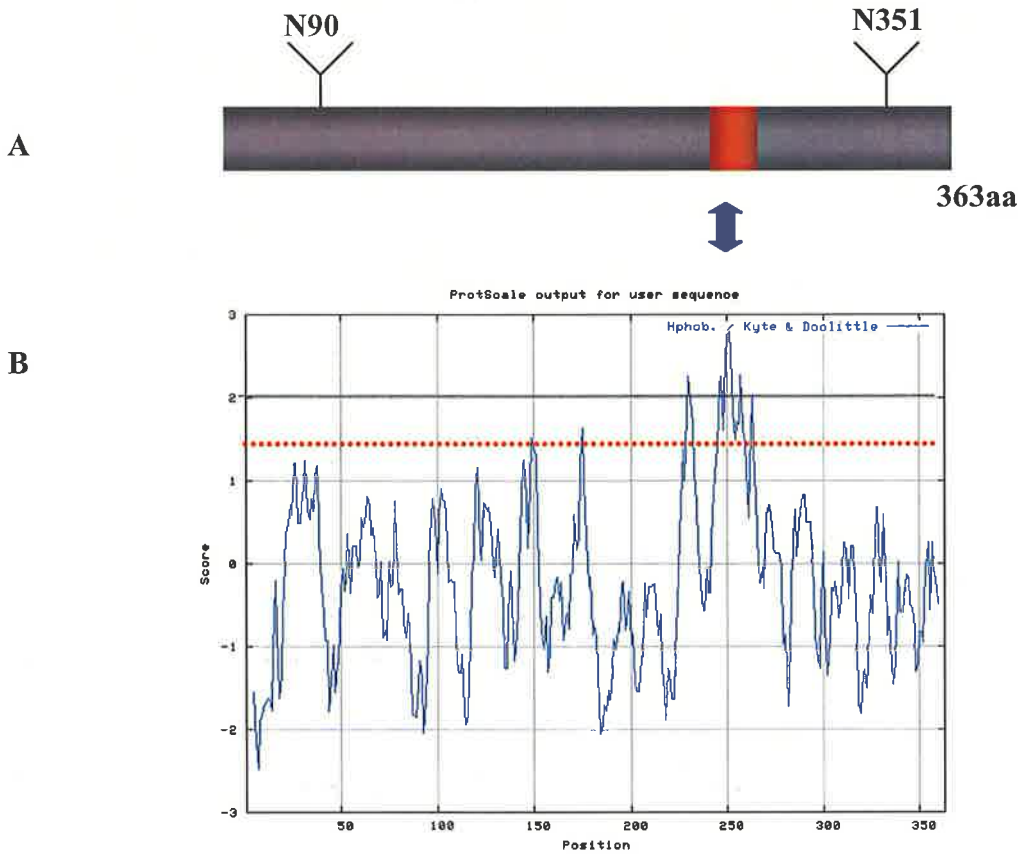

Figure 2.23 Secondary structural prediction of HvGlyT4. **A**: Schematic representation of the *HvGlyT4* protein. The predicted putative glycosylation sites and the hydrophobic region and the number of amino acids are shown. **B**: Hydropathy plot using the Kyte-Doolittle scale failed to demonstrate a defined TMH near the NH_2-terminus, instead a hydrophobic region was predicted close to the COOH-terminus. However, it is not known if this represents a TMH. Y axis = probability of occurrence of TMH and X axis = number of amino acids.

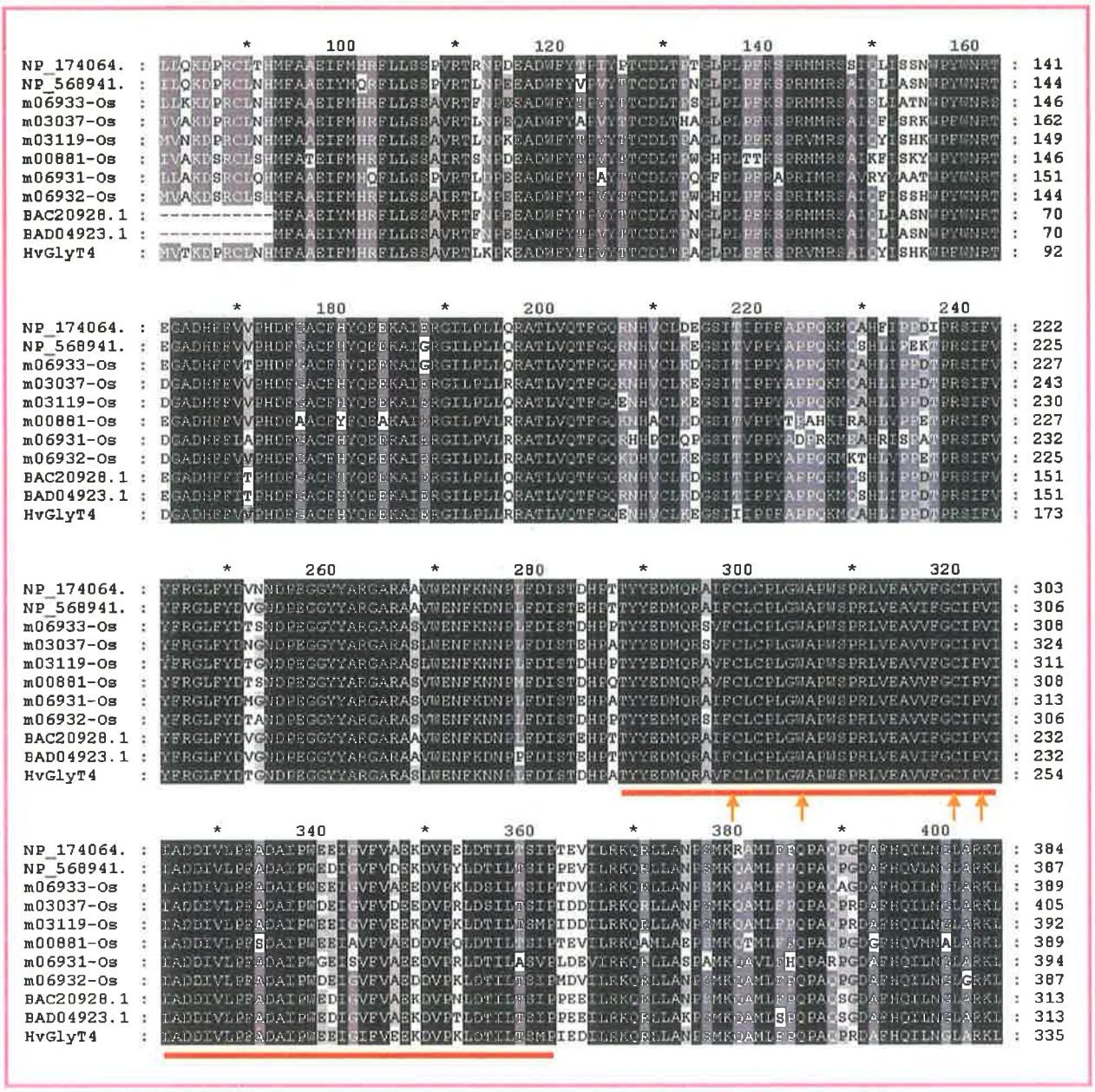

Figure 2.24 Multiple sequence alignment of plant orthologues of HvGlyT4. The TCoffee program was used to align two *Arabidopsis* (Np-174064.1 and NP-568941.1), six rice (ending with Os), *N. plumbaginifolia* (BAC20928.1), *N. tobacum* (BAD04923) and the barley HvGlyT4 sequences. A long amino acid signature motif (underlined in red), which contained amino acid sequences present both in animal and plant kingdoms (Iwai *et al.*, 2002), was recognised. The orange arrows indicate the conserved motifs, including cysteine, glycine, proline and valine in family GT47 (Zhong and Ye, 2003).

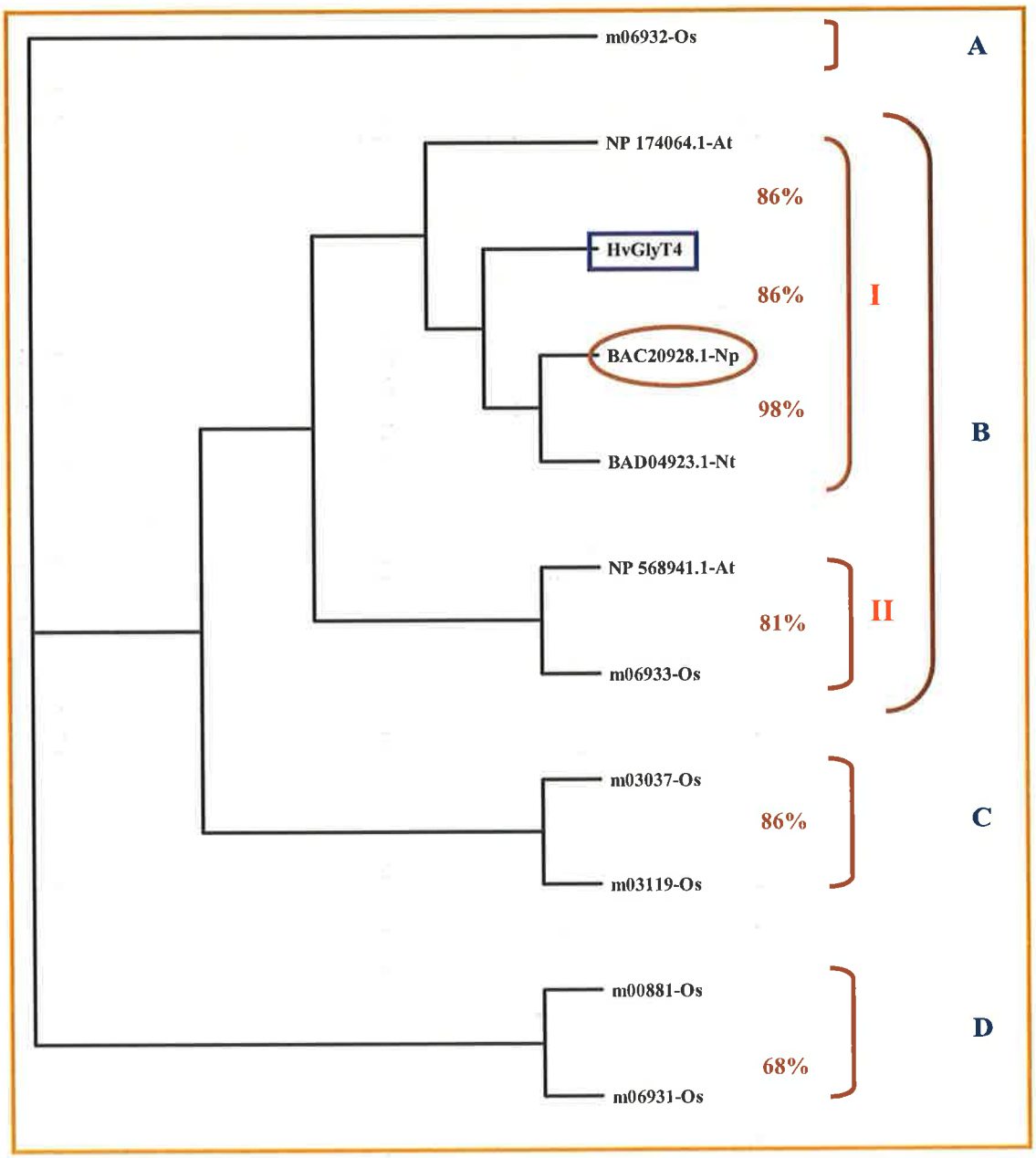

Figure 2.25 Phylogenetic tree of HvGlyT4 and its orthologues. The tree was generated using the TCoffee program and presented using the TreeView software. The tree separates HvGlyT4 orthologues into four clusters A-D; cluster A contains one rice sequence, cluster B contains two subgroups I and II, including two *Arabidopsis* (ending with At), HvGlyT4, *N. plumbaginifolia* (ending with Np), *N. tabacum* (ending with Nt) and one rice sequence (ending with Os), clusters C and D contain two rice sequences each. On the right side of the tree, the identity percentages of amino acids are presented between each pair.

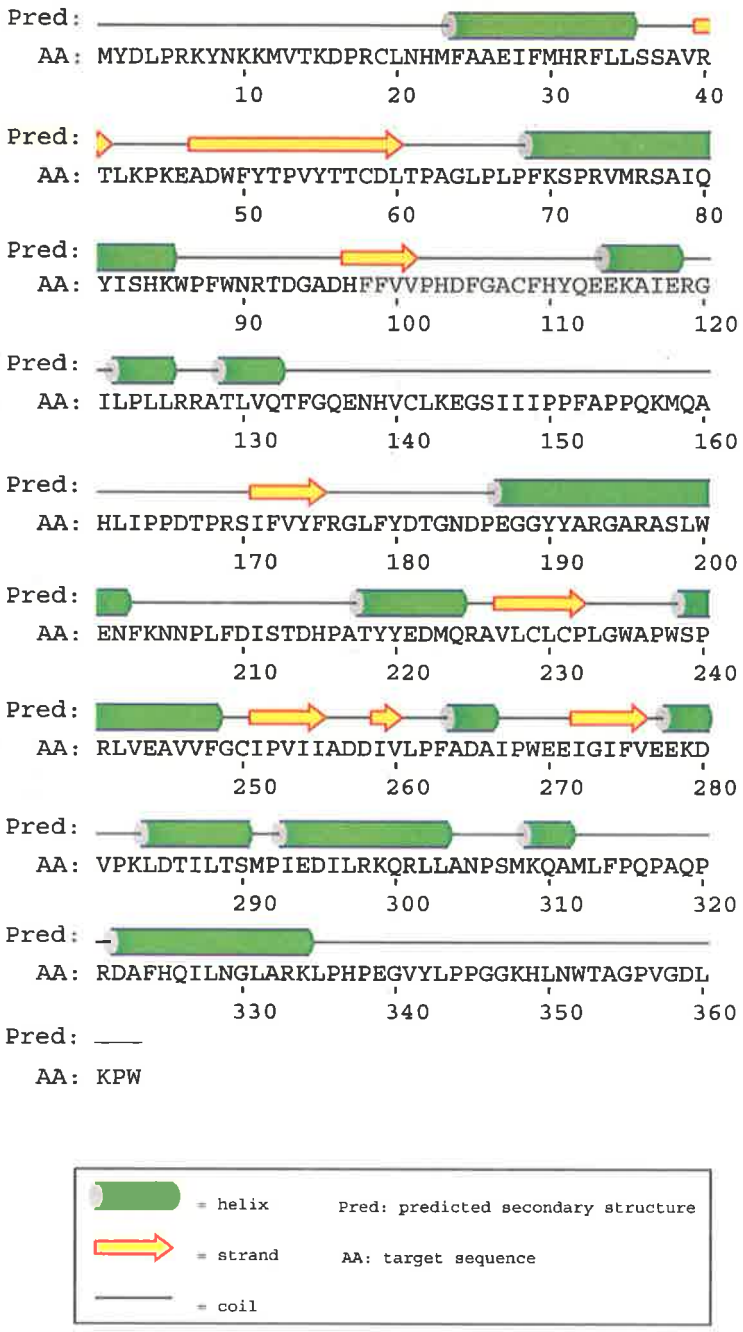

Figure 2.26 Secondary structural element prediction of HvGlyT4 using the PsiPred algorithm. The numbers indicate the amino acids in the primary structure of the protein.

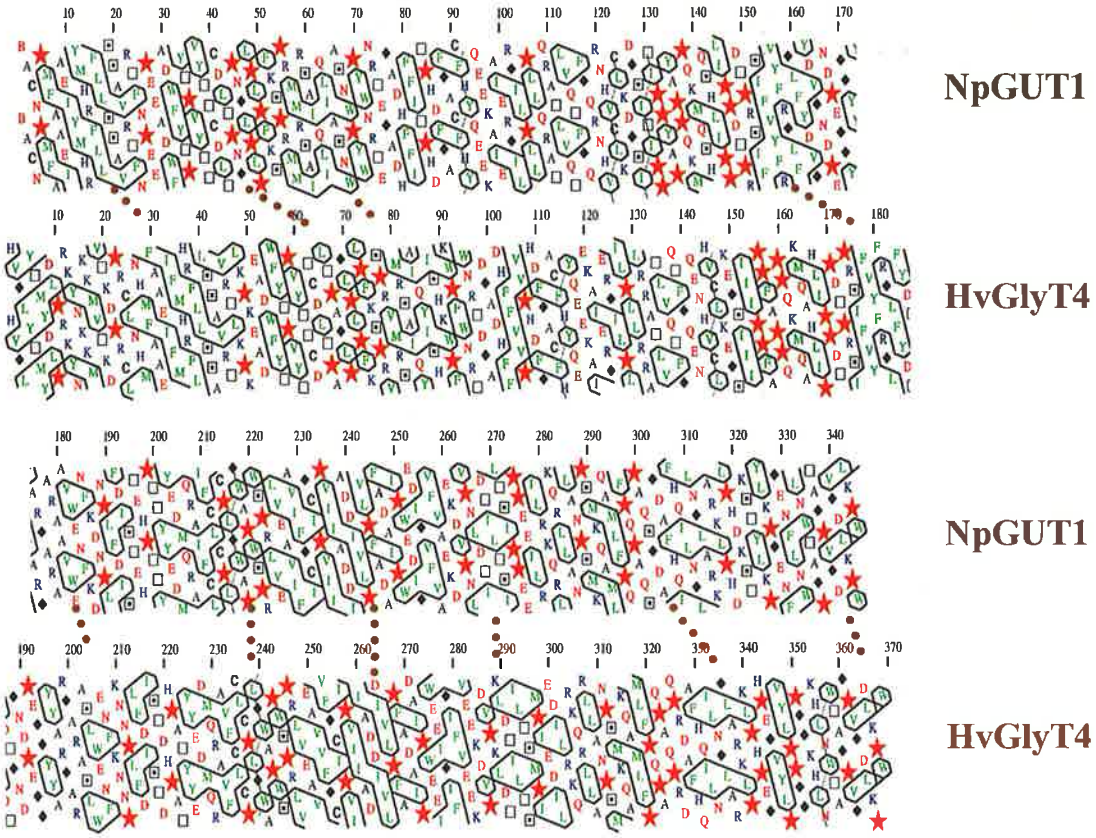

Figure 2.27 Comparison of HCA patterns of HvGlyT4 and *N. plumbaginifolia* glucuronosyltransferase (NpGUT1). The sequences are divided into two parts and the numbers indicate the amino acids in the primary structure of the protein. The dotted brown lines connecting the profiles illustrate very highly identical β-strands and α-helices between these two proteins. Star = proline, diamond = glycine, square with a point = serine, empty square = threonine. Horizontal and vertical boxes represent α-helices and β-strands, respectively.

addition lines were used to assign their map location at the chromosome level. It was shown that *HvGlyT1*, *HvGlyT2*, *HvGlyT3* and *HvGlyT4* are located on chromosomes 5H, 4H, 6H and 2H, respectively (Figure 2.31).

In the case of *HvGlyT5*, sixteen barley parents were screened and polymorphisms were observed between barley varieties Chebec and Harrington and also between Clipper and Sahara (Figure 2.28). In order to investigate the precise map location of *HvGlyT5* within the barley genome, the probe was used against RFLP membranes of 149 double haploid progeny lines of the cross between Clipper and Sahara. The presence and absence of bands was scored to map the location of *HvGlyT5* on a high resolution barley map using Map Manager QTX (Figure 2.29). *HvGlyT5* is located distally on 4HL, and is co-incident with *HvBmy1* (barley β-amylase), showing zero recombination in 104 lines out of 149 lines that were screened (Figure 2.30). This result was further confirmed using the wheat-barley addition lines (Figure 2.31). As mentioned earlier, although the *HvGlyT2* probe did not detect any clear polymorphism in the parental lines, the probe was still used against a doubled haploid population obtained from the cross between Clipper and Sahara. The population showed polymorphism in some lines and the data were collected. When *HvGlyT5* was subsequently mapped, it showed no recombination with *HvGlyT2*, suggesting that they are closely linked and therefore that *HvGlyT2* is possibly found at the same locus as *HvGlyT5*.

Figure 2.28 Southern analysis of barley parental lines probed with *HvGlyT5* 3'UTR. Arrows shaded in red indicate the polymorphism between Chebec (Lane 3) and Harrington (Lane 4) and arrows shaded in yellow indicate the polymorphism between Clipper (Lane 5) and Sahara (Lane 6). The left panel shows restriction digests of extracted DNA from 16 barley varieties with *Bam*HI. The right panel depicts restriction digests of the same DNA samples with *Dra*I. M = DNA size marker, 1 = Galleon, 2 = Haruna Nijo, 3 = Chebec, 4 = Harrington, 5 = Clipper, 6 = Sahara, 7 = Alexis, 8 = WI 2875-1, 9 = Sloop, 10 = Halcyon, 11 = Arapiles, 12 = Franklin, 13 = WI 2585, 14 = Amagi Nijo, 15 = VB 9524, 16 = ND 11231-12.

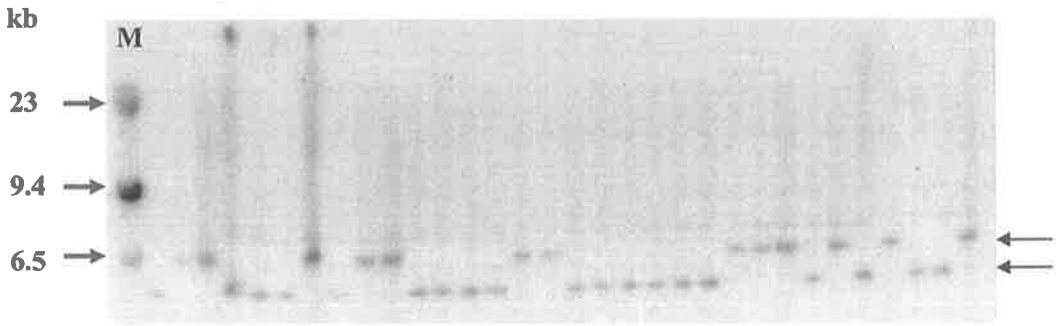

Figure 2.29 Southern analysis of doubled haploid population obtained from the cross between Clipper × Sahara, probed with *HvGlyT5* 3'UTR. A representative section of the population is shown. The black arrows indicate the presence or absence of bands. The genomic DNA from the progeny was digested with *Bam*HI.

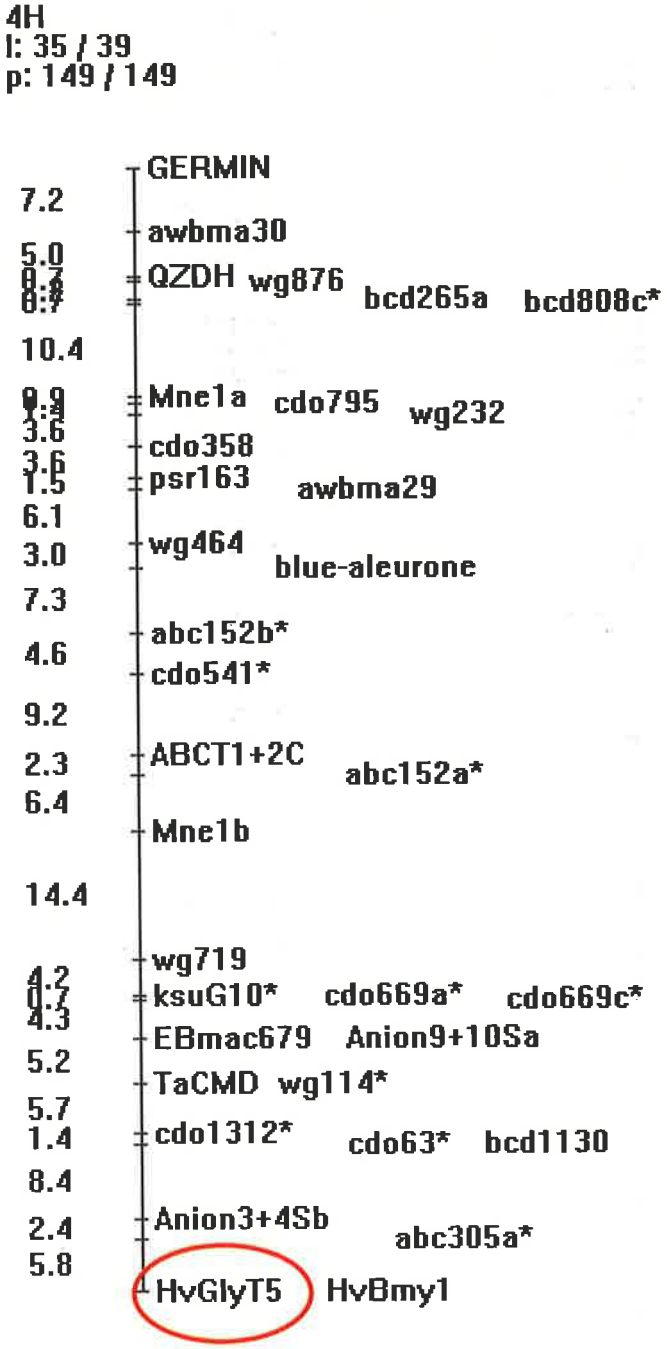

Figure 2.30 The map location of *HvGlyT5* on the long arm of chromosome 4H. The red circle shows the *HvGlyT5* locus linked to *Hvbmy1*. No other markers have been identified distal to the *HvGlyT5* gene. Numbers indicate the distance between markers in centiMorgans.

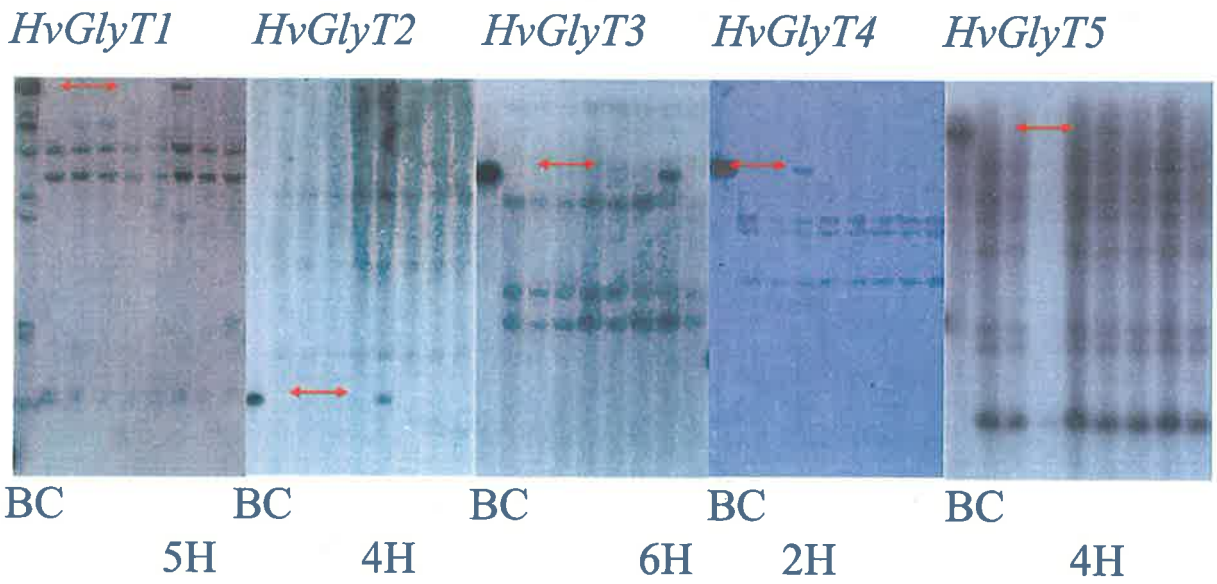

Figure 2.31 Map location of *HvGlyTs* using addition lines. Addition lines were used to locate *HvGlyT1*, *HvGlyT2*, *HvGlyT3*, *HvGlyT4*, and *HvGlyT5* on chromosomes 5H, 4H, 6H, 2H, and 4H, respectively. M is the DNA size marker. C is the Chinese Spring wheat parent and B is the Betzes barley parent. Red arrows indicate the positive bands on each blot. The probes used for Southern analysis were obtained from 3′UTRs.

2.4 DISCUSSION

In the Chapter, experiments are described through which members of glycosyltransferase families GT34 and GT47 from barley have been isolated and characterised. This was the first step in a broader strategy to identify glycosyltransferase enzymes responsible for the addition of α-L-arabinosyl and α-D-glucuronosyl residues to (1→4)-β-D-xylan chains during arabinoxylan biosynthesis in barley. Given that there was no real indications from the literature as to which family might contain these enzymes, barley orthologues to putative glycosyltransferase genes from plants were cloned progressively as the sequences of the other plant genes were reported. In the following sections, the results obtained for these putative barley glycosyltransferases from the two families GT34 and GT47 are discussed.

2.4.1 Barley members of family GT34 glycosyltransferases

Following the report of the isolation and functional assignment of *Trigonella foenum-graecum* galactomannan (1→6)-α-galactosyltransferase (Edwards *et al.*, 1999), the barley EST database was searched with this sequence to identify homologues. As the project progressed, the search led to the isolation of four partial-length barley ESTs belonging to family GT34. Three near full-length cDNAs, designated *HvGlyT1-3,* and one partial-length cDNA, designated *HvGlyT5*, corresponding to barley glycosyltransferases were eventually isolated (Figures. 2.3, 2.9 and 2.14). Genetic mapping demonstrated that the genes were scattered across the genome on different chromosomes. These data confirmed the existence of a GT34 gene family in barley. Similar results were obtained when the *Arabidopsis* genome was searched, resulting in the identification of eight members in family GT34 (Faik *et al.,* 2002). Also, an *in silico* analysis of the rice genome revealed the existence of a gene family containing seven members (data not shown). This suggested that the barley gene family might also contain 7-8 members, although only four representatives were isolated here. Nevertheless, it was likely that the four barley glycosyltransferase cDNAs represented the most highly expressed members of the GT34 gene family in barley.

The barley genes belonging to family GT34, as with homologues in *Arabidopsis* and rice, encode proteins of more than 400 amino acid residues in length. Structurally, and moving from the NH_2- to the COOH-terminus, the proteins contain a short cytosolic region, a TMH, a loosely-defined stem region and a catalytic domain that is possibly oriented towards the lumen of the Golgi. This structure is typical of type II membrane-bound glycosyltransferases [Figures 2.4, 2.10 and 2.15 (Kleene and Berger, 1993; Breton and Imberty, 1999)]. It has been shown that the hydrophobic amino acids present in the TMH have a role in plant glycosyltransferase retention in the Golgi membrane (Pagny *et al.,* 2003). However, amino acid replacement in the TMH seems to have no effect in targeting the enzyme to the Golgi (Colley *et al.,* 1992). Hydrophobic cluster analysis of the stem region, containing a stretch of hydrophilic amino acids that is located between the catalytic domain and the TMH, also shows a proline rich area (Figures. 2.4, 2.10 and 2.15, Panel C) that might be important in the stability of type II membrane proteins (Pagny *et al.*, 2003).

In many cases the predicted putative signal peptide cleavage site was located within the putative TMH (Figures 2.3, 2.9 and 2.14). While it is assumed that the TMH sequences are real, and serve to anchor the mature glycosyltransferases into membranes, this remains to be demonstrated experimentally. A DxD motif just after a hydrophobic cluster of amino acids, which is believed to be involved in coordination of the divalent cation associated with the activated sugar nucleotide (Breton *et al.,* 1998), is present in all plant protein sequences belonging to family GT34 (Figure 2.19). This motif, containing negatively charged residues, appears in a loop after a hydrophobic cluster of amino acids (Figures 2.5, 2.11 and 2.16), possibly bringing it up to the surface of the protein molecule and making it accessible for substrate binding. However, there are no reported three-dimensional structures for family GT34 enzymes, so this remains speculative.

Multiple sequence alignments of plant members of family GT34 (Figure 2.17) reveal that they can be classified into two main groups: one contains an internal sequence of approximately 50 amino acid residues that is seen in the fenugreek galactomannan (1→6)-α-galactosyltransferase (Edwards *et al.*, 1999) and the other does not contain this sequence, as seen in the *Arabidopsis* xyloglucan (1→6)-α-xylosyltransferase

(Faik *et al.*, 2002). All the barley members of the GT34 family so far isolated belong to the latter group and resemble the primary structure of the *Arabidopsis* xyloglucan (1→6)-α-xylosyltransferas. The phylogenetic analyses separate the plant members of family GT34 into seven main groups (Figure 2.20). In most cases, barley members fall into the same cluster as rice members, as expected. The percentage amino acid sequence identity between orthologues appears to be higher than that between the paralogues within a given species (Figure 2.20).

The number of predicted α-helices and β-strands also differ among the barley glycosyltransferases, as shown in Figures 2.5, 2.11 and 2.16. Excluding the TMH, HvGlyT1, HvGlyT2 and HvGlyT3 contain 11, 13, 16 and 8, 14 and 11 α-helices and β-strands, respectively. Thus, while these barley enzymes all belong to family GT34, they nevertheless carry significant variation in secondary structures, which may suggest differences in tertiary structures. This may have a bearing on solving the crystal structure of members of this family, although at this stage no three dimensional structures are available for family GT34 glycosyltransferases.

2.4.2 Barley members of the family GT47 glycosyltransferases

Subsequent to the isolation of a rhamnogalacturonan II β-glucuronosyltransferase from *N. plumbaginifolia* (*NpGUT1*) (Iwai *et al.*, 2002), a near full-length orthologue of this gene was isolated from barley and designated *HvGlyT4* (Figure 2.22). A fragment of the cDNA was used for mapping purposes, and this located *HvGlyT4* to chromosome 2H (Figure 2.31). The sequence analysis revealed that *HvGlyT4* contains less than 50% GC content (44%) at the third position of codons, despite the fact that monocot genes often contain a higher GC content in this position (Murray *et al.*, 1989). The low GC content presumably results from selection pressure against codon bias. A multiple sequence alignment of plant glycosyltransferase homologues of NpGUT1 is shown in Figure 2.24. The high percentage identity between these sequences (more than 68% at the amino acid level) strongly suggests that relatively little divergence has occurred between monocots and dicots during evolution for this

gene. Furthermore, the high percentage identity suggests the functional relatedness of these genes and that the barley *HvGlyT4* gene might be a β-glucuronosyltransferase.

Animal exotoxin β-glucuronosyltransferases, involved in the synthesis of heparan sulfate, were the first glycosyltransferases to be functionally defined in family GT47 (Lind *et al.,* 1998). Two plant members, *Nicotiana plumbaginifolia* rhamno-galacturonan type II β-glucuronosyltransferase (*NpGUT1*) (Iwai *et al.*, 2002) and *Arabidopsis* xyloglucan β-galactosyltransferases (*mur3*) (Madson *et al.,* 2003), were identified in this family, and these carry the structural motif pfam03016 that is representative of the glucuronosyltransferase domain of animal exostosins (Zhong and Ye, 2003; Li *et al.*, 2004). When Zhong and Ye (2003) aligned all 39 *Arabidopsis* sequences in family GT47, they managed to identify conserved amino acids ($CX_4GX_{17}P$), including cysteine, glycine, proline and valine in the long amino acid signature. Zhong and Ye (2003) showed that the *Arabidopsis* members of family GT47 fall into four major groups (A-D), and that group A can be further divided into four subgroups (I-IV). The *Mur3* gene belongs to group D, whereas *NpGUT1* falls into subgroup I of group A with two of its *Arabidopsis* orthologs. Subgroup I members have a hydrophobic region near the COOH-terminus of the enzyme and lack a defined TMH (Figure 2.21). This suggests that they are either cytosolic or peripheral proteins when compared to the type II glycosyltransferases, which are mostly integral proteins. At this stage it would appear that HvGlyT4 might be a member of subgroup I of group A.

The *HvGlyT4* cDNA encodes a protein of 363 amino acid residues. Its high percentage identity with *NpGUT1* suggests the enzyme is more likely to be a β-glucuronosyltransferase involved in pectin biosynthesis than an α-glucuronosyltransferase involved in arabinoxylan synthesis. The TMH prediction programs failed to identify a TMH, suggesting that HvGlyT4 is less likely to be an integral membrane protein. Multiple sequence alignments (Figure 2.24) revealed the presence of the conserved amino acid residues of family GT47 in HvGlyT4 and its orthologues, which are similar to the conserved sequence motif of pfam036016 from animal enzymes. HCA revealed a highly similar secondary structure between

HvGlyT4 and NpGUT1 (Figure 2.27), which suggested that the two enzymes might also share a similar 3D structure.

On the basis of sequence homology and the functions of related enzymes from other plants, the barley glycosyltransferases belonging to family GT34 are most likely, at this stage, to have an α-xylosyltransferase function and to be involved in xyloglucan biosynthesis. The functional prediction of HvGlyT5 based on amino acid sequence is still pending because a full-length sequence is not yet available. However, the phylogenetic tree (Figure 2.20) groups these sequences away from the *Arabidopsis* xyloglucan (1→6)-α-xylosyltransferase (Faik *et al.*, 2002), which may suggest other functional roles or different acceptor and/or substrate specificities for the barley glycosyltransferases of family GT34. On the other hand, HvGlyT4 contains not only a high percentage sequence identity, but also shares a very similar secondary structure (Figure 2.27), with NpGUT1 (Iwai *et al.*, 2002). These data suggest a similar functional role for HvGlyT4, probably as a β-glucuronosyltransferase involved in the biosynthesis of pectins.

However, these possibilities are based predominantly on sequence similarities and it was decided to examine the transcriptional patterns of the barley glycosyltransferase genes and to attempt to correlate the transcript profiles with those of other candidate genes that might be involved in the synthesis of well-characterised polysaccharides in barley. The transcript profiling experiments are described in the next Chapter.

CHAPTER 3 TRANSCRIPT ANALYSIS OF BARLEY GLYCOSYLTRANSFERASE GENES

3.1 INTRODUCTION

In Chapter 2, the isolation and characterisation of five barley glycosyltransferase cDNAs were described. Although the isolation of the cDNAs was based on the sequences of putative glycosyltransferase genes from other plant species, few of these have been completely characterised with respect to their substrate specificities and functions. Thus, the next objective was to undertake a series of experiments to define the functions of the barley glycosyltransferases isolated in this work. As a first step in this process, transcript analyses were performed to define the locations and relative abundance of mRNAs corresponding to the five cDNAs.

Comprehensive spatial and temporal analyses of transcription patterns of a gene or a gene family, coupled with comparisons with transcript profiles of other genes of known biological function, may provide informative clues as to the function of the target genes. Northern blots, *in situ* hybridisation (Parker and Barnes, 1999), RNAse protection assays (Hod, 1992; Saccomanno *et al.*, 1992), reverse transcription polymerase chain reaction (RT-PCR) (Weis *et al.*, 1992), cDNA arrays (Bucher, 1999), and quantitative real-time PCR (Higuchi *et al.*, 1992; Higuchi *et al.*, 1993) are methods that have been widely used to measure transcript levels.

Northern hybridisation analysis can be used to assess the size and quality of isolated RNA (Bustin, 2000). *In situ* hybridisation (Parker and Barnes, 1999) has been used to locate a transcript to a specific tissue or cell type. The RNAse protection assay (Hod, 1992; Saccomanno *et al.*, 1992) provides valuable information regarding the start codon and location of exons and introns in a gene. However, the major disadvantages of these three methods, despite the wealth of information that they provide, are their low sensitivity, labour intensive nature and low-throughput capacity (Bustin, 2000; Ding and Cantor, 2003). Screening of a cDNA microarray provides information about differentially expressed genes and the relative abundance of transcripts in a variety of tissues in a high throughput manner, but this technique requires sophisticated instruments to manufacture the cDNA arrays and specialised software for interpretation of what is usually cumbersome and sometimes confusing data (Ding

and Cantor, 2003). Compared with the methods mentioned above, RT-PCR is a relatively quick and sensitive technique used to quantify, approximately at least, the transcript level of a gene within a tissue or cell type (Wang and Brown, 1999). In RT-PCR, isolated mRNA is converted into a complementary DNA (cDNA) *via* reverse transcriptase, and the cDNA molecules corresponding to the mRNA of interest are amplified by means of specific primers (Rappolee *et al.,* 1989).

The mRNA level of a particular gene can be measured either semi-quantitatively or quantitatively (Ferre, 1992). In the semi-quantitative method, a sample of the PCR products is taken for dot blot analysis (Montgomery and Dallman, 1997) to compare the amounts from different tissues. Competitive and non-competitive RT-PCR are two versions of a quantitative method based on how the PCR is set up (Wang *et al.*, 1989; Vanden Heuvel *et al.*, 1993; Bustin, 2000). In competitive RT-PCR, the target sequence is co-amplified next to an increasing amount of standard RNA sample in which the same primer recognition sites and internal sequence are present (Freeman *et al.*, 1999; Bustin, 2000). The standard and the target sequences compete with each other for amplification using the same PCR reagents. The different amounts of standard allow the calculation of a "standard curve" for quantification of the target sequence (Bustin, 2000). The amplicons can be distinguished from each other by incorporating a restriction site or an intron in the standard (Gilliland *et al.,* 1990). In a recent development, a high-throughput matrix-assisted laser desorption ionization time-of-flight (MALDI-TOF) mass spectroscopy (MS) technique was used to differentiate and separately quantify the standard from the target sequence (Ding and Cantor, 2003). This technique, known as real competitive PCR (rcPCR), is capable of quantifying the absolute amount of transcripts in a highly sensitive and reproducible fashion (Ding and Cantor, 2003).

In non-competitive RT-PCR, a dilution series of a previously amplified target sequence is provided as a standard that is run in parallel with the synthesis of the target cDNA. The standards provide a range of absolute cDNA quantity at the same time that they are used to assess the relative abundance of target sequence within the transcripts present in a given cell or tissue. The amount of the amplified products can be measured either by gel electrophoresis and band intensity measurements, or by

equipping the PCR machine with fluorescent detection capabilities to detect the quantity of fluorescent PCR products (Bustin, 2000). In the latter application, the quantity of PCR products is measured instantaneously, at each PCR cycle, so the technique is called Real-Time Quantitative RT-PCR (McMaugh and Lyon, 2003). In this thesis, this is referred to as Q-PCR.

Q-PCR is currently the method of choice for accurate gene expression analysis. It provides a rapid and sensitive quantification technique for measurement and detection of nucleic acids (Ding and Cantor, 2004). Despite its benefits, Q-PCR has some disadvantages, including tube to tube variation, being relatively low-throughput compared with some other techniques, and because of the need for expensive chemicals and instruments (Ding and Cantor, 2004).

Q-PCR quantifies the amount of transcripts by tracking the level of fluorescence in the reaction. An increase in fluorescence is proportional to the accumulation of amplified DNA in real time (Ding and Cantor, 2004; Gachon *et al.*, 2004) (Figure 3.1). Ethidium bromide was the first intercalating dye used to quantify the amount of nucleic acid present (Wittwer *et al.,* 1997; Wittwer *et al.,* 1997), but because of its relatively lower affinity for double stranded DNA, it has been replaced with other dyes (Gachon *et al.,* 2004). With regards to the chemistry of fluorescent dyes, three types are available (Bustin, 2000; McMaugh and Lyon, 2003). These include intercalating compounds such as SYBR Green (Morrison *et al.,* 1998), dual fluorescence resonance energy transfer (FRET) based on excitation (Wittwer *et al.,* 1997), and quenching probes (Heid *et al.*, 1996; Tyagi and Kramer, 1996; Whitcombe *et al.*, 1999). The latter two chemistry types are not used in work described in this thesis and will not be discussed further.

SYBR Green I, the most commonly used dye in Q-PCR, is a dsDNA-specific binding dye, which binds largely to the minor groove of DNA, with more than 100 times the affinity of ethidium bromide (Wilhelm and Pingoud, 2003). The emitted fluorescence from the bound dye is much higher than the free dye, which makes the monitoring of

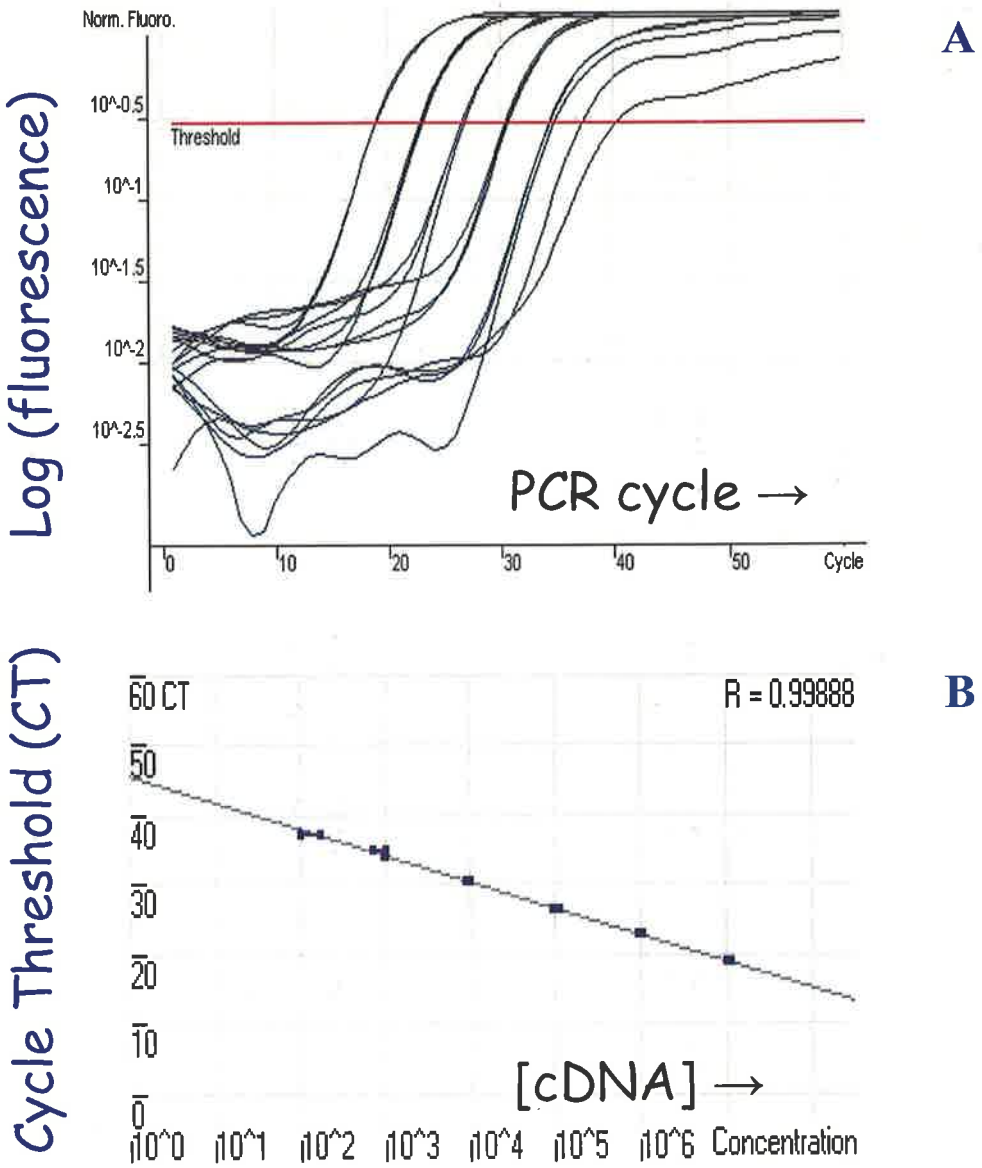

Figure 3.1 The graphs generated by a Q-PCR run (graphs taken from Corbett Rotogene software version 4.0). **A**: Intercalation of SYBR Green into the dsDNA PCR products causes the fluorescence signal to increase as the reaction proceeds and passes the threshold line. Threshold line is the point of detection of fluorescence at which reaction fluorescence intensity reaches above the background level. The X axis is the number of PCR cycles and the Y axis is the logarithmic value of the fluorescence signal. **B**: The relationship of accumulated DNA concentration with cycle threshold (CT) through a linear regression. CT is the cycle at which the sample crosses the threshold line. CT is normally 10 times the standard deviation of the average fluorescence signal and under perfect conditions equals to the inverse logarithmic amount of template concentration (Gibson *et al.*, 1996; Ding and Cantor, 2004). R = linear correlation coefficient.

the amplified product possible during PCR (Wittwer *et al.,* 1997; Morrison *et al.,* 1998). The precision of SYBR Green I in quantification is reported to be as high as other fluorescence dyes mentioned earlier (Schmittgen *et al.,* 2000; Wilhelm *et al.,* 2003). In this project, the SYBR Green I detection dye was used to quantify transcript levels throughout the Q-PCR procedure.

Q-PCR provides one dimensional information of the transcript amounts within a tissue or a cell type. It considers one gene at a time and measures its transcript level independently of other processes within a given cell or a tissue. One way to investigate the spatial relationships of the genes, their probable involvement in a particular pathway (*e.g.* cell wall biosynthesis), or their controlled co-expression with other genes, is to consider the transcript values of these genes obtained *via* Q-PCR and establish a bivariate correlation. The correlation data can be presented as a cluster of co-ordinately expressed genes in a number of tissues. Although the correlation analyses are informative, it is important to consider that two or more series of data might bear a high correlation without having any actual functional relationship. Apart from looking at one gene at a time through Q-PCR, one can take advantage of the high-throughput methods that were introduced in Chapter One (section 1.3.2). These techniques, including oligonucleotide arrays, provide information about the presence or absence of mRNAs and also the magnitude of up- or down-regulation of gene expression within different tissues or cells of a single organism. In this manner, genes that might be jointly involved in a particular pathway can be identified or characterised through their similar transcript profiles.

In this Chapter, transcriptional profiling of barley glycosyltransferases was performed through Q-PCR and *in silico* analysis of microarray data in a range of tissues from barley.

3.2 MATERIALS AND METHODS

3.2.1 Materials

QuantiTect SYBR Green PCR reagent was purchased from Qiagen (Valencia, CA, USA). pUC19 was from Geneworks (Adelaide, SA, Australia). Restriction enzymes were obtained from New England BioLabs, Inc. (Beverly, MA, USA). Triethyl ammonium acetate and acetonitrile were purchased from BDH (England). EDTA was obtained from Merck Pty Ltd (Vic, Australia). The Zorbax Eclipse DS DNA column used on the HPLC was from Agilent Technologies (Palo Alto, CA, USA). HPLC was performed on a series II 1090 liquid chromatograph, which was purchased from Hewlett-Packard (Palo Alto, CA, USA). Big Dye 2, Big Dye 3 reagents and SYBR Green I dye were from Applied Biosystems (Foster City, CA, USA). The Rotor Gene 23000 Real-Time Cycler coupled with DNA sample analyser v4.2 software was purchased from Corbett Research (Martlake, NSW, Australia).

3.2.2 Growth of barley tissues

Dr. Rachel Burton (University of Adelaide, SA, Australia) isolated total RNA and synthesised cDNA preparations for 10 barley tissues, as described below. This series of cDNAs is referred to as the barley "tissue series", and has been used in several extensive transcript analyses as described by Burton *et al.* (2004).

Leaf tissues were prepared by germinating barley grains (cv. Sloop) in damp vermiculite in the dark for 3 days at 20°C until the coleoptiles emerged. Germinated grains were transferred to a light/dark regime of 14/10 h at 20°C for a further three days. The first leaves of the barley seedlings were harvested and divided into five segments (A-E); "A" for leaf tip and "E" for leaf base as shown in Figure 3.2. Segment "E" includes dividing and some elongating cells, cell elongation is occurring in segment "D", and the maturation of cells has occurred in segments "B" and "C" (Schünmann *et al.*, 1997; Wenzel *et al.*, 2000).

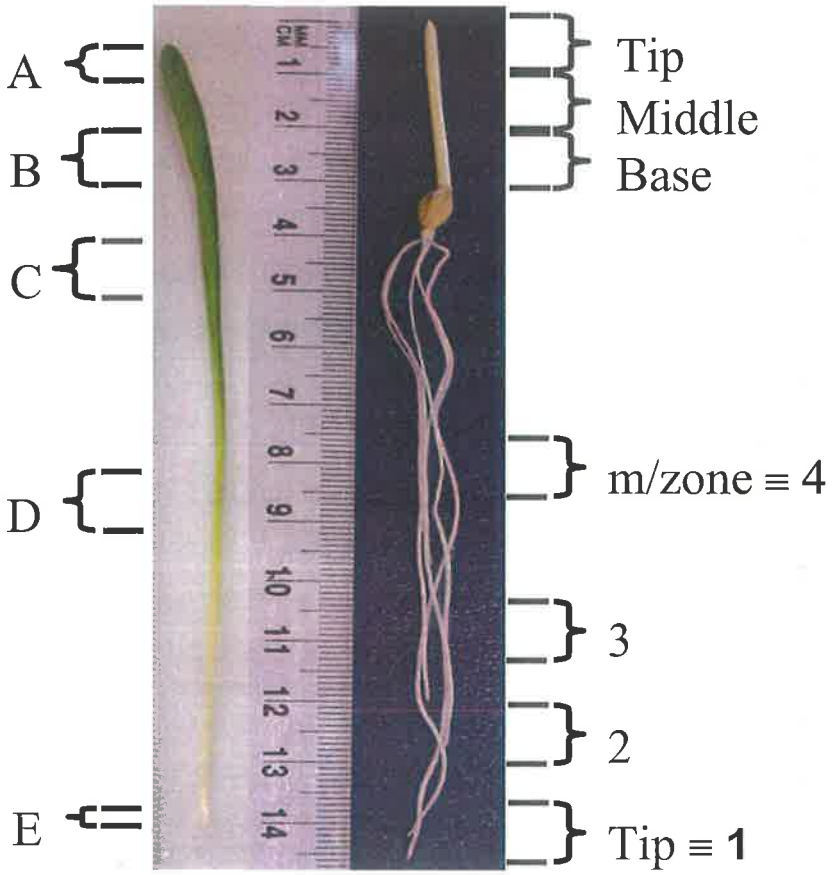

Figure 3.2 Segments of barley vegetative tissues used for isolation of RNA. The leaf sub-sections (A-E) are shown on the left and young root (maturation zone, 3, 2 and tip) and 5-d-old coleoptile segments (tip, middle and base) are depicted on the right. Photo is courtesy of Dr. Rachel Burton.

Root and coleoptile tissues were prepared by germinating barley grains on damp paper towels in the dark for 3-6 days at 20°C. As shown in Figure 3.2, the root was divided into four sub-sections. Cell division and elongation occurs in section 1 (5 mm, containing the root cap, meristem and elongation zone), the completion of cell growth and initiation of secondary wall formation occurs in segment 2 and xylem maturation and lateral root formation occur in segments 3 and 4 respectively (personal communication with Dr. Brian Atwell). The coleoptile tip (shortest cells in coleoptile), middle (fully expanded cells) and base (expanding cells) were also prepared (Figure 3.2).

Floral tissues, stems, developing endosperm and developing grains were prepared by growing barley plants in a greenhouse under a day/night temperature regime of 23°C/15°C. Anthers and pistils were collected at two time points (12-14 days before anthesis and at anthesis). The upper internode of the stem (*i.e.* below the peduncle) was harvested as the mature stem tissue. Developing endosperm was harvested with a needle from 2-11 days post anthesis under a dissecting microscope. Developing grain was harvested at two time points after anthesis (3-5 and 10-13 days).

The harvested tissues were frozen in liquid nitrogen and stored at -80°C. The RNA extraction and cDNA synthesis were performed as described in section 2.2.2. Synthesised cDNAs were used at a 1:10 dilution in the Q-PCR experiments unless the cDNA concentration was very low, in which case undiluted cDNA was used.

3.2.3 Primer design for Q-PCR

Q-PCR uses a fluorescence dye for quantification of the target sequence. Any amplification of non-specific products, such as primer dimers, reduces the efficiency of the measurement and produces systematic errors (Wilhelm and Pingoud, 2003). In our laboratory, Dr. Andrew Harvey (University of Adelaide, SA, Australia) developed a protocol for efficient primer design, utilising a number of software components, which take into account the Q-PCR requirements. The steps involved in primer design were as follows: Primer3 (http://www.broad.mit.edu/cgi-in/primer/primer3_www.cgi)

and Net Primer programs (http://www.primerbiosoft.com/netprimer/netprlaunch/netpralaunch.html), available at the molecular biology tool web site (http://www.molbiol.net), were used to design PCR primers for Q-PCR. For each gene a highly variable sequence of between 150-300 bp was selected for amplification. Initially, Primer3 was used to identify a number of potential primers. Net Primer was used to investigate the potential occurrence of primer dimers and secondary structure formation. A pair of potentially suitable primers identified by this method were checked by a BLAST search against the non-redundant (nr) and EST (est-others) database (http://www.ncbi.nlm.nih.gov/BLAST/). The BLAST results were used to assess the uniqueness of these primers in amplifying the target sequence. The primers were designed to avoid three identical bases in a row and more than two purines in the last 5 bases. Furthermore, primer pairs were designed to contain a hairpin ΔG of less than 0.5 kcal/mol. The ΔG for dimer formation was less than -4.0 kcal/mol and melting temperatures (T_m) of primers varied by only a few degrees.

3.2.4 Determination of fluorescence acquisition temperature

The noise from non-specific binding of primers to the template can be avoided by increasing the temperature at which the fluorescence data is acquired (Bustin, 2000). The optimal temperature can be calculated either through prediction of the amplicon T_m using software programmes such as Primer3 or measuring this directly in the Q-PCR thermocycler. In the present study, the thermocycler (Rotor Gene 23000 Real-Time Cycler) was used to produce a plot of fluorescence as a function of temperature to generate a melting curve (Figure 3.3) for the amplicon following an established protocol (Ririe *et al.,* 1997). The peak of the melt curve (usually ~77°C) was used to determine the optimum temperature at which to collect the fluorescence data (personal communication with Dr. Neil Shirley, University of Adelaide, SA, Australia).

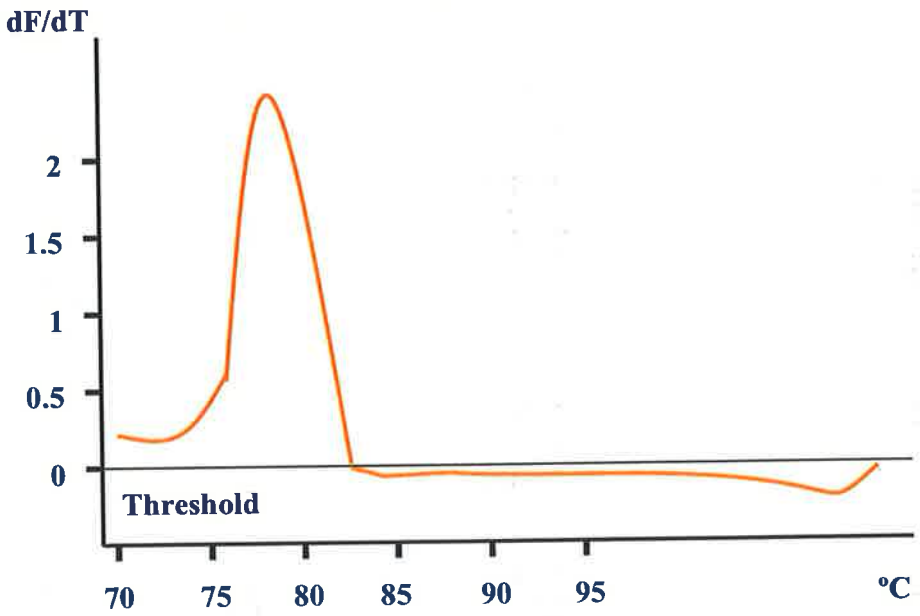

Figure 3.3 Schematic representation of a melt curve. A plot of fluorescence (F) as a function of temperature (T) is generated by the thermocycler. The peak of the melt curve is the optimum temperature for the acquisition of fluorescence data. The thermocycler produces a melt report containing the melt curve and the detected fluorophors' efficiency of the light channels that were used to generate the melt curve.

3.2.5 Q-PCR

Transcript levels were quantified using a Rotor Gene 23000 Real-Time Cycler coupled with DNA sample analyser v4.2 software. Dr. Neil Shirley (University of Adelaide, SA, Australia) is acknowledged for his valuable advice, HPLC purification and quantification of the standard template, and his great assistance in finding suitable control genes for each cDNA and for analysis of the results.

PCR products of both the gene of interest and control genes were amplified from a root cDNA population using specific primers for the barley cultivar Sloop (Table 3.1). It is important to mention that some genes can differ slightly in sequence between barley cultivars and this needs to be considered if another variety is tested by Q-PCR. The PCR mixture contained 10 µl QuantiTect SYBR Green PCR reagent, 3 µl each of 4 µM forward and reverse primers, 3 µl water and 1 µl cDNA template. The PCR was performed with an initial denaturation at 95°C for 15 min, followed by 45 cycles [95°C for 20 sec; 55°C for 30 sec; 72°C for 30 sec], and 80°C for 15 min in an RG 23000 Rotor-Gene Real Time Thermal Cycler. At the end of the amplification, a melt curve was produced by heating the sample from 70°C to 99°C. Fluorescence data were collected at 72°C and 80°C to determine the optimal temperature for acquisition (Table 3.1). The PCR products (four to six independent 20 µl PCRs) were purified by HPLC (Hewlett-Packard series II 1090) on an Agilent Zorbax Eclipse DS DNA column (2.1 mm × 150 mm × 3.5 µm) (Wong *et al.,* 2000). Solution A (100 mM triethylammonium acetate and 0.1 mM EDTA, pH 7.0) and B (100 mM triethylammonium acetate, 0.1 mM EDTA and 25% w/v acetonitrile, pH 7.0) with a flow rate of 0.2 ml/min were used to equilibrate the column and elute the DNA from the HPLC column respectively. HPLC purification of DNA was performed using a gradient range from 35% to 70% of solution B for 30 min (including 10 min equilibration with solution A) at 40°C. The purified PCR products were quantified based on comparison with a peak generated from pUC19 digested with *Hpa*II. The digested fragments (147 bp, 190 bp, 242 bp representing 55 ng, 71 ng and 90 ng respectively) from 2 µl of a 500 ng/µl solution were used as the reference peak (Figure 3.4). An average value of the above data (representing the nanograms per unit

Gene	Forward Primer	Reverse primer	PCR size	Acquisition temperature
			bp	°C
GAPDH	GTGAGGCTGGTGCTGATTACG	TGGTGCAGCTAGCATTTGAGAC	198	80
HSP70	CGACCAGGGCAACCGCACCAC	ACGGTGTTGATGGGGTTCATG	108	83
α-Tubulin	AGTGTCCTGTCCACCCACTC	AGCATGAAGTGGATCCTTGG	248	80
Cyclophilin	CCTGTCGTGTCGTCGGTCTAAA	ACGCAGATCCAGCAGCCTAAAG	122	79
HvElf1	GGTACCTCCCAGGCTGACTGT	GTGGTGGCGTCCATCTTGTTA	164	80
HvCesA1	TGTGGCATCAACTGCTAGGAAA	CGTACAAAGTGCCTCATAGGAAA	267	75
HvGlyT1	GGCGCGCGGCGGGAACAAGTAG	CCTCGGCAACCTTGGCGTCAGC	170	82
HvGlyT2	CCGCCAAGCCATTGTGAT	GAAGAAAGAAGCATCCATTTG	196	79
HvGlyT3	TGGTCTCTTCAAGGTCAG	GTCCCGCAAGAAAGTAGCA	222	77
HvGlyT4	CGGTGGGAAGCATCTGAA	ACCTGCGGCACTGTGTTTC	152	77
HvGlyT5	CTGCGGCGGCAAGCCCAACGAGAT	GCAAGCAACGCTGTCATTTCA	251	77

Table 3.1 QPCR primers and product sizes in base pairs together with optimal acquisition temperatures (Burton *et al.*, 2004).

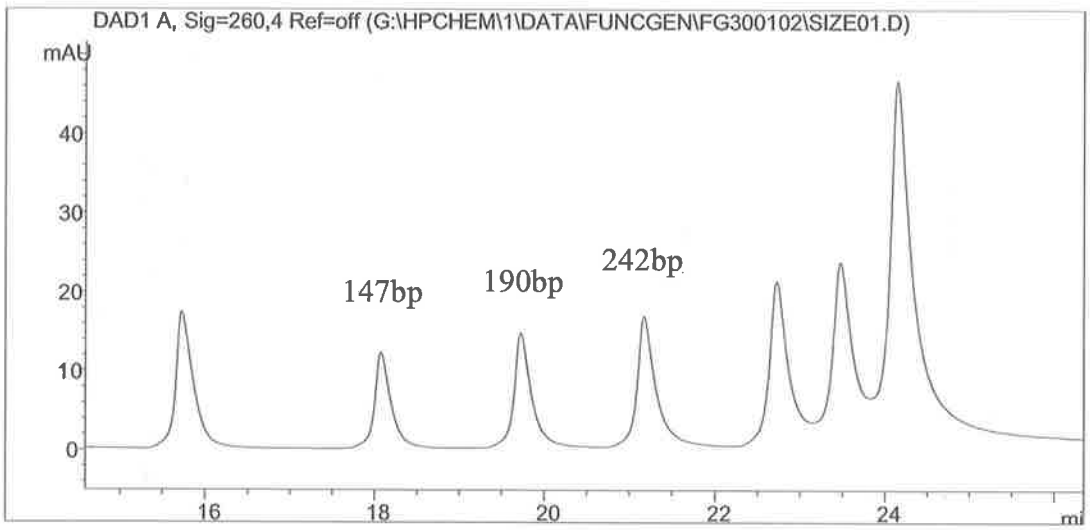

Figure 3.4 Profile of HPLC separation of 1 µg pUC19 digested with *Hpa*II. The three peaks with a defined fragment size were used as standards to quantify the PCR-amplified fragment made using gene specific primers.

area of the peak) was calculated for use in the quantification of the PCR products. The products were dried and resuspended in water to make a 20 ng/µl stock solution. The stock solution (1 µl) was subjected to DNA sequencing to confirm identity. A stock dilution of this standard containing 10^9 copies of the target sequence per microliter was prepared as a base for the subsequent standard dilution series (10^7-10^1 molecules μl^{-1}).

The dilution series was used to generate a standard curve for quantifying PCR products. PCR amplification was conducted on tissue-specific cDNAs (section 3.2.2) in quadruplicate next to standards with three replicates and two no-template negative controls in a 72-well Real-Time Cycler. For all genes except *HvGlyT1*, a 1:10 dilution of the cDNA was used to generate the expression data with a reasonable standard deviation value. For *HvGlyT1*, undiluted cDNA templates were used because of its low abundance.

Each PCR included 10 µl QuantiTect SYBR Green PCR reagent, 3 µl of a 4 µM solution of each of the primers (Table 3.2), 0.6 µl 1000-fold dilution of SYBR Green I dye and 1 µl of either the cDNA or the standard in a total reaction volume of 20 µl. The amplification was carried out with an initial denaturation at 95°C for 15 min followed by 45 cycles [95°C for 20 sec; 55°C for 30 sec; 72°C for 30 sec and 15 sec at the optimal acquisition temperature (Table 3.1)]. The product melt curve, which indicates product purity, was produced at the end of the amplification by heating from 70°C to 99°C. Agarose gel electrophoresis (2.5% w/v agarose-tris-borate/EDTA with ethidum bromide) was performed for all reactions, including the standards and negative control, to confirm the presence of a PCR product (Figure 3.5). The software developed by Corbett Research (Rotor-Gene V4.6) was used to calculate the optimal cycle threshold from the dilution series, the mean expression level and standard deviations (SDs) for each cDNA quadruplet.

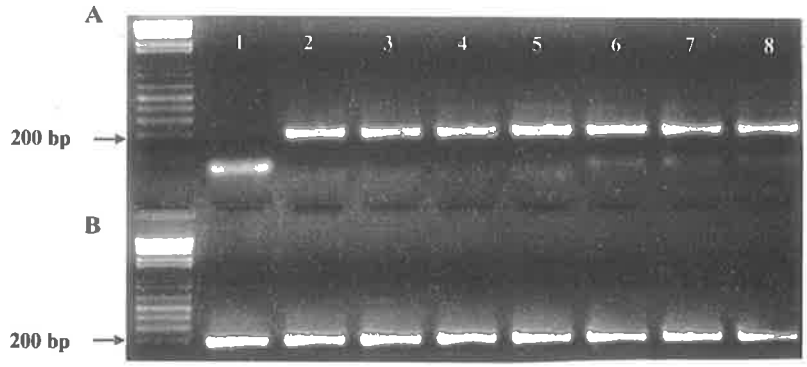

Figure 3.5 Products of a Q-PCR run. An example of agarose gel electrophoresis (2% agarose gel) of Q-PCR products. Lane 1, Panel A = negative control, Lanes 2-8 = standards, Panel B, Lanes 1-8 = cDNAs from eight different tissues, which were randomly chosen.

3.2.6 Normalisation factors (NFs) for Q-PCR

A transcript analysis of a variety of metabolically distinct tissues made without using a correction factor (CF), also termed a normalisation factor (NF), causes discrepancies in the comparison of Q-PCR results (Vandesompele *et al.,* 2002). Vandsompele *et al.* (2002) developed a normalisation technique, which uses internal control genes that are relatively stably expressed in a range of tissues. The normalisation provides the opportunity to either eliminate or reduce sampling errors (such as quality and quantity of RNA). Data obtained from Q-PCR for barley glycosyltransferases were normalised with the best three control genes out of six stably expressed genes, including glyceraldehyde-3-phosphate (*HvGAPDH*), α-tubulin (*HvTub*), heat shock protein-70 (*HvHSP70*), cyclophiline (*HvCycl*), elongation factor 1 (*HvElf1*) and cellulose synthase (*HvCesA1*). Control genes tend to be more highly expressed in metabolically active tissues, such as meristems or rapidly growing tissues, so the normalisation value is usually also greater in these tissues (Table 3.2). A higher level of expression of control genes in metabolically active tissues directly opposes the earlier assumption of the constant expression of internal genes across different tissues. In order to minimise this effect, the three most suitable control genes were selected using software specifically designed for the purpose (Burton *et al.*, 2004).

The geNorm programme is a Visual Basic Applet (VBA) for Microsoft Excel, which was developed by Vandesompele *et al.* (2002) to identify the best stably expressed genes that have the lowest average expression stability (M value). The elimination of less stable genes was performed progressively, starting with five genes and eliminating genes one by one to reach the lowest M value. For most cDNAs, except for the root tip, no difference was seen using either five or two control genes. Three control genes, *HvGAPDH*, *HvCycl* and *HvTub*, were used to calculate normalisation values for the tissue series (Table 3.2). On the basis of the data obtained from the broad tissue series, transcript analysis was carried out in some narrower tissue sub-series. The NF value was calculated for each tissue sub-series (Table 3.3). NF values

Tissue	Normalisation Factor (NF)
First leaf tip	0.24
First leaf base	1.55
Root tip	2.66
Root m/zone	0.49
Floral early	1.79
Floral anthesis	2.57
Developing Grain (3)	3.18
Developing Grain (13)	0.12
Coleoptile 3 day	1.40
Stem	0.84

Table 3.2 Calculated normalisation factors of barley tissue series. Normalisation factors calculated by geNorm for cDNAs of the tissue series based on the best combination of three control genes (*HvGAPDH*, *HvCycl* and *HvTub*).

Tissue	Control Genes	Normalisation Factor (NF)
Leaf E (base)	*HvCycl, HvGAPDH, HvHSP70*	3.15
Leaf D	*HvCycl, HvGAPDH, HvHSP70*	0.92
Leaf C	*HvCycl, HvGAPDH, HvHSP70*	0.72
Leaf B	*HvCycl, HvGAPDH, HvHSP70*	0.54
Leaf A (tip)	*HvCycl, HvGAPDH, HvHSP70*	0.89
Mature leaf base	*HvTub, HvGAPDH, HvCesA1*	0.42
Mature leaf B	*HvTub, HvGAPDH, HvCesA1*	0.66
Mature leaf C	*HvTub, HvGAPDH, HvCesA1*	5.29
Mature leaf D	*HvTub, HvGAPDH, HvCesA1*	0.68
Root 4 (m/zone)	*HvCycl, HvCesA1, HvTub*	0.32
Root 3	*HvCycl, HvCesA1, HvTub*	0.91
Root 2	*HvCycl, HvCesA1, HvTub*	0.76
Root 1 (tip)	*HvCycl, HvCesA1, HvTub*	4.56
Coleoptile base	*HvCycl, HvTub, HvGAPDH*	1.25
Coleoptile middle	*HvCycl, HvTub, HvGAPDH*	0.36
Coleoptile top	*HvCycl, HvTub, HvGAPDH*	2.19
Developing endosperm day 2	*HvCycl, HvTub, HvElf1*	0.61
Developing endosperm day 3	*HvCycl, HvTub, HvElf1*	0.62
Developing endosperm day 4	*HvCycl, HvTub, HvElf1*	0.55
Developing endosperm day 5	*HvCycl, HvTub, HvElf1*	0.34
Developing endosperm day 6	*HvCycl, HvTub, HvElf1*	1.59
Developing endosperm day 7	*HvCycl, HvTub, HvElf11*	1.22
Developing endosperm day 8	*HvCycl, HvTub, HvElf1*	0.34
Developing endosperm day 9	*HvCycl, HvTub, HvElf1*	0.4
Developing endosperm day 10	*HvCycl, HvTub, HvElf1*	0.36
Developing endosperm day 11	*HvCycl, HvTub, HvElf1*	0.38

Table 3.3 Calculated normalisation factors of the barley tissue sub-series. Normalisation factors were calculated by geNorm for the barley tissue sub-series. A combination of the best three control genes were chosen to normalise each tissue segment.

Tissue	Control 1	Control 2	Control 3	A	B	C	D	E	F
1	509205	319258	273480	76938	12708	354258.454	0.3114	247069	40809
2	2285528	846565	853455	856855	83424	1181977.282	1.0389	824706	80294
3	1181685	4878555	4420690	4110873	420493	2942801.688	2.5868	1589184	162554
4	681735	64090	929673	331460	9037	343752.039	0.3021	1096950	29908
5	2495395	679445	2541053	525183	71268	1627180.565	1.4303	367177	79827
6	3262168	826395	2174140	989980	84776	1802992.062	1.5848	624646	53491
7	5221848	1227395	2854920	1483743	141605	2635122.600	2.3163	640559	61134
8	285500	62380	96478	46518	9430	119773.068	0.1053	441833	89564
9	1067015	312273	1033360	912375	88134	700893.400	0.6160	1480889	143052
10	813763	887093	555458	610568	50252	737404.537	0.6482	941953	77526
11						1181535.57			

Table 3.4 Example of processing of a series of hypothetical data obtained from a range of tissues and three control genes *via* Q-PCR. Column 1 = 10 different tissues, Controls 1, 2 and 3 = average value of raw data for 3 control genes obtained from 4 replications, A = average value of raw data for the hypothetical gene obtained from 4 replications, B = standard deviation of raw data obtained from 4 replications, C = geometric mean of 3 control genes, 11 = average value of geometric means, D = normalisation value (C divided by 11), E = A divided by D to normalise the raw data, F = B divided by D to normalise the raw standard deviation values. A graph was plotted based on the data obtained from E for the tissue series and error bars were plotted based on values obtained from data present in column F (Figure 3.6 is an example of these plots).

were used to normalise Q-PCR data for *HvGlyTs* (dividing the raw data by the NF value). An example of how the data was processed is presented in Table 3.4.

3.2.7 Bivariate correlation analysis of Q-PCR data belonging to cell wall-related enzymes

The Q-PCR non-normalised data of barley glycosyltransferases, along with some other cell wall-related enzymes were used for bivariate correlation analyses and to generate a transcript similarity tree. The data for other cell wall-related enzymes were obtained from Dr. Neil Shirley, Dr. Rachel Burton, Dr. Qisen Zhang, Dr. Andrew Harvey (University of Adelaide, SA, Australia) and Ms. Ann Medhurst (University of Melbourne, Vic, Australia).

The bivariate analyses were carried out using Gene Cluster software (downloadable from http://rana.lbl.gov/EisenSoftware.htm), followed by uploading the matrix of genes versus tissues' Q-PCR data into this software. The raw data were transformed logarithmically and genes centred based on their mean value. Complete linkage clustering was performed and the data were viewed using TreeView (downloadable from http://rana.lbl.gov/EisenSoftware.htm).

3.2.8 Transcript profiling using cDNA microarray reference data

A barley Affymetrix chip was made, under the guidance of the Initiative for Future Agriculture and Food Systems (IFAFS) group (USDA), from fifteen barley tissues prepared from two barley varieties (Golden Promise and Morex) at the Scottish Crop Research Institute (SCRI). The information about the tissue types and varieties are available at http://bioinf.scri.sari.ac.uk/affy/WEB_TISSUES/tissue_types.htm. The chip represents 22,500 barley transcripts in three replicates. A set of control genes not found in the barley genome such as hygromycin, luciferase, and β-glucuronidase were included on the chip to normalise the data. All data were normalised using the Robust Multi-array Analysis (RMA) method (Irizarry *et al.*, 2003). The hybridisation and

normalisation of data was performed at the Department of Agriculture-Agricultural Research Service, Iowa State University (Close *et al.*, 2004). During this work, the barley glycosyltransferase sequences, which were amplified during Q-PCR were used to retrieve a chip Contig number using either HarvEST version 1.07 (http://harvest.ucr.edu/) or the Barley Base database (http://barleypop.vrac.iastate.edu /BarleyBase/). The Manhattan analysis program was developed by Dr. Neil Shirley (University of Adelaide, SA, Australia) to find genes with the closest expression patterns based on Manhattan distance, also known as city-block metric and rectilinear distance (Kruscal, 1964). In this programme, a mean value was defined for genes that were co-ordinately expressed and the absolute distance values from the mean value ($d = \Sigma \mid X_i - Y_i \mid$) were used to find and plot the putative, so-called "partner" genes.

3.3 RESULTS

3.3.1 Q-PCR analysis of barley glycosyltransferases

The abundance of individual barley glycosyltransferase transcripts was measured in a range of barley tissues *via* Q-PCR (Figure 3.6). Transcript levels were further investigated in relevant tissue sub-series and data are presented for each individual glycosyltransferase in the following sections.

3.3.1.1 Transcript analysis of *HvGlyT1 via* Q-PCR

The overall transcript level for *HvGlyT1* is very low and was only reliably detectable in the root tip (Figure 3.6, Panel A). The root sub-series was examined to investigate the distribution of transcript along the root profile (Figure 3.7, Panel A). This showed that the mRNA level increased gradually from a very low copy number in the root maturation zone to its maximum in the root tip. Affymetrix data (Figure 3.8, Panel A) revealed five genes with a similar expression pattern to *HvGlyT1* (Contig No. 20744). Among these genes, some were unidentified, whilst others had been assigned a putative role such as a Bowman Birk trypsin inhibitor in rice (Contig No. 20696) and a polyamine oxidase in barley (Contig No. 6513). Another gene that showed a similar transcript profile to *HvGlyT1*, based on both Affymetrix data and Q-PCR results, was a cellulose synthase-like gene (*CslC3*) from rice (HF22106r). This gene is the equivalent of the barley Hv*CslC3*.

3.3.1.2 Transcript analysis of *HvGlyT2 via* Q-PCR

The expression level for *HvGlyT2* was higher than *HvGlyT1* in most of the tissues analysed, but again showed a relatively very low amount overall (Figure 3.6, Panel B). The data showed that *HvGlyT2* mRNA is more abundant in roots than in other tissues.

Further analysis of the root sub-series (Figure 3.7, Panel B) illustrated that the mRNA was distributed evenly along the root. A search of the Affymetrix data showed that this gene was not represented on the chip.

3.3.1.3 Transcript analysis of *HvGlyT3 via* Q-PCR

Amongst the barley genes isolated in this project, *HvGlyT3* showed the most abundant transcript level in all tissues (Figure 3.6, Panel C). The highest amounts of transcript were found in the more metabolically active tissues such as root tip and coleoptiles. The abundance of mRNA was further measured in the root (Figure 3.7, Panel C), leaf (Figure 3.9, Panel A), coleoptile (Figure 3.10, Panel A) and floral (Figure 3.11, Panel A) sub-series. The data showed that *HvGlyT3* is expressed most highly in the root tip with lower amounts found in other root segments. In leaf segments, the mRNA is highly abundant in the leaf base, lower in the middle segments and very low in the less metabolically active segment of the leaf tip. The transcript level was almost equal in coleoptile sections, which contained expanding and short cells (at the coleoptile base and tip respectively); transcript was found in a considerable amount in the fully expanded cells in the middle segment (Figure 3.10, Panel A). Transcripts of *HvGlyT3* increased markedly between anthers taken from 1 to 2 weeks pre-anthesis to the stage of anthesis, whereas in pistils there was a decline during the same period (Figure 3.11, Panel A).

Dr. Qisen Zhang (University of Adelaide, SA, Australia) generously provided details of the neutral momosaccharide composition of cell wall polysaccharides (Table 3.5) determined from 7 d old barley seedlings by gas chromatography-mass spectrometry (Zhang *et al.*, in press). The data showed a higher level of arabinose in the leaf base (60%) and root tips (20%) compared with other parts of the leaf and root segments. These results were consistent with the *HvGlyT3* transcript data, which may suggest an arabinosyltransferase role for this enzyme.

A Contig (No. 15389) representing *HvGlyT3* was found on the Affymetrix chip (Figure 3.8, Panel B). The chip was searched to locate genes with similar expression profiles. The BLAST search results showed that the best four hits were syntaxin (HA22E11r-s), a putative vacuolar proton ATPase subunit 1 (Contig No. 13933) and two unknown proteins from rice.

3.3.1.4 Transcript analysis of *HvGlyT4 via* Q-PCR

The root maturation zone and leaf tip (less metabolically active zones of root and leaf) were tissues in which *HvGlyT4* was highly expressed, (Figure 3.6, Panel D). Besides these two tissues, *HvGlyT4* was consistently expressed elsewhere in the plant at relatively lower amounts (Figure 3.6, Panel D). *HvGlyT4* mRNAs were highly expressed in all root segments except the root tip (Figure 3.7, Panel D). Segment B (wall maturation zone) of the leaf had the highest amount of *HvGlyT4* mRNA amongst all tissues (Figure 3.9, Panel B). The *HvGlyT4* transcript pattern was similar to that of *HvGlyT3* in coleoptile segments and at different stages of floral development (Panel B in Figures 3.10 and 3.11). Figure 3.11, Panel B shows a five fold increase in transcript level in anthers at anthesis compared with the pre-anthesis stage. Affymetrix data analysis (Figure 3.8, Panel C) revealed that several other genes are expressed with a similar pattern to *HvGlyT4* (Contig No. 8844). A peroxisomal targeting receptor 1 from *Nicotiana* (Contig No. 8870) and a steroid membrane binding protein from rice (Contig No. 10724) were among these genes (Figure 3.8, Panel C).

3.3.1.5 Transcript analysis of *HvGlyT5 via* Q-PCR

The transcript levels of *HvGlyT5* were not high, with a peak of 6,000 copies per microlitre in developing grain (Figure 3.6, Panel E). Since the highest transcript level was observed in developing grain tissues, the detailed transcript pattern was further studied in developing endosperm (2-11d post anthesis). The transcript profile showed increasing expression, beginning at day 4 and reaching its maximum at days 6 and 7.

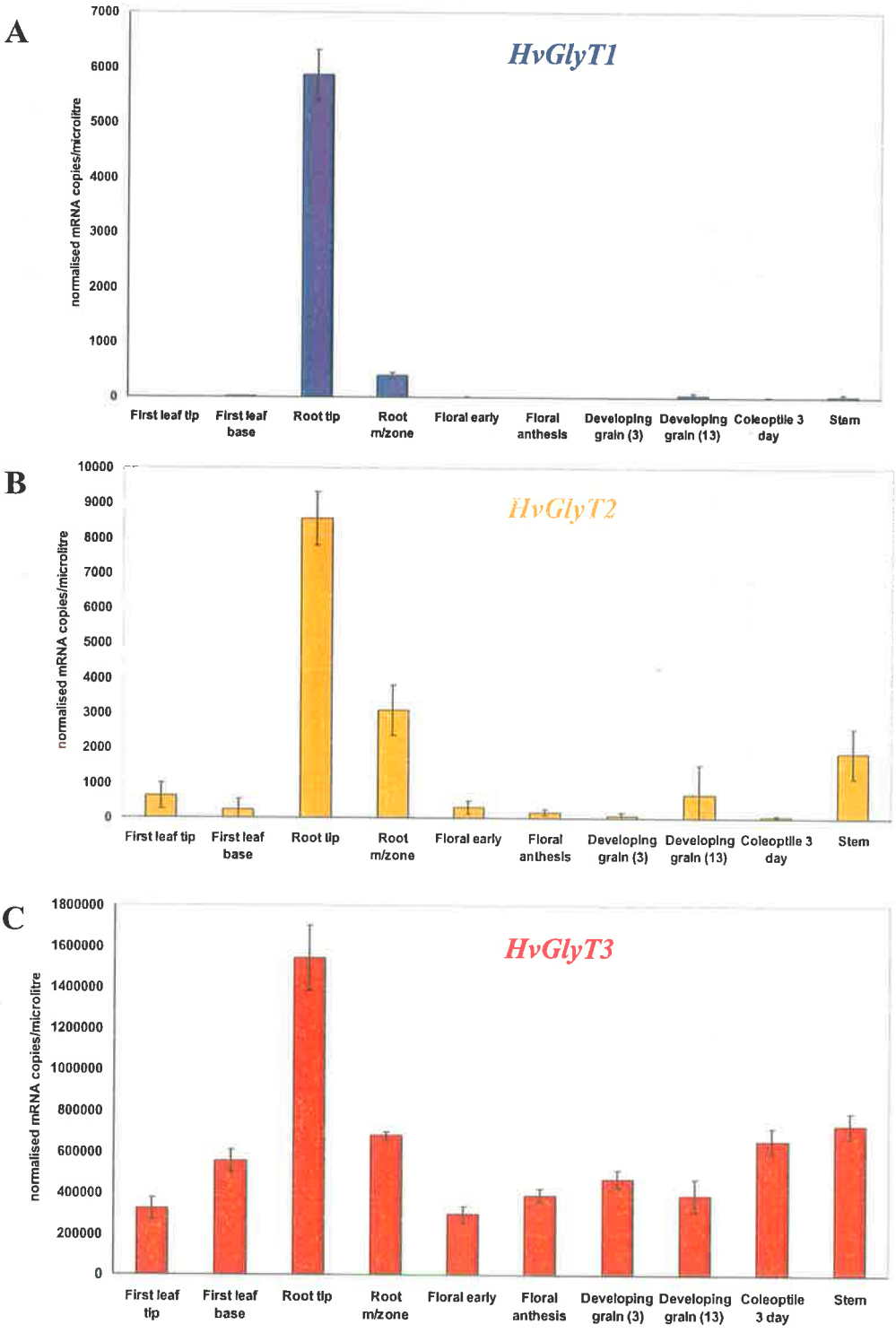
A
HvGlyT1
normalised mRNA copies/microlitre
7000
6000
5000
4000
3000
2000
1000
0
First leaf tip
First leaf base
Root tip
Root m/zone
Floral early
Floral anthesis
Developing grain (3)
Developing grain (13)
Coleoptile 3 day
Stem
B
HvGlyT2
normalised mRNA copies/microlitre
10000
9000
8000
7000
6000
5000
4000
3000
2000
1000
0
First leaf tip
First leaf base
Root tip
Root m/zone
Floral early
Floral anthesis
Developing grain (3)
Developing grain (13)
Coleoptile 3 day
Stem
C
HvGlyT3
normalised mRNA copies/microlitre
1800000
1600000
1400000
1200000
1000000
800000
600000
400000
200000
0
First leaf tip
First leaf base
Root tip
Root m/zone
Floral early
Floral anthesis
Developing grain (3)
Developing grain (13)
Coleoptile 3 day
Stem

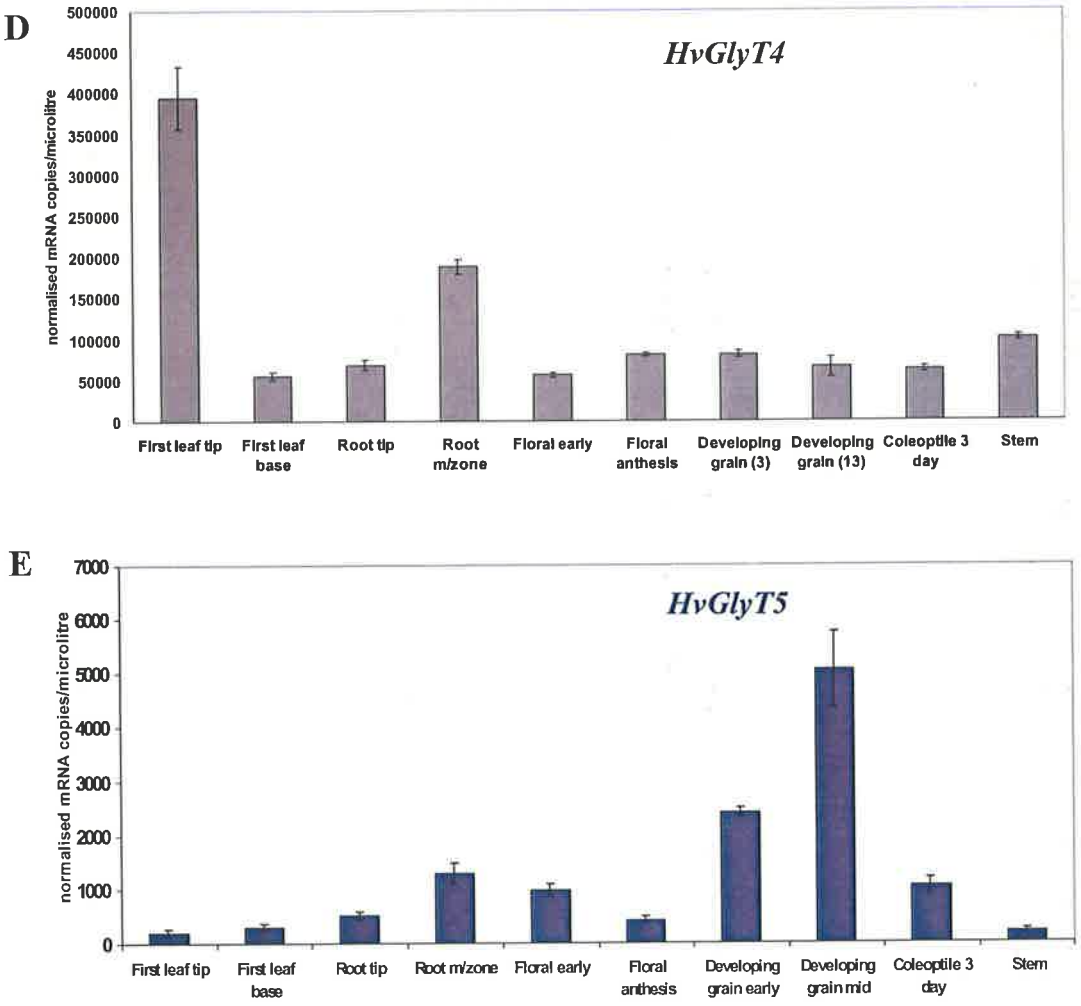

Figure 3.6 Normalised expression levels of five barely glycosyltransferase genes in a range of tissues. Levels of mRNA are presented as the number of copies per microlitre of cDNA after normalisation. Error bars = standard deviations for each mRNA. **A**: the expression pattern for *HvGlyT1*, which is most highly expressed in root tip. **B**: the transcript profile for *HvGlyT2*, which is most abundant in the root tip. **C**: the expression profile for *HvGlyT3*. The transcripts of *HvGlyT3* have been found in all tissues examined at a relatively high level. **D**: the expression pattern for *HvGlyT4*, which is also detected in all tissues, and peaks in the first leaf tip and the root maturation zone. **E**: the expression pattern for *HvGlyT5*, which is detected at a very low level in all tissues. It is more abundant in developing grain and levels increase as the grain develops.

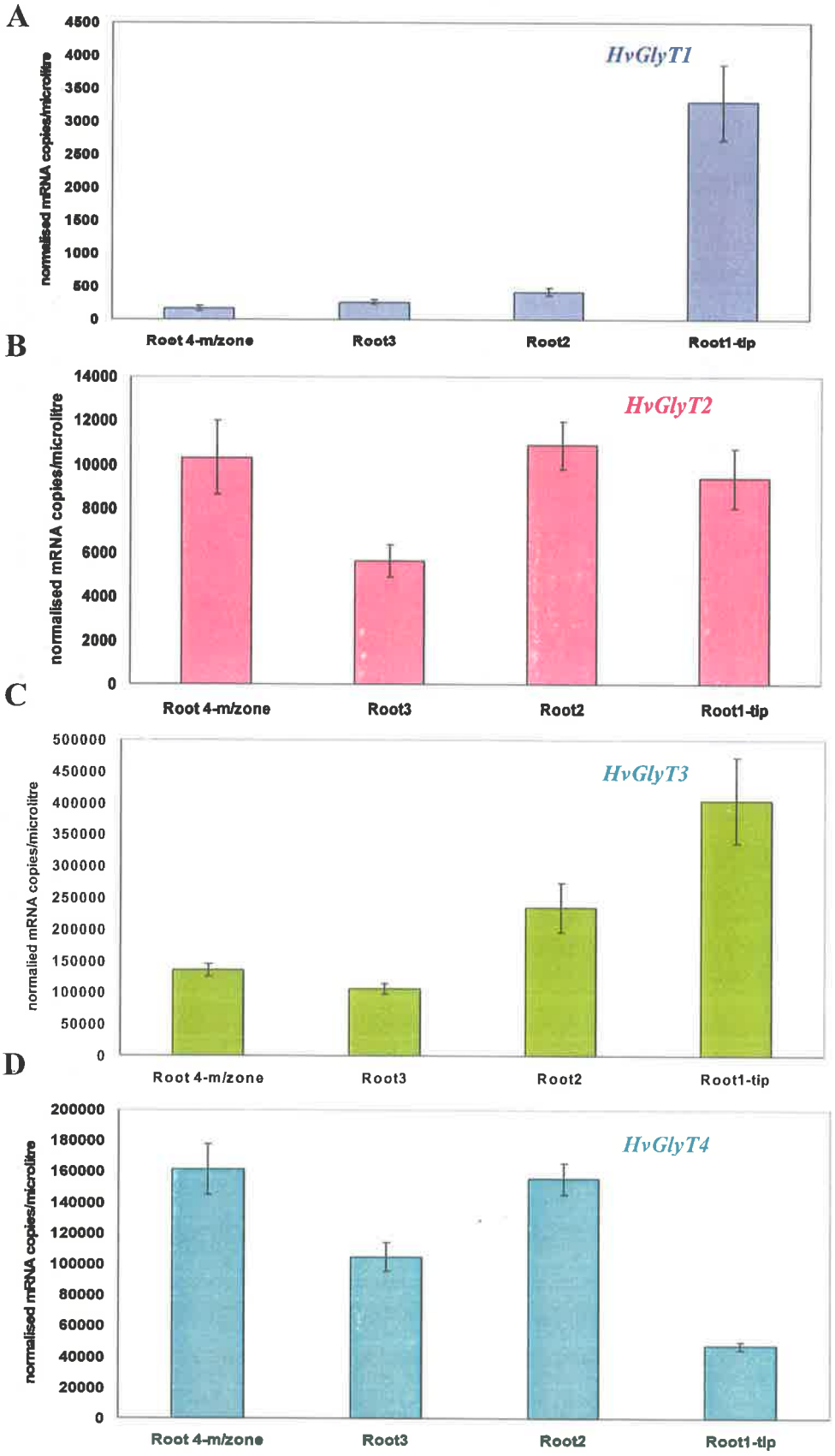
A
HvGlyT1
normalised mRNA copies/microlitre
4500
4000
3500
3000
2500
2000
1500
1000
500
0
Root 4-m/zone
Root3
Root2
Root1-tip
B
HvGlyT2
normalised mRNA copies/microlitre
14000
12000
10000
8000
6000
4000
2000
0
Root 4-m/zone
Root3
Root2
Root1-tip
C
HvGlyT3
normalied mRNA copies/microlitre
500000
450000
400000
350000
300000
250000
200000
150000
100000
50000
0
Root 4-m/zone
Root3
Root2
Root1-tip
D
HvGlyT4
normalised mRNA copies/microlitre
200000
180000
160000
140000
120000
100000
80000
60000
40000
20000
0
Root 4-m/zone
Root3
Root2
Root1-tip

Figure 3.7 Normalised expression levels of barley glycosyltransferases (*HvGlyT1*, *HvGlyT2*, *HvGlyT3* and *HvGlyT4*) in segments of roots. Error bars = SDs. **A**: The expression pattern for *HvGlyT1*; note its high expression level in the root tip. **B**: The transcript levels of *HvGlyT2*, which is evenly distributed along the root without any preference for a specific segment. **C**: The expression profile of *HvGlyT3* showing an increase in the transcript level towards the root tip. **D**: *HvGlyT4* is expressed highly in less metabolically active segments of the root.

Thereafter *HvGlyT5* transcript levels decreased sharply (Figure 3.12). *HvGlyT5* is represented on the Affymetrix chip (Contig No. 18015) and a few other genes with hypothetical functions showed similar transcript patterns (Figure 3.8, Panel D).

3.3.2 Bivariate correlation analysis of Q-PCR data

A tree (Figure 3.13) was generated based on normalised Q-PCR data as described in section 3.2.7. The tree clusters the genes with similar transcript profiles in a range of 10 barley tissues. *HvGlyT1* and *HvGlyT2* fall in the same cluster as *HvCslJ1* (Burton *et al.*, unpublished data) and *HvCslC3*. *HvGlyT3* clusters with *HvCslD1* and *HvUGEP2* (barley UDP-glucose epimerase 2). *HvGlyT4*, *HvCslD2* are grouped in one cluster. Finally, *HvGlyT5* has a very similar transcript profile to *HvCslE2*.

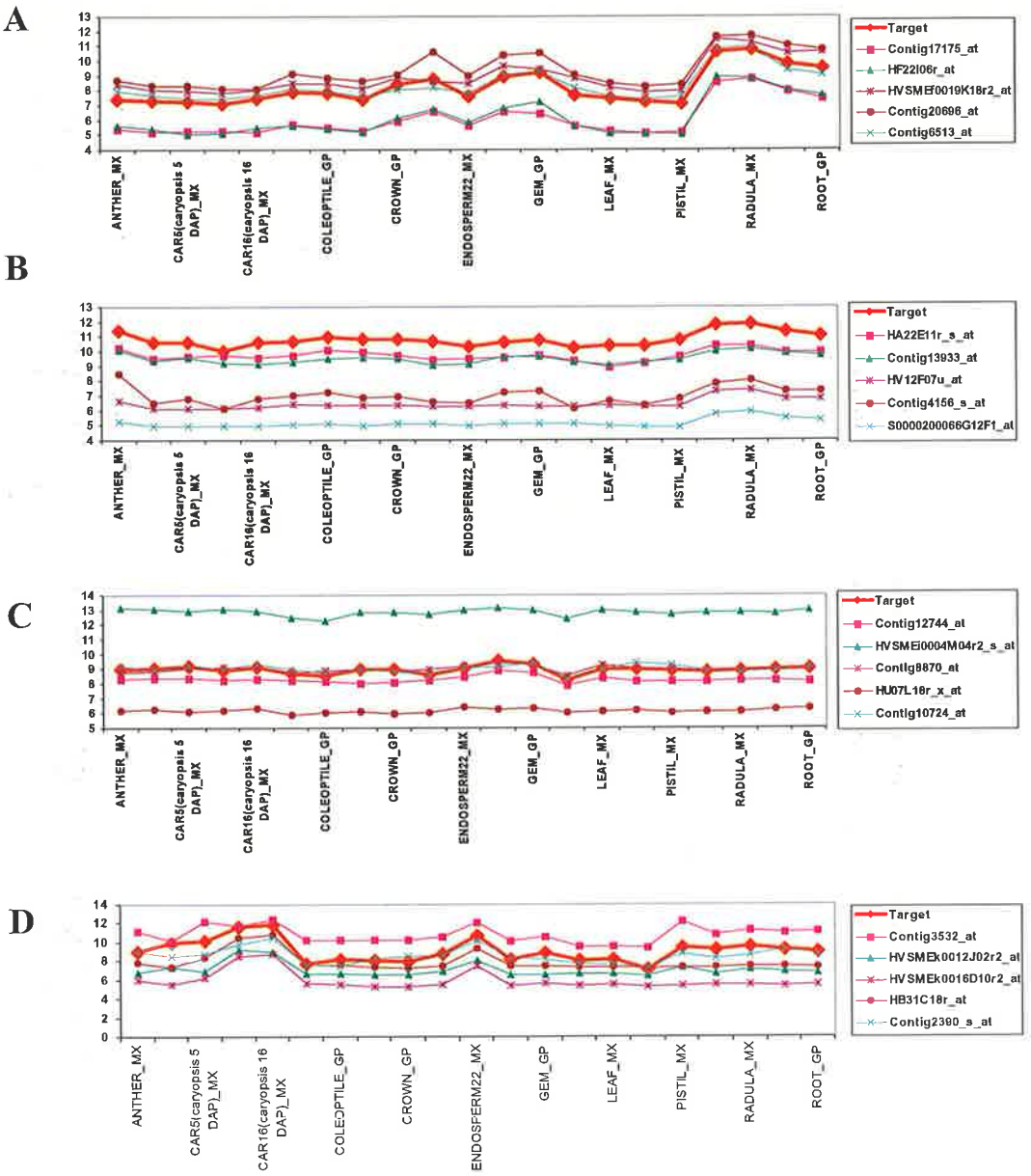

Figure 3.8 Transcript profiling *via* Manhattan analysis. The barley Affymetrix chip was used to reveal genes with a similar expression pattern to barley glycosyltransferases. Panels A, B, C and D show the *HvGlyT1*, *HvGlyT3* *HvGlyT4* and *HvGlyT5* transcript patterns (indicated as target in the legend) and the genes present on the chip with the closest transcript profile to those genes respectively. *HvGlyT2* is not present on the chip.

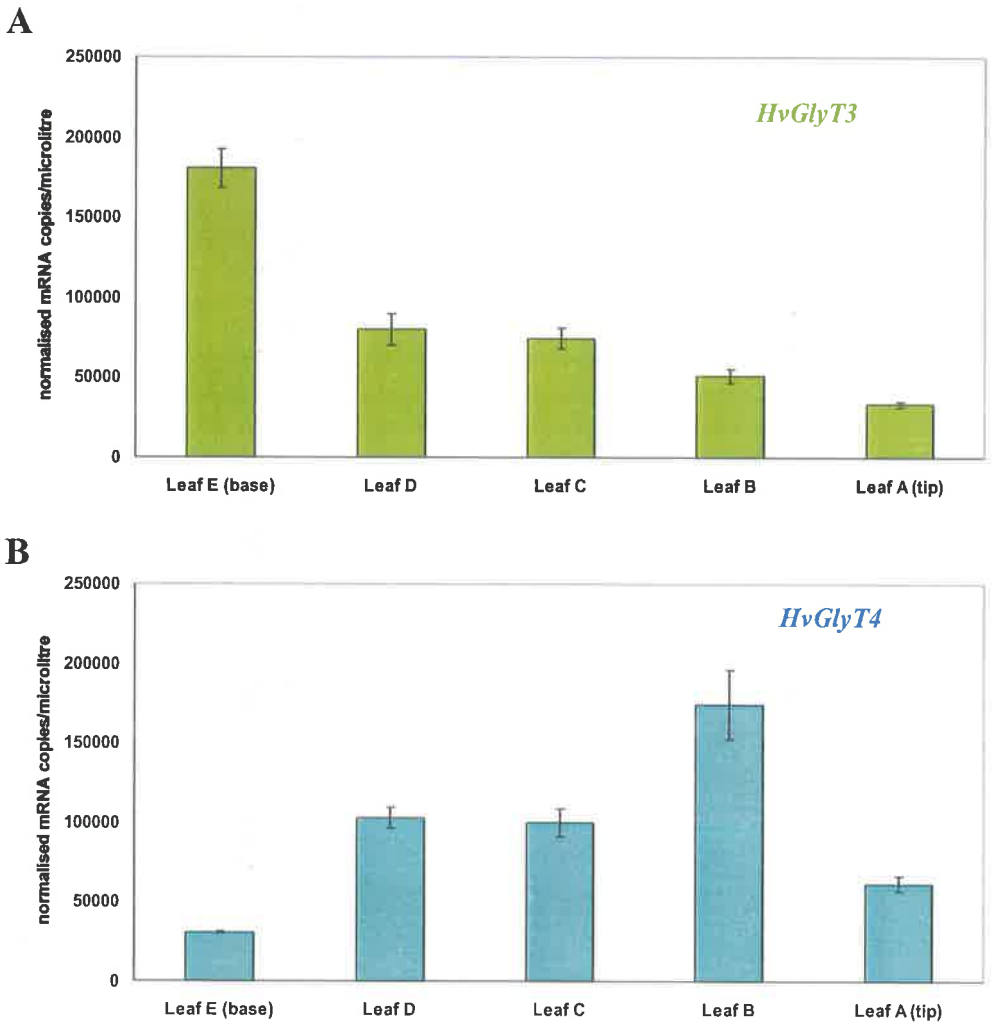

Figure 3.9 Normalised expression levels of barley *HvGlyT3* and *HvGlyT4* in leaf segments. **A**: High expression of *HvGlyT3* in the leaf base. **B**: The expression pattern of *HvGlyT4* in leaf segments, where the highest amount is found in segment B. Error bars = SDs.

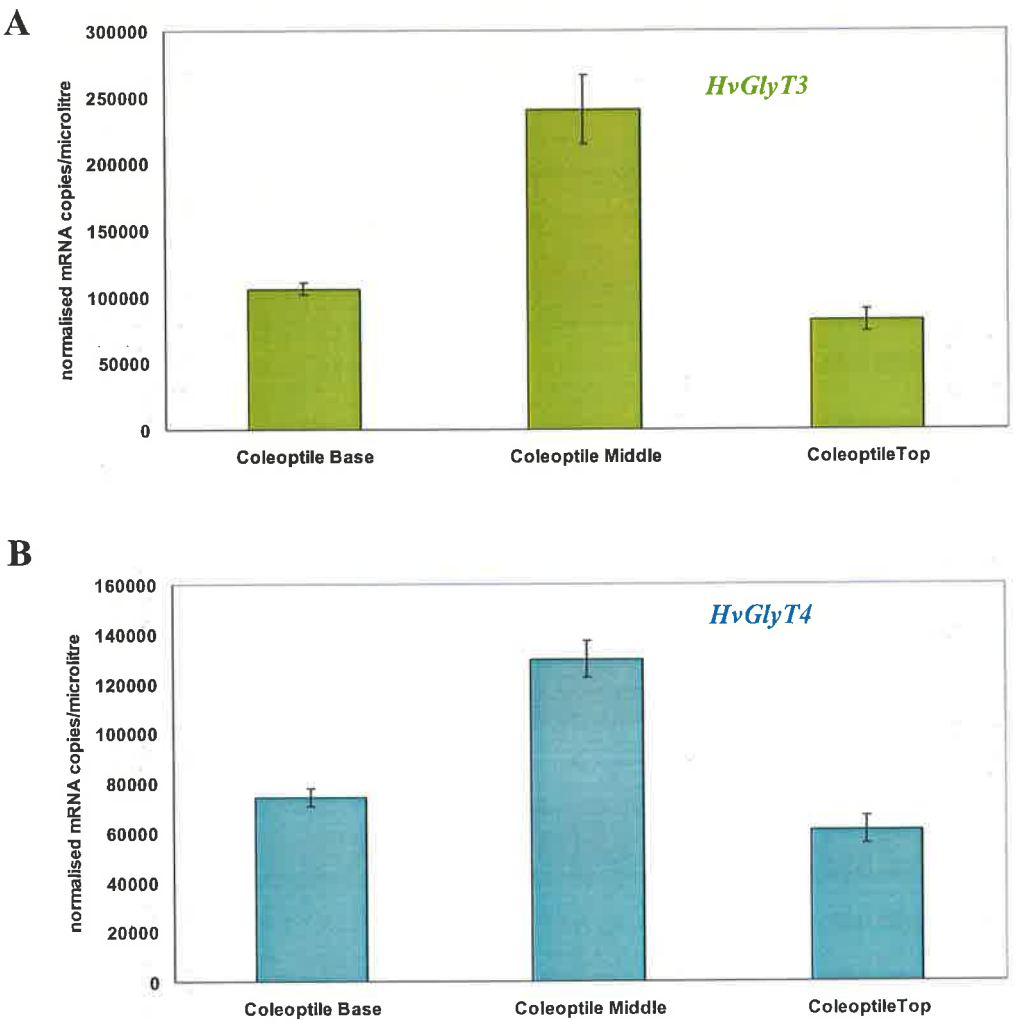

Figure 3.10 Normalised expression levels of barley *HvGlyT3* and *HvGlyT4* in coleoptile segments. **A**: *HvGlyT3* is mostly expressed in the middle section of the coleoptile with relatively high expression level in the other segments. **B**: The expression pattern of *HvGlyT4*, which follows the same pattern as *HvGlyT3* but at a relatively lower amount. Error bars = SDs.

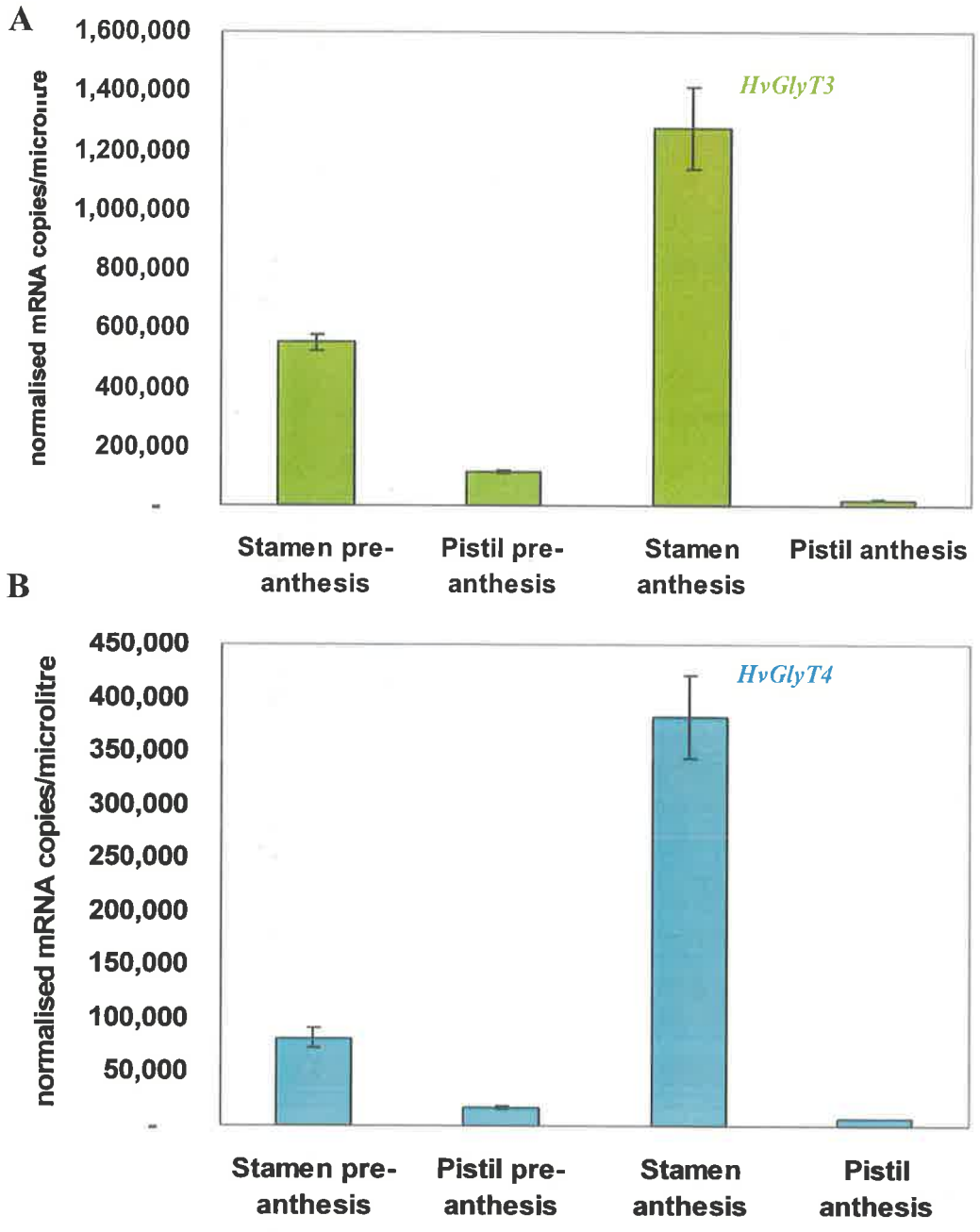

Figure 3.11 Normalised expression levels of barley *HvGlyT3* and *HvGlyT4* in the floral sub-series. Both Panels show that the transcript level in stamens is generally higher than in pistils. For both genes, the transcript level increases considerably in the stamens from the pre-anthesis stage to anthesis, whilst it reduces in the pistils over the same period. Error bars = SDs.

Molar%	Leaf tip	Leaf Centre	Leaf base	Root tip	Root base
Arabinose	6	6	10	10	8
Xylose	22	21	21	27	28
Mannose	nd	nd	2	1	nd
Glucose	69	72	64	58	61
Galactose	2	1	4	4	4

Table 3.5 Composition of neutral sugars in 7 d old barley seedling. Leaf tip, centre, and base correspond to leaf segments A, C and E in Figure 3.2. Root tip and base correspond to root segments 1 and 4 in Figure 3.2. The data are mean values of two replications with variations not more than 1% for arabinose, mannose, and galactose and 3% for xylose and glucose (Zhang *et al.*, in press). nd = not detectable

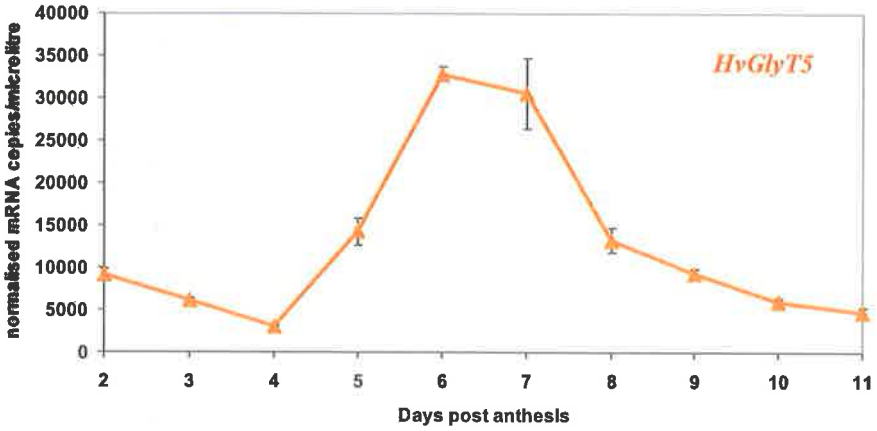

Figure 3.12 Expression pattern of *HvGlyT5* in developing endosperm (2-11 d post anthesis). The transcript level starts increasing at 4 d post anthesis, reaches its highest amount at days 6 and 7, and declines sharply afterwards.

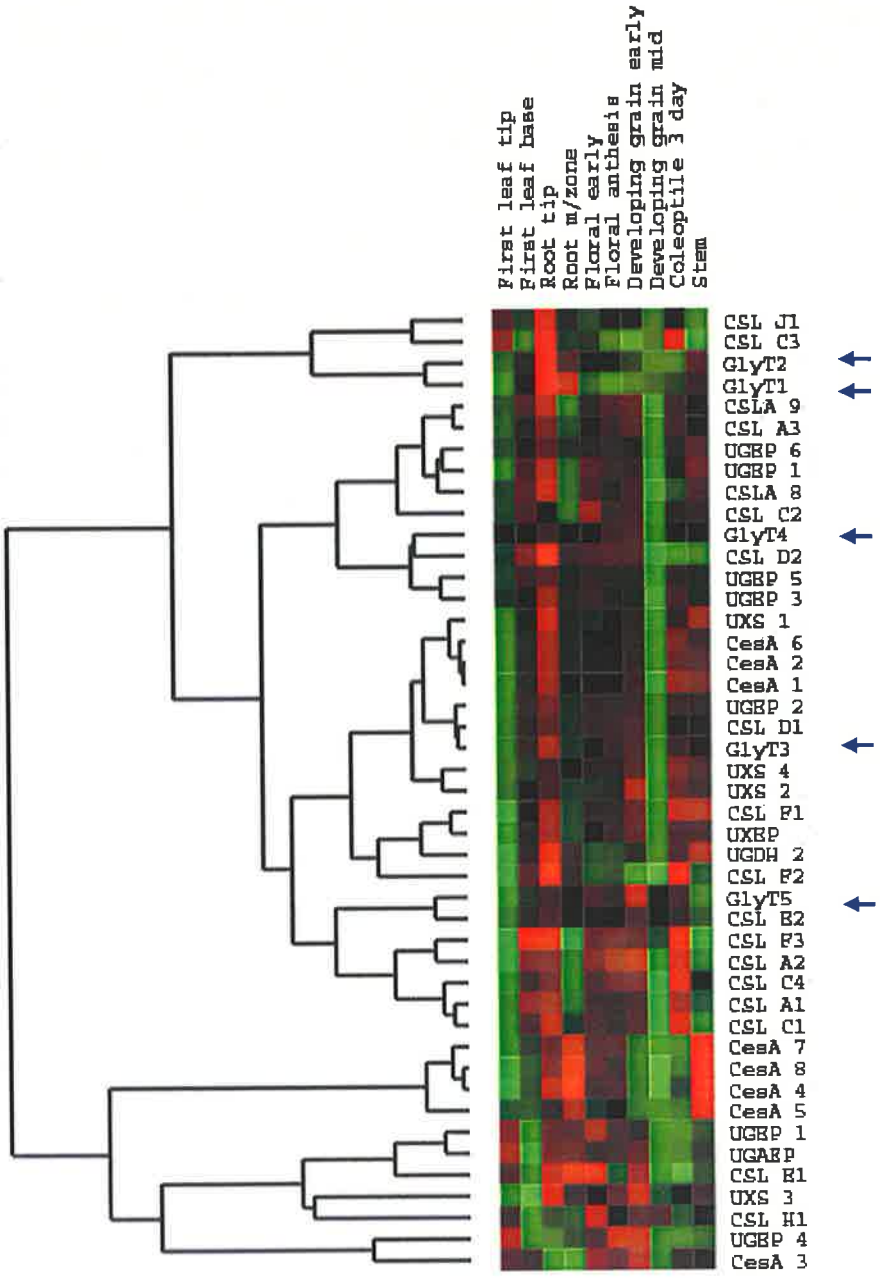

Figure 3.13 Bivariate correlation analyses of a range of cell wall-related biosynthetic enzymes in 10 barley tissues. The red and green squares indicate up- and down-regulation of transcripts in comparison with the average transcript value respectively. The black squares indicate no change compared with the average value. CesA = cellulose synthase, CSL = cellulose synthase like, UGEP = UDP-glucose epimerase, GlyT = barley glycosyltransferase, UXS = UDP-xylan synthase, UGDH = UDP-glucose dehydrogenase, UXEP = UDP-xylose epimerase, UGAEP = UDP-glucuronic acid epimerase. Letters and numbers after each gene are indicative of family members.

3.4 DISCUSSION

The total amounts of mRNAs in cells and tissues provides a picture of different anatomical and physiological states, whilst comparative transcript profiling, for a range of genes may point to putative relationship(s) of genes and gene products in biochemical pathways or processes. This is possible especially where most cellular activity is dedicated to a particular pathway (Liepman *et al.*, 2005). For example, a galactomannan galactosyltransferase and a mannan synthase were isolated from fenugreek and guar seeds, respectively, where galactomannan is the most abundant polysaccharide (Edwards *et al.*, 1999; Dhugga *et al.*, 2004). As discussed earlier, there are a number of ways to gather and interpret such information, and while apparent co-expression of genes might often have no basis in cellular function, co-expression analysis can reveal interesting and unexpected results that can be used subsequently to develop testable biological hypotheses. It must also be remembered that "gene expression", as measured by transcript abundance, is an imprecise term that does not necessarily reflect the final level of expression of the gene product in its correct cellular compartment. Here, Q-PCR and barley Affymetrix data were used for transcript profiling of the putative barley glycosyltransferases cloned during this work.

The Q-PCR results suggested possible roles for some of the barley glycosyltransferases when linked to previous studies and existing knowledge on cell wall composition. Transcript data showed that *HvGlyT1* was only transcribed in roots, with higher amount in the root tip. This finding suggested its involvement in the biosynthesis of a polysaccharide that is specific to the root tip. It has been shown that the root tip, more specifically the root cap, exudes a pectic mucilage that is rich in xylogalacturonan (XGal) (Willats *et al.*, 2004). A xylogalacturonan-specific monoclonal antibody (LM8), which recognises XGal highly substituted with xylose, showed that this polysaccharide was present in legume seed testa and maize root caps (Willats *et al.*, 2004). Thus, the location of the XGal in maize root caps, coupled with the low abundance of this polysaccharide (XGal) in the most monocot cell walls, might indicate a possible involvement of *HvGlyT1* in the biosynthesis of XGal as a

putative xylosyltransferase. However, this is a long extrapolation and any such role needs to be confirmed by further work.

One of the enzymes that showed a similar transcript profile to *HvGlyT1* in the Affymetrix data was polyamine oxidase (*POA*). POAs are enzymes that oxidise polyamine substrates to produce hydrogen peroxide (Slocum and Furey, 1991). It has been shown that this enzyme is embedded in the cell wall (Federico and Angelini, 1991; Slocum and Furey, 1991; Liu *et al.*, 1995). Localisation to the cell wall may imply involvement of this enzyme with reactions that are coupled to the presence of H_2O_2 in the cell wall, such as biosynthesis of extensins (Wilson and Fry, 1986) and lignin (Grisebach, 1981). Despite the involvement of POA in the re-structuring of the cell wall, at this stage establishing any relationship between *POA* and *HvGlyT1* is premature. The bivariate correlation analyses of the Q-PCR data (Figure 3.13) showed that *HvGlyT1* clusters with *HvGlyT2*, *HvCslC3* and *HvCslJ1*. *HvGlyT1* showed a particularly high level of correlation with *HvCslC3,* using both Q-PCR and Affymetrix data, and this might suggest a functional relationship. As mentioned earlier, if HvGlyT1 is involved in xylosyltransferase activity in the synthesis of XGal then HvCslC3 might be a polygalacturonate synthase.

The distribution of *HvGlyT2* mRNA is restricted to the barley root, with an even distribution along the root. This suggests that HvGlyT2 might be involved in construction of a polysaccharide that is specific to the root cell wall and is not found elsewhere. Since the detailed polysaccharide compositions of the walls of many barley tissues is still not available, speculation on function *via* transcript analyses for *HvGlyT2* awaits the emergence of such data in the future.

The high expression levels of *HvGlyT3* suggest its involvement in the biosynthesis of a polysaccharide that is abundant in the barley cell wall. As mentioned earlier, arabinoxylans are major components of graminaceaus walls. Hence, at this stage arabinosyltransferase activity may be proposed as a function for *HvGlyT3*. A search for transcripts with a similar profile to *HvGlyT3* in the Affymetrix data identified a number of genes. Amongst them, syntaxin might be functionally relevant to HvGlyT3. Syntaxins are a subfamily of integral membrane proteins named SNARE,

which mediate membrane fusion events during vesicle transport (Block *et al.,* 1988; Collins *et al.,* 2003; van Vliet *et al.,* 2003). The similarity of the transcript profiles of syntaxins and *HvGlyT3* may suggest the possible involvement of syntaxin as a carrier of *HvGlyT3* to the Golgi apparatus. However, any proposed role for HvGlyT3 must remain speculative at this stage.

The expression pattern of *HvGlyT4* showed that its mRNA is present in all tissues, but at a higher concentration in mature vegetative tissues. Although the widespread transcription of the gene makes it difficult to draw any conclusion in regards to function, the high level of sequence similarity of *HvGlyT4* with a known pectin glucuronosyltransferase (Iwai *et al.*, 2002) may suggest that *HvGlyT4* is also a pectin glucuronosyltransferase, as discussed in Chapter 2.

Evaluating the transcription pattern of *HvGlyT5* in the tissue series revealed the presence of mRNA in all tissues at a relatively low copy number. The highest amount was found in developing grain. The transcript analysis of a developing endosperm series showed that *HvGlyT5* transcript abundance assumed a bell-shaped (Figure 3.12) with the peak at day 6. The fact that *HvGlyT5* was expressed in minor amounts may suggest its involvement in the biosynthesis of a relatively low abundance polysaccharide in the wall. Galactomannan is one such polysaccharide in monocots.

In general, the transcript profiles showed that some of the glycosyltransferases are highly regulated in a tissue-specific and/or developmentally-regulated manner, while some others have a more widespread distribution. Transcripts of *HvGlyT1, HvGlyT2* and *HvGlyT5* were less abundant in all tissues when compared with *HvGlyT3* and *HvGlyT4*. The high levels of transcripts for *HvGlyT3* and *HvGlyT4* were comparable with highly abundant barley transcripts such as those for *HvCesA1* (Burton *et al.,* 2004). Analysis of the Affymetrix data revealed some genes with similar expression patterns to *HvGlyT1*, *HvGlyT3*, *HvGlyT4* and *HvGlyT5*. However, at this stage any interpretation of these is must be considered preliminary, at best.

As part of the ongoing process of defining a biological function for the barley glycosyltransferase genes, it was decided to investigate potential protein-protein

interactions between the HvGlyT proteins and any other proteins that might bind to them, such as nucleotide sugar interconverting enzymes and cellulose synthase-like proteins. Accordingly, the yeast two-hybrid system was used to investigate any such protein-HvGlyT interactions. The results of these experiments are described in the next Chapter.

CHAPTER 4 YEAST TWO-HYBRID SCREENING FOR PROTEIN-PROTEIN INTERACTIONS

4.1 INTRODUCTION

Following the isolation of the five barley glycosyltransferase cDNAs, the focus of the work was shifted towards the functional analyses of the genes. Although the transcript analyses described in Chapter 3 provided valuable information on the differences in transcriptional activity of the various *HvGlyT* genes, they did not lead to unequivocal conclusions on the possible functions of the genes. The availability of a functional yeast two-hybrid system allowed an investigation of proteins that might interact with the five HvGlyT proteins. In particular, interaction of one of the HvGlyT proteins with a *Csl* or *CesA* gene might shed light on enzyme complexes that might be necessary to synthesise heteropolysaccharides, such as arabinoxylans or xyloglucans. In this Chapter, possible protein-protein interactions involving the two transcriptionally most abundant barley glycosyltransferases were examined by screening the cDNAs against two yeast two-hybrid wheat cDNA libraries. In addition a cDNA encoding a UDP-xylose epimerase (Q. Zhang and G. B. Fincher; unpublished data) was screened against the library, because this enzyme is likely to be active when arabinoxylans are being synthesised.

Cellular processes, such as the formation of macromolecules by enzymatic complexes and the regulation of signal transduction pathways, can be mediated by several proteins that interact with each other (Thaminy *et al.*, 2004). Proteins can interact either by chemically binding to each other, or by binding together through a third protein (Rost *et al.*, 2003). Thus, investigating protein-protein interactions in either a cellular or developmental context may provide clues to the function of candidate genes (Cobbe and Heck, 2004). To define interacting partners of specific proteins in the cell, biochemical and genetic approaches have been used (Chien *et al.*, 1991; Van Criekinge and Beyaert, 1999). These techniques are versatile and can be classified into *in vitro* and *in vivo* types (Table 4.1).

Affinity chromatography and co-immunoprecipitation are the two common types of *in vitro* assays. In affinity chromatography, the extracted protein sample passes through a column containing an immobilised protein of interest. The proteins interacting with

Type	Methodology	Example	Reference
In vitro	Co-immunoprecipitation (pull-down assay)		(Birge *et al.*, 1993; Warne *et al.*, 1993)
	Affinity chromatography		(Formosa *et al.*, 1991)
	Two-dimensional blue/native SDS gel electrophoresis		(Schagger *et al.*, 1994; Camacho-Carajal *et al.*, 2004)
In vivo	Fluorescence assays	FRET	(Gordon *et al.*, 1998; Immink *et al.*, 2002)
		BiFc	(Hu *et al.*, 2002; Hu and Kerppola, 2003; Bracha-Drori *et al.*, 2004; Walter *et al.*, 2004)
	cDNA Library-based assay	*E. coli* or yeast two-hybrid screening	(Hu *et al.*, 2000)

Table 4.1 Common biochemical approaches towards the investigation of protein-protein interactions. Co-immunoprecipitation (pull-down assays) and affinity chromatography are amongst the *in vitro* biochemical methods. *In vitro* techniques are often time consuming and take a lot of effort to find the interacting proteins (Bracha-Drori *et al.*, 2004), but they have been used as complementary techniques and as supporting evidence for data derived from genetic methods (Van Criekinge and Beyaert, 1999; Cobbe and Heck, 2004). Fluorescence resonance energy transfer (FRET), bimolecular fluorescence complementation (BiFC) and cDNA library-based assays, including two-hybrid systems are amongst the *in vivo* assays.

the protein of the interest bind to the column and are later eluted and characterised. In contrast, antibodies are used to separate the interacting antigen and all other interacting partners of the antigen *via* co-immunoprecipitation to unravel the nature of the complex that the antigen is involved in. In two-dimensional blue native/SDS electrophoresis, multi-protein complexes (MPC) are initially separated based on charge *via* a blue native polyacrylamide gel (BN-PAGE). The first dimension separation followed by a SDS-PAGE to separate the proteins present within each complex. This step is completed by the identification of proteins of interest, either *via* immunoblotting or silver staining. Subsequently the co-shifted proteins, present in the MPC, can be identified by other analytical methods, such as Edman sequencing or liquid chromatography coupled with tandem mass spectrometry (LC-MS/MS).

On the other hand, *in vivo* techniques are used to study the interaction of proteins within the cell, and include fluorescence and cDNA library-based assays. The fluorescence assays include fluorescence resonance energy transfer (FRET) and bimolecular fluorescence complementation (BiFC), which work on the basis of measuring the generated fluorescent light. In the library-based assays, such as yeast two-hybrid screens, the activation of reporter genes are measured *via* development of colour upon interaction of proteins attached to fluorophores or upon growth on selective plates. Given that the yeast two-hybrid system was used in this research, its application, benefits and drawbacks are discussed here.

The yeast two-hybrid system has become a powerful tool for the study of protein interactions since its first introduction by Fields and Song (1989). In this technique (Figure 4.1), a cDNA encoding the protein of interest is fused to a DNA-binding domain (BD), such as Gal4 or LexA. This is called "bait" and is used to screen either a yeast line expressing another specific cDNA or a cDNA library fused to an activation domain (AD). The library is referred to as "prey". The interaction between bait and prey is detected by transcriptional activation of a reporter gene in the nucleus of the yeast cell. The reporter gene becomes active when the AD of the yeast Gal4 gene is brought into close proximity of BD. The reporter gene will develop a blue colour in the presence of the substrate 5-bromo-4-chloro-3-indolyl-β-D-

galactopyranoside (X-Gal) indicating a putative protein-protein interaction (Figure 4.1).

The yeast two-hybrid system has been used successfully as an in vivo assay for revealing putative partner proteins, but it does have some limitations (Table 4.2). Some of these include the detection of false positive clones during the screening of a library (Bartel *et al.*, 1993), self-activation where reporter gene expression is switched on by either bait or prey constructs alone (Walhout and Vidal, 1999), and the difficulty of finding the interacting partners of membrane-bound proteins (Fetchko *et al.*, 2003).

False positives are identified prey clones for which the probability of interaction with the bait protein is very low to impossible (Serebriiskii *et al.*, 2000). Ribosomal subunits, heat shock proteins, proteosome subunits and cytoskeletal components are examples of proteins that can be considered false positives (http://www.fccc.edu/research/labs /golemis/InteractionTrapInWork.html). In order to avoid confusion and misleading results, the detection of false positives is a critical issue. Several factors are known to be responsible for false positive interactions, including proteins that directly bind to and activate promoters (Bartel *et al.*, 1993). The amount of activation sensitivity depends on the differential access of bait proteins to reporter promoters (Golemis and Brent, 1992). This was demonstrated with fusion proteins that activate strongly in higher concentrations, but failed to activate the transcription machinery when expressed at lower levels (Golemis and Brent, 1992). Furthermore, a particular biological function of a protein or the presence of charged amino acids and/or coil-coil interactions sometimes lead to false positives. These types of proteins, such as ribosomal subunit proteins, heat shock and proteosome subunits, are called "sticky proteins" (Serebriiskii *et al.*, 2000).

Self-activation is another inherent problem with the yeast two-hybrid system that may occur during library screening. Self-activators are proteins that activate transcriptional machinery in both the organism of origin and in yeast. Some other proteins are not transcriptional activators, but when tethered with the yeast promoters, exhibit transcriptional activity (Walhout and Vidal, 1999). Self-activation can also

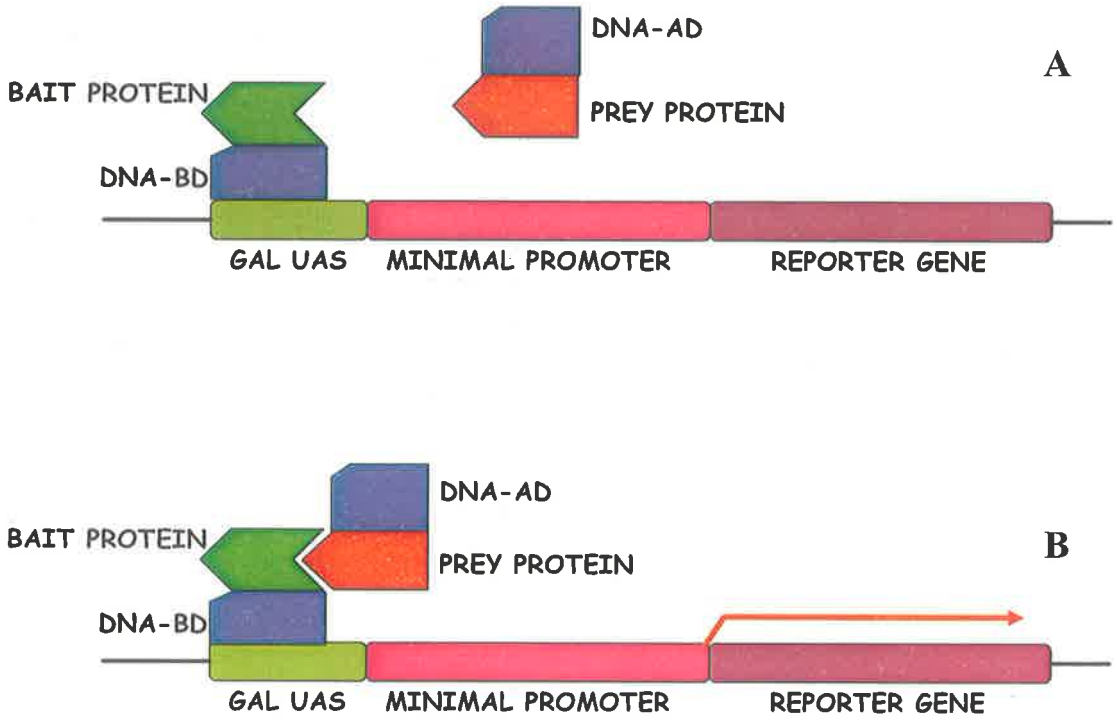

Figure 4.1 Schematic view of the yeast two-hybrid system. In Panels A and B, two chimeric cDNAs, one containing a DNA binding domain (DNA-BD: blue rectangle) and one that contains an activation domain (DNA-AD: blue square) are co-transformed into an appropriate yeast strain. If the fusion partners (orange and green) were to interact with each other (Panel B), the AD and BD would be brought into close proximity, allowing binding to the *Gal4* upstream activation sequence and the commencement of transcription of the reporter gene (GUS), which results in a blue colouration of the yeast colony when X-α-gal is present as the substrate of α-galactosidase. Here, Matchmaker™ Two-Hybrid System 3 was used in order to screen cDNA libraries (http://www.clontech.com/). This system uses yeast AH109, which contains four reporter genes, ADE2, HIS3, lacZ and MEL1. These reporter genes are incorporated into the yeast genome under the control of distinct GAL4-responsive UASs and TATA boxes. Their distinction eliminates occurrence of false positives caused as a result of interaction with the upstream region of the reporter construct and interaction with certain promoter elements, GAL4 and TATA box.

Limitations	Reasons
Proteins misfold and are inactive	• Use of yeast as the host is not suitable for all proteins • Lack of proper post-translation modification in yeast such as disulfide bridges, glycosylation and phosphorylation • All fusion proteins are targeted to the nucleus in this system, while some of these proteins contain other types of signal peptides and require targeting to other organelles • Attachment of binding and activation domains to the protein
Weak representation of cDNA library	• Only 1 in 3 of the fused cDNAs are in the right frame • Many cDNAs present in the library are partial-length and so may not carry the interacting domain
Toxicity of some proteins in yeast	• Proteins such as cyclines or homeobox gene products are toxic when expressed and targeted to the yeast nucleus.
False interaction	• The interaction in yeast does not always represent a true interaction in the plant

Table 4.2 Disadvantages in the use of the yeast two-hybrid system. Taken from Van Criekinge and Beyaert **(1999).**

occur as a result of other factors, including a frame shift in the prey vector during construction of the cDNA library, leading to expression of spurious proteins that activate transcriptional machinery (Walhout and Vidal, 1999). Similarly, there may be interactions of subunits of proteins with multiple TMHs during non-specific aggregation of their multimeric structure in the hydrophilic yeast nucleus (Creasey *et al.*, 2003). Despite these problems, both bait and prey proteins can be screened for self-activation prior to yeast two-hybrid screening in order to avoid misleading results.

Membrane-bound proteins have crucial roles in many cell processes, including cell wall biosynthesis. They appear in the insoluble fraction during protein isolation, due to either their hydrophobic nature or because they interact with other molecules such as lipids. Insolubility may also be caused by palmitoylation, farnesylation and myristoylation (Kohler and Muller, 2003). Difficulties in protein isolation can hamper the identification of protein complexes and interacting partners (Fetchko *et al.*, 2003). Despite its intrinsic drawbacks, the yeast two-hybrid system has been widely used to unravel the nature of many interacting proteins (Auerbach *et al.*, 2002), but it has received remarkably little attention as a tool to investigate the existence of interacting proteins participating in cell wall biosynthesis. The fact that almost all steps in cell wall biosynthesis occur in the membrane might explain why it has not been used extensively in this field. Emergence of new techniques such as the "split-ubiquitin yeast two-hybrid system" (Stagljar *et al.*, 1998; Iyer *et al.*, 2005) for the study of interacting membrane-bound proteins may provide new opportunities to define these interactions. In this system, two fragments of ubiquitin cDNA are fused to two interacting cDNAs. The proteins can be encoded by both membraneous or at least one must be a membrane protein (Figure 4.2). When the two proteins interact, the split parts of ubiquitin are brought together, which leads to the release of the transcription factor bound to the protein of interest. Upon release, the transcription factor moves to the nucleus and activates the reporter genes.

Glycosyltransferases are likely to interact with other proteins in a transient manner to perform a range of essential processes in the cell (Phizicky and Fields, 1995; Van Criekinge and Beyaert, 1999). Since these are membrane-bound proteins and the

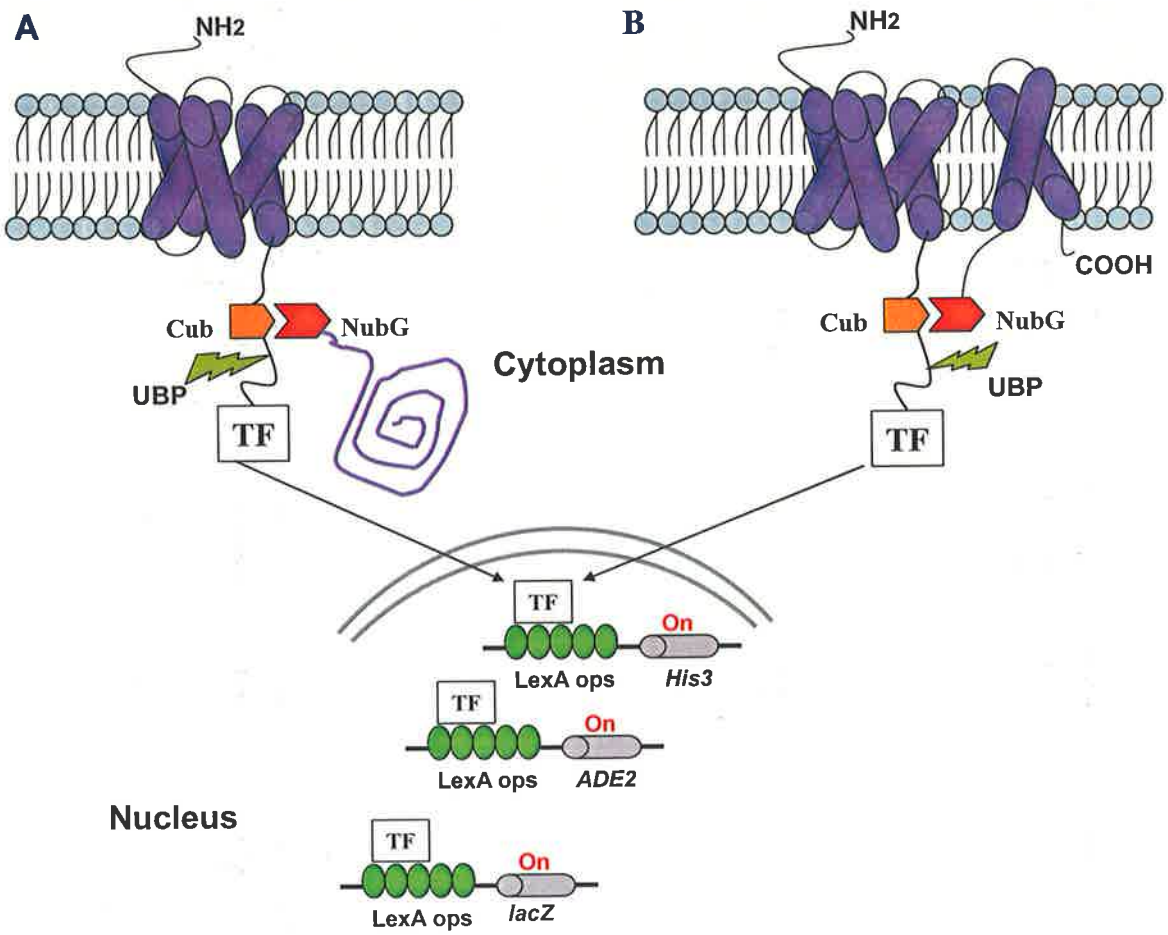

Figure 4.2 Outline of "split-ubiquitin yeast two-hybrid system" (modified after Thaminy *et al.*, 2004; Iyer *et al.*, 2005). **A:** A membrane-bound "bait" protein is fused to COOH-terminal half of ubiquitin (Cub), along with an artificial transcription factor (TF). A cytosolic "prey" is fused to the NH_2-terminal half of ubiquitin (Nub), which upon interaction of the two proteins the two halves of ubiquitin reconstitute to produce ubiquitin. The presence of so-called "split-ubiquitin" is recognised by ubiquitin-specific proteases (UBP), which cleaves the TF. Subsequently, the released TF enters the nucleus and causes the activation of reporter genes, such as *His3*, *lacZ* and/or *ADE2*. The activation of reporter genes can be monitored by growth on selective plates or by calorimetric assays. **B:** Similar to above a membrane-bound "bait" protein may interact with a membrane-bound "prey" protein and lead to the cellular processes mentioned above. NubG = a modified Nub (isoleucine to glycine at position 13 of the Nub moiety), which prevents spontaneous association with Cub. LexA ops = LexA operator sites.

interactions might be transient in nature, the functional analysis of the proteins *via* protein-protein interactions might be a difficult task. As a result, few examples of such studies are reported in the literature. However, there is one example in which a highly conserved region of a protein (EXT2) in the heparan sulfate biosynthesis pathway was shown to interact with a specific glycosyltransferase [*N*-acetylgalactosaminyl transferase (GalNAc-T5)]. This interaction was demonstrated when EXT2 was screened against human keratinocyte and lymphocyte cDNA libraries *via* yeast two-hybrid screening, using an *in vitro* binding assay (Simmons *et al.*, 1999). The result showed that the EXT2 protein interacts with a "GalNAc-T5" that is involved in the initiation of mucin *O*-linked chain biosynthesis. In another study, Hong *et al.* (2001) demonstrated the interaction of an *Arabidopsis* UDP-glucose transferase (UGT1) with phragmoplastin, a protein involved in synthesis of the cell plate.

If cell wall biosynthesis is considered in a broad context, nucleotide sugar transporters, nucleotide sugar interconverting enzymes, glycosyltransferases and glycan synthases are potential partners in a complex of interacting proteins. Although technically demanding, the yeast two-hybrid procedure may allow the identification of so-called 'partner' proteins involved in such processes as terminal rosette complex formation for cellulose synthesis or interactions that might occur between glycan synthases and glycosyltransferases during the synthesis of substituted polysaccharides. Thus, identifying a partner with a known function may help to elucidate the function of gene of interest. For example, by biochemical means in an *in vitro* assay, it has been shown that mannan synthase and (1→6)-α-D-galactosyltransferase work together to make a legume seed galactomannan (Edwards *et al.*, 1989; Edwards *et al.*, 2004). Taking this finding into consideration, it was decided in the present study to investigate possible interactions between two transcriptionally abundant barley glycosyltransferases, HvGlyT3 and HvGlyT4, and a barley UDP-xylose epimerase (HvUXEP) as "baits", and two wheat cDNA libraries ("prey"), one made from whole developing grain (1-7 days post anthesis) and the other from developing wheat endosperm (1-7 days post anthesis).

4.2 MATERIALS AND METHODS

4.2.1 Materials

Yeast strains (AH109 and Y187), X-Gal, vectors pGADT7, pGADT7-Rec and pGBKT7, synthetic "Drop-Out" supplements [-Trp, -2 (-Leu/-Trp) and -4 (–Ade/-His/-Leu/-Trp)] and herring testes carrier DNA were purchased from Clonetech (Palo Alto, CA, USA). Kanamycin, acid washed glass beads (212-300 μM), SDS, polyethylene glycol (P3640), lithium acetate and adenine hemisulphate were purchased from Sigma-Aldrich (St. Louis, MO, USA). Yeast nitrogen base without amino acids, bactopeptone and granulated agar were obtained from Becton-Dickinson and Company (Sparks, MD, USA). Restriction enzymes were purchased from Roche Applied Science (Penzberg, Germany). A QIAquik Gel Extraction Kit and a QIAprep Spin Miniprep Kit were obtained from Qiagen (Clifton Hill, Vic, Australia). Oligonucleotide primers were purchased from Geneworks (Adelaide, SA, Australia). Taq DNA polymerase was obtained from Invitrogen (Carlsbad, California, USA). The wheat developing whole grain and endosperm cDNA libraries in pGADT7-Rec (Figure 4.3) were generously provided by Dr. Sergiy Lopato (University of Adelaide, Australia). A full-length barley cDNA clone of UDP-xylose epimerase (*HvUXE*) was obtained from Dr. Qisen Zhang (University of Adelaide, Australia).

4.2.2 Creating HvGlyT3, HvGlyT4 and HvUXE bait constructs

Partial sequences of *HvGlyT3* as described in Chapter 2, lacking the TMH to avoid intrinsic problems associated with membrane proteins, and the full length sequences of *HvGlyT4* and *HvUXEP* were amplified using gene-specific primer sets with an engineered restriction enzyme site at the 5' end of the primers (Table 4.3). The PCR

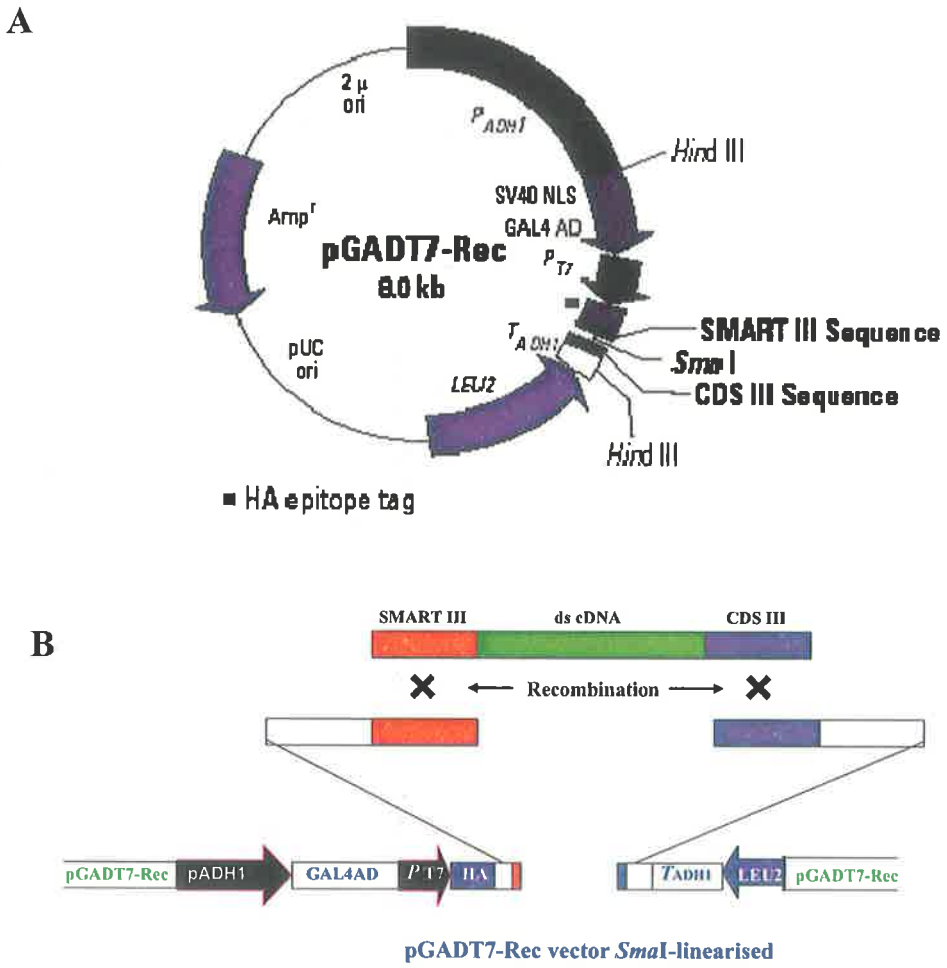

Figure 4.3 The prey vector pGADT7-Rec carries the DNA activation region. A: This vector expresses a protein of interest bearing the GAL4 activation domain (GAL4 AD). Transcription starts after the constitutive ADH1 promoter (P_{ADH1}) and is terminated at the ADH1 transcription termination signal (T_{ADH1}). The fusion protein is targeted to the yeast nucleus by the SV40 nuclear localisation sequences that have been added to the activation domain sequence. The plasmid also contains the T7 promoter (PT7), a hemagglutinin (HA) epitope tag and a MCS. T7 promoter drives the expression of hemagglutinin (HA-tag). pUC and 2 μ are the origin of replications in pGADT7, which are responsible for autonomous replication of the plasmid in *E. coli* and *S. cerevisiae,* respectively. The plasmid carries Amp^r for selection in *E. coli* and the LEU2 nutritional marker for selection in yeast (Chien *et al.*, 1991). **B**: The homologous recombination of double stranded cDNA and *Sma*I linearised pGADT7-Rec in the yeast cell after co-transformation is shown. The wheat cDNA library was cloned into pGADT7-Rec. (http://www.bdbiosciences.com/clontech/techinfo/vectors/vectors F-I/pGADT7-Rec.shtml).

Enzyme	Primer sequences	Restriction enzymes
HvGlyT3	F:GTACAACCATGGTCAACCTCTCCCTCCCGTCC	*Nco*I
	R: CAGTAAGATCTAGAAGTGGTCGGCATCTTGGC	*Bgl*II
HvGlyT4	F:TGCCTTGAATTCATGTTTGCTGCGGAAATATTC	*Eco*RI
	R:AACTCTCTGCAGCCACGGTTTCAGATCTCCAAC	*Pst*I
HvUXE	F:ATGTGCGAATTCATGCTCACCCAGCCACCCTGC	*Eco*RI
	R:TCACTAGGATCCGTGAGTCAAAGAATATATCGA	*Bam*HI

Table 4.3 Primers used for PCR amplification containing the engineered restriction sites. The restriction enzyme sites are underlined in the primer sequences. F= forward primer, R= reverse primer

amplified fragments were digested with the corresponding restriction enzymes as described in section 2.2.7 (Table 4.3). The digested fragments were separated on 1% agarose gels, the bands excised from the gel and purified using the QIAquik Gel Extraction Kit following the instructions provided by the manufacturer. The purified PCR fragments were ligated into the pGBKT7 plasmid digested with the same enzymes (Table 4.3), as described in section 2.2.6 (Figure 4.4). The ligation mixes were transformed into DH5α *E. coli* electrocompetent cells (section 2.2.6) and plated out on LB plates containing 25 mM kanamycin. The plasmid DNA was extracted using a QIAprep Spin Miniprep Kit following the instructions provided by the manufacturer. The pGBKT7 plasmids containing inserts of the correct sizes were subjected to sequencing reactions using T7 (5'TAATACGACTCACTATAGGGC3') and BD (5'TAAGAGCACTTTAAAATTTGTA T3') primers as described in section 2.2.8. The bait vectors, along with empty prey plasmid (empty pGADT7; Figure 4.5), were used to co-transform the yeast strain AH109 to test for self-activation.

4.2.3 Yeast transformation

Saccharomyces cerevisiae strains AH109 and Y187 were streaked out from a frozen glycerol stock onto SD agar plates (0.6% w/v yeast nitrogen base, 2% w/v glucose, 0.083% w/v "Drop-Out" media, pH 5.6 and 0.6% w/v agar). The plates were incubated for 3-5 days at 30°C and kept at 4°C for 3-4 weeks. SD media (1 ml of the above media lacking agar) was inoculated with single colonies from each plate and the clump of cells was dispersed by vortexing. The resuspended cells were used to inoculate 100 ml YPDA media (1% w/v yeast extract, 2% w/v glucose, 2% w/v trypton/peptone and 3% v/v of 0.2% filter sterlised adenine solution) and shaken at 30°C for 16 h or until the OD_{600} reached 1.5. The yeast cells were pelleted at 1000 ×g for 5 min, resuspended in 5 ml fresh YPDA, and the volume was adjusted to 100 ml. The cells were incubated at 30°C for 2 h with shaking. The cells were pelleted at 1000 ×g for 5 min. The herring testes carrier DNA was dissolved in boiling water for 15 min and left on ice. The pelleted cells were resuspended in milli-Q^{TM} water (50 ml) and pelleted at 1000 ×g for 5 min. The cell pellet was resuspended in 2 ml 10 mM Tris-HCl buffer, pH 8.0 containing 1 mM EDTA and 100 mM lithium acetate.

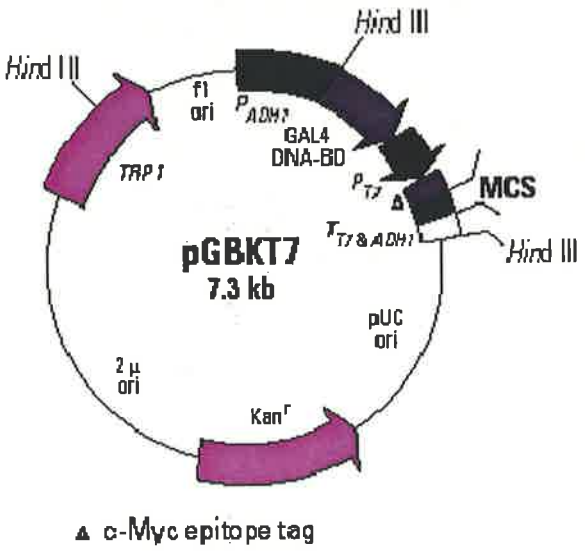

Figure 4.4 pGBKT7 is the DNA-BD vector called the bait vector. This vector expresses proteins fused to amino acids 1-147 of the GAL4 DNA binding domain. In yeast, fusion proteins are expressed at high levels from the constitutive ADH1 promoter (P_{ADH1}) and terminated by the T_{ADH1} transcription terminator signal. T7 promoter is responsible for expression of a c-Myc epitope tag, which is terminated by the T7 transcription termination signal (T_{T7}). The plasmid contains the T7 promoter, a c-Myc epitope tag and a multiple cloning site (MCS). The pUC and 2 µ ori are the origins of autonomous replication in *E. coli* and yeast, respectively. The plasmid contains Kan^r for selection in *E. coli* and the TRP1 nutritional marker for selection in yeast (http://www.bdbiosciences.com/clontech/techinfo/vectors/vectorsFI/pGBKT7.shtml) (Louvet *et al.*, 1997). The barley *HvGlyT3*, *HvGlyT4* and *HvUXE* cDNA fragments were ligated into the MCS of the pGBKT7 to make the bait construct.

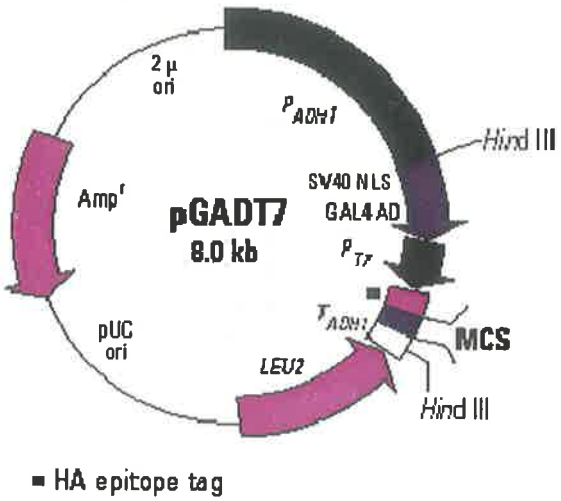

Figure 4.5 pGADT7 is the DNA activation vector called a prey vector. This vector expresses proteins fused to amino acids 768-881 of the GAL4 activation domain (AD). In yeast, fusion proteins are expressed at high levels from the constitutive ADH1 promoter (P_{ADH1}); transcription is terminated at the ADH1 transcription termination signal (T_{ADH1}). The fusion protein is targeted to the yeast nucleus by the SV40 nuclear localisation sequences that have been added to the activation domain sequence. The plasmid also contains the T7 promoter, an HA epitope tag and a MCS. pUC and 2 µ are the origin of replications in pGADT7 which are responsible for autonomous replication of the plasmid in *E. coli* and *S. cerevisiae,* respectively. The plasmid carries Amp^r for selection in *E. coli* and the LEU2 nutritional marker for selection in yeast (Chien *et al.*, 1991). This vector is used for cloning of the interacting partners after a putative interaction *via* the initial screening is established. Either bait or prey protein is cloned into pGADT7 and mated with its partner to confirm that the interaction is real. The plasmid is also used to test the self-activation of the bait vector (**http://www.bdbiosciences.com/clontech/techinfo/vectors/vectorsFI/pGADT7.shtml**). The pGADT7 differs from pGADT7-Rec in a sense that the latter contains adaptor sites which enable the *Sma*I-linearised vector to take up the adaptor ligated dscDNA molecules by means of homologous recombination.

Self-activation of the bait construct, *i.e.* interaction with the empty prey vector (pGADT7), was tested by both transforming and co-transforming the AH109 yeast cells with empty bait vector (1 µl), both bait vectors (1 µl), and empty prey plasmid (1 µl), respectively. The transformation of yeast was performed in a reaction containing herring sperm (5 µl) and resuspended AH109 cells (105 µl).

At the same time, the Y187 yeast strain was transformed with the bait plasmids as above, except for the empty vector preparing the strain ready for mating with the cDNA library. The reactions were mixed and 610 µl transformation solution (1.5 ml 1 M lithium acetate, 1.5 ml 10 × TE and 0.6 ml 50% w/v PEG_{3350} in a total volume of 12 ml) was added to the mixture. The reactions were incubated at 30°C for 1 h with gentle shaking. DMSO (70 µl) was added and, after mixing, the tubes were incubated at 42°C for 15 min, followed by chilling on ice for 2 min. The cells were collected by centrifugation at 1000 ×g for 2 min. The cells were surface washed with 40 µl dH_2O and pelleted at 1000 ×g for 1 min. The cells were resuspended in 100 µl 1 × TE buffer (10 mM Tris-HCl buffer, pH 8.0 containing 1 mM EDTA) and plated on SD agar plates with appropriate selection. The prey vector, pGADT7-Rec contains the nutritional marker "Leu2" that enables the host to grow on a selective media lacking leucine. The bait vector, pGBKT7 bears the nutritional marker "TRP1", which enables the host to grow on selective media lacking tryptophan. Thus, AH109 yeast cells that contained both the prey vector, pGADT7-Rec, and the empty bait vector, pGBKT7, were plated on selective media lacking both amino acids (-Trp/-Leu, also known as -2). Similarly, because Y187 was transformed with pGBKT7, it was plated on selective media lacking tryptophan (Trp). The plates were incubated for 3-5 days at 30°C.

4.2.4 Investigation of self-activation and non-specific protein binding of bait construct

Streaks of individual clones of the transformed AH109 yeast strain containing bait plasmids and empty pGBKT7 were made on SD -2 agar plates (0.6% w/v yeast nitrogen base without amino acids, 2% w/v glucose, 0.6% w/v agar, -Trp/-Leu "Drop-

Out" supplement, pH 5.8) and incubated for 18 h at 30°C. The following day, the clones were replica plated onto SD -2 agar plates and also SD lacking four amino acids (-Ala/-His/-Trp/-Leu, also known as -4), and on agar plates containing 20 mg/ml X-α-Gal (0.6% w/v yeast nitrogen base without amino acids, 2% w/v glucose, 0.6% w/v agar, -Ala/-His/-Trp/-Leu "Drop-Out" supplement, pH 5.8) and incubated for 18 h at 30°C. The lack of self-activation and non-specific protein interactions were checked through observing the lack of development of blue colour on SD -4 plates.

Streaks of individual clones of the Y187 yeast strain, transformed with bait vectors (Section 5.2.3), were made on SD -Trp agar plates and incubated for 18 h at 30°C. An individual clone (2 cm area) was transferred into 100 ml SD –Trp liquid media (0.6% w/v yeast nitrogen base without amino acids, 2% w/v glucose, -Trp "Drop-Out" supplement, pH 5.8) and incubated for 16 h at 30°C with shaking. The yeast cells were pelleted at 800 ×g for 5 min and the pellet was resuspended in 25 ml 2 × YPDA media containing 0.01% adenine hemisulphate and 25 µg/ml kanamycin. The cells were transferred to a 1000 ml vessel and an aliquot of the wheat developing grain or endosperm cDNA libraries in the AH109 yeast strain was added to the vessel. The two yeast strains were left to mate for 16 h at 30°C with very gentle swirling (50 rpm). The following day, the callus-like stack of cells was collected at 800 ×g for 5 min. The cells were washed twice in 0.3-0.5 × YPDA media (50 ml) containing 0.01% (w/v) adenine hemisulphate and 25 µg/ml kanamycin. The cells were pelleted in between washes at 800 ×g for 5 min. The cells were resuspended in 5-7.5 ml of 0.3-0.5 × YPDA media containing 0.01% (w/v) adenine hemisulphate and kanamycin (25 µg/ml) and plated (300 µl) onto SD -4 agar plates. The plates were sealed and incubated up to 5-10 days at 30°C. The clones obtained were collected after two days and streaked on SD -4 agar plates containing 20 mg/ml X-Gal, followed by incubation for 1-2 days. The blue clones, which represent a putative protein-protein interaction, were transferred to YPDA media (5 ml) and incubated at 30°C for 16 h with shaking. Yeast cells (4 ml) were pelleted at 16,000 ×g for 1 min for extraction of yeast plasmid DNA.

4.2.5 Yeast plasmid DNA extraction

Yeast plasmid DNA was extracted from each of the pelleted clones by adding 200 µl extraction buffer (50 mM Tris-HCl buffer, pH 7.4 containing 130 mM NaCl, 5 mM EDTA, 5% w/v SDS), with approximately 30 glass beads (21-300 µm) and 200 µl phenol/chloroform (1:1 v/v). The cells were resuspended twice for 2 min in a platform shaker at 3,000 rpm and incubated on ice between each vortex for 2 min. The cellular debris was removed by centrifugation at 16,000 ×g for 15 min and the supernatant (200 µl) was transferred to a clean tube. Absolute ethanol (600 µl) was added with 20 µl 3 M sodium acetate pH 4.8, followed by a brief vortex. The mixture was incubated at -20°C for 1 h and yeast plasmid DNA was pelleted at 13,000 rpm for 15 min at 4°C. The DNA pellet was washed twice with 500 µl of 75% (v/v) ethanol and dried under vacuum. The DNA was resuspended in 40 µl dH_2O.

4.2.6 Investigation of self-activation and non-specific protein binding of the prey construct

In order to reduce the number of redundant clones requiring investigation, the prey cDNA clones interacting with the bait plasmid were amplified *via* PCR, with an initial denaturation step at 94°C for 30 sec, followed by 35 cycles of [94°C for 30 sec; 50°C for 30 sec; 72 for 2.5 min]. The cDNA fragments were amplified using T7 and 2HRev (5'GGGTTTTTCAGTATCTACGATTC3') primers and half the PCR volume was separated on a 1.2% agarose gel (Figure 4.6, Panel A). The PCR products of a size lower than 400 bp were ignored and the products with a similar size to each other were digested with *Hae*III (section 2.2.7) to identify redundant clones, and half the volume (10 µl) of the digestion reaction was separated on a 3% agarose gel (Figure 4.6, Panel B). The singleton prey plasmids (1 µl yeast DNA) were used to transform *E. coli* electrocompetent cells (DH5α) as described in section 2.2.7. The plasmids were purified using the QIAprep Spin Miniprep Kit. The isolated prey plasmid was used with the empty bait vector (pGBKT7) to co-transform the AH109 yeast strain. These cells were plated onto SD -2 agar plates. The empty bait vector was used to transform the AH109 yeast strain as the negative control when screening for false

positives. The plates were incubated inverted for 2 days at 30°C. A streak of each individual clone was made on an SD -2 agar plate and incubated overnight. The streaks were replica plated onto SD -4 agar plates containing 20 mg/ml X-Gal. The prey plasmids with growth on SD -4 agar plates were eliminated from further screening. The remaining cDNA clones were subjected to a sequencing PCR using the T7 and 2HRev primers, and processed as described in section 2.2.9.

4.2.7 Sequence analysis and screening for false positive clones

The sequences obtained were used to query the translated public databases for sequences of wheat, barley, rice and *Arabidopsis* (BLASTX in: http://www.ncbi.nlm.nih.gov /BLAST/ and http://tigrblast.tigr.org/tgi/). The putative prey vectors most likely to be involved in an interaction were chosen to co-transform the AH109 yeast strain along with the empty bait plasmid (pGBKT7) as the negative control. The transformants were plated onto SD -2 agar plates and incubated at 30°C overnight. A streak of each individual clone was made on one side of a divided SD -2 agar plate with the empty pGBKT7 on the other side and the plates were incubated for 16 h at 30°C. The plate was replica plated onto SD -4 agar containing 20 mg/ml X-Gal and incubated at 30°C for 1-2 days. The positive clones were identified as developing blue colour, but only scored as positive if the empty vector failed to grow in the same media.

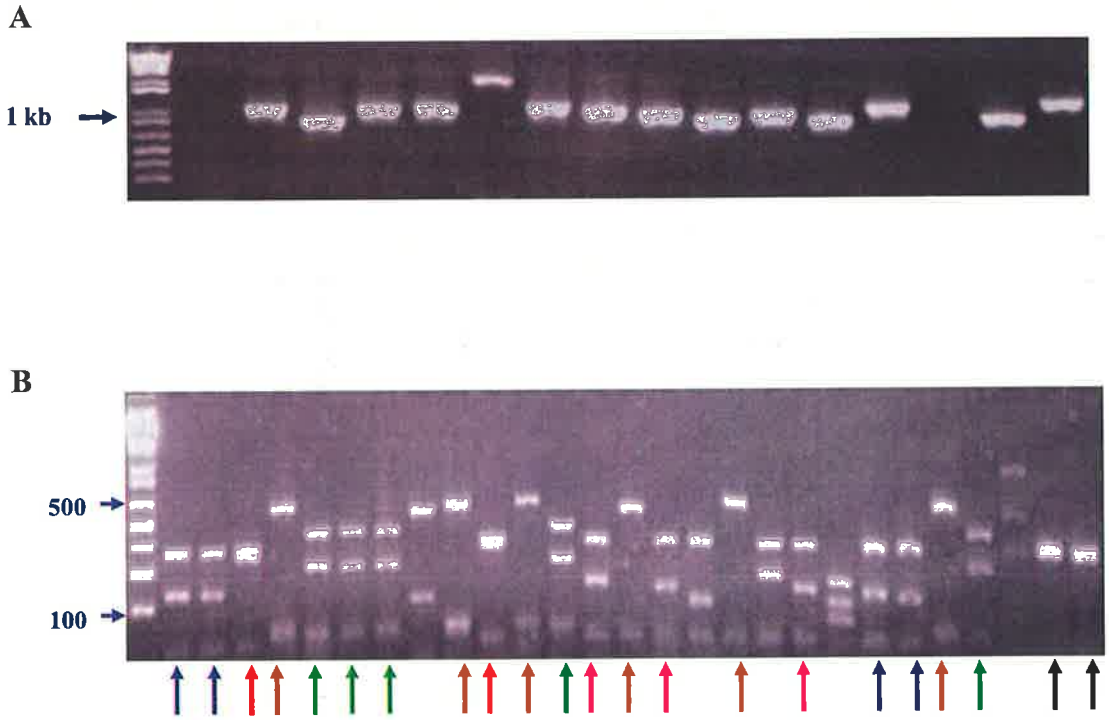

Figure 4.6 Agarose gel electrophoresis of PCR amplified fragments using T7 and 2HRev primers and analysis of digested PCR fragments with *Hae*III. **A:** The primers were used to amplify insert DNA from the interacting prey construct with *HvGlyT3* as bait. The lanes with the same size insert were further analysed with a restriction enzyme digest to eliminate the repetitive clones. **B**: Amplified PCR fragments were from the prey constructs of the wheat developing endosperm cDNA library that interacted with *HvGlyT3* as the bait construct. The lanes containing the same pattern of restricted fragments, indicated with the same coloured arrow, were considered as one clone and one of each in addition to the ones with dissimilar pattern were chosen for sequence analysis.

4.3 RESULTS AND DISCUSSION

4.3.1 Introduction

With the genomes of model plants such as *Arabidopsis* and rice now completely sequenced, it is essential to understand how the individual genes and proteins are organised into biological networks. The discovery of protein complexes and interacting pathways are key elements. Yeast two-hybrid screening is one of the basic approaches that one can carry out to find partner genes and proteins (Fields and Song, 1989). The technique detects direct *in vivo* physical interactions between proteins in a simple and cost effective manner (Fashena *et al.*, 2000). The interaction may be indicative of a true interaction *in vivo* that may reveal a role for the novel protein. Although the technique is very informative, like many others, it has its particular disadvantages (Table 4.2).

Bait constructs were made for the barley members of family GT34 (*HvGlyT3*), family GT47 (*HvGlyT4*) and an important nucleotide sugar interconverter (*HvUXEP*), and used to screen wheat developing endosperm and grain cDNA libraries in order to detect potential interacting proteins. The *HvGlyT3* and *HvGlyT4* cDNAs were cloned because transcript analyses indicated that these were transcribed at relatively higher levels (see Chapter 3). Furthermore, these cDNAs were considered prime candidates for α-arabinosyltransferase and glucuronosyltransferase involved in glucurono-arabinoxylans biosynthesis.

4.3.2 Screening with HvGlyT3 bait construct against the developing wheat grain and endosperm libraries

The *HvGlyT3* bait construct was used to screen the developing wheat grain (1-7 d) and developing endosperm (1-7 d) libraries. The bait construct was tested for self-activation (section 5.2.4) and mated with the libraries to screen for any potential

Interacting protein	Accession Number	Number of positives
Acetyl-CoA carboxylase	7438101	2
Aldehyde dehydrogenase	11995457	1
Amp-binding protein	7670021	1
Ankyrin-like protein	27542766	2
Early responsive to dehydration	1522269	1
GTP binding protein	34911289	2
Hypothetical protein	18415084	5
Hypothetical protein	45661517	1
Hypothetical protein	47205898	1
Hypothetical protein	34910022	1
Hypothetical protein	23237849	1
Hypothetical protein	41053249	1
Hypothetical protein	29788823	1
MYB-like protein	18416582	1
Putative plasmodesmatal receptor protein	46805236	1
Putative polygalacturonase	40253465	1
Putative ABC transporter	37806016	1
Putative purple acid phosphatase	34910020	2
Putative lipid transfer protein	10803445	1
Putative bundle sheath defective protein2	4732091	2
Ribosomal protein	13676681	1
Serine carboxypeptidase	2815493	2
UDP-glucuronic acid decarboxylase	45421832	1

Table 4.4 Putative interacting proteins from screening of the wheat whole grain library using *HvGlyT3* as the bait construct. Protein identity, related accession numbers and the number of repetitions for each clone are listed.

Interacting protein	Accession Number	Number of positives
Serine carboxypeptidase	2815493	15
Unknown protein	19523997	1
	8778845	1

Table 4.5 Putative interacting proteins from screening of the wheat endosperm library using *HvGlyT3* as the bait construct. Protein identity, related accession numbers and the number of repetitions for each protein are listed.

interactions. The proteins that appeared to interact with *HvGlyT3* are listed in Tables 4.4 and 4.5. Two prey clones showed self-activation. The interaction of ankyrin-like protein may be due to non-specific binding as it has appeared in cDNA library screens using other bait constructs (personal communication with Dr. Sergiy Lopato).

A serine carboxypeptidase (accession no. 2815493) appeared to interact strongly (15 positives) with the *HvGlyT3* bait construct during the screening of the wheat endosperm library (Table 4.5). The strong interaction can be described as the number of screened clones of a particular protein, which appears to interact with the protein of interest. Serine carboxypeptidase is an enzyme that specifically removes amino acids from the COOH-terminus of proteins (Doan and Fincher, 1988; Ramirez-Zavala *et al.*, 2004), and is involved in the degradation of storage proteins during grain germination (Muntz *et al.*, 2001). This interaction appeared to be a true interaction, but the biological function or a clear rationale for a GT reacting with a serine carboxypeptidase is not immediately evident.

The interacting protein with the highest number of positives (5) when HvGlyT3 was screened against the whole grain library was an unknown protein of 84 amino acids (accession no. 18415084). This protein had no obvious motifs or properties that would allow its functional identification.

4.3.3 Screening of a whole wheat grain cDNA library using HvGlyT4 and HvUXEP bait constructs

HvGlyT4 and *HvUXEP* bait constructs were used to screen a wheat whole grain cDNA library. The bait constructs were examined for self-activation. The proteins interacting with *HvGlyT4* and *HvUXEP* are listed in Tables 4.6 and 4.7, respectively. It appears that the bait constructs did not interact strongly with any specific protein.

Interacting protein	Accession number	Number of positives
Alcohol dehydrogenase	37787783	1
Phosphoglucanate dehydrogenase	34897872	1
Hypothetical protein	23074079	1
Putative homeodomain protein (controlling seed shattering)	34908294	1
Putative RNA binding protein	40253807	1

Table 4.6 Putative interacting proteins from screening of the wheat whole grain cDNA library using *HvGlyT4* as the bait construct. Protein identity, related accession numbers and the number of repetitions for each clone are listed.

Interacting proteins	Accession number	Number of positives
Ankrin-like protein	34896840	2
Gamma hydroxybutyrate dehydrogenase	29368238	1

Table 4.7 Putative interacting proteins from screening of the wheat whole grain cDNA library using *HvUXEP* as the bait construct. Protein identity, accession numbers and the number of repetitions for each clone are listed.

4.4 SUMMARY AND CONCLUSIONS

The aim of work described in this Chapter was to detect proteins that might interact with HvGlyT3, HvGlyT4 and HvUXEP, and hence to define members of protein complexes that might be involved in cell wall biosynthesis. As mentioned earlier, there are some drawbacks to finding interacting proteins *via* the yeast two-hybrid system, which may lead to weak or false interactions (Table 4.2). The results described in this Chapter failed to produce interpretable information with regards to protein interactions. During the investigating the potential partners for HvGlyT3, interactions were observed with a serine carboxypeptidase and an unknown protein. Although these interactions were strong, it was not possible to draw any firm conclusions, because we were not able to relate the function of a serine carboxypeptidase to a glycosyltransferase. Furthermore, when the unknown protein was subjected to motif searches and analysis of its properties, no conclusive information was obtained. At this stage the interaction between remains undefined, and any biological function will rely on the future identification of protein 18415084. When HvGlyT4 and HvUXEP were used as the baits, no strong interactions with other proteins could be detected.

In the future, assignment of functions to more genes may help to unravel the interactions in a more direct manner, through investigating the interactions of two or more known proteins in a pairwise fashion, rather than screening a cDNA library containing of a large number of genes. Furthermore, recent studies suggest that the co-evolution of genes may facilitate the prediction of interacting proteins through the study of the phylogenetic relationship of the proteins and also by investigating the occurrence of similar transcript profiles (Cobbe and Heck, 2004; Fraser *et al.*, 2004). In relation to cell wall biosynthesis, this matter may be addressed through the investigation of interactions of specific, candidate *CSL* proteins, *GT*s or nucleotide sugar interconverters.

CHAPTER 5 HETEROLOGOUS EXPRESSION OF BARLEY GLYCOSYLTRANSFERASES

5.1 INTRODUCTION

Following the cloning of the five barley putative glycosyltransferases, attention was focused on the functional analyses of these genes. These analyses were initiated by the quantitation of transcript levels in various tissues (Chapter 3). Transcript profiles of the genes were also compared with other genes, using data generated from the barley Affymetrix chip, in attempts to identify underlying correlations that might reveal coordinate expression patterns and therefore suggest functions for some or all of the barley glycosyltransferases. In addition, yeast two-hybrid screening was used (Chapter 4) with the aim of identifying protein partners that might interact with the barley glycosyltransferases, and hence to suggest possible functions on the basis of interactions with other proteins. However, the results obtained from the yeast two-hybrid screening were inconclusive (Chapter 4).

The next step was to subject the cDNAs to heterologous expression and to directly assay expressed proteins for glycosyltransferase activity. It was anticipated this might lead to the assignment of a function to one or more of the enzymes. In the following sections, different heterologous systems are introduced and discussed, the rationale for selecting particular systems is outlined and procedures to produce properly folded active enzymes are described.

5.1.1 Heterologous expression

In the last decade, the identification of genes by high-throughput sequencing of many genomes has raised the question, "What are the structures, properties and functional roles of the corresponding proteins?" At the protein level, many techniques exploiting a range of organisms, including *in vivo* heterologous expression and cell-free protein synthesis from cDNAs encoding the proteins, have been developed to provide sufficient pure protein to directly measure protein activity and function (Sawasaki *et al.*, 2002; Sawasaki *et al.*, 2004). The heterologous expression of recombinant DNA enables rapid production of exogenous proteins and thus plays an

important role in modern functional genomics (Kost, 1997; Dubessay *et al.*, 2004). However, this technique can be successful only if the expressed protein does not have a significant effect on the physiology of host system (Endo and Sawasaki, 2004), and if the host system is able to provide the conditions required for the production of a functionally active protein. One of the key requirements is to develop conditions that allow correct folding of the expressed protein, which in some cases may demand the formation of disulphide bridges or specific post-translational modifications such as glycosylation (Gustafsson *et al.*, 2004). A high level of transcription does not always lead to a high quality active protein (Olins, 1996). A range of biological systems has been utilised as hosts for heterologous expression, including bacterial, yeast, fungal, viral, mammalian and insect cell systems, alongside transgenic plants and animals (Kost, 1997). Each of these systems has advantages and pitfalls that affect protein yield, proper folding, post-translational modification, cost, speed and ease of use (Braun and LaBaer, 2003). In general, biological and biochemical properties of the protein of interest dictate the type of expression system to use (Geisse *et al.*, 1996). For instance, it has been shown that different isoforms or orthologues of a single enzyme isoform will be preferentially expressed in soluble, active form (Persans *et al.*, 2001). Because many of the enzymes of interest are likely to be membrane-bound, their functional analysis through heterologous expression will critically depend on the ability to produce correctly folded proteins in lipid phases or liposomes (Opekarova and Tanner, 2003), such as ergosterols, phosphatidyl choline and phosphatidyl ethanolamine (Opekarova *et al.*, 1999; Robl *et al.*, 2000). Considerable evidence confirms that membrane proteins are dependent on these lipid bodies for their structural integrity and function (Opekarova and Tanner, 2003). These lipids act as cofactors for the membrane-bound protein function or as "co-structures" for their correct folding and stability (Opekarova and Tanner, 2003).

A more recent approach is the expression of cDNAs to produce proteins in cell-free systems, which can avoid some of the inherent difficulties of the intact biological system (Sawasaki *et al.*, 2002; Endo and Sawasaki, 2004; Sawasaki *et al.*, 2004). Although this technique has been successful for some proteins, it requires further optimisation for future success. In the following section, the host systems that have been used in this project, in addition to the ones that have been reported in the

Techniques	Methodology	Examples	Problems
Manipulating the cellular folding apparatus	Amino acid substitution to suppress aggregation	Enhancing electrostatic interactions, hydrophobic interactions and chain configuration	- Which amino acid to substitute? - What is the effect of mutation on the function and stability of the protein?
	Co-overexpression of chaperones	• Heat shock protein (Hsp70) family ○ dnaK in bacteria • Chaperonins ○ GroEL in bacteria	- Finding the correct substrate-chaperone is a major task - Sometimes has detrimental effect through cell septation and filamentation depending on the level of expression of the chaperones (Blum *et al.*, 1992)
	Co-expression of foldases	• PDI • PPIase	Requires optimisation
Manipulating the expression conditions	Choice of expression vector	Strong/weak and inducible/constitutive promoter	
	Reduction of protein synthesis rate	- Lower induction temperature - Lower concentration of inducer	
	Tagging the protein with other highly soluble proteins	See Table 5.2	

Table 5.1 Common techniques that can be used in heterologous expression systems to obtain properly folded proteins. These techniques can be divided into two sub-categories (Wetzel, 1994; Georgiou and Valax, 1996; Weickert *et al.*, 1996; Braun and LaBaer, 2003). Chaperones and foldases are the two classes of accessory proteins that can prevent misfolding of expressed recombinant proteins by assisting the folding and maturation of proteins. Chaperones improve the tertiary structure of proteins through coordinated binding and releasing of partially folded polypeptides, but they do not increase the rate of protein folding (Raikhel and Chrispeels, 2000; Spremulli, 2000). Protein disulfide-isomerase (PDI), an ER-localised enzyme, restores the proper conformation of the expressed proteins *via* establishing disulfide bridges and also by accelerating protein folding in cysteine-rich polypeptides by repeatedly breaking and forming new disulfide bonds (Raikhel and Chrispeels, 2000; Spremulli, 2000). Peptidyl prolyl isomerases (PPIase) are other class of enzymes, which speed up the final folded conformation of proteins *via* the *cis-trans* isomerisation of X-Proline bonds (Spremulli, 2000). A minority of peptide bonds containing a proline residue acquire a *cis* conformation. Thus, PPIases facilitate the formation of the final configuration (Spremulli, 2000).

literature to enable the functional assignment of cell wall glycosyltransferases, are described in more detail.

Escherichia coli

The expression of heterologous genes in bacterial host systems is the simplest and cheapest available technique for synthesising proteins. Heterologous cDNAs are cloned into low copy number plasmids, which should contain a Shine-Dalgarno (SD) sequence complementary to the *E. coli* 3′ end of the 16S rRNA gene and the consensus sequence 5′TAAGGAGG3′ before the start codon (ATG) in order to drive the initiation of translation (Baneyx, 1999). It has been reported that the synthesis of a protein chain occurs every 35 sec, due to the virtually simultaneous events of gene transcription and translation in *E. coli* (Lorimer, 1996), but correct protein folding remains a great challenge in achieving active proteins in this host system (Baneyx and Mujacic, 2004). Thus, despite the ease of use and limited requirements of this system, the production of eukaryotic functional proteins in *E. coli* has often been difficult, since many are either misfolded or unfolded (Weickert *et al.*, 1996). Generally, short proteins containing less than 100 amino acid residues can fold into their native conformation as a result of their fast folding kinetics. In contrast, large protein molecules often aggregate to produce inactive protein masses, known as inclusion bodies, or are targeted for degradation (Baneyx and Mujacic, 2004). A number of techniques for manipulating the cellular folding apparatus have been developed to avoid the formation of inclusion bodies (Table 5.1). In the first set of methodologies, amino acid substitution and the use of accessory proteins such as chaperones may increase the chance of correct folding. Alternatively, alterations in growth or expression conditions leading to slower folding kinetics, providing enough time for each amino acid to find its right configuration within the whole structure of the polypeptide, may result in properly folded proteins. Although these techniques control folding during expression in bacteria, they still do not prevent

misfolding caused by improper and/or insufficient post-translational modifications, such as intra- or intermolecular disulfide bond formation and glycosylation (Bencurova *et al.*, 2003). Concerning the expression of glycosyltransferases in *E. coli*, Pagny *et al.* (2003) showed that glycosylation is an absolute requirement for the activity of GTs from *Arabidopsis*. Thus, *E. coli* might not be a suitable system for expression of the barley GTs.

Codon bias is another important factor and can have profound impacts, not only on expression levels but also on the misfolding of expressed proteins in prokaryotic systems (Gustafsson *et al.*, 2004). Every host species has a specific subset tRNA molecules, which recognise the numerous amino acid codon combinations (Kurland and Gallant, 1996; Gustafsson *et al.*, 2004). The members of each subset vary and thus *E. coli* lacks certain tRNAs, including those that recognise the codons AUA (isoleucine) and AGA or AGG (arginine). If these codons are present in a heterologous cDNA sequence, the protein machinery will freeze during the translation of the corresponding recombinant protein and such a halt in translation may lead to replacement of the amino acid with an incorrect amino acid, which causes an error in the protein sequence. This is referred to as "hungry codon syndrome" (Kurland and Gallant, 1996). One possible solution is to expand the tRNA pool of the host *via* overexpression of genes encoding the rare tRNAs from an introduced plasmid (Gustafsson *et al.*, 2004). Such a plasmid is shown in Figure 5.1. The RIG plasmid carries genes that encode tRNAs for Arg, Ile, Gly, which are deficient in *E. coli* (Baca and Hol, 2000).

Purification tags

Another factor that can contribute to insolubility of the expressed protein is the location and nature of purification tags. For further analysis of the expressed protein, it is usually necessary to purify the protein of interest from a pool of other proteins, which are expressed naturally in the host system. Table 5.2 provides a list of some of the commonly used affinity tags, their sizes and the advantages and the disadvantages of each tag. Although many different proteins, domains or peptides are used as fusion tags, it is difficult to choose the best purification system for an individual protein. Nevertheless, a suitable affinity tag should have the following characteristics: it must

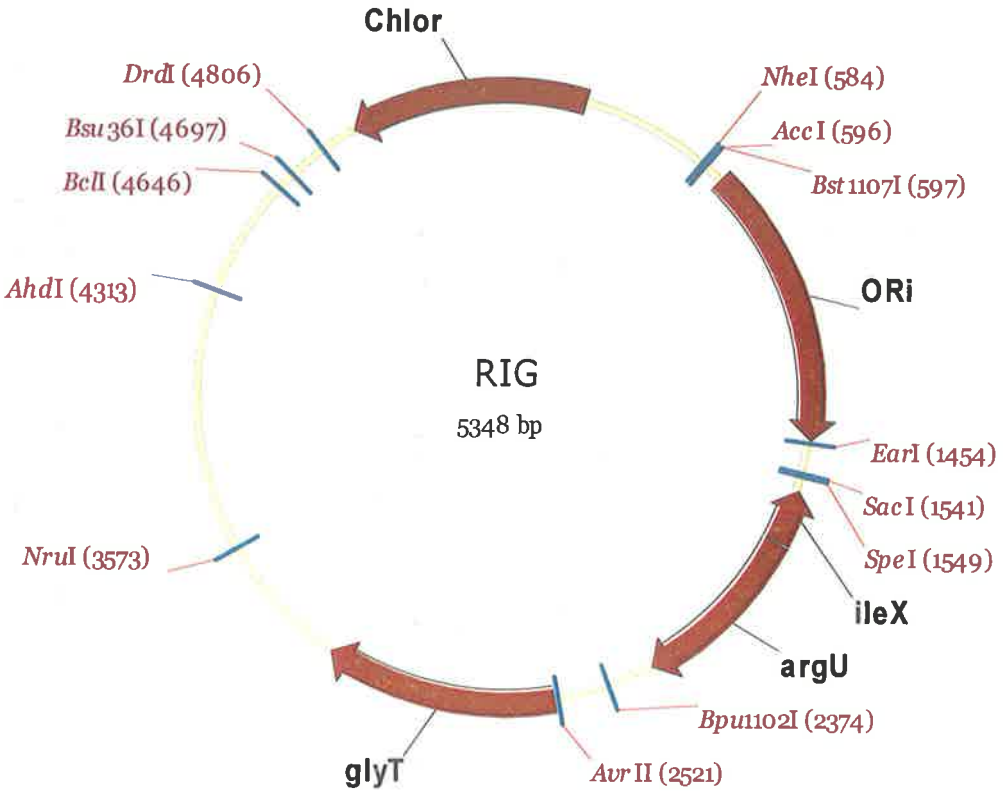

Figure 5.1 The RIG plasmid map with unique restriction sites. RIG is derived from pACYC184 and carries *argU*, *ileX*, and *glyT* genes, which express tRNAs specific for AGG/AGA (arginine), ATA (isoleucine), and GGA (glycine) codons, respectively (Baca and Hol, 2000). Chlor = chloramphenicol resistance.

allow a rapid one-step adsorption purification, it must exert minimal effects on tertiary structure and biological activity, and it must allow for its straightforward and specific removal after purification of the expressed protein (Terpe, 2003).

Purification tags provide a generic purification strategy, usually *via* the affinity of the tag towards immobilised compounds such as metal resins. Additionally, some tags such as maltose binding protein (MBP) and glutathione-S-transferase (GST) are highly soluble, which may increase the solubility of the expressed protein (Kapust and Waugh, 1999; Smith, 2000). Although affinity tags have facilitated the purification of proteins from heterologous expression systems, they sometimes interfere with folding, function and crystallisation of the target protein (Braun and LaBaer, 2003). This might make it necessary to remove the tag. Peptide cleavage sites such as those for thrombin, enterokinase, factor X_a protease and TEV (tobacco etch virus) protease are usually engineered between the affinity tag and the target protein as a linker peptide, to allow removal of the tag following expression. The other approach for removal of the tag is to use self-cleavable tags such as intein, which is more specific and does not require additional chromatographic steps to remove the tag (Chong *et al.*, 1997). In addition to these problems, the presence of the affinity tag does not always guarantee a successful purification of the protein of interest. For instance, the His_6-tag is sometimes buried within the expressed protein, which prevents protein purification *via* nickel-nitrilotriacetic acid (Ni-NTA) affinity chromatography (Terpe, 2003).

Whether to position the purification tag at the COOH- or the NH_2-terminus is another important consideration for the expression of soluble active proteins. Pagny *et al.* (2003) demonstrated that in a (1→2)-β-xylosyltransferase from *Arabidopsis*, anything that interferes with the COOH-terminus of the enzyme, including the His_6-Tag, has to be avoided. A similar result was obtained by Braun and LaBaer (2003).

Tag	Size (kDa)	Purification matrix	Advantage	Disadvantage	Reference
His_6	1	IMAC	• Small size • Detectable *via* immunoassay • Tight binding capability • Functional under denaturing conditions • Uncharged at physiological pH	Poor performance for eukaryotic and HMW proteins	(Hochuli *et al.*, 1987)
GB1	6	IMAC followed by IgG affinity chromatography	• Small size • Stable fold		(Huth *et al.*, 1997)
trxA	11	Osmotic shock or freeze/thaw treatment	• Increase the solubility of eukaryotic proteins	• Weak performance in proteins with HMW • It is not an affinity tag and requires a second tag for purification	(LaVallie *et al.*, 1993)
GST	26	Immobilised glutathione	• High level of expression • Single step purification • Increase in solubility • Detectable *via* either an enzyme assay or immunoassay		(Smith and Johnson, 1988)

MBP	42	Cross-linked amylose, followed by IEC	• Detectable *via* immunoassay • Increase in solubility • High level of expression		(di Guan *et al.*, 1988)
NusA	54	IMAC followed by IEC	• Increase in solubility	• It is not an affinity tag and requires a second tag for purification	(Davis *et al.*, 1999)
CBD-Intein	55	CBD	• Self-cleavable tag		(Chong *et al.*, 1997)

Table 5.2 Purification tags for recombinant proteins. The table provides information regarding the purification tags, which are often used to purify recombinant proteins and sometimes increase the solubility of the heterologously expressed proteins (Braun and LaBaer, 2003; Terpe, 2003). The molecular weight of each tag, its advantages and disadvantages are described in the table. His_6 = poly histidine tag, GB1 = B1 immunoglobulin binding domain of streptococcal protein G, trxA = thioredoxin, GST = glutathione-S-transferase, MBP = maltose binding protein, CBD-intein = chitin-binding domain associated with self-splicing inteins, IMAC = immobilised metal affinity chromatography, HMW = high molecular weight, IEC = ion exchange chromatography

Yeast (Pichia pastoris)

The yeast expression system is easy to use and requires inexpensive growth media (Grisshammer and Tate, 1995), but protein expression takes longer than in *E. coli*. Two species of yeast, *Saccharomyces cerevisiae* and *Pichia pastoris*, have been extensively used for heterologous expression of eukaryotic genes. However, in relation to the expression of active GTs, *P. pastoris* has been shown to be more successful (Malissard *et al.*, 1999). It is likely that *S. cerevisiae* hyperglycosylates the expressed proteins with polymannans consisting of 50-100 mannosyl residues, which may impair the biological activity of the recombinant protein (Malissard *et al.*, 1999). In contrast, *P. pastoris* incorporates 8-14 mannosyl residues on potential glycosylation sites of the expressed protein (Eckart and Bussineau, 1996; Malissard *et al.*, 1999). Besides glycosylation, yeast performs other eukaryotic post-translational modifications such as the removal of the NH_2-terminal methionine, the addition of acetyl groups to the NH_2-terminus, the formation of COOH-terminal methylation complex, myristylation and farnesylation (Eckart and Bussineau, 1996). These modifications, especially the last three, are important in intracellular membrane targeting of expressed proteins, which suggests that yeast would be a relatively good system for the expression of membrane proteins (Grisshammer and Tate, 1995; Eckart and Bussineau, 1996). However, yeast may not share the same eukaryotic protein trafficking and post translational modification steps as mammals, which may prevent it from being a good heterologous system for some proteins (Sadhukhan and Sen, 1996). Gustafsson *et al.* (2004) showed that yeast is one of the closest hosts to plants in terms of containing a similar codon bias, which makes it a potential system for the expression of plant proteins that are not overly sensitive to hyperglycosylation and which are not membrane-bound. The other limiting factor using yeast for the expression of membrane-bound proteins is that the yeast lacks plant specific sterols (sito-, stigma- and campesterol) required for some correct folding and activity of the translated protein. Although yeast contains yeast-specific ergosterol, it often does not result in fully functional heterologous proteins (Opekarova and Tanner, 2003).

Apart from the intracellular steps involved in expressing and processing proteins, it has been shown that expression in yeast requires optimisation of a number of external factors. The position of the affinity tag, temperature, cell density, medium

formulation, variation between clones, the length of the expression period and the type of promoter (constitutive/inducible) need to be tested (Bencurova *et al.*, 2003). In a comparison of eight expressed GTs derived from different organisms, all of which mediated *N*- and *O*-linked oligosaccharide biosynthesis in *P. pastoris*, it was shown that reduction of the expression temperature from 30°C to 16°C decreases yeast growth but increases the overall yield of active protein (Bencurova *et al.*, 2003). Bencurova *et al.* (2003) also concluded that prior to the expression of GTs in *P. pastoris*, a number of plasmids needs to be constructed to test the efficiency of each one, including the full-length cDNA containing the TMH encoding region, and partial-length cDNA lacking the TMH region, under the control of either constitutive or induced promoters. They also studied the effects of affinity tag location, in the expectation that the best position may depend on the location of the catalytic domain in relation to the tag and, in the case of GTs where the catalytic domain is closer to the COOH-terminus, it might therefore be better to fuse the tag to the NH_2-terminus. The use of *P. pastoris* to express cell wall related GTs was described in detail in Chapter 1 and will not be discussed further here. However, yeast might be a useful expression system if all the relevant complexities mentioned above are considered.

Insect cells

Insect cells represent another relatively inexpensive host system for recombinant protein production. They are capable of performing the co- and post-translational protein processing seen in other eukaryotes, which may be important in producing properly folded proteins (Geisse *et al.*, 1996; McCarroll and King, 1997). To introduce the recombinant plasmid containing the gene of interest into the insect cells, two methodologies of transfection have been developed. One is plasmid uptake *via* standard methods such as calcium phosphate coprecipitation, and the other is the introduction of the plasmid into an insect virus so that the recombinant plasmid is subsequently transferred *via* infection of insect cells. The latter involves more steps and also has effects on the insect cell secretory pathway and the integrity of the plasma membrane (McCarroll and King, 1997).

The common insect cells that are used for the purpose of foreign gene expression are derived from *Spodoptera frugipedra* (*Sf*9), usually used with a baculovirus vector, and

Drosophila Schneider cells (S2). The insect cells may be transiently transformed in preliminary experiments and, if successful, a stable transformation can subsequently be performed, and can result in the production of milligram quantities of recombinant protein (McCarroll and King, 1997). The difference between the two transformation techniques is that for stable transformation, in addition to the plasmid bearing the gene of interest, another plasmid carrying a selectable marker is used to transfect the insect cells. Pagny *et al.* (2003) used a baculovirus vector system to express *Arabidopsis* (1→2)-β-xylosyltransferase in *Sf*9 cells, not only to demonstrate its glycosylation function, but also to identify important amino acid residues or domains for GT activity. In another study, Liepman *et al.* (2005) used *Drosophila* S2 cells to define the enzymic functions of *Csl* genes from *Arabidopsis* and rice. The results showed that members of the *CslA* gene family encode β-mannan synthases; the expressed enzyme showed biochemical activity in the presence of GDP-mannose. When both GDP-mannose and GDP-glucose were provided, a glucomannan was synthesised and, in the presence of GDP-glucose alone, (1→4)-β glucan polymers were obtained (Liepman *et al.*, 2005). This work confirmed that of another group (Dhugga *et al.*, 2004), which identified this enzyme through an EST sequencing approach involving guar seed cDNAs.

Mammalian cells

In comparison with other expression systems, working with mammalian cells appears to require sophisticated facilities and expensive reagents (Braun and LaBaer, 2003). Many factors, at both transcription and translation levels, need control the efficient heterologous expression in mammalian cells, including RNA processing, gene copy number, mRNA stability, position effect at the site of chromosomal integration and genetic properties of the cell type (Makrides, 1999). Mammalian cells are able to perform the proper protein folding, together with complex and authentic post-translation modifications (Marino, 1989). Mammalian cells, as with yeast expression systems, hyperglycosylate the expressed protein (Daly and Hearn, 2005) and application of tunicamycin, a sugar analogue of UDP-GlcNAc, can be used to reduce the extent of glycosylation (Elbein, 1984).

Two common strategies, using either viral- or plasmid-based vectors, are generally used to introduce foreign DNA into mammalian cells (Makrides, 1999; Colosimo *et al.*, 2000). Viral expression vectors can transfer the gene of interest to the mammalian cells through infecting the cells, while the other types of vectors can be delivered to the cells *via* both chemical and physical methods, as reviewed by Colosimo *et al.* (2000). These vectors can be used to carry and express the gene of interest either transiently or stably. Transient gene expression facilitates the rapid production, with 2-3 days, of small quantities of proteins for evaluating the system. Baby hamster kidney (BHK), African green monkey kidney CV1 also known as COS cells, human embryonic kidney (HEK)-293 and baby hamster kidney (HEK)-293 cells are amongst the cell lines that are used for transient gene expression (Makrides, 1999). In contrast, stable gene expression is used for expression of genes of interest in Chinese hamster ovary (CHO), Madin-Darby canine kidney (MDCK) or myeloma cells. In addition to these vectors, which integrate foreign DNA into the genome, episomal elements have also been used for gene transfer (Makrides, 1999; Colosimo *et al.*, 2000). These episomal vectors, such as the Epstein-Barr virus (EBV), do not integrate DNA into the genome and the expression of the gene of interest is not subjected to positional effects (Colosimo *et al.*, 2000).

Mammalian cells have been used for expression of plant proteins. One of the earliest attempts was the identification of plasma membrane water channels when an *Arabidopsis* root cDNA library was used for heterologous expression in COS cells (Kammerloher *et al.*, 1994). Perrin *et al.* (1999) demonstrated the expression of a full-length *Arabidopsis* fucosyltransferase (*AtFT1*) in COS cell lines. The expressed AtFT1 showed 41-fold more fucosyltransferase activity in the presence of tamarind xyloglucan compared with the cell lines transformed with empty vector (Perrin *et al.*, 1999).

*Moss (*Physcomitrella patens*): a plant expression system*

Plants represent an inexpensive, simple, versatile and efficient alternative for the production of recombinant proteins. Furthermore, plant cells are more likely to provide all the conditions required for a plant protein to mature and fold into its active form. *In planta* expression of foreign proteins is not only useful for plant proteins,

but the systems can also be used for other eukaryotic and prokaryotic proteins (Hellwig *et al.*, 2004; Li *et al.*, 2004; Marillonnet *et al.*, 2004; Selth *et al.*, 2004; Wagner *et al.*, 2004). For example, recombinant human glycoproteins produced in plants are more similar to their corresponding native protein when *N*-glycosylation is considered, as compared with the same proteins expressed in systems such as yeast, bacteria and filamentous fungi (Gomord and Faye, 2004).

Mosses are small plants belonging to the Bryophyta and are fast growing in popularity as a model functional genomics system because of a number of features that make them easy to handle, grow and transform (Frank *et al.*, 2005). The mosses lack flowers, true vascular tissues and seeds, and remain in a predominantly haploid state (Figure 5.2) during most of their life cycle (Reski and Cove, 2004). The moss *Physcomitrella patens* is the only known plant that has evolved a highly efficient homologous recombination capability (Landy, 1989; Schaefer and Zryd, 1997). This facilitates the integration of foreign DNA into its genome through a single step, to generate both a null allele and an allelic series. This allows rapid and efficient functional analysis of genes (Decker and Reski, 2004; Reski and Cove, 2004). Additionally, P. patens is highly tolerant to abiotic stresses, which makes it a useful system for studying the plant biochemical processes (Cove and Knight, 1993). Mosses lack some of the disadvantages found when higher plants are used as heterologous expression systems, such as genetic instability, the need for containment and the production of recombinant proteins in low yield (Decker and Reski, 2004). Mosses catalyse post-translational modifications that are similar to those in higher plants, including disulfide bridge formation and complex glycosylation (Koprivova *et al.*, 2003). Additionally, a recent review on cell wall composition of mosses demonstrated that the walls contained no xylan in their cell wall structure (Carfa *et al.*, 2005). This makes the moss a potentially useful host for gain-of-function studies of genes related to arabinoxylan biosyntheis.

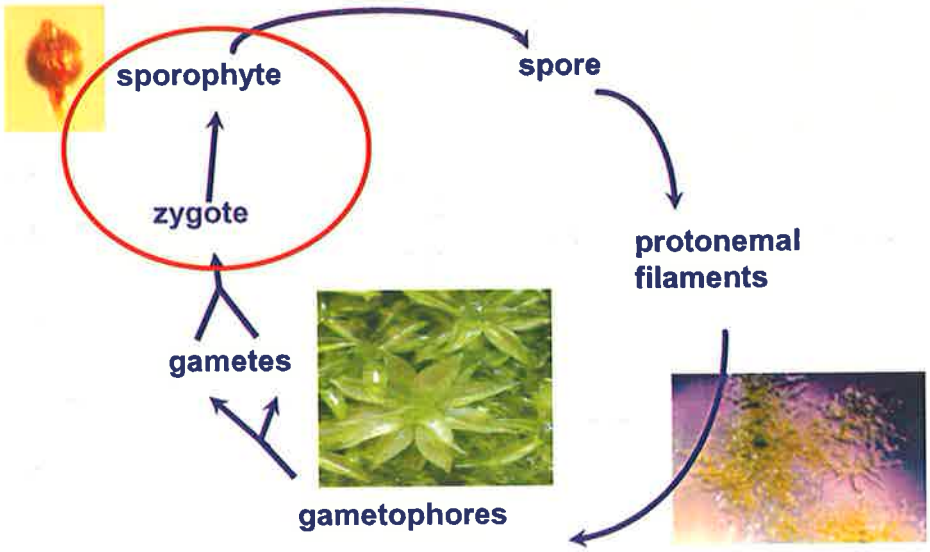

Figure 5.2 Simplified life cycle of moss (*Physcomitrella patens*) (modified after Cove *et al.*, 1997). Haploid gametophyte and diploid sporophyte are the two stages of the moss life cycle. Following mitosis gametes are produced from the gametophyte, and fuse to produce zygotes that develop into the sporophyte. The sporophyte undergoes a meiosis step to produce spores that germinate to produce a long-lived filamentous structure referred as "protonema". Within protonemal stage of the gametophyte, filaments produce branches and extend their length.

5.1.2 Assays for glycosyltransferase activity

Once a recombinant protein is expressed, a convenient assay is required to determine both the functionality of the expressed protein and its substrate specificity. In cases where the recombinant protein is properly folded and has undergone the proper post-translational modifications, the active protein can be further analysed for kinetic and equilibrium properties.

Radioactivity enzyme assays have been routinely used in the study of substrate specificity and activity measurement of cell wall glycosyltransferases, as mentioned in Chapter 1. The requirements for these enzyme assays are: a suitable buffering system, a divalent cation usually Mn^{+2} (see Chapter 1), an enzyme either in a relatively pure form or obtained from a crude extract such as microsomal preparations, and a selection of appropriate substrates. The enzyme reaction is usually started by the addition of a radiolabelled sugar nucleotide substrate, followed by incubation at temperatures lower than 30°C for more than 1 h. In this project [^{14}C]-sugar nucleotides were used as substrates to measure the activity of the recombinant glycosyltransferases.

In parallel to these experiments, a "free sugar" assay was used to screen for unknown GT activity (Bruckner *et al.*, 2000). Instead of using an oligosaccharide as the acceptor substrate, in these assays high concentrations (0.5 M) of neutral sugars are used to "force" the enzymatic reaction towards producing a disaccharide in the presence of the radioactive donor substrate. The unincorporated radioactivity is separated *via* an anion exchange column and the incorporation of radioactivity into the acceptor is measured in a scintillation counter. In both of the above enzyme assay techniques, the outcomes can be further confirmed with specific enzymatic digestion of the reaction products.

In summary, the aim of heterologous expression is to produce biochemically active proteins with technological ease and at a low cost. Unfortunately, individual proteins require specific conditions for correct folding and, in some cases, the only way to

achieve this is by trial and error, using different host systems. Further, a key drawback of heterologous systems is that successfully expressed proteins may display no activity. For example, when Liepman *et al.* (2005) expressed CslE1 and CslH1 proteins in *Drosophila* cells, detectable soluble protein was observed, but neither exhibited measurable activity. This lack of activity might be attributed either to the absence of the proper acceptor or donor substrate in the assay reaction, or the involvement of the enzymes in an enzyme complex (Dhugga, 2005). *In vitro* assays of undefined glycosyltransferases require the inclusion of a range of substrate molecules, some of which are not readily available (Perrin *et al.*, 2001), and in cases where they are available the number of possible combinations make the examination of substrate specificity a large and expensive task. For example, Faik *et al.* (2002) managed to express a number of *Arabidopsis* GTs belonging to family GT34 in *P. pastoris* but they managed to define the function of only one: it was a xyloglucan (1→6)-α-xylosyltransferase, transferring the first xylosyl residue to the glucan backbone. It was proposed that the other family members might also be a xylosyltransferases, but that they required a different substrate such as a glucan backbone substituted with one or more xylosyl residues (Faik *et al.*, 2002).

Although a few Csl proteins (Dhugga *et al.*, 2004; Liepman *et al.*, 2005) and GTs (Edwards *et al.*, 1999; Perrin *et al.*, 1999; Faik *et al.*, 2000; Faik *et al.*, 2002) have shown to be autonomously functional, biochemical and transcript data have indicated that other glycan synthases (Meikle *et al.*, 1991; Dhugga and Ray, 1994; Kudlicka and Brown, 1997; Tanaka *et al.*, 2003; Burton *et al.*, 2004) and some of the GTs (Perrin *et al.*, 1999) require partners for efficient function. It might be possible to overcome this requirement for a complex of enzymes by using *in planta* expression systems (Voinnet *et al.*, 2003; Gleba *et al.*, 2004; Komarnytsky *et al.*, 2004; Marillonnet *et al.*, 2004) and assaying either the crude extract or an enriched protein by the use of an affinity tag. Appropriate design of gene constructs may also be possible where proteins that have previously been shown to require partners for efficient function, such as CesA proteins, are co-expressed at similar levels from a poly-cistronic mRNA driven by a single strong promoter. The interspersion of Internal Ribosome Entry Site (IRES) (Bonnal *et al.*, 2003) sequences between each gene is used to mediate such expression and there is a growing number of these that may be used in vector design

(http://ifr31w3.toulouse.inserm.fr/IRESdatabase). Another more general problem associated with the GT assay is that prediction of function based on sequence relatedness with previously characterised enzymes is often not possible. Although GTs have been classified into families (Campbell *et al.*, 1997), within a family it is possible to find different substrate specificity among paralogues or orthologues of the enzymes. For example, family GT34 contains both xyloglucan α-xylosyltransferases and galactomannan α-galactosyltransferases (Edwards *et al.*, 1999; Faik *et al.*, 2002).

In our study, although some predictions of functions of the cloned barley GT cDNAs were made based on both sequence information and transcript analysis, for the unequivocal definition of gene function it was necessary to produce the enzymes *via* a range of heterologous expression systems, and to assay the expressed proteins for GT activity using a broad range of sugar nucleotide substrates and oligosaccharide, polysaccharide and free sugar acceptors. Based on sequence homology to previously characterised enzymes, it was predicted that HvGlyT1, HvGlyT2 and HvGlyT3 might be α-xylosyltransferases and HvGlyT4 and HvGlyT5 might be α-galactosyl-transferases and glucuronosyltransferases, respectively (see Chapter 2). Transcript data were consistent with α-xylosyltransferase, α-arabinosyltransferase and α-galactosyltransferase roles for the *HvGlyT1*, *HvGlyT3* and *HvGlyT5* genes, respectively (see Chapter 3). The barley genes were evaluated in several heterologous expression systems, including *E. coli*, insect cells, mammalian cells and *Physcomitrella*. The experimental procedures and results are described below.

5.2 MATERIALS AND METHODS

5.2.1 Materials

PCR primers were designed using the Netprimer program available at http://www.premierbiosoft.com/netprimer/netprlaunch/netprlaunch.html and synthesised by Geneworks (Adelaide, Australia). The dNTPs were from Fisherbiotech (West Perth, WA, Australia). Elongase enzyme mix, BenchMark™ Pre-Stained Protein Ladder, pDONR™201, pDEST™17, pET-DEST42, BP clonase enzyme mix, LR clonase enzyme mix, Schneider 2 (S2) *Drosophila* cells, a DES expression system kit, Schneider's *Drosophila* Medium, Nonidet P-40, SF-900 II SFM, $pF_{AST}B_{AC}$ HTa plasmid vector and T4 DNA Ligase were purchased from Invitrogen (Carlsbad, CA, USA). Acrylamide (40%)/Bis solution (29:1) and Precision Plus Protein™ standards were purchased from BioRad (Hercules, CA, USA). Western blue stabilised reagent was bought from Promega (Madison, WI, USA). The electrophoresis power supply ECPS 3000/150 was purchased from Amersham Biosciences Pty Ltd (Castle Hill, NSW, Australia). BD71 dye was purchased from Aldrich (Milwaukee, WI, USA). The Nucleospin extraction kit was from Macherey-Nagel (Duren, Germany). Agarose was obtained from Becton Dickinson (Sparks, MD, USA). Restriction enzymes and BSA (bovine serum albumin) were purchased from New England BioLabs (Beverly, MA, USA). The pET-3a plasmid was obtained from Novagen (Madison, WI, USA). The pET3a was modified by Dr. Helen Healy (University of Adelaide, SA, Australia) and named the pET3a-HT expression vector. Instant skim milk was purchased from Diploma (New Zealand). Mighty Smart II (a SDS-PAGE electrophoresis tank) was supplied by Hoefer Scientific Instruments (San Francisco, USA). Western analysis was performed using a Semi-dry blotter EBU-4000, which was supplied by CBS Scientific Co (CA, USA). Nitrocellulose membrane was obtained from Osmonics (MA, USA). Fuji medical X-ray film was supplied by the Fuji Photo Film Co. (Tokyo, Japan). Luminol was purchased from ICN Biochemicals Inc. (SC, Ohio, USA). Hydrogen peroxide was obtained from BDH Chemicals (Vic, Australia). *E. coli* strains DH5-α and BL-21 were from Stratagene (La Jolla, CA, USA). The pQE-30, pQE-31 and pQE-32 plasmid expression vectors and nickel-nitrilotriacetic acid (Ni-NTA) spin columns were

purchased from QIAGEN Pty Ltd (Clifton Hill, Vic, Australia). Dowex G-55 (Cl-form), UDP-^{14}C-glucuronic acid, UDP-^{14}C-galactose, UDP-xylose, UDP-glucuronic acid, UDP-galactose, chloramphenicol, kanamycin, bromophenol blue, Coomassie Brilliant Blue R, RNase A, *p*-coumaric acid, guar galactomannan, monoclonal anti-polyhistidine (alkaline phosphatase conjugate), leupeptin, IPTG, CHAPS and X-Gal were obtained from Sigma-Aldrich (St Louis, MO, USA). Coomassie protein assay reagent was obtained from Pierce (Rockford, Illinois, USA). Tween 20, sodium bicarbonate, PEG_{4000}, $MgCl_2$, sodium dodecyl sulfate (SDS), glucose, galactose, rhamnose, arabinose, xylose, mannose, fucose, $MnCl_2$, CH_3Cl, 2-mercaptoethanol (2-ME), Triton X-100, N,N,N',N'-Tetramethyl ethylenediamine (TEMED), bacto-trypton, bacto-yeast extract and glycerol were purchased from Merck Pty Ltd (Kilsyth, VIC, Australia). Ecolume scintillation liquid was obtained from ICN Biochemicals (Costa Mesa, CA, USA). Scintillation tubes were purchased from Packard Bioscience (Groningen, Netherlands). PMSF was obtained from Roche Diagnostics (NSW, Australia). Xylotetraose, xylopentaose, mannohexaose, cellopentaose, sugar beet arabinan, carob galactomannan, tamarind seed xyloglucan, gum arabic galactan, apple pectic acid and soybean rhamogalcturonan were purchased from Megazyme International Ireland Ltd Pty (Wicklow, Ireland). Wheat arabinoxylan and oat xylan were isolated and generously donated by Dr. Richard Steward (University of Adelaide, SA, Australia). Gum arabic AGP was donated by Professor Bruce Stone (La Trobe University, Melbourne, Australia). Moss, pMBL6 and pJIT145-Kan plasmid vectors were generously donated by Dr. Celia Knight (University of Leeds, UK). Sonifier B-12 was supplied by Branson Sonic Power Company (Danbury, CT, USA). A TH4 Thermoregulator water bath was purchased from RATEK instruments Pty Ltd (Australia). A liquid Scintillation Counter LS 3801 and an Avanti J-E centrifuge were obtained from Beckman Coulter (NSW, Australia).

5.2.2 PCR amplification and restriction enzyme digestion to generate an expression construct

A set of PCR primers was designed and used in a PCR for selected fragments of GT cDNAs (section 2.2.2). The PCR was performed as described in section 2.2.4 using

Elongase DNA polymerase. The PCR products were separated on a 1% agarose gel. Bands were excised and DNA purified using the QIAquick Gel Extraction Kit, following the manufacturer's instructions. Both full- and partial-length cDNA fragments containing engineered restriction sites at both ends were PCR amplified. The amplified fragments were digested as explained in section 2.2.7 and the digested fragments were ligated into the relevant expression vector (digested with the same restriction enzymes) as mentioned in section 2.2.6. The pET (Figure 5.3), pQE-30, -31 and -32 (Figure 5.4) expression plasmid vectors were used for cloning and subsequent expression in an *E. coli* system. The constructs were transformed into *E. coli* electrocompetent cells (DH5α or XL1Blue), where they were sequenced to check the integrity of the construct as described in section 2.2.8. The correct plasmid DNA, in-frame with the start codon, was transferred into either BL21 (for the pET expression vector) or M15 (for pQE expression vectors) for heterologous expression as described in section 2.2.6. In order to check the sequence integrity of the pET and pQE vectors, the following primers were used; T7: 5′TTAATACGACTCACT ATCGG3′ and T7-terminator: 5′GCTAGTTATTGCTCAGCGG3′ for pET, and pQE-F: 5′CGGATAACAATTTCACACAG3′ and pQE-R: 5′GTTCTGAGGTCATTACT GG3′ for pQE.

The Gateway expression system was also used to generate expression plasmid vectors (Figure 5.6) in pDEST^{TM}17 (expressing protein with the His_6-tag at the NH_2-terminus) and pET-DEST42 (expressing protein with the His_6-tag at the COOH-terminus). In order to amplify the gene of interest, primers contained the attB1 (5′GGGGACAAGTTTGTACAAAAAAGCAGGCTNN; the last two bases must not be AA, AG or GA) in the sense primer and the attB2 site (5′GGGGACCACTTTGTA CAAGAAAGCTGGGTN) in the antisense primer, followed by an 18-25 bp sequence of the gene of interest (Hartley *et al.*, 2000; Walhout *et al.*, 2000). Either TEV or thrombin cleavage sites were engineered into the primer for the post-expressional removal of the His-tag; the cleavage site was engineered between the attB1 and the gene-specific sequence for an NH_2-terminus His-tag, and between the attB2 site and the gene-specific sequence for a COOH-terminus His-tag.

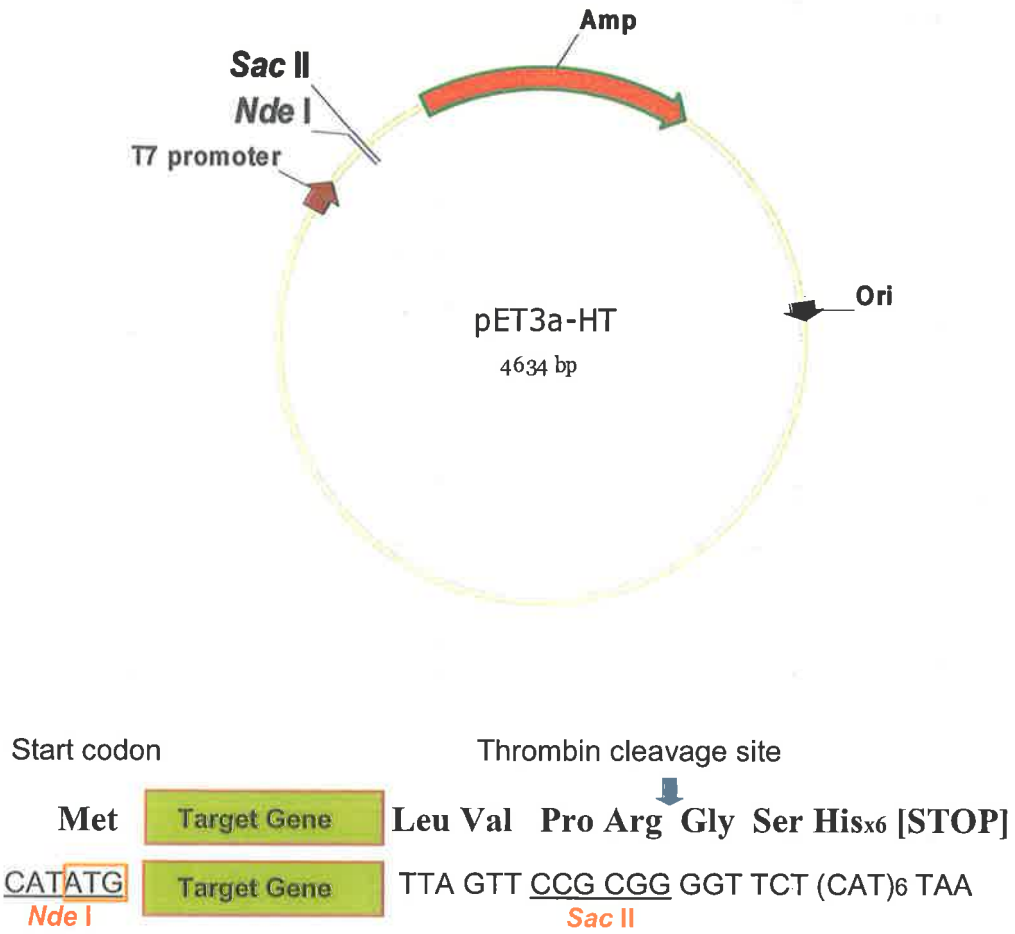

Figure 5.3 The pET3a-HT expression vector. The vector contains a strong T_7 promoter driving the expression of the target gene cloned into *Nde*I/*Sac*II restriction sites. The vector allows affinity column purification *via* the inclusion of an in-frame poly-histidine (His) tag at the COOH-terminus of the open reading frame. A thrombin cleavage site is located before the histidine tail to facilitate the removal of the poly-His tag after affinity purification of the target protein. The selection marker is ampicillin (Amp^R). The ATG of the *Nde*I restriction site is the start codon.

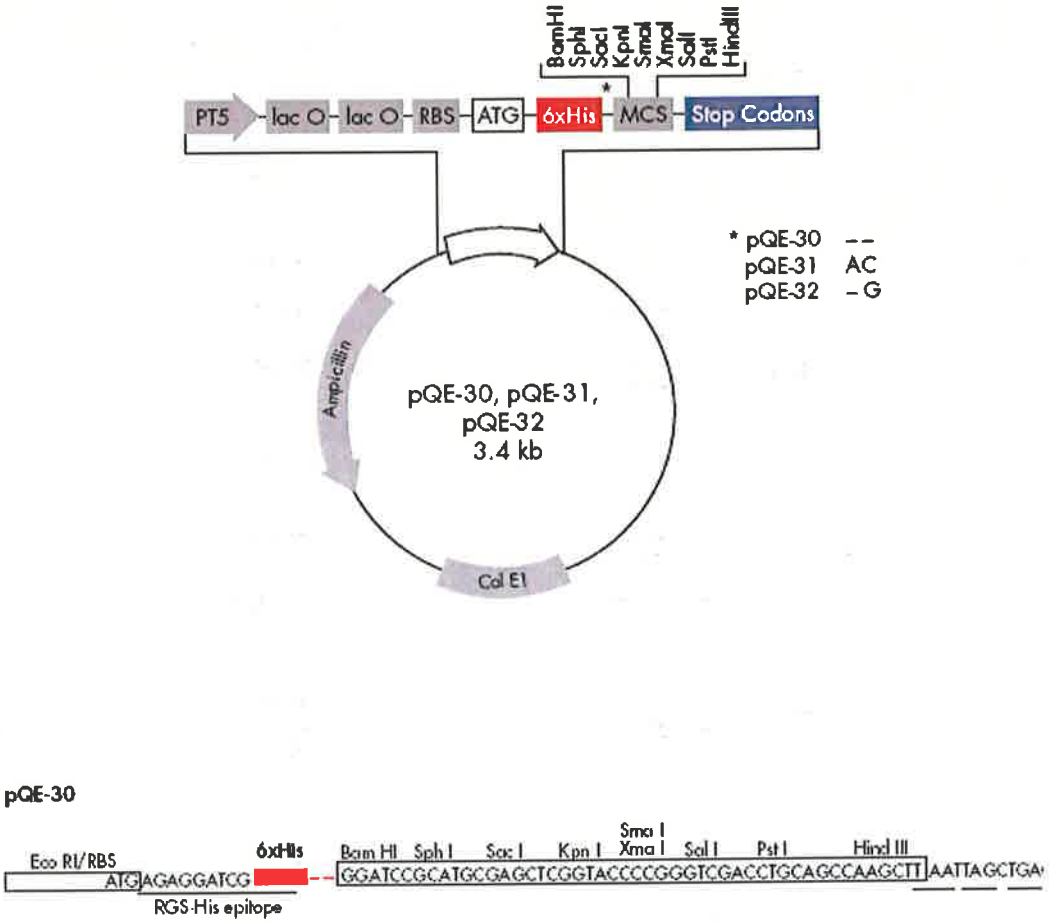

Figure 5.4 pQE expression plasmid vectors for NH_2-terminal His_6-tag constructs (http://www1.qiagen.com/). The vector contains a T5 promoter (pT5) driving the expression of the target gene cloned into the multiple cloning site (MSC). The synthetic ribosomal binding site (RBS) increases the rate of translation. The β-lactamase gene (*bla*) confers resistance to ampicillin at 10 μg/ml as the selectable marker. ColE1 is the origin of replication. lac O = lac repressor, which regulates recombinant protein expression, * = indicates three different reading frames for pQE vectors, t_0 = transcriptional terminator from phage lambda, RGS-His epitope is an amino acid sequence for detection of the His_6-tag using RGS-His antibody.

The fragments were amplified using Elongase as described 2.2.4. Each amplified fragment was separated on a 1% agarose gel and purified from the gel using the Nucleospin kit. The purified PCR fragment was used in a donor vector (pDONR^{TM}201, Figure 5.5) recombination reaction, also known as a BP reaction to create an entry clone. The BP reaction (2 µl amplified fragment, 100-200 ng donor vector, 2 µl BP reaction buffer, 3 µl TE buffer and 2 µl BP clonase enzyme mix) was performed for 16 h at 25°C and stopped by heating to 94°C for 5 min. The BP reaction mix (2 µl) was used in the transformation of XL1Blue *E. coli* cells as described in section 2.2.6 and plated out on LB agar containing 50 µg/ml kanamycin. The plasmid DNA was prepared as described in section 2.2.7 and the integrity of the sequence within the donor vector was checked through DNA sequencing as described in section 2.2.8, using proximal attL1 5′TCGCGTTAACGCTAGCATGGATCTC3′ and proximal attL2 5′GTAACATCAGA GATTTTGAGACAC3′ primers.

Final expression constructs were generated *via* homologous recombination between the entry clone and the expression vector in an LR reaction. The LR reaction (2 µl LR reaction buffer, 1 µl LR clonase enzyme mix, 100-200 ng of both the entry vector and the destination vector) was performed at 25°C for 16 h and stopped by heating to 94°C for 5 min. The newly recombined destination vector was used to transform XL1Blue *E. coli* cells as described in section 2.2.6 and plated out on LB agar containing 100 µg/ml ampicillin. Plasmid DNA was isolated and the presence of the insert within the destination vector was checked through a restriction enzyme digest as described in section 2.2.7. The isolated plasmid was used to transform BL21 *E. coli* cells for protein expression as described in section 4.2.5.

5.2.3 Heterologous expression in E. coli

The transformed *E. coli* clones were grown in "Terrific Broth" (TB: 100 ml 0.17 M KH_2PO_4, 0.72 M K_2HPO_4 added to 900 ml base broth; 1.33% w/v tryptone, 2.66% w/v yeast extract, 0.44% v/v glycerol) containing 50 µg/µl ampicillin and either 25 µg/µl chloramphenicol for BL21 or 25 µg/ml kanamycin for M15 at 37°C for 16 h overnight in a rotary shaker. A 150 µl aliquot of this overnight culture was used to

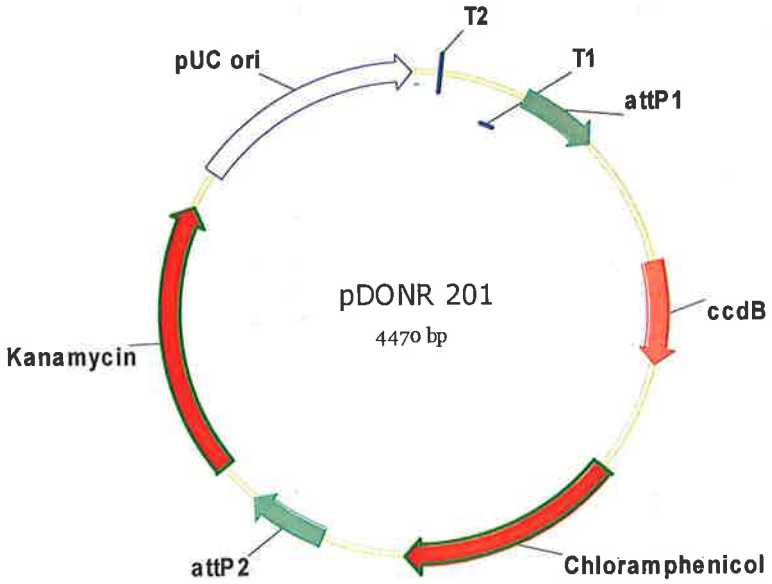

Figure 5.5 Map of the pDONR^{TM}201 (http//www.invitrogen.com). The amplified fragment of the gene of interest with its incorporated recombination signal sequence replaces the *ccdB* and Chloramphenicol genes through BP reaction. This homologous recombination occurs *via* attP1 and attP2. Kanamycin and chloramphenicol resistance allow the selection and counter-selection of expression clones in *E. coli*, respectively. Negative selection of transformants is performed by the presence of *ccdB* gene. T1 and T2 are transcription termination sequences.

A

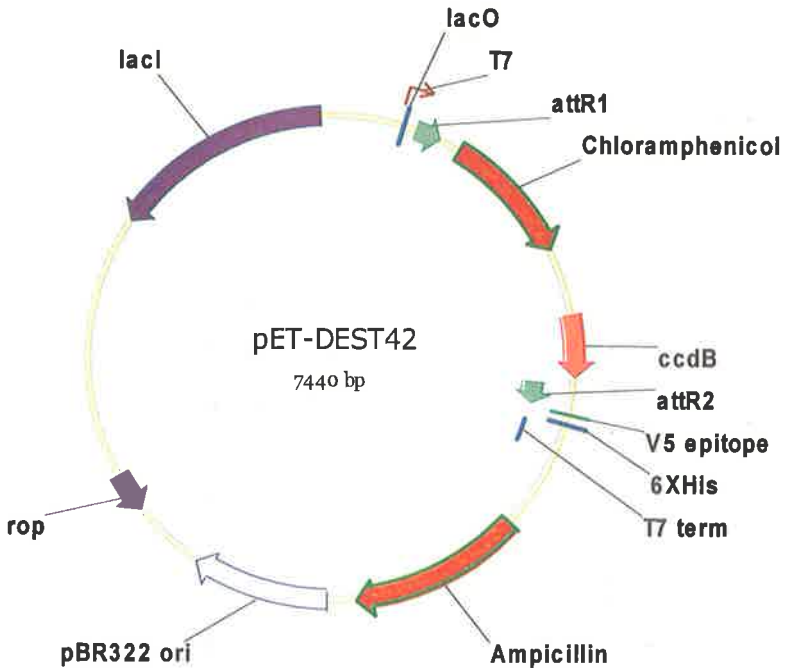
lacO
T7
lacI
attR1
Chloramphenicol
pET-DEST42
7440 bp
ccdB
attR2
V5 epitope
6XHis
T7 term
rop
pBR322 ori
Ampicillin

B

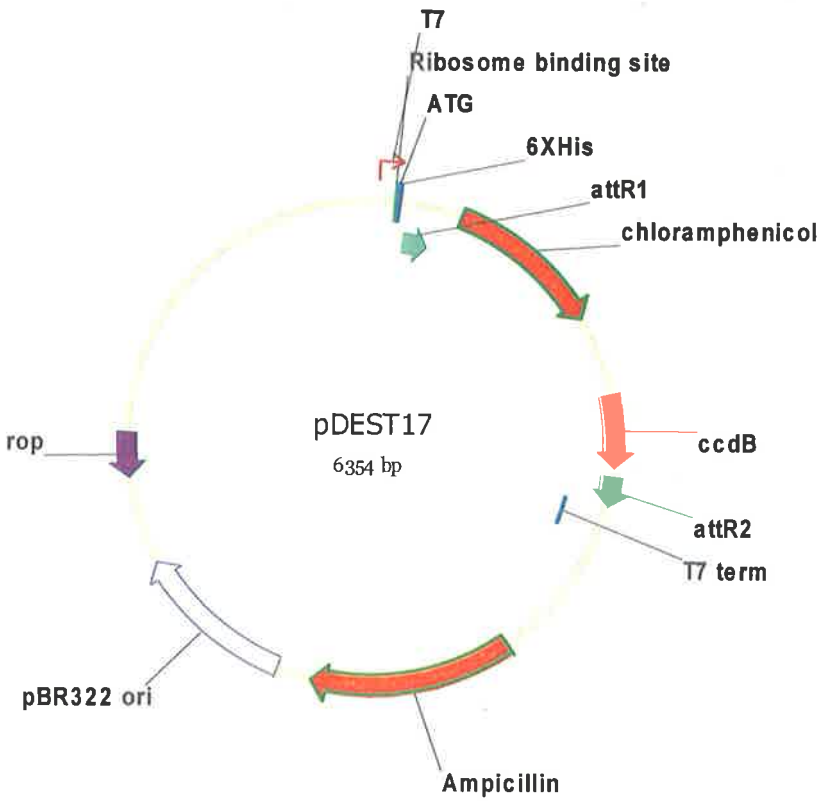
T7
Ribosome binding site
ATG
6XHis
attR1
chloramphenicol
pDEST17
6354 bp
rop
ccdB
attR2
T7 term
pBR322 ori
Ampicillin

Figure 5.6 Map of the Gateway destination vectors for protein expression (http//www.invitrogen.com). **A**: Map of pETDEST42 with a COOH-terminus His_6-tag. **B**: Map of pDEST^{TM}17 with an NH_2-terminus His_6-tag. Homologous recombination occurs between plasmid pDONR^{TM}201 (Figure 5.5), bearing the gene of interest, and the destination vector *via* attR1 and attR2 sites. As a result, the cassette bearing the gene of interest replaces the chloramphenicol and *ccdB* genes in destination vectors. The T7 promoter allows high-level and IPTG-inducible expression of the recombinant protein and also drives the expression of chloramphenicol resistance and *ccdB* genes. Ampicillin and chloramphenicol resistance allow the selection and counter-selection of expression clones in *E. coli*, respectively. lacI = an open reading frame, which encodes the lac repressor to reduce basal transcription from the T7lac promoter, lacO = lac operator, which serves as a binding site for the lac repressor and functions to further repress T7 RNA polymerase-induced basal transcription of the gene of interest in BL21 strains. Rop = an open reading frame, which interacts with pBR322 origin to facilitate low-copy replication in *E. Coli*.

seed 15 ml TB containing the same antibiotics and left to grow until the culture reached an optical density (OD) of 0.5-0.7 at 600 nm. An aliquot (1 ml) was stored as an uninduced fraction and the rest of the culture was induced with 0.5 mM IPTG. The culture was shaken at room temperature for a further 4 h and an aliquot was stored as the induced fraction. The rest of the cells were centrifuged at 2000 ×g for 20 min at 4°C and the pellet was snap frozen in liquid nitrogen. The pellet was resuspended in chilled sodium phosphate buffer (0.5-1 ml) and the cells were ruptured using a sonifier at the output control setting of 7. The ruptured cells were centrifuged at 16,000 ×g for 20 min at 4°C to separate the soluble protein fraction from the insoluble fraction (inclusion bodies). The supernatant (200 µl) was transferred to a 1.5 ml Eppendorf tube as the soluble fraction and the pellet was resuspended with 0.5 ml 8 M urea and labeled as the insoluble fraction. The fractions, uninduced, induced, soluble and insoluble, were separated on an SDS-PAGE gel.

5.2.4 Polyacrylamide gel electrophoresis

The fractions and relative controls were prepared for electrophoresis by boiling in loading dye (0.125 M Tris-HCl buffer, pH 6.8, containing; 4% w/v SDS, 20% v/v glycerol, 5% v/v 2-mercaptoethanol, 0.0005%w/v bromophenol blue) for 10 min. The samples were separated on an SDS-PAGE gel (Laemmli, 1970) (5% w/v polyacrylamide stacking gel and 12.5% w/v polyacrylamide resolving gel) at 40 mA in running buffer (25 mM Tris-HCl buffer, pH 8.3 containing; 250 mM glycine and 0.1% w/v SDS) in a Hoefer protein electrophoresis tank. Gels were stained in 0.625 (w/v) Coomassie Blue R solution containing 25% (v/v) methanol and 7% (v/v) acetic acid for 1 h at 50°C and destained in the same methanol/acetic acid solvent. Either a LMW SDS marker kit (protein sizes ranging from 14.4 to 94 kDa) or a pre-stained marker (protein sizes ranging from 10 to 250 kDa) was used to estimate the size of the protein bands.

5.2.5 Western analysis

Proteins from the SDS-PAGE gel were transferred onto an Osmonics nitrocellulose membrane using a semi-dry blotter under constant amperage (100 mA) for 1 h. The transfer of the protein was performed in an assembly of filter paper (4 pieces of 3MM Whatman paper), nitrocellulose membrane, SDS-PAGE gel and filter paper (16 pieces the same size as the gel) piled on top of one another. All the components were submerged briefly in transfer buffer (12 mM Tris-HCl buffer, pH 8.3, containing 96 mM glycine and 20% v/v methanol). Prior to incubation of the membrane with the antibody, the membrane was stained with 0.008% (w/v) DB71 reagent in 40% (v/v) ethanol/10% (v/v) acetic acid for 2 min to check for successful blotting (Hong *et al.*, 2000). The stained membrane was rinsed briefly with 40% (v/v) ethanol/10% (v/v) acetic acid and the stain was removed by incubation for 5-10 min in a mixture of absolute ethanol:1 M sodium bicarbonate:water (10:3:7). The membrane was blocked using 5% (w/v) skim milk in 1 × TTBS (20 mM Tris-HCl buffer, pH 7.5, containing; 0.5 M NaCl and 0.05% v/v Tween 20) for 30 min at room temperature. The membrane was washed with TTBS twice for 10 min each and incubated with the primary antibody (specific to the antigen or to the epitope tag) in TTBS (1:1000) for 16 h on a rotary shaker followed by three washes, 10 min each, with TTBS. The membrane was incubated with a secondary antibody, either goat anti-rabbit IgG-alkaline phosphatase conjugate or goat anti-rabbit IgG-horseradish peroxidase conjugate in TTBS (1:2000), for 1 h on a rotary shaker, followed by three washes with TTBS. For alkaline phosphatase conjugated secondary antibodies, Western blue stabilised reagent was added as the substrate. Chemiluminscent substrate (90% v/v luminol, 1% v/v *p*-coumaric, 0.06% v/v H_2O_2) was used for developing membranes treated with antibody conjugated with peroxidase for 5 min, followed by exposure to radiography film for a few seconds.

5.2.6 Affinity purification of expressed protein

Depending on the buffering system that was used for resuspension of the pellet (soluble or insoluble fraction), the expressed fraction was separated from the rest of

the proteins present in the solution *via* affinity purification on Ni-NTA columns. All steps in the purification of the soluble fraction were carried out at 4°C, while those for the insoluble fraction were performed at 22°C. If the protein was in the insoluble fraction, the Ni-NTA column was equilibrated with buffer B (8 M urea, 0.1 M NaH_2PO_4, 0.01 M Tris-HCl buffer, pH 8.0). The insoluble fraction containing the His_6-tagged protein (600 µl) was loaded onto the column and the flow-through was collected. The column was washed three times with buffer C (600 µl) containing the same solvents as buffer B with the addition of 0.01 M Tris-HCl buffer, pH 6.3. The His_6-tagged protein was eluted from the column using buffer E (200 µl) containing the same solvents as buffer B but with 0.01 M Tris-HCl buffer, pH 4.5. If the His_6-tagged protein was present in the soluble fraction, the Ni-NTA column was equilibrated with 600 µl lysis buffer (50 mM NaH_2PO_4, 300 mM NaCl, 10 mM imidazole, pH 8.0). The soluble fraction was loaded onto the column and the flow-through was collected. The column was washed 3 times with wash buffer containing the same solvents as the lysis buffer with the addition of 20 mM imidazole. The His_6-tagged protein was eluted with 200 µl elution buffer (50 mM NaH_2PO_4, 300 mM NaCl, 250 mM imidazole, pH 8.0).

5.2.7 Quantification of purified protein

The proteins expressed in heterologous expression systems or protein extracts from plant tissues were quantified using the Bradford assay (Bradford, 1976). In this method, the dye (Coomassie Brilliant Blue G-250) binds to arginine and aromatic amino acid residues, where the anionic form of the residues has a maximum absorbance at 595 nm. A standard series of bovine serum albumin (BSA) solutions containing 0, 10, 20, 50, 100, and 200 µl 0.1 mg/ml BSA was prepared, and 400 µl aliquots were mixed with 400 µl Bradford dye. At the same time, 5 µl test protein extract was added to 400 µl water followed by the addition of the dye. Concentrations of proteins were measured at 595 nm after 5 min incubation at room temperature. A standard curve was prepared and the protein was quantified based on the standard curve and a best fit regression formula.

5.2.8 Generation of baculovirus expression constructs

Constructs were made in $pF_{AST}B_{AC}$ HTa (Figure 5.7) as described in section 5.2.2 and given to Dr. Sassan Asgari (University of Adelaide, SA, Australia) to carry out the expression in *Sf9* cells, using the baculovirus transformation technique. The insect cells expressing the foreign protein were harvested at 24 h, 48 h, and 72 h post-infection. The insect cells (4×10^7) were resuspended in 1 ml lysis buffer (LB I; 10 mM Tris-HCl buffer, pH 7.5, containing 10 mM NaCl, 1.5 mM $MgCl_2$, 10 mM 2-mercaptoethanol) containing proteinase inhibitor (1 mM PMSF and 4 µg/ml leupeptin) and incubated for 30 min on ice. The cells were pelleted at 10,000 ×g for 10 min, the supernatant (S1, soluble fraction) was stored and the pellet was resuspended with 1 ml LB II buffer (20 mM Tris-HCl buffer, pH 7.5, containing 300 mM NaCl, 10 mM $MgCl_2$, 0.5% v/v Triton X-100, 20% v/v glycerol, 10 mM 2-mercaptoethanol) containing proteinase inhibitor. The suspension was sonicated 5 × for 10 sec at an output control setting of 2 on ice, followed by centrifugation at 10,000 ×g for 10 min. The supernatant was named S2 and stored on ice, and the pellet was resuspended with 1 ml LB III (20 mM Tris-HCl, pH 7.5, 500 mM NaCl, 10 mM $MgCl_2$, 2% v/v Triton X-100, 10 mM imidazole, 50% v/v glycerol, 10 mM 2-mercaptoethanol) containing proteinase inhibitor. The suspension was sonicated 5 × for 20 sec at an output control setting of 3 on ice, followed by centrifugation at 10,000 ×g for 10 min. The supernatant was called S3. All three fractions, S1, S2, and S3, were analysed through Western analysis using the anti-His antibody as described in 5.2.5.

5.2.9 Generation of moss (Physcomitrella patens) *expression construct for HvGlyT2*

A near full-length *HvGlyT2* cDNA (1347 bp) was amplified using Elongase (section 5.2.2) with the following primers: FPhysT2: 5′GCGAGC*AAGCTT*ATGCATCATCATCATCATCATCAT**GAAAACTTGTATTTTCAAGGG**GCGGAAGAACACGCCGGCGACCAGCATGAG3′; underlined is a His_6-tag and in bold is the TEV cleavage site, RPhysT2: 5′GGATCC*GAATTC*TCACAATGGCTTGGCGGCCCTGAACTC3′; italics indicate restriction enzyme sites. Two-step PCR was begun with an initial

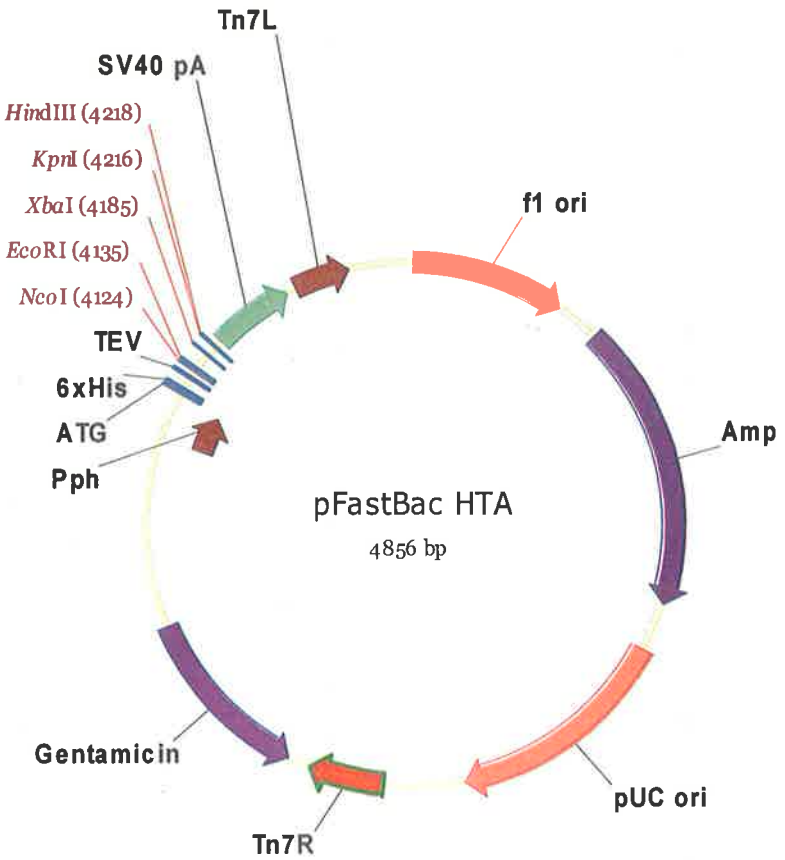

Figure 5.7 pFastBac^{TM}HTA plasmid map. The fragments were inserted in multiple cloning sites under the control of polyhedrin promoter (Pph) for expression of proteins in insect cells. The mini-Tn7 contains an expression cassette containing a gentamicin resistance gene, Pph, a multiple cloning site, and an SV40 poly-(A) signal inserted between the left and right arms of Tn7. f1 ori = f1 origin, Amp = ampicillin resistance gene, pUC ori = pUC origin, TEV = TEV recognition site for cleavage of 6 × His tag after protein purification, SV40 pA = SV40 polyadenylation signal.

denaturation at 94°C for 1 min followed by 35 cycles of 94°C for 30 sec; 72°C for 70 sec and ending with 72°C for 5 min. The amplified fragment was cloned into pGEM-T Easy as described in 2.2.6. The fragment was excised from the plasmid using *Hin*dIII and *Eco*RI (section 2.2.7) and cloned into pJIT145-Kan between the *Hin*dIII and *Eco*RI sites, followed by the insertion of a cassette from pMBL6 bearing the CaMV 35S promoter driving the nptII selectable marker, into the *Spe*I site of pJIT145-Kan to produce pJIT-GlyT2-pMBL6 (Figure 5.8). Following sequence confirmation, the plasmids, containing and lacking the full-length *HvGlyT2* cDNA, were linearised with *Sph*I and used for moss transformation. Moss transformation and all the steps involved in transformation, including selection for transgenic moss and sub-culture, were performed by Dr. Christina Lunde (Australian Centre for Plant Functional Genomics, University of Adelaide, Australia).

5.2.10 Total protein extraction from moss

Moss protonemal (Figure 5.2) tissue (1 g) was ground in liquid nitrogen with 2 ml grinding buffer (0.2 M Na_2HPO_4, 0.2 M NaH_2PO_4, pH 7.0) containing 25 µl protease inhibitor. The grinding was continued on ice until a homogenised mixture was obtained. The mixture was centrifuged for 20 min at 4°C and the supernatant was collected as the soluble fraction. The pellet was resuspended in 1 ml the same buffer containing 10% SDS and, after brief grinding, incubated at 100°C for 30 min. The homogenised mixture was centrifuged at room temperature for 20 min and the supernatant collected as the insoluble fraction. Both the soluble and insoluble fractions were used in Western analysis as described in section 5.2.5.

5.2.11 Heterologous expression in mammalian cells

Constructs were made in pME18S (Figure 5.9) and handed over to Dr. Tim Adams (CSIRO, Division of Health Sciences and Nutrition, Vic, Australia) to transiently express in the human embryonic kidney cell line, 293 T, and evaluate the expression *via* Western analysis.

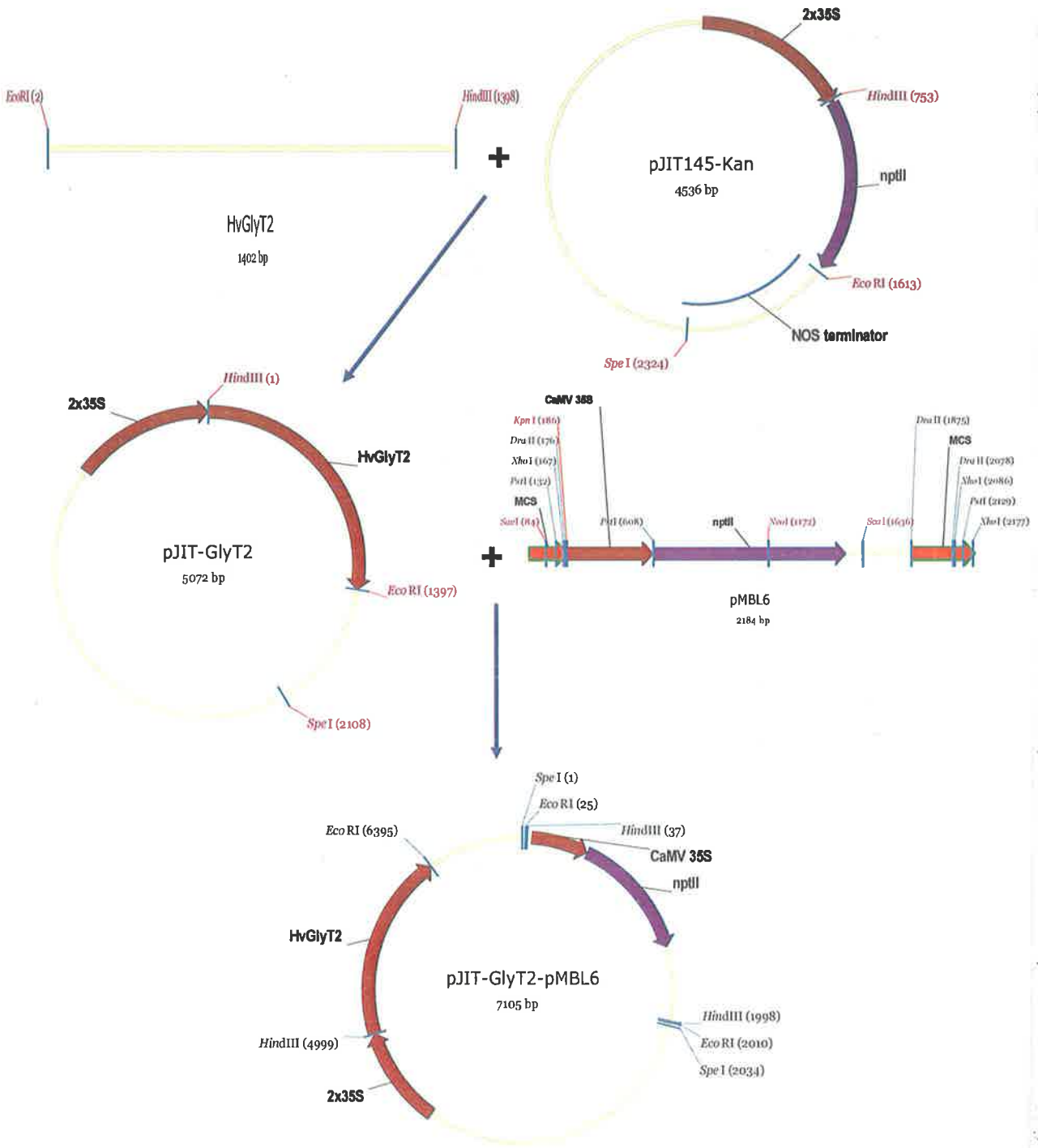
EcoRI (2)
HindIII (1398)
HvGlyT2
1402 bp
2x35S
HindIII (753)
pJIT145-Kan
4536 bp
nptII
Eco RI (1613)
NOS terminator
Spe I (2324)
HindIII (1)
2x35S
HvGlyT2
pJIT-GlyT2
5072 bp
Eco RI (1397)
Spe I (2108)
CaMV 35S
MCS
nptII
pMBL6
2184 bp
Spe I (1)
Eco RI (25)
HindIII (37)
CaMV 35S
nptII
Eco RI (6395)
HvGlyT2
pJIT-GlyT2-pMBL6
7105 bp
HindIII (4999)
2x35S
HindIII (1998)
Eco RI (2010)
Spe I (2034)

Figure 5.8 Generating the moss expression vector for *HvGlyT2*. *HvGlyT2* was cloned into pJIT145-Kan between the *Hin*dIII and *Eco*RI restriction sites. The construct was digested with *Spe*I to accommodate the cassette from pMBL6, which provides the nptII selectable marker driven by the 35S promoter.

5.2.12 Free sugar assays

The supernatant of heterologously expressed proteins in baculovirus were used to assay the protein activity using 0.5 M sugars (glucose, galactose, rhamnose, arabinose, xylose, mannose, and fucose) as the acceptor molecules. The assay reaction (50 µl) contained 25 mM ammonium formate, pH 7.5, 10 mM $MnCl_2$, 100 µM UDP-[^{14}C]-sugars (galactose, xylose), 0.5 M free sugar and 2 µl insect culture (*Sf9*) supernatant. The empty plasmid vector, boiled supernatant, water and no acceptor substrates were the negative controls designated within each experiment. The assay reaction was started by adding the culture supernatant to the assay reaction and was incubated at 30°C for 1-, 4- and 24 h. The assay reaction was passed through an equilibrated Dowex G-55 (Cl-form) anion exchanger column with ammonium formate, by centrifugation in a micro-centrifuge for 1 min. To prepare the anion exchanger column, the Dowex resin was rinsed with 20% (v/v) ethanol and washed with sterile water three times. The resin (0.7-0.8 ml) was loaded into a pierced Eppendorf tube with a ball of cotton wool to drain the unincorporated substances into a 10 ml tube. The bound material was washed with with H_2O (0.45 ml) twice by centrifugation at 30 ×g for 1 min. The eluate was collected and the radioactivity was counted in a liquid scintillation counter. Because glucuronic acid is negatively charged in solution and binds to the anionic column, UDP-[^{14}C]-glucuronic acid was not used in free sugar assays.

5.2.13 Enzyme assays

A range of oligo- and polysaccharides (Table 5.3) were used as the substrate acceptor for the heterologously expressed enzymes. The assay reaction (100 µl) contained 200 mM Tris-HCl buffer, pH 7.5, 200 mM $MnCl_2$, 1% w/v acceptor substrate, 20 µl enzyme supernatant and 10 mM UDP-[^{14}C]-sugars (galactose, xylose, and glucuronic acid). The reaction was started with the addition of culture supernatant and incubated at 25°C for 1-, 4-, and 24 h. The reaction was stopped by addition of acetic acid (50 µl), followed by boiling for 2 min. The acceptor molecule was precipitated by

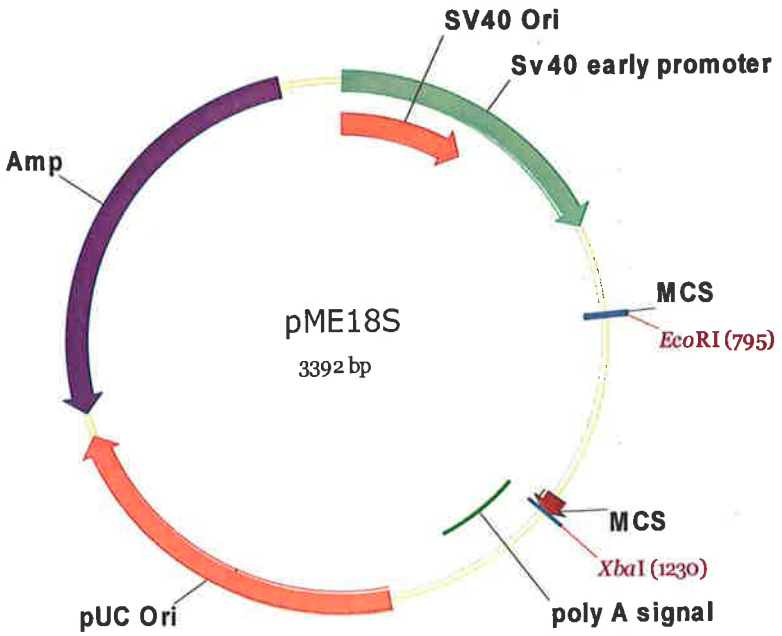

Figure 5.9 pME18S mammalian expression vector. The fragment was inserted between the *Eco*RI and *Xba*I restriction sites under the control of the SV40 early promoter. The plasmid carries resistance to ampicillin.

addition of cold absolute ethanol (750 µl) and the pellet washed three times with 70% (v/v) ethanol (70°C) to remove any unincorporated radioactivity, followed by incubation on ice for 10 min. For each ethanol wash, the pellet was dispersed by vortexing the tube, incubating on a hot block (70°C) for 20 min, on ice for 10 min and centrifugation at 16,000 ×g for 20 min. In cases where short oligosaccharides were used the precipitation was carried out using 80% (v/v) cold ethanol and the rest of the steps were performed on ice except the centrifugation. In all cases a visible pellet formed, which indicated that the oligosaccharide acceptors were indeed precipitated by the ethanol treatment. The final pellet was resuspended in 2 × 200 µl water and collected for a radioactivity count in a liquid scintillation counter.

Sugar molecules	Acceptor substrate	Source
Oligosaccharides	Xyloltetraose	
	Xylopentaose	
	Mannohexaose	
	Mannoheptaose	
	Cellopentaose	
Polysaccharides	Arabinan	Sugar beet
	Galactomannan	Carob
	Xyloglucan	Tamarind seed
	Galactan	Gum Arabic
	Pectic acid	Apple
	Arabinoxylan	Wheat
	AGP	Gum Arabic
	Xylan	Oat
	Rhamnogalacturonan	Soybean pectic fibre
	Arabinoxylan digested with AXAH	Wheat

Table 5.3 The acceptor substrates, oligo- and polysaccharides that were used in the enzyme assays. AXAH = arabinofuranohydrolase (Lee *et al.*, 2001)

5.3 RESULTS

5.3.1 Heterologous expression in E. coli

Although many different expression systems were used in this project, *E. coli* was always the first choice due to its ease of use, low cost and rapid turn around time. The experiments were performed as the cloning of each full-length cDNA was accomplished. A comprehensive attempt at heterologous expression was carried out using *HvGlyT1*. This included the use of different vector systems bearing both the partial-length (- TMH) and the full-length cDNA (+ TMH), co-transformation of the cells with RIG vector (see section 5.1.1), trying to optimise cell growth conditions and performing the enzyme assay on various cellular extracts. The enzyme assay was performed at a time when only one functionally characterised glycosyltransferase, galactomannan (1→6)-α-galactosyl- transferases (Edwards *et al.*, 1999), had been reported in the literature and as a result only UDP-[^{14}C]-galactose was considered as a donor substrate. Furthermore, at the time no UDP-[^{14}C]-xylose or UDP-[^{14}C]-arabinose were available.

As the project progressed and *HvGlyT3* became the prime candidate as a potential α-L-arabinosyltransferase and because of the high homology of *HvGlyT4* to a previously characterised RGII glucuronosyltransferase (Iwai *et al.*, 2002), heterologous expression in a range of host systems became focused more on these two cDNA clones. In cases where the expressed proteins were detected only in inclusion bodies as an insoluble fraction, no enzyme assay was performed.

HvGlyT1

A partial-length 1023 bp fragment of *HvGlyT1*, which lacked the TMH, was amplified using IcGal5′EXP and IcGal3′EXP primers (Table 5.4). The fragment was digested with *Sph*I and *Kpn*I and ligated into pQE-31 digested with the same restriction enzymes, followed by transformation into XL1Blue electrocompetent cells. The integrity of the construct was checked by DNA sequencing and used to transform

M15 electrocompetent cells. The transformed cells were grown in TB medium as described in section 5.2.3. A protein with the predicted size of 40 kDa was expressed in a doublet form, possibly due to the presence of a second internal start codon (Figure 5.10), and was purified from the insoluble fraction using a Ni-NTA resin column as described in 5.2.6. Attempts were made to obtain the protein in the soluble fraction by altering other parameters, including trying different concentrations of IPTG (0.005, 0.05, and 0.5 mM) and expression at 16°C for 24 h. However, ultimately this was not successful even though, in general, these conditions lower the expression rate and may allow the protein to fold better (see section 5.1.1).

Once the full-length *HvGlyT1* sequence was obtained, both partial-length (lacking 40 amino acid residues at the NH_2-terminus) and near full-length (424 amino acid residues) fragments with a His_6-tag at both the NH_2- and COOH-termini were inserted into Gateway expression plasmids as described in section 5.2.2. The pDEST17 and pET-DEST42 plasmids were used. The primers that were used to PCR amplify the fragments are listed in Table 5.4. Heterologously expressed proteins from both cDNAs were only observed in the insoluble fraction (Figure 5.11). When co-transformed with the RIG plasmid to provide the rare tRNAs, there was no positive effect on the solubility of the expressed proteins (Figure 5.12). Although the partial-length HvGlyT1 protein with the NH_2-terminal His_6-tag was only detected in the insoluble fraction, a crude extract of expressed protein resuspended in 20 mM Tris-HCl buffer, pH 7.5, was used to investigate total enzyme activity (Table 5.5). The assay result showed that there was no difference between the uninduced and induced samples, when galactomannan, xyloglucan and galactan were used as the acceptor substrate in the presence of UDP-[^{14}C]-galactose.

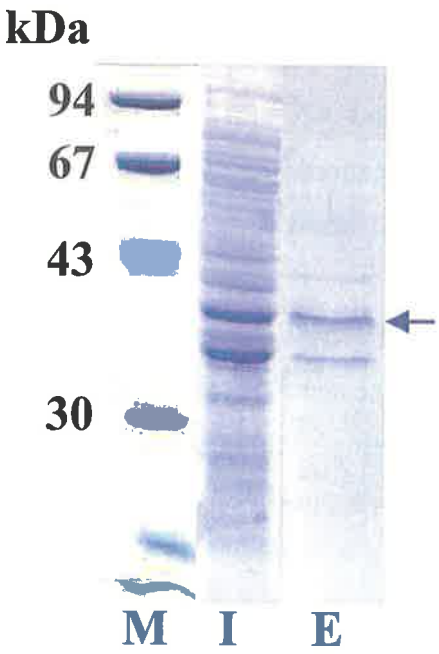

Figure 5.10 SDS-PAGE of the expression of HvGlyT1 in M15 *E. coli* cells. The expected size of the protein is 40 kDa, which is indicated by an arrow. The other band of smaller size indicates the possibility of the presence of an internal start codon. M = markers, I = insoluble fraction, E = insoluble eluate of the Ni-NTA affinity column.

Vector	Primer name	Primer sequence	Cleavage type
pQE-31	IcGal5′EXP (**F**)	TCGACACTAGT*GCATG* CAAAGGTA	*Sph*I
pQE-31	IcGal3′EXP (**F**)	GACAATCTGCAG*GGTACC*TATTACTCCTGCC	*Kpn*I
pDEST17	NHisFF-TEV (**F**)	GGGGACAAGTTTGTACAAAAAAGCAGGCTT C GAAAACTTGTATTTTCAAGGGATGCAGAAGA CCATCAACAACGTC	TEV
pDEST17	NHisFP-TEV (**P**)	GGGGACAAGTTTGTACAAAAAAGCAGGCTT C GAAAACTTGTATTTTCAAGGGGCGGCAGCTG ACGCCAAGGTTGCC	TEV
pDEST17	N3′end-TEV	GGGGACCACTTTGTACAAGAAAGCTGGGTC **TCA**AGTTTCGATCTTGGCGTCCATCTT	
pET-DEST42	CHisFF-Throm (**F**)	GGGGACAAGTTTGTACAAAAAAGCAGGCTT C ATGCAGAAGACCATCAACAACGTC	
pET-DEST42	CHisFP-Throm (**P**)	GGGGACAAGTTTGTACAAAAAAGCAGGCTT C GCGGCAGCTGACGCCAAGGTTGCC	
pET-DEST42	N3′end-Throm	GGGGACCACTTTGTACAAGAAAGCTGGGTC CGACCCCCTGGGCACTTTAGTTTCGATCTTG GCGTCCATCTT	Thrombin

Table 5.4 Primers that were used to amplify *HvGlyT1* partial- or full-length cDNAs to be expressed in *E. coli*. The first column indicates the expression vectors used for cloning purposes. Underlined sequences are the TEV or Thrombin cleavage sites for the removal of the His_6-tag. Restriction sites are indicated by italics. The stop codon is indicated in bold. A bold F or P in the second column indicates the primers that were used for the amplification of near full-length (F) or partial length (P) *HvGlyT1*, respectively.

Acceptor substrate	Expressed enzyme	CPM		Boiled extract
		R1	R2	
galactomannan	+	21	21	25
	–	24	29	33
xyloglucan	+	28	24	27
	–	23	26	27
galactan	+	16	23	22
	–	22	24	21

Table 5.5 Enzyme activity measurement of a crude extract of *HvGlyT1* partial-fragment, lacking the TMH, expressed in *E. coli*. There was no difference between the induced fraction (+), uninduced fraction (-) or with the boiled extract. cpm = count per minute.

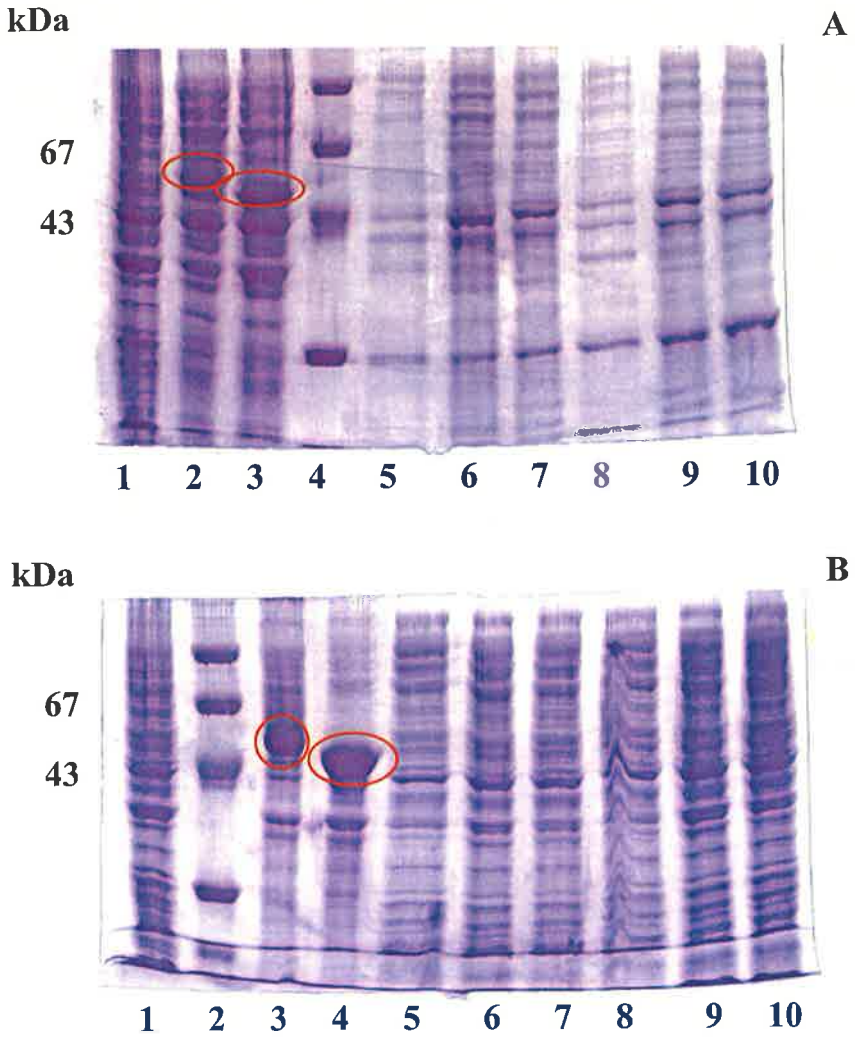

Figure 5.11 SDS-PAGE separation of proteins expressed in the BL21 strain of *E. coli* using the Gateway expression system. **A:** HvGlyT1 fragments were cloned into pET-DEST42; 1 = uninduced, 2, 3 = induced insoluble fractions of the full-length with an expected size of 50 kDa and the partial-length with an expected size of 46 kDa, 4 = marker, 5, 6, 7 = soluble fractions (full-length) resuspended in sodium/phosphate buffer, 5% w/v CHAPS, 5% v/v triton X-100, respectively, 8, 9, 10 = soluble fractions (partial-length) in the same buffering condition as above. **B:** HvGlyT1 fragments were cloned into pDEST17; 1= uninduced, 2 = marker, 3, 4 = induced insoluble fractions of full- and partial-length HvGlyT1, 5-10 = as above in A. Red circles indicate the likely HvGlyT1 protein.

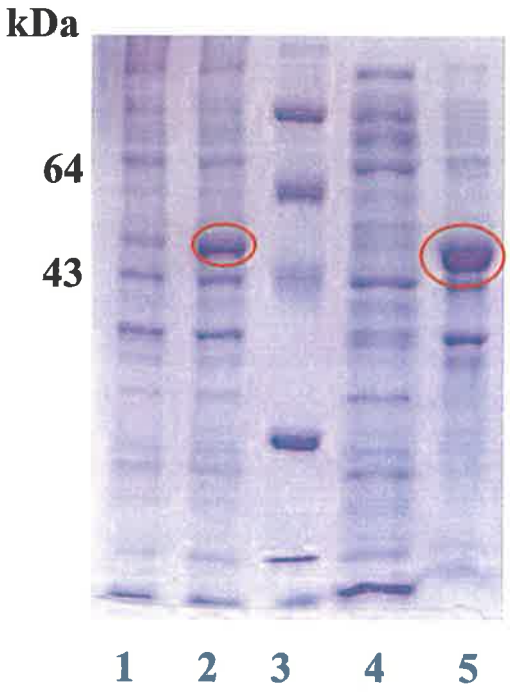

Figure 5.12 SDS-PAGE gel of partial-length HvGlyT1 protein expressed in the pDEST17 vector in the presence of the RIG vector in the BL21 strain of *E. coli*. Lane 1 = uninduced fraction, Lane 2 = induced fraction, Lane 3 = markers, Lane 4 = soluble fraction, Lane 5 = insoluble fraction. The circled protein band is predicted to be HvGlyT1 protein.

HvGlyT3

A partial-length 1221 bp fragment of *HvGlyT3* (- TMH) was amplified using EFPT3: 5′ACAATTGGTACCAACCTCTCCCTCCCGTCCCAACCC3′ and ERT3: 5′TCTTC AAAGCTTTCAAGAAGTGGTCGGCATCTTGGC3′, cloned into pQE-30 between the *Kpn*I and *Hin*dIII restriction sites as described in sections 2.2.6 and 2.2.7, and sequenced as described in section 2.2.8. The expression of this protein was induced in M15 *E. coli* cells as described in section 5.2.3 and was checked by SDS-PAGE. The polyacrylamide gel showed that no expression of the HvGlyT3 protein had occured (Figure 5.13).

HvGlyT4

A near full-length 1089 bp *HvGlyT4* cDNA, for which no TMH was predicted, was amplified using EFT4: 5′AAGGTTGGTACCTACGACTTGCCAAGAAAATA CAAC3′ and ERT4: 5′GGAAACAAGCTTCTACCACGGTTTCAGATCTCCAAC3′, cloned into pQE-30 between the *Hin*dIII and *Kpn*I restriction sites as described in sections 2.2.6 and 2.2.7, and sequenced as described in section 2.2.8. The protein was expressed in M15 *E. coli* cells as described in section 5.2.3 and was checked by SDS-PAGE. The protein was found to be expressed only in the insoluble fraction (Figure 5.14) and was therefore not assayed.

5.3.2 Heterologous expression using the baculovirus expression system

On the basis of published work by Edwards *et al.*, (1999), which reported the expression of a partial-length (- TMH) galactomannan (1→6)-α-galactosyltransferase in *P. pastoris*, it was decided to generate constructs of the barley GTs lacking the TMH. Partial-length fragments of *HvGlyT1* (1245 bp), *HvGlyT2* (1197 bp), *HvGlyT3* (1230 bp), and *HvGlyT4* (1023 bp) were PCR amplified using gene-specific primers containing suitably engineered restriction sites (Table 5.6). The amplified fragments were digested, ligated into $pF_{AST}B_{AC}$ HTa and sequenced to check they were in frame with the start codon as described in section 5.2.2. The constructs were used for protein expression using *Sf9* insect cells as described in section 5.2.8. The expressed proteins were detected *via* Western analysis using the anti-His antibody (primary

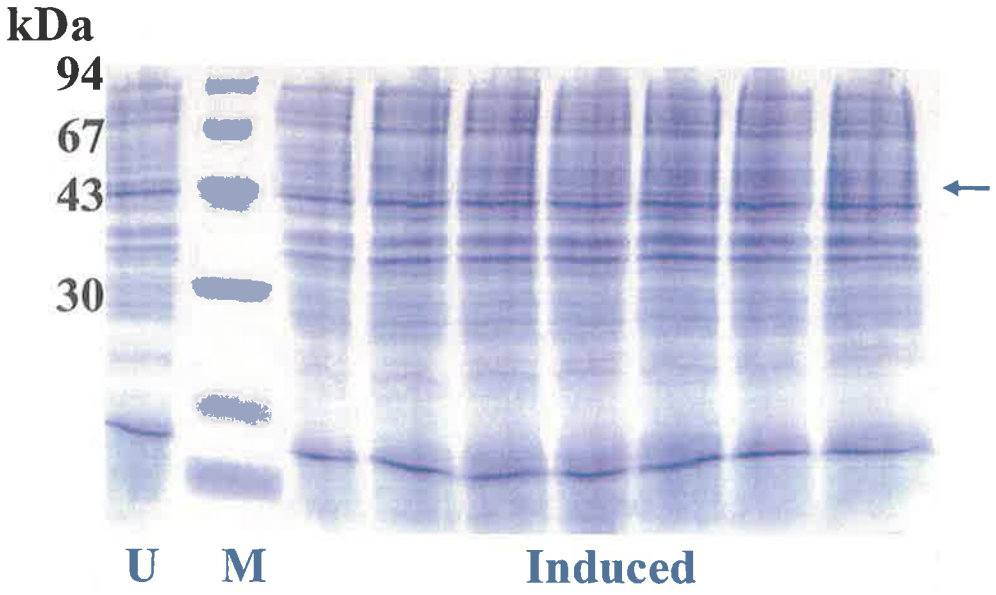

Figure 5.13 SDS-PAGE gel analysis of partial-length HvGlyT3 protein expression in *E. coli*. Seven individual clones were tested for expression of the HvGlyT3 protein. All were negative as judged by a total protein extract. Arrow indicates the expected size of the protein.

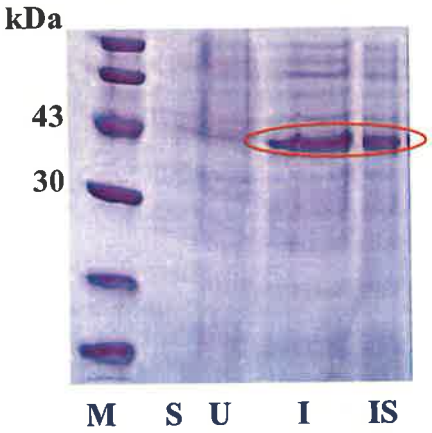

Figure 5.14 SDS-PAGE gel of proteins expressed in the *E. coli* system (BL21) with an *HvGlyT4* construct. M = marker, S = soluble fraction, U = uninduced, I = induced, IS = insoluble fraction. The red circle shows the expressed protein with an expected size of 43 kDa. Since the protein was located in the insoluble fraction, no enzyme assay was performed.

antibody) in S2 and S3 fractions (section 5.2.8) as described in section 5.2.5 (Figure 5.15). Attempts to purify the expressed proteins using the His-tag affinity column failed. Therefore, crude S2 fraction (sometimes a mixture of S2 and S3 fractions) of *Sf9* insect cells containing the expressed proteins were used to assay the activity of proteins as described in sections 5.2.12 and 5.2.13. It should be noted that the S1 fraction was the soluble fraction and the others were only partially soluble, obtained through sonication and the use of detergent to solublise the membrane-bound proteins.

HvGlyT1

When the free sugar assay was performed for HvGlyT1 (Table 5.7), the amount of incorporation was generally lower than the negative control. The negative control was the boiled crude extract in which it is possible that proteins aggregate and entrap some radioactivity, thus causing higher cpm values in the boiled extract controls.

HvGlyT2

The free sugar assay showed the possibility of the incorporation of UDP-[^{14}C]-xylose onto 0.5 M glucose, in just one experiment (Table 5.8). The experiment was repeated with 0.5 M glucose, 2% (w/v) xyloglucan and 2% (w/v) cellopentaose as putative acceptor substrates (Table 5.9). Although the results showed some incorporation when compared to negative controls, the incorporation of radioactivity was not high enough to confirm HvGlyT2 as a xylosyltransferase. Further free sugar assays (Table 5.10) with two partially solublised HvGlyT2 fractions (S2 and S3) also suggested that this enzyme might be a xylosyltransferase, but the results were not reproducible and the amount of incorporated radioactivity was not convincing.

HvGlyT3

An initial free sugar assay was performed with the S2 + S3 fractions of a partially solublised, expressed HvGlyT3 from *Sf9* cells as described in section 5.2.8. The results showed a comparatively higher amount of incorporation of [^{14}C]-galactose onto glucose and galactose and also [^{14}C]-xylose onto glucose (Table 5.11). Another assay was performed (Table 5.12) in the presence of UDP-[^{14}C]-galactose as the donor substrate and 0.5 M glucose, 0.5 M galactose, 2% (w/v) polygalacturonic acid

Primer name	Primer sequence	R.E
F-BGlyT1	GGCACCGAATTCATCAACCTCATCGCCTTCTCC	*Eco*RI
R-BGlyT1	TTGTCGGTACC**TCA**AGTTTCGATCTTGGCGTC	*Kpn*I
F-BGlyT2	ACCGACGAATTCCTCCCACGCATCCGCATCGAG	*Eco*RI
R-BGlyT2	GATCCAAGCTT**TCA**CAATGGCTTGGCGGCCCTG	*Hin*dIII
F-B-PaT3	GTACATCCATGGTCAACCTCTCCCTCCCGTCCCAACCCTCCGAG	*Nco*I
R-B-PaT3	TCTTCAAAGCTT**TCA**AGAAGTGGTCGGCATCTTGGCCTTCAC	*Hin*dIII
F-BGlyT4	CTTAATGAATTCTTTGCTGCGGAAATATTC	*Eco*RI
R-BGlyT4	GGAAACAAGCTT**CTA**CCACGGTTTCAGATCTCC	*Hin*dIII

Table 5.6 Primers that were used to amplify the partial fragments of *HvGlyT1*, *HvGlyT2*, *HvGlyT3*, and *HvGlyT4* for heterologous expression in *sf9* insect cells. Underlined sequences are the restriction enzyme sites (R.E). Bold sequences are the stop codon.

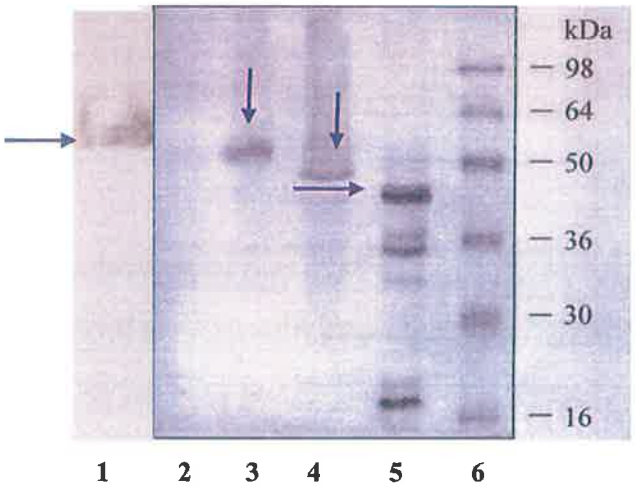

Figure 5.15 Western analysis of heterologously expressed proteins in *Sf9* insect cells using the anti-His antibody. S2 fraction of HvGlyT3, empty $pF_{AST}B_{AC}$ HTa plasmid vector, HvGlyT1, HvGlyT2, HvGlyT4, and protein size marker are shown in Lanes 1-6. HvGlyT4 appears to be degraded in Lane 5 in this Western analysis. The expected sizes for HvGlyT1-4 were 50, 47, 49, 40 kDa, respectively. The Figure is courtesy of Dr. Sasan Asgari. Arrows are indicative of expressed proteins present in the S2 fraction.

		CPM				
Donor	**Acceptor**	**R1**	**R2**	**R3**	**R4**	**N**
UDP-[^{14}C]-galactose	glucose	65	80	195	151	320
	galactose	86	124	226	239	305
	rhamnose	76	84	150	380	336
	arabinose	73	73	176	151	355
	xylose	74	85	203	156	416
	mannose	73	80	128	237	327
	fucose	90	78	200	228	318
UDP-[^{14}C]-xylose	glucose	75	95	209	178	195
	galactose	70	65	142	164	214
	rhamnose	67	71	116	147	155
	arabinose	69	81	151	179	180
	xylose	81	90	207	237	265
	mannose	62	58	182	234	234
	fucose	81	92	376	224	208

Table 5.7 A free sugar assay for HvGlyT1 (S2 fraction) expressed in *Sf9* insect cells. The specific activity of 5.5 nmol UDP-[^{14}C]-galactose and 40 nmol UDP-[^{14}C]-xylose were 5650 and 559.69 cpm/nanomoles, respectively. Two different batches of enzymes were used for the enzyme assay, referred to as old and new. R1 and R2 are cpm values of two replications of the old batch and R3 and R4 are cpm values of two replications of the new batch. N is the cpm values of boiled extract used as negative control. It is clear from the table that the cpm values of the negative controls are generally higher than the active enzyme. It is possible that the denatured enzyme entraps some radioactivity while it aggregates during incubation and thus produces higher values. CPM = counts per minute.

		CPM		
Donor	**Acceptor**	**R1**	**R2**	**N**
UDP-[^{14}C]-galactose	glucose	106	74	ND
	galactose	270	106	ND
	rhamnose	85	121	ND
	arabinose	99	87	ND
	xylose	69	171	50
	mannose	118	89	ND
	fucose	90	80	ND
UDP-[^{14}C]-xylose	glucose	1250	90	60
	galactose	96	89	ND
	rhamnose	87	143	ND
	arabinose	100	109	ND
	xylose	139	93	ND
	mannose	83	92	ND
	fucose	80	100	ND

Table 5.8 A free sugar assay for HvGlyT2 S2 (40%) + S3 (60%) fractions expressed in *Sf9* insect cells. The specific activity of 5.5 nmol UDP-[^{14}C]-galactose and 40 nmol UDP-[^{14}C]-xylose were 5650 and 559.69 cpm/nanomoles, respectively. R1 and R2 are cpm values of two replications of the assay reaction. N is the cpm values of boiled extract used as the negative control. Since the radioactive source is not readily available only two controls were considered. ND = not determined, CPM = counts per minute.

		CPM	
Enzyme fraction	**Acceptor**	**R1**	**R2**
S2	glucose	337	312
	cellopentaose	69	114
S3	glucose	244	165
	cellopentaose	58	65
S2 + S3 (1:1)	xyloglucan	286	110
Boiled extract	glucose	137	ND
	cellopentaose	65	ND
S2 + S3 (1:1)	no acceptor	114	ND
No extract	glucose	139	ND

Table 5.9 Enzyme assay for HvGlyT2 (S2 and S3) fractions expressed in *Sf9* insect cells in the presence of UDP-[^{14}C]-xylose. A part of the experiment presented in Table 5.8 was repeated using 0.5 M glucose, 2% (w/v) xyloglucan and 2% (w/v) cellopentaose as the acceptor substrates. The data shows the incorporation of radioactivity onto glucose and xyloglucan, but not cellopentaose. However, the amount of cpm is not high enough to allow a definite conclusion. The specific activity of 40 nmol UDP-[^{14}C]-xylose was 559.69 cpm/nanomoles. R1 and R2 are cpm values of two replications of the assay reaction. Boiled extract and water were used as the negative controls. Since the radioactive source is not readily available only one replication was considered for negative controls. ND = not determined, CPM = counts per minute.

	CPM			
Enzyme fraction	**R1**	**R2**	**R3**	**R4**
S2	545	418	612	1320
S3	1310	354	1320	403
Boiled extract	ND	ND	431	ND
No UDP-[^{14}C]-xylose	42	ND	ND	ND
No extract	169	ND	73	ND

Table 5.10 A free sugar assay for HvGlyT2 (S2 and S3) fractions expressed in *Sf9* insect cells in the presence of UDP-[^{14}C]-xylose as the donor substarte and 0.5 M glucose as the acceptor substrate. The specific activity of 40 nmol UDP-[^{14}C]-xylose was 559.69 cpm/nanomoles. Although some level of incorporation is apparent, the results were not reproducible even within the same experiment. R1 and R2 are replicates of an enzyme assay, incubated at 30°C with agitation for 16 h. R3 and R4 are the replications of an enzyme assay, incubated at 30 °C for 4 h without agitation. Since the radioactive source is not readily available not all the controls were replicated. ND= not determined, CPM = counts per minute.

and 2% (w/v) galactan. The results showed some incorporation of [^{14}C]-galactose onto galactose when compared to the negative control, but the level was not considered to be significant.

HvGlyT4

As mentioned earlier, a free sugar assay was not performed using UDP-[^{14}C]-glucuronic acid as the donor substrate. Instead enzyme assays were performed with a number of oligo- and polysaccharides (Table 5.13) as the acceptor substrate in the presence of UDP-[^{14}C]-glucuronic. However, when the cpm values were compared with negative controls the differences were not significant.

*5.3.3 Heterologous expression of HvGlyT2 in moss (*Physcomitrella patens*)*

The steps involved in generating an expression construct for moss and moss transformation were described in section 5.2.9. A few moss transformants were obtained and showed resistance to the selective antibiotic. Protein was extracted (section 5.2.10) from transformed moss tissue, quantified (section 5.2.7) and 10 µg protein was loaded on an SDS-PAGE gel for Western analysis using the anti-His antibody as described in sections 5.2.4 and 5.2.5 (Figure 5.16). Western analysis failed to reveal any expressed protein and therefore further work to produce stable transgenic lines was not pursued.

5.3.4 Heterologous expression of HvGlyT1 in mammalian cells

Partial- (1146 bp) and full-length (1272 bp) fragments of *HvGlyT1* were amplified using F-Mam and R-Mam, FMam2 and R-Mam, respectively (Table 5.7). The fragments were cloned into pGEM-T Easy as described in section 2.2.6 and subjected to DNA sequencing as described in section 2.2.8. The fragments were excised from the vector using *Eco*RI and *Xba*I, and cloned into the pME18S mammalian expression vector as described in sections 2.2.6 and 2.2.7. The integration of the inserts within the expression vector was examined with restriction enzyme mapping and DNA

sequencing. The plasmids bearing the *HvGlyT1* inserts were used for protein expression as described in section 5.2.11. Western analysis with the anti-cMyc antibody failed to detect any expressed protein (data not shown).

		CPM	
Donor	**Acceptor**	**R1**	**R2**
UDP-[^{14}C]-galactose	glucose	513	1122
	galactose	495	477
	rhamnose	354	450
	arabinose	219	310
	xylose	207	240
	mannose	202	210
	fucose	254	228
UDP-[^{14}C]-xylose	glucose	492	600
	galactose	175	175
	rhamnose	176	249
	arabinose	113	119
	xylose	122	125
	mannose	134	99
	fucose	149	235

Table 5.11 An initial screening of the suitable substrates for the free sugar assay for HvGlyT3 S2 (40%) + S3 (60%) fractions expressed in *Sf9* insect cells. The specific activity of 5.5 nmol UDP-[^{14}C]-galactose and 40 nmol UDP-[^{14}C]-xylose were 5650 and 559.69 cpm/nanomoles, respectively. R1 and R2 are cpm values of two replications of the assay reaction. Since the radioactive source is not readily available no controls were included in the preliminary experiment. Initial data suggests the possibility of incorporation onto either glucose or galactose. The experiment was repeated using these free sugars, which is represented in Table 5.12. CPM = counts per minute.

Donor	Acceptor	Enzyme fraction	CPM R1	CPM R2
UDP-[^{14}C]-galactose	glucose	S2	463	543
		S3	502	578
	galactose	S2	1194	900
		S3	970	825
	polygalacturonic acid	S2 + S3 (1:1)	81	63
	galactan	S2 + S3 (1:1)	190	155
No extract	galactose	S2 + S3 (1:1)	190	ND
No acceptor	-	S2 + S3 (1:1)	50	ND
Boiled extract	galactan	S2 + S3 (1:1)	58	ND
UDP-[^{14}C]-xylose	glucose	S2	418	289
		S3	260	369

Table 5.12 Enzyme assay for HvGlyT3 expressed in *Sf9* insect cells. Based on initial screens (Table 5.12) another assay was performed, which suggests the incorporation of UDP-[^{14}C]-galactose onto 0.5 M galactose with 3% nmole incorporation. When the assay was repeated with polysaccharides as the acceptor substrates the same result was not obtained. The specific activity of 5.5 nmol UDP-[^{14}C]-galactose and 40 nmol UDP-[^{14}C]-xylose were 5650 and 559.69 cpm/nanomoles, respectively. Since the radioactive source is not readily available the controls were not replicated. ND = not determined, CPM = counts per minute.

Acceptor	CPM		
	R1	R2	R3
AGP	326	578	449
RG	433	675	634
galactomannan	747	752	1119
xylopentaose	271	776	ND
wheat arabinoxylan	1407	1661	950
no acceptor	294	676	ND
boiled extract	2536	ND	ND
no extract	5827	ND	ND
no UDP-GluA	34	ND	ND

Table 5.13 Enzyme assay for HvGlyT4 expressed in *Sf9* insect cells. The specific activity of 80 nmol UDP-[^{14}C]-glucuronic acid was 293.8 cpm/nanomoles. Although the amount of incorporation was high with some of the polysaccharides when compared to negative controls the cpm values were not significant. Since the radioactive source is not readily available the controls were not replicated. ND= not determined, CPM = counts per minute.

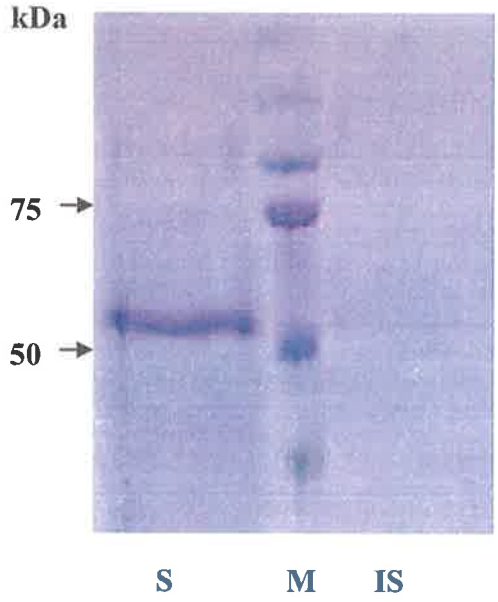

Figure 5.16 Western membrane of protein extract from moss (*Physcomitrella patens*) transformed with the *HvGlyT2* expression construct and stained with DB71. S = soluble fraction obtained from supernatant, M = protein size marker, IS = insoluble fraction obtained from tissue pellet. The strong band in the soluble fraction is probably Rubisco. A 50 kDa protein was expected to be expressed. Arrows indicate the sizes of protein marker.

Host system	cDNA template	Primer name	Primer sequence	R.E.
Mammalian	*HvGlyT1*	F-Mam	GAATTCCCACCATGGCTGACGCC AAGGTTGCCGAGGAC	*Eco*RI
		F-Mam2	GAATTCCCACCATGCAGAAGACC ATCAACAAC GTCAAGA TC	*Eco*RI
		R-Mam	TCTAGA**TCA**CAGATCCTCTTCAGA GATGAGTTTCTGCTCAGTTTCGAT CTTGGCGTCCATCTT	*Xba*I

Table 5.14 Gene-specific primer sequences and their engineered restriction enzyme (R.E.) sites for amplification of cDNA fragments for cloning in protein expression vectors specific for the mammalian system. Underlined sequences are the R.E.s and the bold sequence is the stop codon.

5.4 DISCUSSION

Although heterologous expression of proteins provides us with the best and the most direct approach towards the functional analysis of genes, in many cases the expressed protein may not adopt its correct 3D structure and activity can not be measured. As a result, a number of host systems have to be tried in order to produce a functionally active protein.

Following the isolation of barley glycosyltransferase cDNA clones, the focus was shifted towards the analysis of their function and specificity through heterologous expression. Several available host systems, ranging from *E. coli* to mammalian cells, were used (Table 5.15). Some systems such as mammalian cells failed to express any protein. It has been shown previously that mammalian systems are not always appropriate for the expression of glycosyltransferases, because mammalian cells often silence genes that are not required for cell survival (Potvin and Stanley, 1991; Hagen *et al.*, 1993). Additionally, the mammalian host system may be complicated to some extent as a result of the presence of similar endogenous proteins (Strous and Berger, 1982).

When *E. coli* was used as the host system to express genes with and without the TMH, it failed to produce soluble proteins. As shown in Table 5.1, the expression system can be optimised by manipulating the cellular folding apparatus and the expression conditions, or by using a highly soluble protein as a tag to enhance solubility. However, for the expression of proteins such as glycosyltransferases where post-translational modifications such as glycosylation may be crucial in the formation of an active enzyme (Pagny *et al.*, 2003), the *E. coli* system may not be suitable because it lacks the required post-translational machinery. Later in the study, partially solublised proteins were obtained using mild detergent (section 5.2.8) when the baculovirus system was used as the expression system, but the proteins could not purified by affinity chromatography (see section 5.1.1). Thus, the crude lysates of the cells were assayed for enzymic activity.

System	Enzyme	TMH	Expression	Test for activity	Result
E. coli	HvGlyT1	±	Insoluble	Crude extract	No activity
	HvGlyT3	-	No expression	ND	ND
	HvGlyT4	-	Insoluble	ND	ND
Insect	HvGlyT1	-	PS	Crude extract	NC
	HvGlyT2	-	PS	Crude extract	NC
	HvGlyT3	-	PS	Crude extract	NC
	HvGlyT4	-	PS	Crude extract	NC
Mammalian	HvGlyT1	±	No expression	ND	ND
Moss	HvGlyT2	+	No expression	ND	ND

Table 5.15 A summary of the experimental work described In this Chapter. The barley GTs were expressed in a number of host systems with (+) and without (-) TMH. Sometimes no expression was observed and in cases with expression, the expressed enzymes were either insoluble or partially soluble. When the enzymes were insoluble, the assay for activity was not performed except on one occasion. A crude extract of the *E. coli* was used to test activity. This did not show any incorporation of the radioactive donor substrate onto the acceptor substrate. When the cDNAs were expressed in insect cells, the soluble fraction did not contain any expressed protein and therefore the insoluble fraction was resuspended twice in mild detergent (section 5.2.8) and called a partially soluble fraction. The attempts to purify the enzyme *via* Ni-NTA affinity tag failed to recover the His_6-tagged proteins. Crude extracts were used to perform enzyme activity (Tables 5.7-5.13) assays. In some cases some minor activities were observed, but these did not represent a true activity especially when compared with the negative controls. ND = not determined, PS = partially soluble, NC = not conclusive.

Initially, the expressed proteins were examined *via* a free sugar assay to pinpoint the putative acceptor substrate. This assay was not performed using UDP-[^{14}C]-glucuronic acid as the donor substrate. Enzyme assays using both oligosaccharides and polysaccharides were performed. These assays for protein activity failed to produce consistent outcomes when the assays were repeated. Similar results were obtained when the *Arabidopsis* members of family GT34 were expressed in the baculovirus system and used for activity assays (Keegstra, K, personal communication).

Heterologous expression within plant tissues, as discussed earlier in this Chapter, is most likely to provide all the requirements for expression and accurate folding of plant proteins. When moss was used as the host to produce a barley glycosyltransferase, no expression occurred, possibly as a result of a failure in the integration of the construct within the moss genome. The technology for heterologous expression in moss is in its infancy and expression vectors and suitable promoters have just recently started to emerge (Koprivova *et al.*, 2003; Horstmann *et al.*, 2004; Jost *et al.*, 2005). Because of time constraints, plant systems other than moss were not used in this project.

The inconclusive or negative results obtained with the various heterologous expression systems (Table 5.15) indicated that a new approach to define the functions of the barley GlyT genes was required. Accordingly, we decided to take a less direct, loss-of-function approach in which barley was transformed with dsRNAi constructs that would silence the target gene in the expectation that the transgenic lines would show a phenotype that might be linked to cell wall biosynthesis. These experiments will be discussed in the next Chapter.

CHAPTER 6 TRANSIENTLY-INDUCED GENE SILENCING OF BARLEY GLYCOSYLTRANSFERASES

6.1 INTRODUCTION

In the previous Chapter, attempts to use heterologous expression to directly address the functions of barley glycosyltransferase proteins was described. However, despite using a number of different host systems, expression of active protein was not achieved and no enzymatic activity was detected. The next step was to use reverse genetics to address the potential involvement of the barley GlyTs on cell wall polysaccharide biosynthesis.

Following the complete sequencing of the *Arabidopsis* and rice (*Oryza sativa*) genomes, the number of potential proteins expressed from these genomes was predicted to be at 25,000 and 55,000, respectively. Functions were assigned to some proteins through sequence homology, but the functional analysis of many of the proteins is still pending (*Arabidopsis* Genome Initiative, 2000; Goff *et al.*, 2002; Yu *et al.*, 2002). Taking a reverse genetics approach to disrupt gene function and subsequently to study the phenotypic effects at either the macro or micro level may provide hints about the relatedness of these proteins to different steps of plant cell growth and development (Waterhouse and Helliwell, 2003; Horiguchi, 2004). The gene silencing approach to the reverse genetics experiments may employ a variety of techniques, outlined in Chapter 1, which can affect gene function at either the transcriptional or post-transcriptional levels. These techniques differ in their effectiveness and have their own benefits and drawbacks.

Post transcriptional gene silencing (PTGS) is a type of sequence-specific RNA degradation (Figure 6.1) and it has been termed RNA interference (RNAi), RIP and quelling in animals, flies and fungi, respectively (Finnegan *et al.*, 2001; Horiguchi, 2004). A three-step model has been developed to explain the mode of action of PTGS (Figure 6.1). These steps are: the formation of a double-stranded RNA molecule (dsRNA), conversion of the dsRNA to 21- to 26- nucleotide small interfering RNA (siRNA), and cleavage of the endogenous target

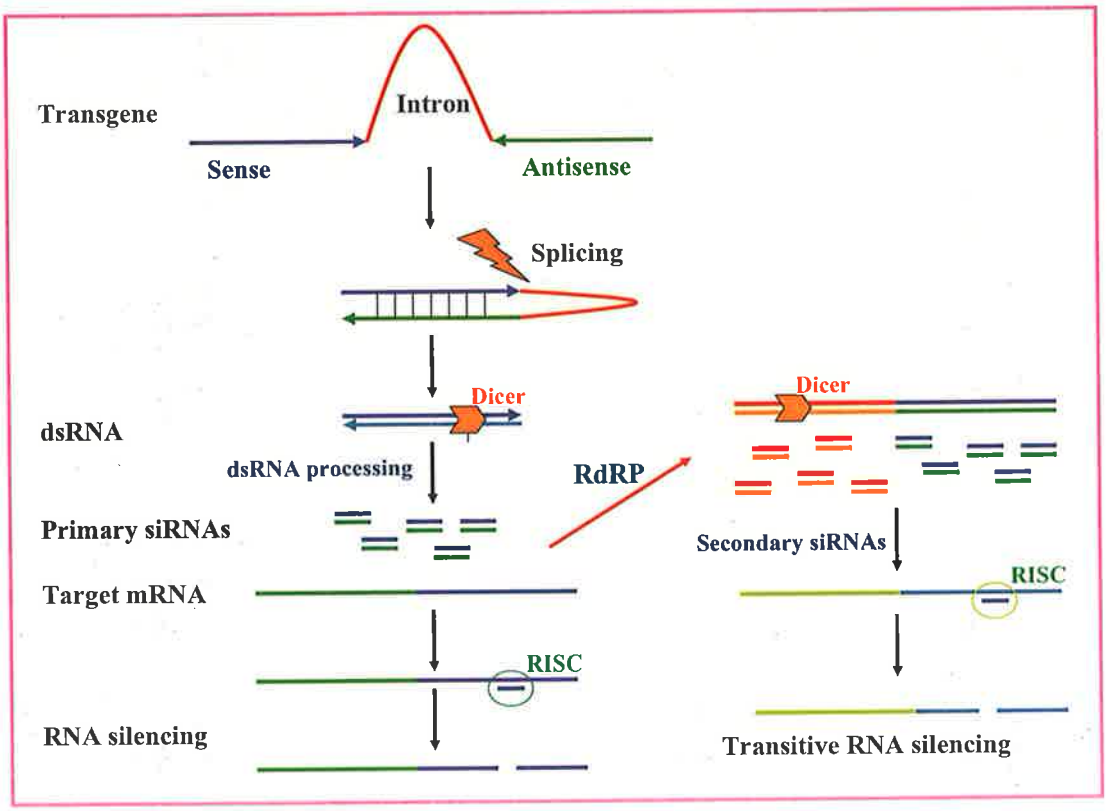

Figure 6.1 The current model of RNA-mediated gene silencing in plants (modified after Horiguchi, 2004). Processing of dsRNA in PTGS occurs *via* two putative methods; Direct RNA silencing and Transitive RNA silencing. A fragment of the gene of interest is cloned into a plasmid under the control of a strong promoter (Sense: Intron: Antisense). This plasmid is used to transform either the plant or of interest. After integration of the plasmid into the genome of the target plant, it produces an intron-hairpin RNA (ihpRNA) from the cassette, which goes through normal RNA processing where the intron is excised and a dsRNA is formed (Wesley *et al.*, 2001). The dsRNA is processed into 21- to 26-nucleotide (nt) dsRNA fragments called siRNAs by the action of an RNase III-like endonuclease. This enzyme is termed Dicer in animals (Bernstein *et al.*, 2001) and Dicer-like in plants (Tang *et al.*, 2003). Activity of another protein with an unknown function, HEN1, also has been reported during the processing of dsRNA (Boutet *et al.*, 2003). Finally, in an RNA-induced silencing complex (RISC) contains the siRNA cleavage of the target RNA with a complementary sequence to the siRNA sequence occurs (Hamilton and Baulcombe, 1999; Matzke *et al.*, 2001; Horiguchi, 2004). In transitive RNA silencing (right Panel), siRNAs are converted to dsRNA by the action of RNA dependent RNA polymerase (RdRP) and the resultant dsRNA then also follow the above-mentioned pathways.

RNA *via* binding of the siRNA to its complementary sequence in a complex named the RNA-induced silencing complex (RISC) (Horiguchi, 2004).

PTGS was first described in transgenic plants and named co-suppression as a result of degradation of both the transgene, which was used to overexpress the chalcone synthase gene to boost the flower color in petunia, and the homologous endogenous gene resulting in changes in pigment levels in petals (Napoli *et al.*, 1990). Shortly after, similar results were seen by introduction of an endogenous gene or cDNA under the control of an exogenous promoter, and it became evident that PTGS was a widespread phenomenon (Smith *et al.*, 1990; van der Krol *et al.*, 1990). PTGS has also manifested to introduce virus resistance in plants in a way to degrade both the viral RNA and the virus-derived transgene mRNA (Baulcombe, 1999). Transgenic plants producing an inverted-repeat dsRNA hairpin homologous to viral endogenous sequences have been reported to give rise to highly efficient virus resistance plants (Smith *et al.*, 2000; Tenllado *et al.*, 2004). Thus, exogenously supplied dsRNA could be utilised in crop protection against virus diseases.

Hamilton *et al.* (2002) reported the presence of two size classes of siRNAs produced as a result of the action of an enzyme called Dicer through the study of the different effects of viral suppressors during RNA silencing. The first class of 21-22 nucleotides (short) is involved in local RNA silencing of transgenes, and in virus resistance as a result of siRNAs derived from viral sequences. In contrast, the longer siRNA of 24-26 nucleotides are involved in both transcriptional silencing *via* the methylation of genomic DNA, and systemic PTGS (Hamilton *et al.*, 2002; Mallory and Vaucheret, 2004). Further biochemical studies showed that the exogenous [^{32}P]-radiolabeled dsRNA molecules are degraded in wheat germ and cauliflower extracts into two classes of RNAs, containing 21- and 24-nucleotides (Tang *et al.*, 2003). The data from wheat germ extract showed that the longer siRNAs are more abundant than the short class by a factor of about 4 (Tang *et al.*, 2003), which may support the fact that the longer siRNAs are required for more than one function within the plant. The systemic movement of siRNAs is *via*

plasmodesmata in cell to cell movement and for long distances through the phloem (Palauqui *et al.*, 1997; Voinnet *et al.*, 1998; Klahre *et al.*, 2002; Mlotshwa *et al.*, 2002; Himber *et al.*, 2003; Yoo *et al.*, 2004). This movement of RNA silencing contributes in non-cell-autonomous signaling, which means it can be induced locally and then spread within the organism (Mlotshwa *et al.*, 2002). However, mechanisms of intercellular trafficking of the siRNAs remain elusive, since we still do not know how and why this systemic movement occurs (Yoo *et al.*, 2004). There are reports in *Caenorhabditis elegans* that a protein with multiple TMH is essential in systemic silencing (Winston *et al.*, 2002), which may act as a receptor or a membrane channel (Mlotshwa *et al.*, 2002). After reports emerged in relation to the presence of siRNA molecules, attention was turned to the cloning and identification of endogenous small RNA molecules called microRNAs (Mette *et al.*, 2002; Park *et al.*, 2002; Reinhart *et al.*, 2002; Llave *et al.*, 2002a).

MicroRNAs are probably present in all multicellular organisms (Xie *et al.*, 2004) and use the same RISC complex and cellular machinery as siRNA molecules (Llave *et al.*, 2002b; Tang *et al.*, 2003). MicroRNAs (miRNAs) are derived from intergenic regions of the genome (Ambros *et al.*, 2003) and are involved in down-regulation of developmentally important endogenous genes (Bartel and Bartel, 2003; Carrington and Ambros, 2003; Hake, 2003; Hunter and Poethig, 2003). Searches for complementary regions of miRNAs in sequenced plant genomes revealed that miRNAs bind to their target sequences in a perfect manner (Rhoades *et al.*, 2002), which makes mRNA molecules potential targets for cleavage and repression of translation (Mallory and Vaucheret, 2004).

A number of methods were developed to deliver the foreign DNA into plant cells to investigate the effects of gene silencing transiently. These methods include agroinfiltration, virus induced gene silencing (VIGS) and particle bombardment (Horser *et al.*, 2002). The transient techniques are often used to evaluate the efficacy of gene silencing prior to the use of stable transformation *via Agrobacterium* because of the ease

of related evaluation and detection steps. In cases where the use of transient methods lead to a particular phenotype, the phenotype can be further investigated through stable transformation using either particle bombardment or *Agrobacterium* methods. The VIGS technique involves infecting host plants with a virus carrying a sequence with homology to a host nuclear gene, and the high level expression of gene under the control of viral promoters later triggers cytoplasmic RNA degradation (Baulcombe, 1999). This technique requires a pathogenic virus with the ability to infect the host plant and was developed in *Nicotiana benthamiana*. Until recently, attempts to use a virus to induce PTGS in monocots were not successful, but a vector derived from the barley stripe mosaic virus (BSMV) showed that this phenomenon can be induced in barley (Fitzmaurice *et al.*, 2002; Holzberg *et al.*, 2002; Lacomme *et al.*, 2003). The use of BSMV is restricted in Australia due to quarantine regulations. As a consequence of this limitation for monocots, a new technique based on particle bombardment called transiently induced gene silencing (TIGS), was developed by Dr. Rachel Burton and Dr. Keith Gatford (University of Adelaide, SA, Australia) as an in-house method (Burton *et al.*, 2003). The method uses a plasmid developed by Wesley *et al.* (2001) to produce dsRNA molecules transiently within the cell; the plasmid is introduced into the cells by particle bombardment. The vector contains two multiple cloning sites separated by an intron, which accommodates both a sense and an antisense fragments. After introducing the plasmid to an organism, the transcripts include a dsRNA molecule, which is an inverted repeat separated by an intron (Wesley *et al.*, 2001).

Biolistics have been used previously in barley as an effective approach to study gene silencing (Azevedo *et al.*, 2002). A dsRNAi construct disrupted the function of dihydroflavonol-4-reductase (Ant18 dsRNA), which resulted in the inhibition of anthocyanin accumulation in barley (Schweizer *et al.*, 2000). In the same study, the effect of dsRNA on the production of *Mlo* barley plants that were resistant to the barley powdery mildew [*Blumeria graminis* f.sp. *hordei* (Bgh)] was studied. In a similar study, the *SGT1* gene, which is the barley orthologue of yeast protein that is an essential cell cycle regulator, was shown to interact with *Rar1*, a pathogen resistance signaling gene, in

barley (Azevedo *et al.*, 2002). Silencing of both *Rar1* and *SGT1* showed a great reduction of resistance to powdery mildew, which suggested a role in plant defence mechanisms. There are many other reports of PTGS in other plants as a functional analysis tool (Schweizer *et al.*, 2000; Xiao *et al.*, 2003; Zhao *et al.*, 2003). In a study to reveal the function of a galactomannan galactosyltransferase gene involved in cell wall biosynthesis from *Lotus japonicum*, PTGS was used to disrupt the activity of the galactosyltransferase in order to establish a relationship between loss of function and possible changes in cell wall structure (Edwards *et al.*, 2004). The T1 generation seed showed a range of effects and some contained galactomannan with a higher ratio of Man to Gal as a result of a silencing effect on galactosyltransferase activity.

Here, a post-transcriptional gene silencing approach (PTGS) was used in barley as a method of choice to study possible cell wall changes in relation to the silencing of all family GT34 members, and of three individual genes (*HvGlyT1*, *HvGlyT2* and *HvGlyT3*). At the time of experiment, *HvGlyT4* cDNA was not cloned and therefore family GT47 did not consider in these experiments. The dsRNA constructs were generated essentially as described above, and were introduced into immature barley embryos by microparticle bombardment.

6.2 MATERIALS AND METHODS

6.2.1 Materials

The pHANNIBAL vector (Figure 6.2) was generously donated by Dr. Peter Waterhouse (CSIRO, Canberra, Australia). Spermidine, Tris, toluidine blue, glutaraldehyde, osmium tetra oxide, 10 × Murashige-Skoog macronutrient and micronutrient, 1000 × Murashige-Skoog vitamin solution, 2,4-D and agar grade M were purchased from SIGMA-Aldrich (St Louis, MO, USA). Isopropanol, glacial acetic acid, formaldehyde, sodium phosphate, sodium chloride, acetone, calcium chloride, and ethanol were purchased from Merck Pty Ltd (Kilsyth, VIC, Australia). Oligonucleotide primers were synthesised by Geneworks (Adelaide, SA, Australia). The pGEM-T Easy vector system I kit was provided by Promega (Madison, WI, USA). Restriction endonucleases were supplied by New England BioLabs, Inc. (Beverly, MA, USA). Gold microcarrier (0.6 micron in size), rupture discs (900 psi), the PD-1000/He particle delivery gun for biolistics and carrier discs were obtained from BIO-RAD Laboratories Pty Ltd (NSW, Australia). Low melting point agarose (EEO $\leq$ 0.12) was obtained from Edwards Instrument Co. (NSW, Australia). A polaron H1200 vibrating microtome used to prepare the cross-sections of tissues was from BIO-RAD microscience division (Cambridge, MA, USA). Elongase enzyme mix was purchased from Invitrogen (Melbourne, Australia). Calcofluor White M2RS NEW (Fluostain) was kindly provided by Professor Bruce Stone (La Trobe University, Melbourne, Australia). CM Sepharose CL-6B was supplied by Amersham Life Sciences (Buckinghamshire, UK). Leica MZFLIII and Leica 1M1000 image manager software were purchased from Leica (Heerbrugg, Switzerland). An Axioskop 20 microscope was obtained from Carl Zeiss Pty Ltd (Sydney, NSW, Australia).

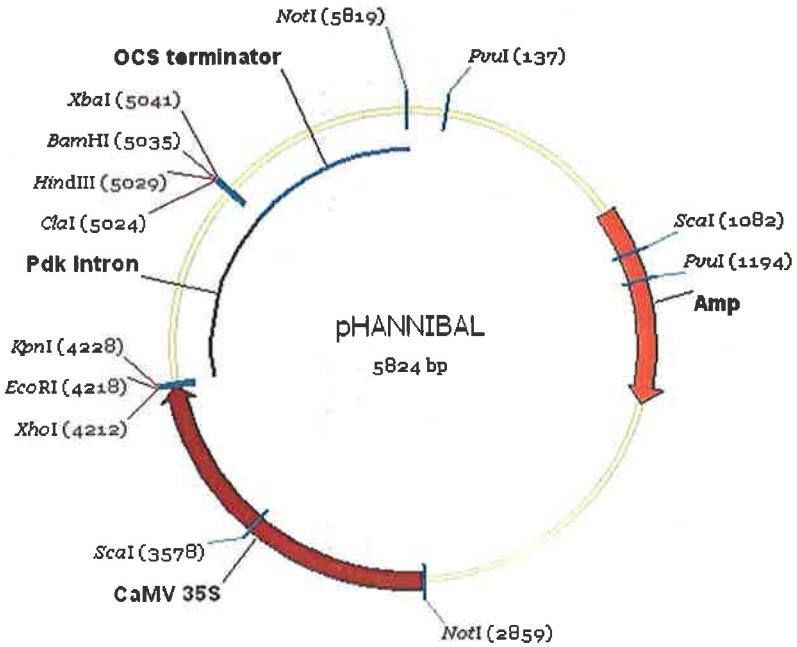

Figure 6.2 Map and multiple cloning sites for pHANNIBAL. PCR products from the target gene are cloned into both polylinkers of the plasmid, using relevant restriction sites engineered into the PCR primers to ensure the opposite orientation of both inserts. For example, PCR products were cloned into either *Eco*RI/*Kpn*I or *Hin*dIII/*Xba*I, respectively. The two polylinkers are separated by the Pdk intron isolated from *Flaveria*. The 35S cauliflower mosaic virus promoter drives transcription to produce a hairpin loop RNA (hpRNA).

6.2.2 PCR Amplification of sense and antisense fragments

A multiple sequence alignment was carried out using three barley members of family GT34 to find a conserved sequence region sharing at least 21 identical nucleotides. However, locating a stretch of 21 bp was not possible, so a fragment (267 bp) with the highest homology between the three barley glycosyltransferase cDNA clones was amplified (Figure 6.3). *HvGlyT1* was chosen as the template and primers (Table 6.1) were designed to amplify sense and antisense copies of the conserved region. To generate the dsRNAi vectors, primers (Table 6.1) containing suitable restriction sites based on available sites in the multiple cloning site of the pHANNIBAL vector (Figure 6.2), were designed to amplify the sense and antisense fragments. The fragments were amplified in a 50 µl PCR using Elongase as the DNA polymerase with an initial start at 94° C for 2 min, followed by 35 cycles of [94°C for 30 sec; lowest T_m of the gene-specific primers for; 30 sec; 68° C for 30 sec].

In order to silence *HvGlyT2* and *HvGlyT3* specifically, the 3'UTR of these genes was amplified as described above. For *HvGlyT2* and *HvGlyT3*, fragments of 164 and 457 nucleotides were amplified using the primers with suitable restriction sites (Table 6.1).

6.2.3 Generation of dsRNAi silencing constructs in pHANNIBAL

Amplified fragments (both sense and antisense) were cloned into pGEM-T Easy as described in section 2.2.6. The sequences of the fragments were confirmed as described in section 2.2.8 and fragments were excised from pGEM-T Easy using their respective enzymes (sense fragments: *Xho*I and *Eco*RI, antisense fragments: *Xba*I and *Hin*dIII) as described in section 2.2.7. The excised fragments were cloned into the pHANNIBAL plasmid sequentially, *i.e.* sense fragment (*Eco*RI/*Xho*I) first and antisense fragment (*Xba*I/*Hin*dIII) second, after digestion of pHANNIBAL with the corresponding enzymes.

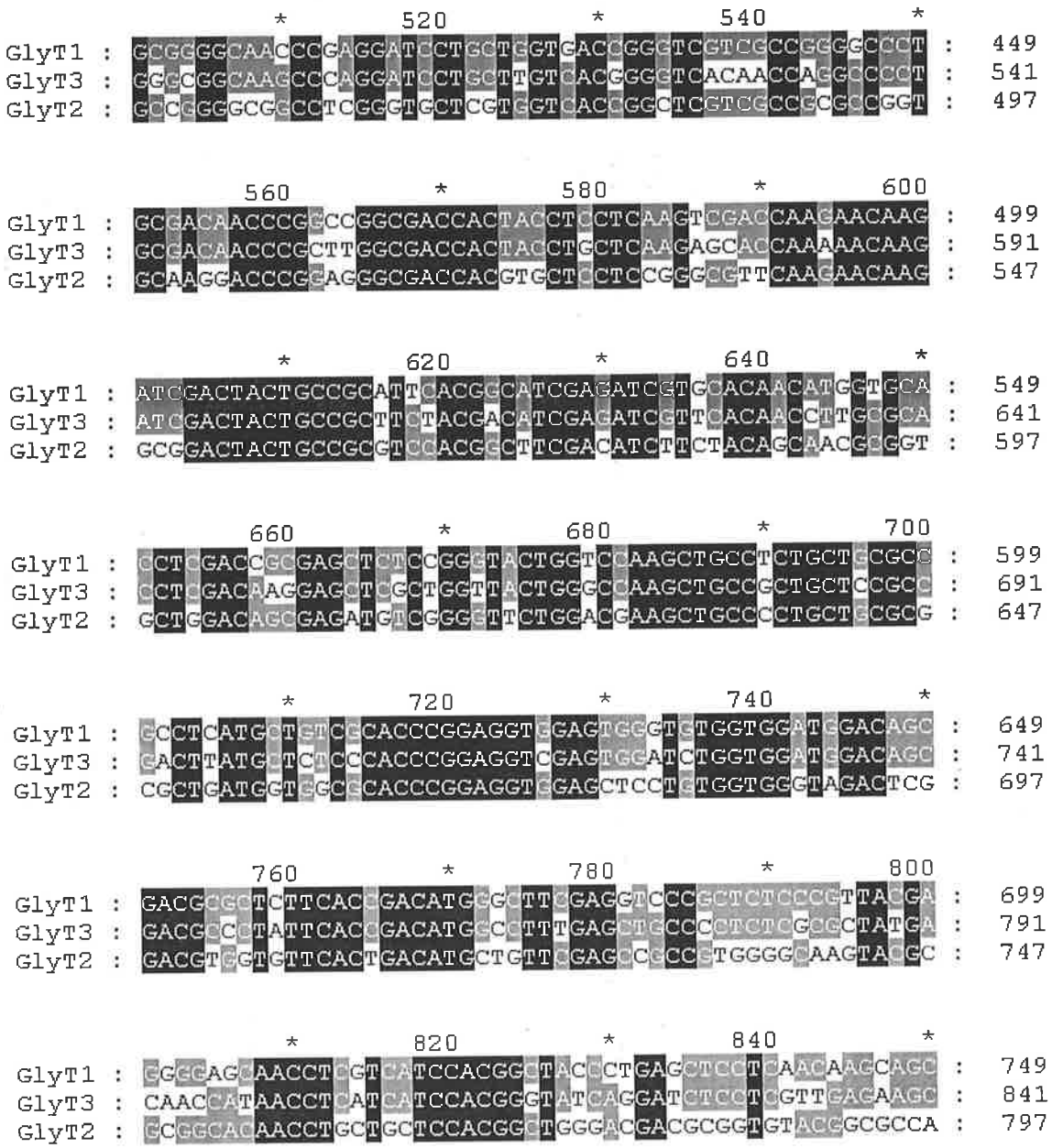

Figure 6.3 Partial multiple sequence alignment of three barley glycosyltransferas cDNA clones. GlyT1, GlyT2 and GlyT3 denote the barley glycosyltransferases (*HvGlyT1*, *HvGlyT2* and *HvGlyT3*).

The dsRNAi plasmid constructs were isolated as described in section 2.2.7 and purified using a Sepharose Cl-6B column. Insertions were confirmed by restriction enzyme digests of the cloned fragment from the pHANNIBAL vector (Figure 6.4). The extra cloning steps in pGEM-T Easy resolve the inherent difficulties that may arise from sequencing of inverted repeat sequences in the pHANNIBAL vector.

6.2.4 Preparation of immature embryos

Barley (cv. Sloop) was grown in a glasshouse at 25/18° C day/night temperature, under 12-13 h daylight. At 25 d post anthesis, immature plump grains (green to yellowish in colour) were harvested in the afternoon and after dehusking kept at 4°C under a wet tissue. The following morning, the grains were surface sterlised with 70% (v/v) ethanol for 2 min. Grains were rinsed three times for 5 min each with sterlised water. The immature embryos were excised under a microscope in sterile conditions and placed onto osmotic treatment (OS1) media (20% v/v 10 × Murashige-Skoog macronutrient solution, 10% v/v 10 × Murashige-Skoog micronutrient, 0.1% v/v 1000 × Murashige-Skoog vitamin solution, 1 mg/ml 2,4-D, pH 5.8, 24% w/v sucrose, and 0.9% w/v agar) modified after Murashige and Skoog (1962) for 24 h.

6.2.5 Preparation of gold microcarrier particles

Gold microcarrier particles (60 µg of 0.6 micron) were washed with absolute ethanol (1 ml) by vortexing for 1 min followed by a 3 min sonication. The particles were left at room temperature until they had all settled, and were subsequently centrifuged for 1 min at 9,000 ×g. The supernatant was discarded and the microcarriers were washed twice with sterile water as above to remove any excess ethanol. Sterile water (1 ml) was added and after a brief vortex, the tube containing the gold particles was left in the sonicator while aliquoting the particles. Microcarriers were aliquoted (20 µl) into separate tubes followed by the addition of sterile water (30 µl). The gold particles were stored at 4°C.

Gene	Orientation	Sequence	R.E
HvGlyT1	S-F	CTCGAGCCTGCTGGTGACCGGGTCGTCG	*Xho*I
	S-R	GAATTCGGGACCTCGAAGCCCATGTCGGT	*Eco*RI
	A-F	TCTAGAGGGACCTCGAAGCCCATGTCGGT	*Xba*I
	A-R	AAGCTTCCTGCTGGTGACCGGGTCGTCG	*Hin*dIII
HvGlyT2	S-F	CTCGAGCAGGGCCGCCAAGCCATTGTGATC	*Xho*I
	S-R	GAATTCGACGTACAGTTCACAATGGTGCC	*Eco*RI
	AS-F	TCTAGAGACGTACAGTTCACAATGGTGCC	*Xba*I
	As-R	AAGCTTCAGGGCCGCCAAGCCATTGTGATC	*Hin*dIII
HvGlyT3	S-F	CTCGAGATGCGGAAGCTATGGTGATTATC	*Xho*I
	S-R	GAATTCGCAAGAAAGTAGCACTGAAATG	*Eco*RI
	AS-F	TCTAGAGCAAGAAAGTAGCACTGAAATG	*Xba*I
	AS-R	AAGCTTATGCGGAAGCTATGGTGATTATC	*Hin*dIII

Table 6.1 PCR primers showing the engineered restriction site (underlined).
S-F = sense forward, S-R = sense reverse, A-F = antisense forward, A-R = antisense reverse, R.E = restriction endonuclease.

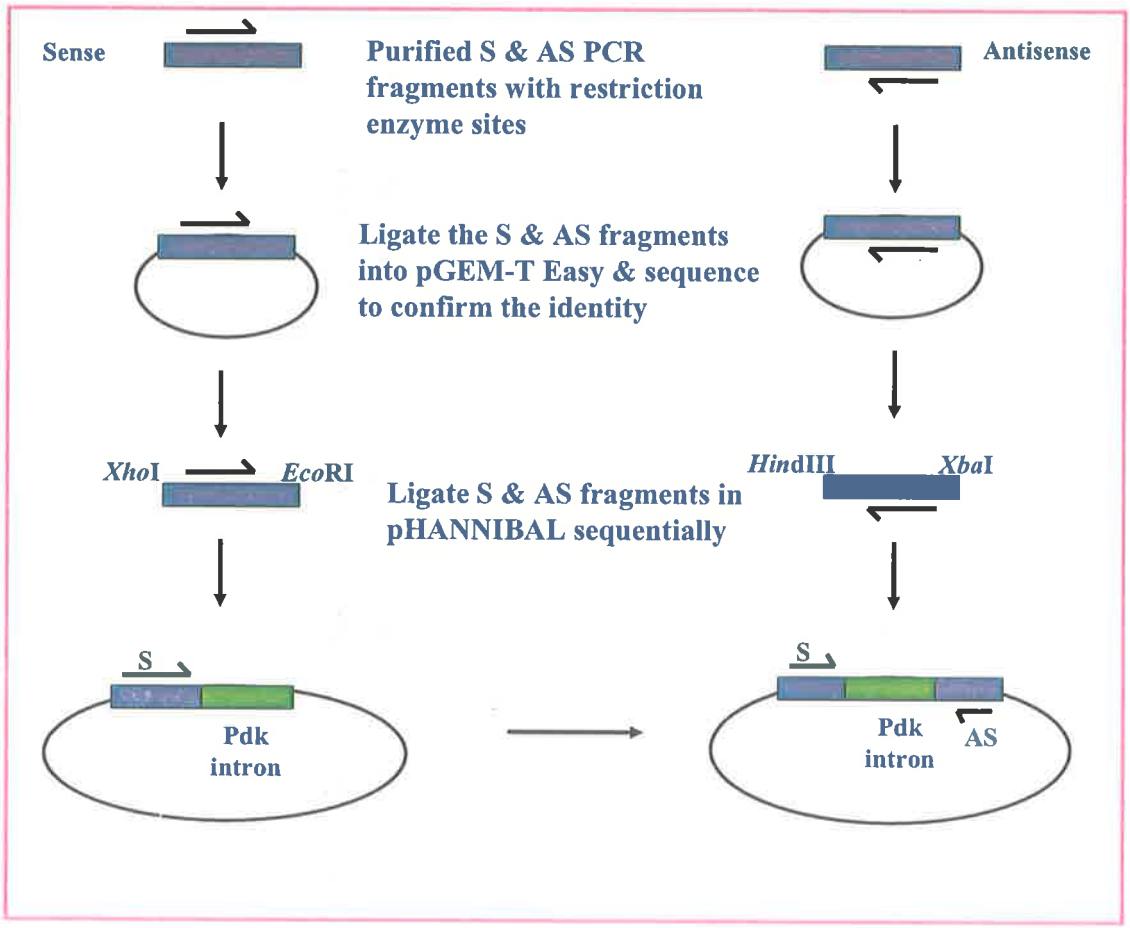

Figure 6.4 Schematic representation of the steps involved in building dsRNAi constructs in the pHANNIBAL vector. S = sense, AS = antisense.

6.2.6 Particle bombardment of immature embryos

The dsRNAi silencing plasmid prepared in section 7.2.3 (2.3 µg) along with the empty pHANNIBAL vector (2.3 µg) was added to two separate tubes containing the gold particles. Spermidine (20 µl 0.1 M) and 50 µl 2.5 M $CaCl_2$ were mixed in the lid of each tube. The lid was closed and the mixture vortexed for 3 min. The mixture was incubated on ice for 5-10 min to precipitate the DNA-coated gold particles followed by centrifugation at 3,000 ×g for 10 sec. The supernatant was discarded and absolute ethanol (250 µl) was added. After a brief vortex, tubes were allowed to stand on ice for another 5-10 min and after centrifugation at 3,000 ×g for 10 sec, the supernatant was discarded. Absolute ethanol (100 µl) was added and the mixture incubated on ice until the bombardment.

A Biolistic PD-1000/He particle delivery gun (Figure 6.5), rupture discs (900 psi) and carrier discs were surface sterlised with 70% (v/v) ethanol, 100% (v/v) isopropanol and absolute ethanol, respectively. The carrier discs were coated with 10-15 µl of the incorporated microcarriers, left to dry and placed on the stopping screen. A rupture disc was installed and the Petri-dish containing the immature embryos was placed on the target shelf. Vacuum was applied to the chamber to 27 Inches of Hg. Helium pressure (1500 psi on tank) was applied to the disc by activating the fire button to force the plasmid-coated particles into the immature embryos. The plates containing the bombarded immature embryos were sealed and incubated in the dark at 20°C overnight.

The following day the bombarded immature embryos were transferred onto half strength MS media solidified with 1.6% (w/v) agar (5% v/v 10 × Murashige-Skoog macronutrient solution, 5% v/v 10 × Murashige-Skoog micronutrient solution, 0.05% v/v 1000 × Murashige-Skoog vitamin solution, 3% w/v sucrose, pH 5.8) modified after Murashige and Skoog (1962). The plates were incubated in the dark at 20°C for 5 d following bombardment.

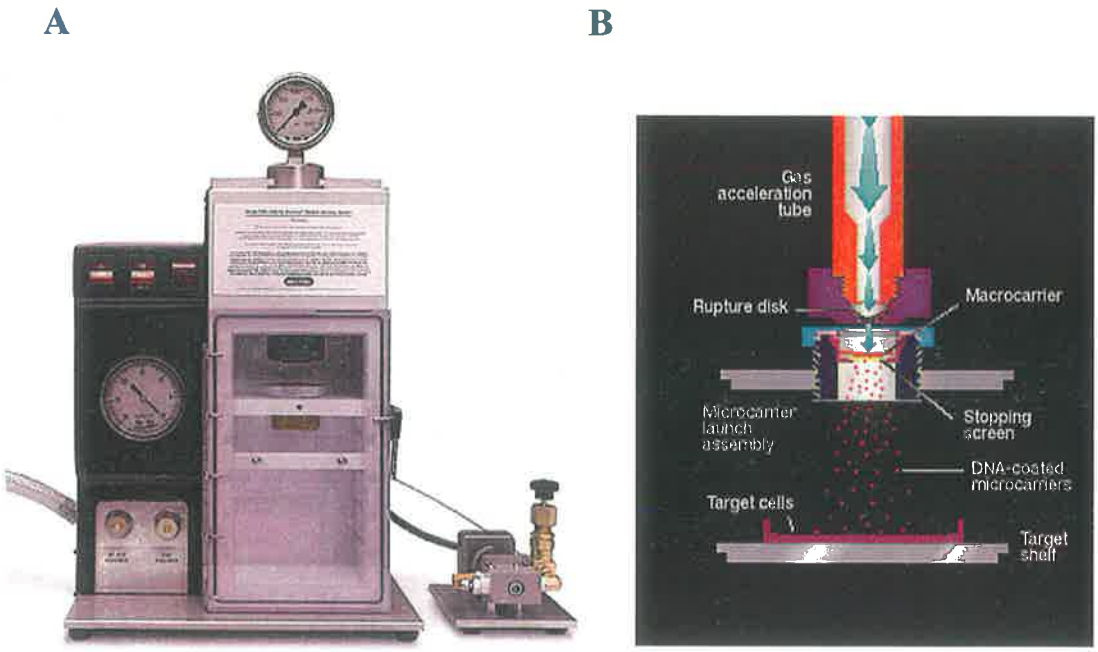

Figure 6.5 A view of the Biolistic PDS-1000/He unit and a schematic representation of micro projectile bombardment. **A:** Biolistic unit and its main chamber containing the microcarrier launch assembly and the helium pressure gauge (on top). The central gauge (left) shows the vacuum within the chamber and two lower knobs adjust the vacuum flow and vent rates. The helium metering valve is next to the main chamber. **B:** Illustration of how the instrument accelerates the microcarriers into the target cells. After applying the vacuum in the system to lower any frictional drag on the DNA-coated microcarriers, the helium gas is released to hit the rupture disk. At the burst pressure of the rupture disk, a gas shock is applied to the chamber and it carries the microcarriers towards the target cell or tissue. A wire-mesh stopping screen inhibits the carry over of the plastic disk (macrocarrier), while allowing the passage of microprojectiles (the photos are adapted from http://fisio.dipbsf.uninsubria.it/scuola/biolistic.html).

6.2.7 RNA extraction and first strand cDNA synthesis

Total RNA was extracted from 5 d old barley (cv. Sloop) primary/seminal root base, root tip and expanding coleoptile and cDNA was synthesised as described in section 2.2.3.

6.2.8 Quantitative (REAL-TIME) PCR and calculation of NF values

The amounts of transcript were measured using Real-Time PCR as described in section 3.2.5 and the data were normalised by calculation of a normalization factor (NF) as described in section 3.2.6.

6.2.9 Fixation and sectioning of bombarded tissues

Sections of barley seminal roots and expanded coleoptiles were harvested 5 d post bombardment from immature embryos treated with either the RNAi construct or the empty pHANNIBAL vector, and incubated in a chilled fresh fixative solution (FAA: 63% v/v absolute ethanol, 5% v/v glacial acetic acid, 2% v/v 37% formaldehyde) for 24 h. The following day fixed tissues were washed three times for 10 min each with washing solution (63% v/v absolute ethanol, 5% v/v acetic acid). The tissues were further rinsed with PBS (10 mM $NaPO_4$, 130 mM NaCl, pH 7.5) and embedded in a molten 5% low-melting point agarose made with 1 × PBS. The embedded tissues were incubated at 4°C overnight. A block of each tissue was excised from the gel and fastened to the specimen block of a vibratome using Superglue. Sections 30-90 µm thick of the tissues were cut in the vibratome chamber filled with sterilised water and sections were collected with a fine paintbrush.

6.2.10 Staining and microscopic analysis of bombarded tissues

Bombarded immature embryos were examined under a Leica MZFLIII microscope. The root and coleoptile tissues were examined carefully and the images were captured using Leica 1M1000 image manager software.

A stock solution of Calcofluor White (1% w/v Calcofluor White, 0.1 M Tris-HCl buffer, pH 9.0) was diluted 100 times with Tris-HCl buffer, pH 9.0 to stain tissue sections. Tissues were observed under UV light with an excitation filter and a barrier filter of 360/40:420 nm). A stock solution of toluidine blue (25% w/v) was diluted 10-fold to stain the tissue sections. The stained tissues were washed with sterilised water and examined under light field.

Tissue sections were mounted on a glass slide and stained separately with calcofluor white (specific for glucans) and toluidine blue followed by removal of any excess stain using water. Toluidine blue develops a pinkish colour with carboxylated polysaccharides, *e.g.* uronic acids, and a blue colour with polyphenols, *e.g.* lignin in secondary cell walls. An Axioskop 20 microscope was used to examine the tissue sections and Leica 1M1000 image manager software was used to capture the images.

6.2.11 Sample tissue preparation and fixation for electron microscopy

The 5 d old barley roots and coleoptiles bombarded with both the empty vector and dsRNAi DNA were fixed using a two step process and dehydrated before coating. In step 1, 2.5% (v/v) glutaraldehyde was used to fix the proteins in the tissue *via* cross-linking of aldehyde groups and amine groups. The tissue was fixed three times with fresh 2.5% (v/v) glutaraldehyde solution at 2 h intervals. The preliminary fixed tissues were rinsed six times with Milli-Q^{TM} water at 1 h intervals. The second step of fixation involved

immobilising proteins and lipids using 1% osmium tetraoxide. The tissues were covered with the OsO_4 for 4 days at 4°C with a brief swirling each morning until the tissues become completely black. The tissues were dehydrated by four consecutive acetone-washes, 25%, 50%, and 75% (v/v), of 2 h each. Finally, the tissues were left in 100% (v/v) acetone until they were coated with gold/palladium alloy.

6.2.12 Scanning electron microscopy

The fixed tissues were dried and mounted on a specimen stub with silver paste or graphite and coated with gold/palladium alloy and stored in a desiccator. Dr. Sarah Wilson (University of Melbourne, Vic, Australia) performed the scanning electron microscopy.

6.3 RESULTS

6.3.1 *Bombardment of barley immature embryos with a dsRNAi construct containing the conserved barley sequence of family GT34*

A dsRNAi plasmid was constructed based on the conserved region of the barley members of family GT34 previously isolated and described. Since the sequence was obtained from *HvGlyT1*, the dsRNAi construct was considered as both a *HvGlyT1* and family GT34 silencer. The immature embryos were bombarded with the construct and after 5 days, the germinated embryos were observed under the light microscope for any phenotypic changes. There were no visible differences between the dsRNAi and the negative control (embryos bombarded with the empty pHANNIBAL vector). Despite this, coleoptiles were used for RNA preparation and cDNA synthesis. Real-Time PCR was carried out for transcript analysis of *HvGlyT1*, *HvGlyT2*, and *HvGlyT3* (Figure 6.6). Table 6.2 shows the normalization factors based on the control genes, *HvCycl* and *HvCesA1* genes, which were used to normalise the raw data. *HvGlyT2* was the only gene that showed slight down-regulation (Figure 6.6). The transcript level of *HvGlyT1* was not down-regulated significantly compared with the control. *HvGlyT3* showed a significant up-regulation.

6.3.2 *Bombardment of barley immature embryos with the HvGlyT2 dsRNAi construct*

Immature embryos were subjected to microprojectile bombardment using a *HvGlyT2*-specific dsRNAi construct. The tissues were examined for any phenotypic changes 5 d post-bombardment. The germinated embryos did not show any visible phenotype. Root tips, the tissue with the highest amount of *HvGlyT2* in barley (Chapter 3), were collected from embryos bombarded with both the empty pHANNIBAL vector and the *HvGlyT2* dsRNAi and total RNA was extracted for cDNA synthesis. The cDNAs were used for transcript analysis *via* Q-PCR and the data were normalised against *HvCycl* and *HvHsp70*

Construct type	Tissue	Normalisation Factor (NF)
Conserved RNAi	Root tip	1.31
	Root base	0.45
Empty pHANNIBAL	Root tip	2.13
	Root base	0.79

Table 6.2 Normalisation factors calculated by geNorm for the cDNAs of root tip and root base. The tissues were collected 5 d post bombardment with the conserved RNAi construct or the empty pHANNIBAL vector and the NF values of the transcript data were based on a combination of two control genes (*HvCycl* and *HvCesA1*).

A

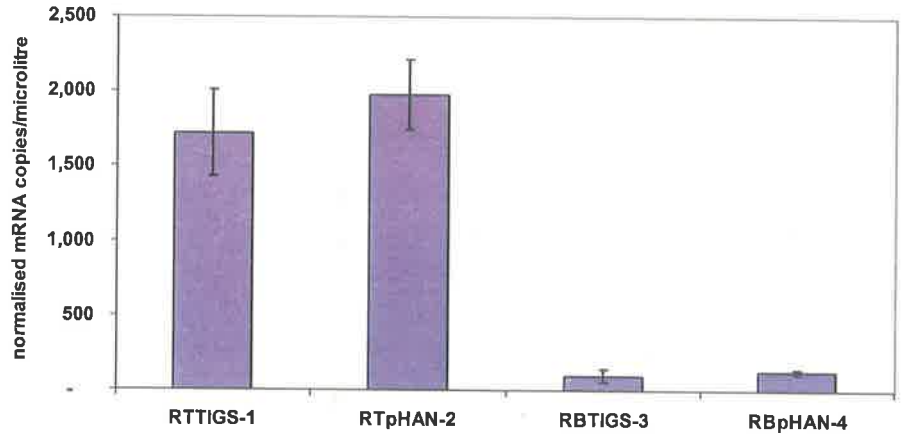
normalised mRNA copies/microlitre
2,500
2,000
1,500
1,000
500
-
RTTIGS-1
RTpHAN-2
RBTIGS-3
RBpHAN-4

B

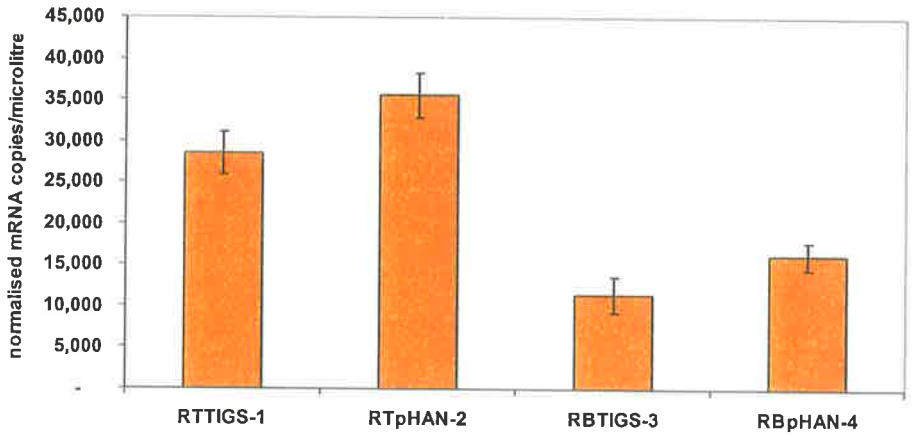
normalised mRNA copies/microlitre
45,000
40,000
35,000
30,000
25,000
20,000
15,000
10,000
5,000
-
RTTIGS-1
RTpHAN-2
RBTIGS-3
RBpHAN-4

C

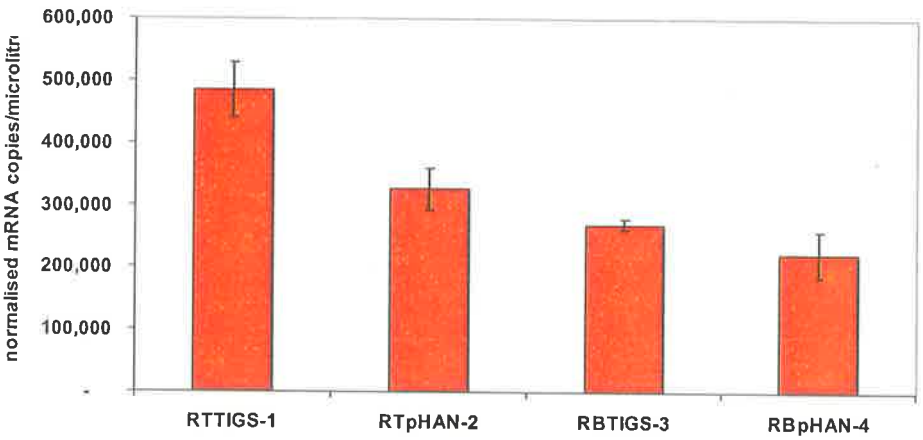
normalised mRNA copies/microlitr
600,000
500,000
400,000
300,000
200,000
100,000
-
RTTIGS-1
RTpHAN-2
RBTIGS-3
RBpHAN-4

Figure 6.6 TIGS using a RNAi construct containing a fragment based on the conserved sequence of *HvGlyT1*, *HvGlyT2* and *HvGlyT3*. The data were normalized with *HvCycl* and *HvCesA1* control genes. RTTIGS-1 = root tip, immature embryo bombarded with RNAi construct, RTpHAN-2 = root tip, immature embryo bombarded with the empty pHANNIBAL plasmid, RBTIGS-3 = root base, immature embryo bombarded with the RNAi construct, RBpHAN-4 = root base, immature embryo bombarded with the empty pHANNIBAL plasmid. **A**: Insignificant down regulation in both root tip and root base for *HvGlyT1*. **B**: Significant down regulation in root tip and base for *HvGlyT2* as the result of RNAi. **C**: Up-regulation of *HvGlyT3* mRNA as the result of dsRNAi silencing in both root tip and base. Note the mRNA level (copies/microlitre) for each gene on the Y axis.

as the control genes (Figure 6.7). The transcript level was shown to have decreased as much as 40% but, as mentioned above, despite the significant reduction in transcript level, this was obviously not enough to cause phenotypic changes.

6.3.3 Bombardment of barley immature embryos with the HvGlyT3 dsRNAi construct

A *HvGlyT3*-specific dsRNAi construct was used to bombard barley immature embryos using the empty pHANNIBAL vector as the negative control. The ultrastructure of the germinated immature embryos was examined under the microscope for any subtle changes. A hairy root tip phenotype was seen among the embryos bombarded with the *HvGlyT3* dsRNAi construct, which was not seen in the embryos bombarded with the control plasmid (Figure 6.8).

Since the frequency of the roots showing the phenotype was relatively low (5% of all the bombarded embryos), pooled samples of root tip, root base, and coleoptile were collected for total RNA extraction and cDNA synthesis. The cDNAs were subjected to Q-PCR for transcript analysis (Figure 6.9) followed by normalization of the raw data with the control genes as described in Chapter 3. The transcript level was up-regulated in coleoptiles as a result of sampling error, since a pooled sample was used for cDNA synthesis. In both root base and tip however, the transcript level was slightly reduced although the down-regulation in the root base was not significant. In contrast, the root tip showed a 25% reduction in transcript level. The coleoptile and roots were subjected to further analysis using the light and electron microscopes.

In each bombarded immature embryo showing a phenotype, only one of the rootlets out of three emerged displayed a hairy root tip phenotype and this was used to prepare sections for light microscopy. The two remaining rootlets and emerged coleoptile from the same embryo were fixed for electron microscopy. The root tip segments were fixed, sectioned and stained for light microscopy as described in sections 7.2.9 and 7.2.10

(Figures 6.10 and 7.11). The root tip sections stained with Calcofluor White, which is a dye used for staining cellulose and other β-glucans, had bigger cells compared with the control and no separating walls at the sub-epidermal layer were present. A similar pattern was seen when the root tip sections were stained with another wall specific dye, toluidine blue. Bigger cells and the collapse of the epidermal layer leading to hairy root tip phenotype were clear. These changes in the cell wall structure clearly suggest the involvement of *HvGlyT3* in cell wall biosynthesis in barley.

The intact roots and coleoptiles were further analysed with SEM. The roots, which did not show the hairy root tip phenotype, were no different from the control. However, the coleoptile tissue appeared to have a patchy structure where elongating cells had not expanded properly and had caused stress fractures in contrast to the control (Figure 6.12). This result reaffirmed the idea that *HvGlyT3* is likely to be involved in cell wall biosynthesis and demonstrated the need to examine target tissues carefully and thoroughly following bombardment for signs of a phenotype.

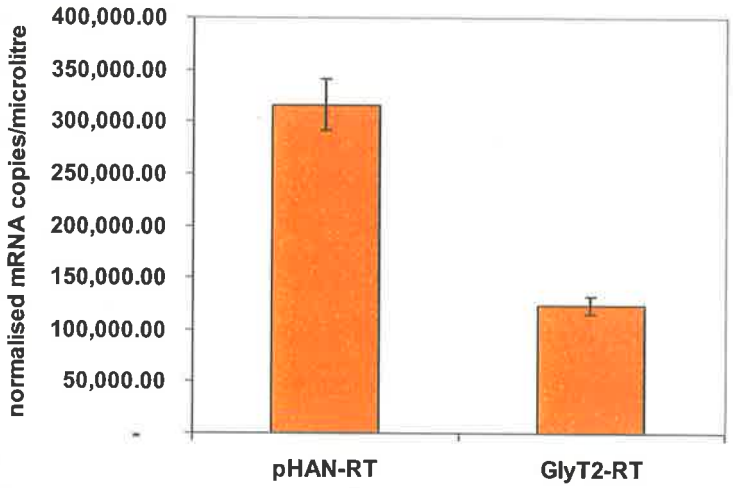

Figure 6.7 Gene silencing using a dsRNAi construct containing the 3'UTR of *HvGlyT2*. The data were normalised against *HvCycl* and *HvHSP70* as control genes. Root tip cDNAs were prepared from 5 d old immature embryos bombarded with both the empty pHANNIBAL plasmid (pHAN-RT) and *HvGlyT2* RNAi construct (GlyT2-RT). The NF values were 3.28 and 0.31 for pHAN-RT and GlyT2-RT, respectively. As a result of gene silencing a reduction of about 40% was observed in the transcript level of *HvGlyT2*.

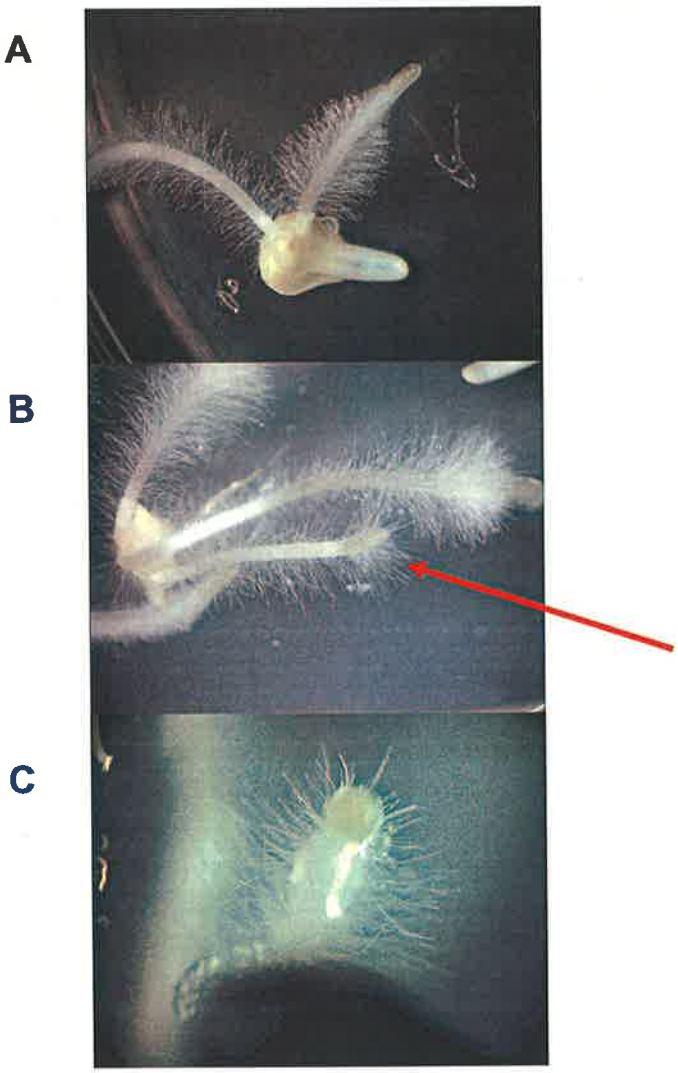

Figure 6.8 Immature embryos bombarded with the empty pHANNIBAL vector and the *HvGlyT3* RNAi construct. **A**: Germinated immature embryo after being bombarded with the empty vector. **B**: RNAi effect on the root ultrastructure. A hairy root tip is present on one out of three rootlets emerged from the embryo. **C**: A close up of the hairy root tip phenotype.

A

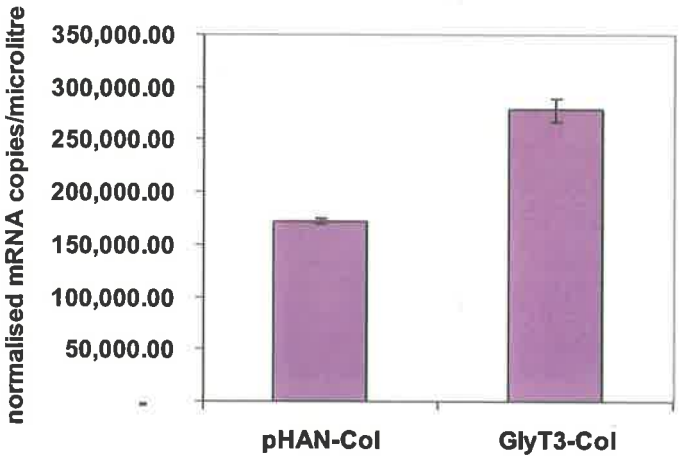
normalised mRNA copies/microlitre
350,000.00
300,000.00
250,000.00
200,000.00
150,000.00
100,000.00
50,000.00
-
pHAN-Col
GlyT3-Col

B

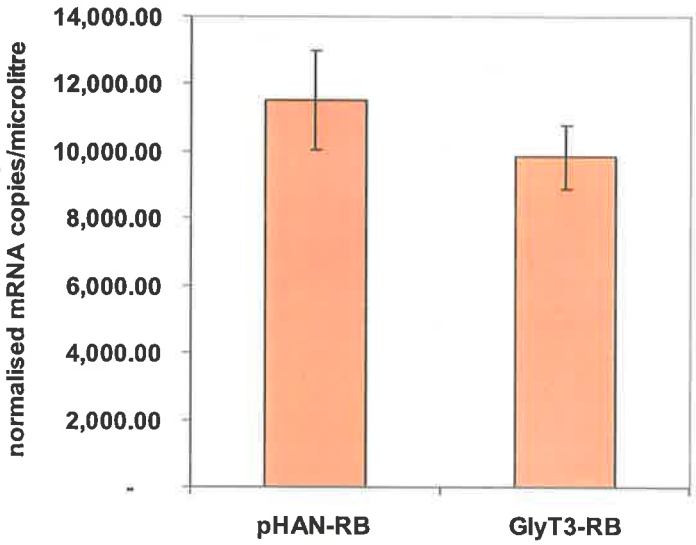
normalised mRNA copies/microlitre
14,000.00
12,000.00
10,000.00
8,000.00
6,000.00
4,000.00
2,000.00
-
pHAN-RB
GlyT3-RB

C

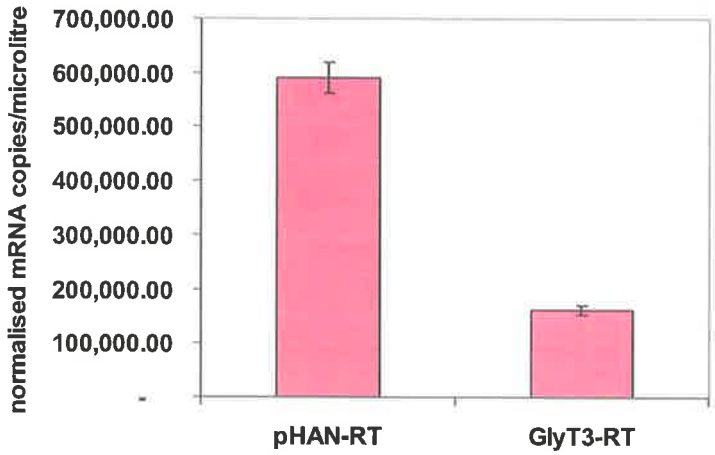
normalised mRNA copies/microlitre
700,000.00
600,000.00
500,000.00
400,000.00
300,000.00
200,000.00
100,000.00
-
pHAN-RT
GlyT3-RT

Figure 6.9 Gene silencing using a dsRNAi construct containing the 3'UTR of *HvGlyT3*. The data were normalised with *HvCycl* and *HvHSP70* for coleoptile and root base and *HvCycl* and *HvTub* for root tip. pHAN = immature embryos were bombarded with the empty pHANNIBAL plasmid, GlyT3 = immature embryos were bombarded with the RNAi construct containing the 3'UTR of *HvGlyT3*, Col = coleoptile, RB = root base, RT, root tip. After bombardment and germination, a significant up-regulation in coleoptile (Panel A), insignificant down regulation in root base (Panel B) and a significant (~25%) reduction were seen in transcript level of root tip (Panel C). The transcript data are presented as copies/microlitre.

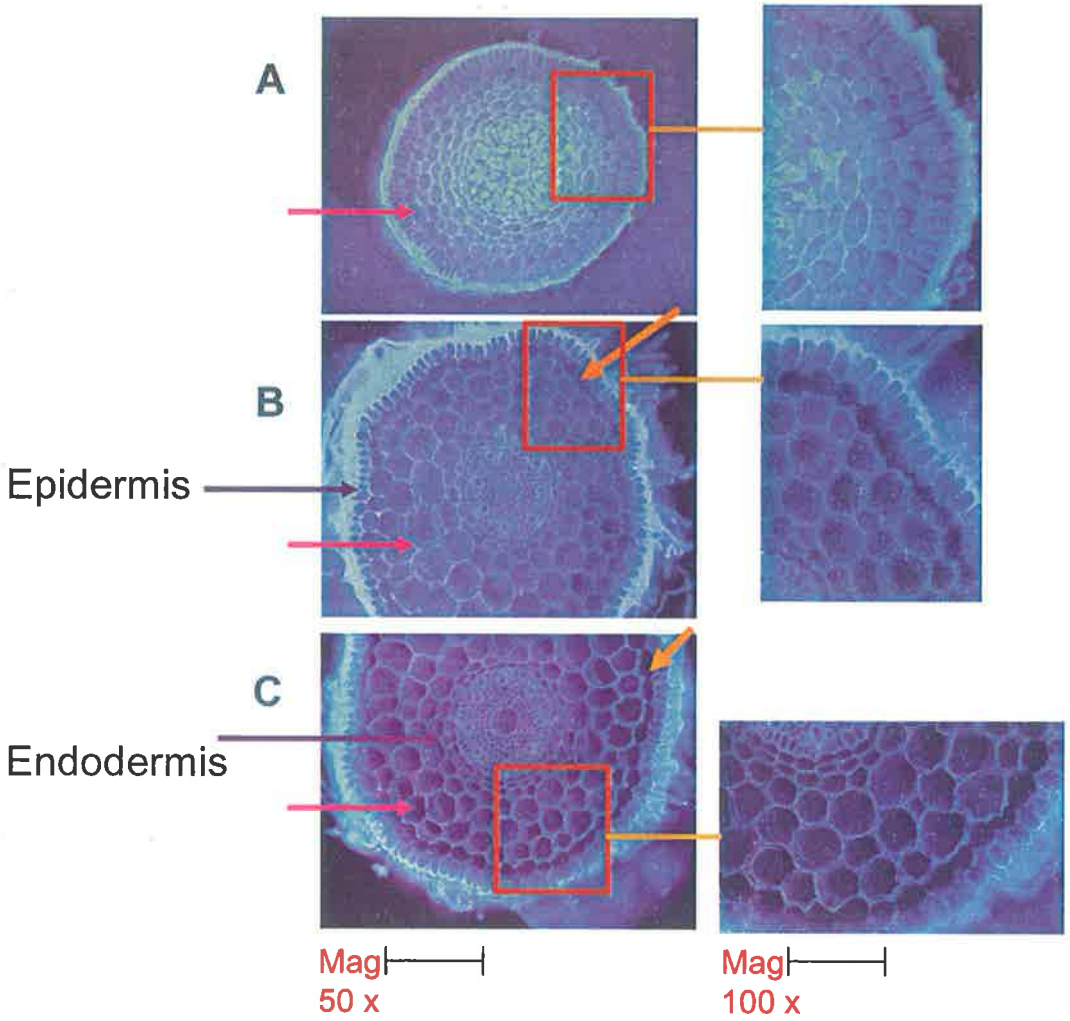

Figure 6.10 Root sections stained using calcofluor white. **A**: A root section excised from an immature embryo bombarded with the empty pHANNIBAL vector as the control. The cells were normal in size and shape and the root layers (epidermis, parenchyma, and endodermis) were intact. **B** and **C**: Different views of a root cross-section excised from an immature embryo bombarded with the *HvGlyT3* RNAi construct. Cells are bigger in size (pink arrows) compared with the control (Panel A). The cell walls between sub-epidermal layer are distorted and there are no separating walls present (orange arrows). The photos on the right are the enlarged pictures.

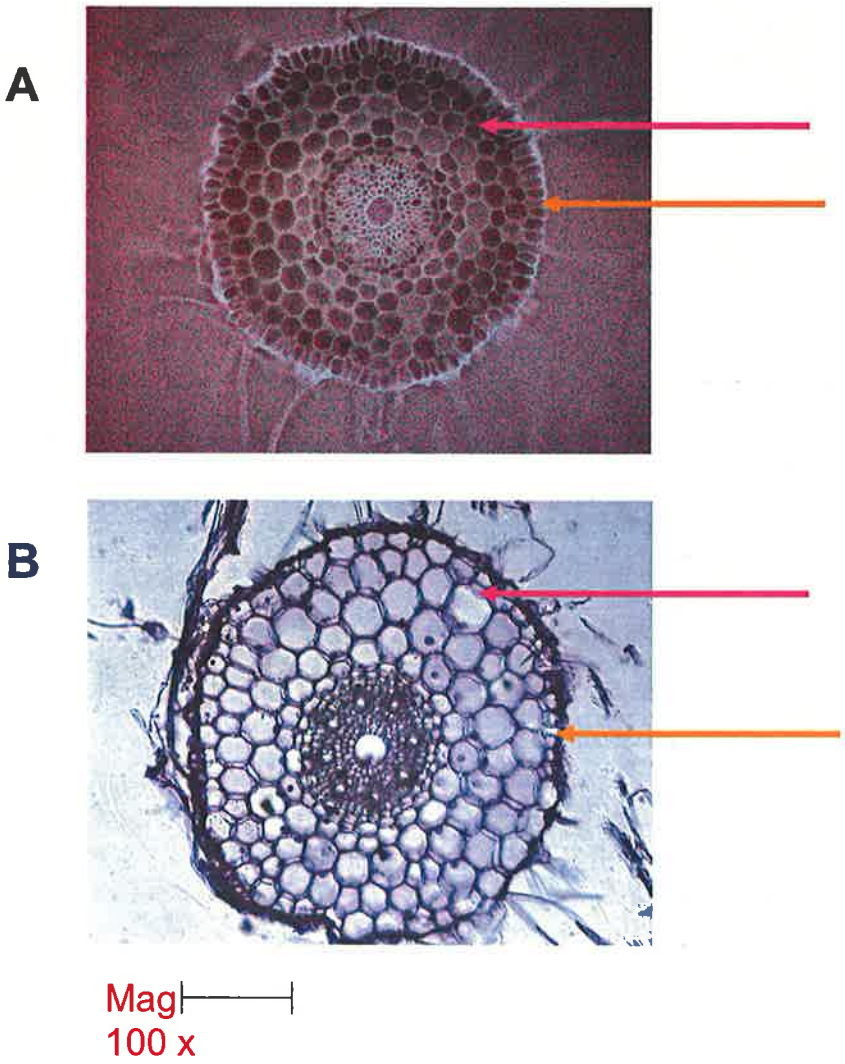

Figure 6.11 Root sections stained using toluidine blue. **A**: A cross-section of a root excised from immature embryos bombarded with the empty pHANNIBAL vector as control. The epidermis is present as normal. **B**: A cross-section of a root excised from immature embryos bombarded with the *HvGlyT3* dsRNAi construct. In contrast to the cross-section obtained from the control, the cells are bigger (pink arrow) and collapse of epidermis is visible (orange arrow). The intensity of toluidine blue staining between the root sections at A and B is an artifact of reproduction.

A

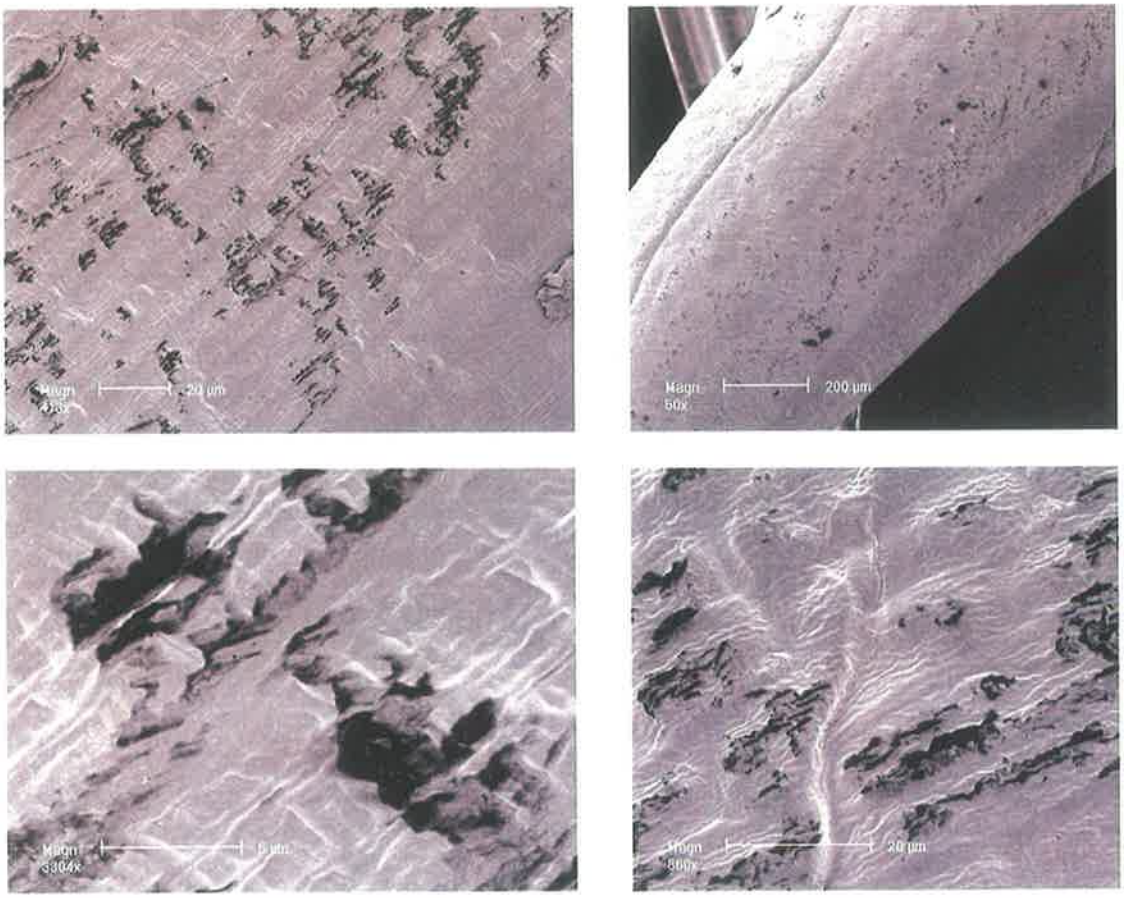
Magn
20 µm
Magn
200 µm
50x
Magn
5 µm
3304x
Magn
30 µm
800x

B

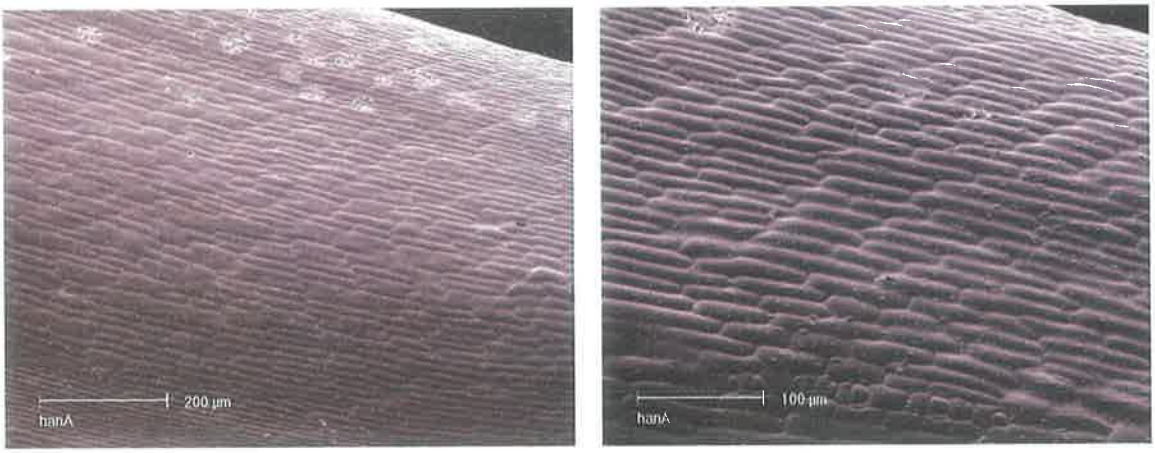
200 µm
hanA
100 µm
hanA

Figure 6.12 Scanning electron microscopy of whole coleoptiles subjected to dsRNAi silencing. A: Coleoptiles from immature embryos bombarded with the *HvGlyT3* RNAi construct. Elongating cells are damaged and stress fractures are as a result of RNAi silencing as opposed to panel B, which shows coleoptiles from immature embryos bombarded with the empty pHANNIBAL vector, which showing no similar phenotype.

6.4 DISCUSSION

An efficient way of provoking cellular RNA degradation, dsRNAi gene silencing, promises to be a useful tool for rapid functional analysis. Gene silencing through down-regulation of corresponding transcripts may lead to the production of a mutant phenotype. In the context of the cell wall, new phenotypes may emerge if interacting polysaccharides in the complex structure of the wall fail to establish a network (Bouton *et al.*, 2002; Iwai *et al.*, 2002) or silencing causes a failure in the biosynthesis of a particular polysaccharide, which contributes to the wall's overall structure, such as cellulose, and/or arabinoxylans in monocots, and xyloglucans in dicots (Burton *et al.*, 2000; Ryden *et al.*, 2003). These alterations may be detected and measured in a number of ways such as microscopy, transcript analysis, wall composition analysis, and wall extensibility analysis. Taking all these factors into consideration, it was decided to investigate the relationship of the barley cDNA clones from family GT34 with the biosynthesis of the cell wall, *via* RNAi silencing.

The dsRNAi constructs, both gene- and family-specific, were made and introduced into immature embryos using microprojectile bombardment. The germinated embryos were examined for phenotypic changes and analysed for transcript level alterations. Down-regulation of transcripts was observed. This was sometimes tissue-specific and in some cases deemed to be insignificant. In other cases the transcript level was up-regulated in particular tissues. The reason for the increase in transcript level may be due to either sampling error or compensatory effects in wounded cells, which were not silenced or in cells which were neither wounded nor silenced but which receive signals from damaged neibouring cells (Burton *et al.*, 2000).

Microprojectile bombardment is a random event and it is possible that many cells are not hit during the process. As a consequence of this, the pooled sample may under-represent the effect of RNAi silencing as transcripts from the majority of cells may mask any

effect. Furthermore, the target gene may be up-regulated in wounded cells rather than silenced ones as a physiological response to being damaged. These effects seen to be more prominent in relation to cell wall biosynthetic genes (our unpublished data). As a result, this up-regulation might be misinterpreted as an up-regulation within the silenced cells. In summary, the attempt to silence all family members using a conserved dsRNAi construct did not produce a spectacular effect. It is noteworthy to mention that only three members of family GT34 were investigated here and that other unknown members may be causing compensatory effects, which may mask a phenotype.

When the immature embryos were bombarded with a specic *HvGlyT3* dsRNAi construct a reproducible hairy root tip phenotype was observed. Unfortunately, the frequency of the phenotype was low (5% of the transformants) which did not allow us to analyse the wall composition in comparison with control roots. However, although wall composition analyses were not carried out, the phenotype observed suggested a level of weakening in the structure of root cell walls leading to the emergence of root hairs in an unusual place. Previously, Favery *et al.*, (2001) reported a class of *Arabidopsis* root hair mutants with defective cell walls called *Kojak* (*kjk*). They showed that the roots of the mutants split open at their tips. Further analysis showed that *KOJAK* encodes an *Arabidopsis* cellulose synthase-like protein, AtCslD3. The transcript analysis of *AtCslD3* showed a preference in epidermal cells, suggesting its involvement in the process of root outgrowth.

Root hairs emerge from trichoblasts, which are specialised subsets of epidermal cells, as a result of the involvement of a few genes that are sensitive to hormonal and environmental factors (Leavitt, 1904; Schiefelbein, 2000). As a result of local thinning and loosening of the trichoblasts' cell wall, initiation of root hair development begins by a bulging of the cell wall, followed by tip growth and polarised outgrowth of an elongated hair-like structure (Leavitt, 1904; Schnepf, 1986; Carol and Dolan, 2002; Cho and Cosgrove, 2002). In our case, by silencing an important cell wall biosynthetic enzyme, we artificially created a loosened cell wall at the root tip that undergoes bulging as a result of turgor pressure and other internal propulsive forces, so producing a root hair

at the tip of the root. This loosening, and the absence of cross-walls within the sub-epidermal layer (Figures 6.10 and 6.11), was further observed *via* light microscopy in root cortical cells showing the phenotype. Furthermore SEM micrographs showed an effect in the elongating coleoptile cells arising from the same immature embryo. These cells appeared damaged and stress fractures were visible. These phenotypic changes at the macro level in the form of the hairy root tip, and the micro level as changes in coleoptile cells, support the hypothesis that *HvGlyT3* is in fact involved in cell wall biosynthesis.

CHAPTER 7 SUMMARY AND FUTURE DIRECTIONS

7.1 SUMMARY OF EXPERIMENTAL RESULTS

The overall aim of this project was to characterise glycosyltransferases from barley (*Hordeum vulgare* L.) that are involved in the biosynthesis of important cell wall polysaccharides. The major barley cell wall polysaccharides, similar to the other members of Poaceae family, are cellulose, arabinoxylans, and (1→3,1→4)-β-D-glucans. The specific aim was to isolate and characterise α-arabinosyltransferases and glucuronosyltransferases, which are involved in the biosynthesis of barley arabinoxylans. Bearing in mind that the functional annotation of glycosyltransferases based on sequence homology is almost impossible due to their low percentage identity (Breton *et al.*, 2002), other approaches, including transcript analysis, investigating protein-protein interactions, heterologous expression and dsRNAi silencing were used as tools for the characterisation of the cDNA clones isolated.

Initially attempts were focused on isolating as many cDNA clones as possible, based on information from previously characterised wall glycosyltransferases from other plants (see Chapter 1). A number of techniques, such as cDNA library screening, BAC library screening, RACE3′-PCR, RACE5′-PCR and genomic walking were used to isolate the cDNA clones. Multiple sequence alignment of the isolated barley cDNAs belonging to family GT34, which includes *HvGlyT1*, *HvGlyT2*, *HvGlyT3* (Figure 2.19) showed a higher similarity towards the characterised (1→6)-α-xylosyltransferase from *Arabidopsis* (Faik *et al.*, 2002), suggesting a similar function in barley. The other partially cloned member of GT34, *HvGlyT5*, showed a higher similarity to the characterised (1→6)-α-galactosyltransferase from fenugreek (Edwards *et al.*, 1999). HvGlyT4 was a member of GT47 and showed a high homology to RGII glucuronosyltransferase from *Nicotiana plumbaginifolia* (Iwai *et al.*, 2002). There followed a detailed transcript analysis of the isolated cDNA clones in the hope of establishing a relationship between transcript levels and a particular wall component. That is, abundant transcripts for a given GT may well correspond to an abundant polysaccharide in the wall of a particular tissue. Transcript

analyses were performed using two different techniques; Q-PCR and *in silico* analysis of microarray data. The results implied putative roles for some of the isolated cDNA clones. *HvGlyT1* appeared at very low abundance and was specific to the root tip where the roots exude mucilage, a compound rich in xylogalacturonan (Willats *et al.*, 2004). The *HvGlyT1* is coordinately expressed with the barley *CslC3* gene and polyamine oxidase, a chemical involved in defense response mechanisms (Slocum and Furey, 1991). Based on this transcript and co-expression data, HvGlyT1 might be an α-xylosyltransferase involved in the biosynthesis of xylogalacturonan as a consituent of mucilage, which may play a defensive role in root structures against soil pathogens.

Transcript analysis of *HvGlyT2* using Q-PCR revealed that like *HvGlyT1* it is expressed at low levels and is specific to roots. A lack of detailed comparative information about root wall composition makes it difficult to pinpoint a putative role for HvGlyT2, but based on sequence alignment (Figure 2.19) it shows a high similarity to an α-xylosyltransferase (Faik *et al.*, 2002). In contrast, *HvGlyT3* transcripts are abundant in all tissues with a bias towards dividing and elongating cells in each tissue. A high transcript level may indicate an α-arabinosyltransferase activity for HvGlyT3, which fits well with the high transcript: high arabinoxylan assumption. However, based on sequence homology HvGlyT3 is close to a xyloglucan α-xylosyltransferase (Figure 2.19). Transcript analysis of *HvGlyT4* showed that it is highly abundant in all tissues with a bias towards mature tissues. A high percentage homology with NpGUT1 (Iwai *et al.*, 2002) and the presence of the same long amino acid motif may suggest a similar role as a pectin glucuronosyltransferase in barley (see Chapter 2). Overall, detailed transcript data provided us with some useful clues in relation to the function of the isolated cDNA clones. Other methods were subsequently used in attempts to confirm the roles proposed.

Recent studies have shown that proteins within the same metabolic pathway and with similar expression profiles are most likely to interact *in vivo* (Cobbe and Heck, 2004; Fraser *et al.*, 2004). Thus, assuming that HvGlyT3 was an arabinosyltransferase, and if

screening using this as bait *via* a yeast two-hybrid library reveals an interacting cellulose synthase-like gene, a xylan synthase role for the interacting Csl would be plausible. Thus, in order to try and find genes with related functions it was decided to investigate protein interactions for some of the barley cDNA clones, namely HvGlyT3, HvGlyT4 and a UDP-xylose epimerase, *via* yeast two hybrid screening against whole wheat grain and endosperm cDNA libraries. The UDP-xylose epimerase produces UDP-arabinose, which is an important donor substrate for arabinosyltransferase. HvGlyT3 was shown to interact with a serine carboxypeptidase, but this interaction has no obvious biological significance at this stage. The other two proteins, HvGlyT4 and HvUXEP, failed to interact strongly with any other proteins. Thus, the yeast two-hybrid screening of the wheat cDNA libraries did not provide conclusive results. The next step was to express the enzymes heterologously and to assay the activity of the expressed protein.

Although the best and most direct approach towards the functional analysis of enzymes is heterologous expression, the choice of expression system and the nature of the enzyme itself can make this a challenging task (see Chapter 6). Here, we started the heterologous expression in an *E. coli* system, but the expressed proteins were detected only in inclusion bodies. Other systems, including moss and mammalian cells, failed to express proteins. The only system which provided a partially soluble protein for any of the enzymes was the baculovirus/insect cell system. However, the expressed proteins failed to bind to a Ni-NTA affinity column and a crude extract of the insect cells was therefore used to assay the activity of the proteins. Protein activity was assayed by incubating radiolabelled donor molecules either with oligosaccharide acceptors or with 0.5 M neutral sugars in a suitable buffer and in the presence of divalent cations. The products were collected after removing unincorporated radioactivity, but the levels of incorporated radioactivity were low and revealed no convincing difference between the crude extracts containing the protein of interest and the crude extracts expressing another protein as a negative control. Thus, since heterologous expression failed to produce active and properly-folded protein in a number of systems, the next approach was to investigate HvGlyT function *via* gene silencing.

A frequently used approach in the functional analysis of genes and proteins includes loss-of-function methodologies in which specific genes are silenced in attempts to generate an obvious phenotype. In this project, dsRNAi was used to target transcripts of the three isolated cDNA clones available at the time, *HvGlyT1*, *HvGlyT2* and *HvGlyT3*. A number of constructs, based on a conserved region of all three sequences or on specific regions of *HvGlyT1*, *HvGlyT2* or *HvGlyT3*, produced a reduction in the amount of transcript in some of the tissues examined after particle bombardment. However, *HvGlyT3* was the only construct that produced a detectable phenotype, which was in the form of a hairy root tip and a damaged coleoptile structure. Although the phenotype was obvious, its frequency was not high enough to follow up the experiments with a more detailed transcript or cell wall composition analysis. Nevertheless, we managed to correlate the function of HvGlyT3 to cell wall biosynthesis through observing the loss of a cross-wall between dividing cells in the root sub-epidermal layer and the presence of bigger-sized cells in the cortical region of the roots showing the phenotype when compared with the negative control, which in turn indicated a loosening of the wall. It is believed that non-cellulosic cell wall components are synthesised in the Golgi apparatus, so we decided to produce specific antibodies to explore this aspect further (Appendix 1).

Partially hydrophilic and highly variable regions of HvGlyT1, HvGlyT2, and HvGlyT3 were chosen to be expressed in an *E. coli* system to produce the relevant antigens. Because of the high homology of HvGlyT4 to its paralogues, identifying a specific sequence region was impossible; therefore a partial sequence available at the time was used for expression in *E. coli*. The *E. coli* expression system failed to produce HvGlyT1 and HvGlyT2 antigen, while HvGlyT3 was expressed and purified in the soluble fraction and was used to raise a polyclonal antibodies in rabbit. Although the antibody could recognise the antigen, it failed to specifically detect the HvGlyT3 protein in extracts of barley tissues. Meanwhile, the HvGlyT4 antigen was purified from inclusion bodies and was used to produce a specific antibody, which recognised both antigen and the HvGlyT4 protein in barley protein extracts. This antibody was used to localise the native protein at

the cellular level where it recognised a protein that was most abundant in Golgi stacks, but that was present in minor amounts in the plasma membrane.

In summary, four full-length barley cDNA clones were isolated and located on the barley genome using wheat-barley addition lines. Detailed transcript analysis was performed in attempts to try and correlate transcript levels with the putative function of each gene, and protein-protein interactions were investigated to identify partner proteins. In order to directly assign functions to the cDNA clones, heterologous expression was attempted in number of systems to assay the activity of the expressed protein, but the results were inconclusive. A reverse genetics approach *via* dsRNAi silencing enabled us to correlate HvGlyT3 to cell wall biosynthesis and finally, we managed to localise one of the proteins (HvGlyT4) at the cellular level using a specific antibody.

7.2 FUTURE WORK

The functional analysis of the isolated cDNA clones was the main focus of this project. A definitive role for each gene is yet to be assigned but some alternative methods may be useful in the fulfilment of this goal.

- *Heterologous expression*. By using other systems such as *Drosophila* (Liepman *et al.*, 2005) and vascular plants as the host (Voinnet *et al.*, 2003; Komarnytsky *et al.*, 2004), we may be able to provide the right folding and proper post-translational modification environment for the expression of GT proteins.
- *Immunoprecipitation*. In our case, with the availability of an HvGlyT4 specific antibody it may be possible to affinity purify the native barley protein from plant extracts and use this protein for measuring enzyme activity.
- *Post-transcriptional gene silencing*. PTGS can be triggered using viral vectors (Baulcombe, 1999), which stimulate the dsRNAi (Waterhouse and Helliwell, 2003) pathway inducing gene silencing in a process called virus-induced gene silencing (VIGS). Due to Australian quarantine constraints (see Chapter 6), it was not possible to use VIGS in monocots for this project. Since dsRNAi silencing of genes using both transient and stable transformation has yielded valuable information elsewhere (Fire *et al.*, 1998; Wesley *et al.*, 2004), in this project a transient method was used to evaluate the effect of targeted gene silencing within barley during early seedling growth. This could be followed up with stable transformation experiments to investigate the overall effect on growth and at a whole plant level.

  However, since there is often a high level of gene redundancy (37% of *Arabidopsis* genes belong to families with five or more members, *Arabidopsis* Genome Initiative, 2000), silencing of one family member might be masked by functionally redundant gene homologues. Thus, generating simultaneous double

and triple knockouts using either biolistics or *via* crossing individual insertional mutants into the same background may help us to overcome such effects. The gene silencing approach could be followed up with cell wall analysis to investigate any changes in the composition of wall polysaccharides. Such investigations establish a link between gene function and alterations in the wall composition. Examples of these experiments are described in Chapter 1.

- *Use of other loss-of-function methodologies.* The search for gene-specific mutants in lines generated *via* TILLING (see section 1.3.4, Henikoff *et al.*, 2004) or T-DNA insertion, *i.e.* Salk lines (see section 1.3.4, http://signal.salk.edu/), or Delete-a-gene mutants (Li *et al.*, 2002; Li and Zhang, 2002) provide a powerful reverse genetic procedure for the definition of gene function. Random deletion libraries are made by treating seeds with fast neutrons, followed by PCR screening in the Delete-a-gene methodology. Mutant lines produce shorter amplified fragments compared to the wild type lines when analysed *via* PCR, suggesting a part of the gene has been removed (Li *et al.*, 2002; Li and Zhang, 2002). This approach may also be used to remove tandem arrays of duplicated genes which have a similar function to produce lines that are true nulls (Li *et al.*, 2002). After such treatments, the phenotype can be reversed *via* complementation studies of mutant lines.
- *Gain-of-function.* Overexpression of the cDNA clones, preferentially in places where these cDNAs are not normally expressed, to produce ectopic wall components may be a useful approach. For example, *HvGlyT1* and *HvGlyT2* are two cDNA clones that are root specific. Overexpression of these cDNA clones in other barley tissues, through the use of tissue-specific promoters, may provoke some informative changes in cell wall architecture. Moreover, the barley GTs could be overexpressed in other systems such as *Arabidopsis*, tobacco, yeast, *Drosophila* and a range of mammalian cell lines, which would then facilitate *in vitro* assays of protein activity.

7.3 CONCLUDING REMARKS

As mentioned earlier this project's scope was to define a functional role for the isolated cDNA clones with the hope of characterising either an arabinosyltransferase or a glucuronosyltransferase involved in the biosynthesis of barley glucuronoarabinoxylans. Attempts made in the analysis of these genes did not provide a definitive function, but some tentative conclusions were obtained through the use of multiple sequence alignments, transcript analysis, dsRNAi gene silencing, and immunolocalisation. These results suggest that the identities of the cDNAs may be a xylosyltransferase, an arabinosyltransferase, and a glucuronosyltransferase for HvGlyT1, HvGlyT3 and HvGlyT4, respectively.

APPENDIX 1

A. INTRODUCTION

Despite the isolation of some cell wall polysaccharide biosynthetic glycosyltransferase genes (Pear *et al.*, 1996; Arioli *et al.*, 1998; Edwards *et al.*, 1999; Perrin *et al.*, 1999; Faik *et al.*, 2000; Bouton *et al.*, 2002; Faik *et al.*, 2002; Iwai *et al.*, 2002; Madson *et al.*, 2003; Burton *et al.*, 2004; Edwards *et al.*, 2004), information regarding the precise sub-cellular location of the enzymes that they encode is still not available. Knowledge about the sub-cellular location of enzymes either directly involved in cell wall biosynthesis such as GTs, or indirectly such as sugar nucleotide interconverting and transportering enzymes (Baldwin *et al.*, 2001), may shed light on our understanding of the relationships between these proteins. It may also point to previously uncharacterised mechanisms in polysaccharide biosynthesis. For example, Gardiner *et al.* (2003) proposed a model for cellulose microfibril assembly in developing xylem based on the use of CesA-specific antibodies coupled to green fluorescent protein (GFP), which showed that three CesA proteins are likely to be present in each multi-enzyme complex.

Some biosynthesis of cell wall polysaccharides, and the addition of oligosaccharides to cell wall proteins, occurs in the Golgi apparatus (Neumann *et al.*, 2003). Plant cell Golgi contain individual independent membraneous stacks (Figure 4.1) containing different numbers of cisternae depending on cell type, developmental stage, physiological condition, the functional requirement of a cell, and plant species (Staehelin and Moore, 1995; Andreeva *et al.*, 1998). Each Golgi stack contains many enzymes, including glycosyltransferases, the products of which are sorted and assembled in the *trans*-Golgi network (Staehelin and Moore, 1995). Wee *et al.* (1998) showed that Golgi retention signals, predicted to be embedded in the TMH of the glycosyltransferase, are conserved in plants and mammals since a heterologously expressed rat sialyltransferase was successfully processed in the Golgi of transgenic plants. One of the earliest attempts to demonstrate the involvement of Golgi enzymes in cell wall biosynthesis was radioautographic studies of wheat root tips incubated with D-[1- or 6-^{3}H] glucose

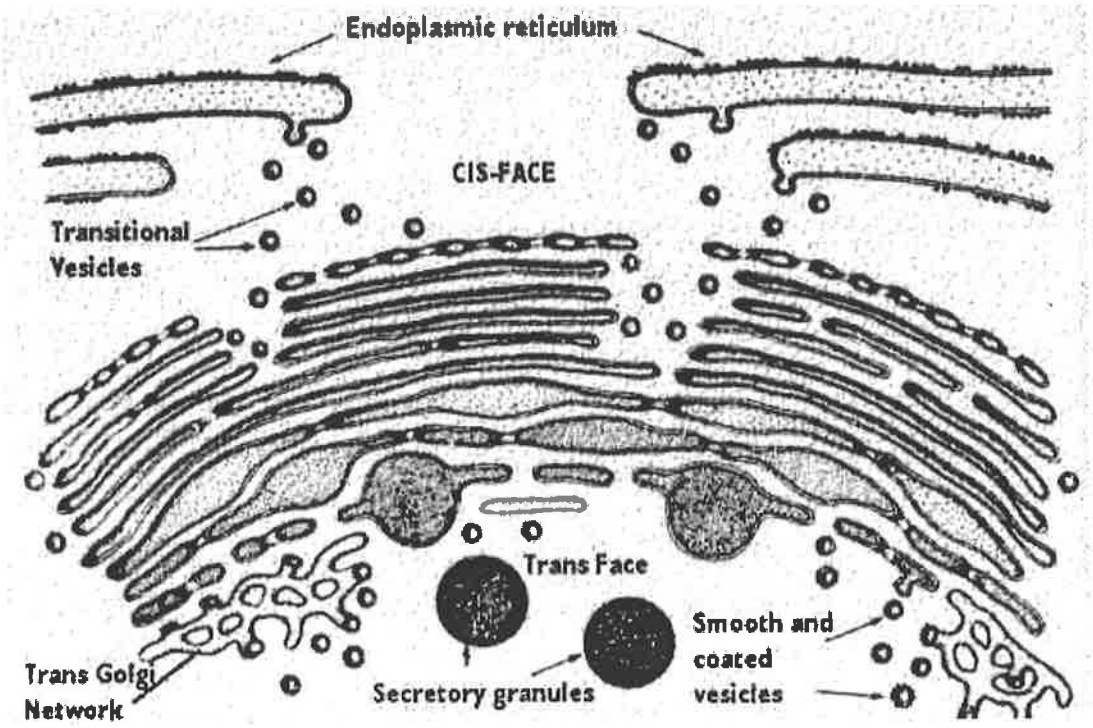

Figure a.1 Golgi apparatus. This schematic picture depicts the interface between the endoplasmic reticulum (ER) and the Golgi stacks. The Golgi apparatus is involved in the secretory pathway of many proteins and is made up of a number of membraneous stacks, which comprise the *cis*, medial, *trans* and *trans*-Golgi networks. The picture is reproduced with permission from the http://cellbio.utmb.edu/cellbio/GOLGI.HTM website.

(Northcote and Pickett-Heaps, 1966). The radiolabeled glucose was formed in the Golgi apparatus of the root-cap cells and moved through the cytoplasm and incorporated into the cell wall. This idea that plant non-cellulosic cell wall polysaccharides are synthesised within the Golgi was further investigated by the immunogold detection of polysaccharides using polysaccharide-specific antibodies, including those for the xyloglucan (XG) backbone (Moore *et al.*, 1991), rhamnogalacturonan I (RG I) (Lynch and Staehelin, 1992), the fucosyl residue of XG (Zhang and Staehelin, 1992), xylan (Northcote *et al.*, 1989), and pectin (Vicre *et al.*, 1998). Lynch and Staehelin (1992) demonstrated that during cell differentiation in the clover root tip, the detection of polysaccharides moves between Golgi cisternae where they shift from the *cis*- and medial Golgi to the *trans*-Golgi network (TGN). This suggests a reorganisation of the Golgi both structurally and functionally depending on the cell type and function. These alterations, such as tailoring the Golgi stacks and TGN, occur to meet the specific synthetic demands of each cell type as a result of the cell being in a different secretary state (Lynch and Staehelin, 1992). For example peripheral root cap cells, synthesising large amount of mucilage, contain larger Golgi stacks with extensive TGN. In contrast, the actively dividing meristematic cells contain smaller Golgi stacks with a lightly staining TGN.

The maturation of polysaccharides can also be described with the use of specific antibodies. For example, it was illustrated that the glucosyl backbone of xyloglucan is synthesised in the *trans*-cisternae whilst the final constituent, a fucosyl residue, is added partly in the *trans*-cisternae and partly in the *trans*-Golgi network (Zhang and Staehelin, 1992) and the XG is finally packaged to ship to the cell wall in the TGN (Driouich *et al.*, 1993). Zhang and Staehelin (1992) described the steps involved in the construction of RG I as follows; backbone assembly occurs in the *cis* and medial cisternae, methylesterification of the carboxyl groups takes place mostly in the medial cisternae, and arabinosylation occurs in the *trans*-cisternae. Based on reports cited above, it appears that the polysaccharides obtained their final structure as they moved towards the cell wall in a sub-compartment of the Golgi apparatus in a *cis*-to-*trans* direction, which

has been called the sequential organisation model (Staehelin and Moore, 1995; Breton *et al.*, 2001). However, it is becoming evident that most glycosyltransferases have an overlapping distribution across the Golgi and that their sub-compartmentation depends on the specific cell type, which in turn may suggest why different cell types differ in their glycosylation patterns (Colley, 1997). Differences in the membranes' composition, cisternal pH and ion concentration, and cytoskeletal proteins from cell to cell are amongst the factors which may govern this sub-compartmentation in different cells (Colley, 1997).

The membranes to which some proteins are targeted have been revealed for a few glycosyltransferases and glycan synthases. Some HvCslCs, HvCslD1 and HvCslD2 (Medhurst, A.; Dewivany, F.; Newbigin, E.; Wilson, S.; and Bacic, T.; unpublished data) are located in vesicles near the plasmamembrane and in the case of CesAs (Kimura *et al.*, 1999), they are restricted to the plasmamembrane. Through sub-cellular fractionation it has been shown that pectin galacturonosyltransferase (Sterling *et al.*, 2001) and arabinan arabinosyltransferase (Nunan and Scheller, 2003) are located in the Golgi fraction. Sub-cellular fractionation requires the preparation of enriched Golgi and other membranous cell fractions involved in the secretory pathways of plant cells (Gregory *et al.*, 2002). Purification of a plant Golgi fraction is difficult, often resulting in low yields or contamination due to copurification with other membranes. This has led to the use of other approaches to overcome these inherent problems, including immunolocation with the use of transmission electron microscopy (TEM) (Dhugga *et al.*, 1997; Wee *et al.*, 1998; Bolwell, 2000; Gregory *et al.*, 2002; Follet-Gueye *et al.*, 2003; Pagny *et al.*, 2003), and heterologous expression combined with epitope tagging followed by visualisation under either the confocal microscope or the TEM (Wee *et al.*, 1998; Follet-Gueye *et al.*, 2003; Pagny *et al.*, 2003). For example, Follet-Gueye *et al.* (2003) demonstrated the location of (1→2)-β-xylosyltransferase, specific for the glycosylation of glycoproteins, to be in the medial cisternae of tobacco BY-2 cells.

In this Appendix, the location of the enzymes in the cell is explored with the use of immunogold labeling and TEM visualisation.

B. MATERIALS AND METHODS

B.1 Materials

PCR primers were designed using the Netprimer program available at (http://www.premierbiosoft.com/netprimer/netprlaunch/netprlaunch.html) and synthesised by Geneworks (Adelaide, Australia). The dNTPs were from FisherBiotech (West Perth, WA, Australia). Elongase enzyme mix and T4 DNA Ligase were purchased from Invitrogen (Carlsbad, CA, USA). QIAquick gel extraction kit, Ni-NTA spin columns and Ni-NTA agarose were bought from QIAGEN Pty Ltd (Clifton Hill, Vic, Australia). Agarose was obtained from Becton Dickinson (Sparks, MD, USA). Restriction enzymes and BSA were purchased from New England Biolabs (Beverly, MA, USA). The pET3a-HT was generously donated by Dr. Helen Healy (University of Adelaide, SA, Australia). Peptides were obtained from Auspep (Melbourne, Vic, Australia). BD71 dye was purchased from Aldrich (Milwaukee, WI, USA). Tween 20, sodium bicarbonate, acetonitrile, trifluoroacetic acid, citric acid, ethanol, acetone, glycerol, imidazole, TEMED, SDS, glycine, acetic acid, methanol, lead citrate, Na_2HPO_4, NaH_2PO_4, KH_2PO_4, urea, imidazole, KCl and NaCl were bought from Merck Pty Ltd (Kilsyth, VIC, Australia). Tris, *p*-coumaric acid, uranyl acetate, IPTG, ampicillin, chloramphenicol, bromophenol blue and Coomassie Brilliant Blue R were obtained from SIGMA-Aldrich (St Louis, MO, USA). Coomassie protein assay reagent was obtained from Pierce (Rockford, Illinois, USA). *E. coli* strains DH5-α and BL-21 were from Stratagene (La Jolla, CA, USA). Luminol was purchased from ICN Biochemicals Inc. (SC, Ohio, USA). H_2O_2 was obtained from BDH chemicals (Vic, Australia). Yeast extract, tryptone and agar were bought from Becton Dickinson (Sparks, MD, USA). Instant skim milk was purchased from Diploma (New Zealand). Nitrocellulose membrane was obtained from Osmonics (MA, USA). Fuji medical X-ray film was supplied by the Fuji Photo Film Co. (Tokyo, Japan). Acrylamide (40%)/Bis solution (29:1) and precision plus protein™ standards were purchased from BioRad (USA). Western blue stabilised reagent was obtained from Promega (Madison, WI, USA). Polyclonal antibodies were made at the IMVS (Adelaide, SA, Australia). Protein A sepharose, electrophoresis power supply ECPS

3000/150, FPLC and LMW electrophoresis calibration kit were supplied by Amersham Biosciences Pty Ltd (Castle Hill, NSW, Australia). Transmission electron microscopy was carried out on a Philips BioTwin CM120 TEM, which was from Nanotechnology Systems Pty Ltd (Vic, Australia). Western analysis was performed using a Semi-dry blotter EBU-4000, which was supplied by CBS Scientific Co (CA, USA). Sonifier B-12 was supplied by Branson Sonic Power Company (Danbury, CT, USA). Mighty Smart II (SDS-PAGE electrophoresis tank) was supplied by Hoefer Scientific Instruments (San Francisco, USA). HPLC series II 1090 and amino acid sequencer G1000A were purchased from Hewlett-Packard (Palo Alto, CA, USA). Type A brass freezer hats were purchased from ProSciTech (Thuringowa, Qld, Australia). An EM High Pressure Freezer, an Ultracut R microtome and an EM automated freezer substitution unit were obtained from Leica (Vienna, Austria). Lowicryl HM20 low temperature resin was bought from Polysciences (Warrington, PA, USA). Colloidal Gold-Affinipure Goat Anti-Mouse IgG was supplied by Jackson ImmunoResearch Laboratories (PA, USA). Formvar coated 200 mesh gold grids were purchased from Holgate Scientific Pty Ltd (Terrigal, NSW, Australia). Gelatin Capsules were obtained from Electron Microscopy Sciences (PA, USA).

B.2 Prediction of antigenicity index

The method of Hopp and Woods (1981) was used to determine the most probable antigenic segment of protein molecules. This method (antigenicity plot) is based on the hydrophilicity scale that is publicly available at http://bioinformatics.org/JaMBW /3/1/7/. Antigenicity was sought with respect to two factors, the first being targeted to the hyper-variable region of the protein to enable differentiation between gene family members, and the other being a minimum fragment size of 12 kDa to avoid protein degradation during expression in either *E. coli* or mammalian cells. Also, peptide sequences were designed based on the most hydrophilic segment of the hyper-variable region to produce monoclonal antibodies. This region of the protein sequence has to contain charged amino acid residues and lack methionine and proline in its sequence. Prior to the synthesis of

peptides, the sequences were used as a query to search the public protein databases in order to confirm the uniqueness of the sequence.

B.3 Heterologous expression in the bacterial system for antigen production

The glycosyltransferases were PCR amplified as described in section 5.2.2 and cloned into the pET vector as described in section 5.2.3. Heterologous expression was carried out as described in section 5.2.3 and the protein extracts were separated on a Polyacrylamide gel as described in section 5.2.4. The expressed protein was affinity purified as described in section 5.2.6.

B.4 HPLC Purification of recombinant protein

A 5 µl aliquot of Ni-NTA eluate was further purified by reverse phase high performance liquid chromatography (RP-HPLC). The two elution solutions were 0.05% (v/v) trifluoroacetic acid (solution A) and 0.04% (v/v) trifluoroacetic acid in 70% (v/v) acetonitrile (solution B). The fraction collected from the highest peak was subjected to amino acid sequencing using an amino acid sequencer model G1000A. The steps involved in the confirmation of the protein sequence were carried out with the help of Mr. Jelle Lahnstein (University of Adelaide, SA, Australia).

B.5 Affinity batch purification of expressed protein

If the protein sequence was confirmed to be correct, the expression of the protein was scaled up to a 250 ml TB culture. Either soluble or insoluble fractions were prepared in 25 ml of a suitable buffer as described in section 4.2.8. Solutions used in the purification of the expressed protein were as described in section 4.2.8. For batch purification of the 6 × His-tagged expressed protein, Ni-NTA agarose resin (1 ml slurry resin for each 25

ml) was used. The resin was equilibrated with a suitable buffer, centrifuged at 2000 rpm for 5 min, and the supernatant was removed. The protein fraction was added to the resin and mixed in a rotary shaker at 200 rpm for 1 h. The slurry was centrifuged at 2000 rpm for 5 min and the supernatant was collected. The resin was washed a further 3 times with 4 ml of wash buffer followed by centrifugation at 2000 rpm for 5 min each. The 6 × His-tagged protein was eluted 5 times by the addition of 0.5 ml elution buffer followed by centrifugation at 2000 rpm for 5 min each. The fraction obtained was checked using SDS-PAGE prior to antibody production.

B.6 Antibody production

Three dilutions of antigen containing 0.5 mg protein each were prepared and sent to the IMVS Veterinary Services Division (Adelaide, SA, Australia) to raise an antibody in a rabbit. The rabbit was pre-bled prior to injection of the first dose of antigen. The injection was repeated three times at three week intervals and prior to the third injection, the rabbit was bled to test the specificity of the antibody. The test bleed was used against the antigen and a plant tissue extract and if a satisfactory result was obtained, the rabbit was injected for the third time and then bled to collect the antibody. Also, synthetic peptides were used to immunise mice to prepare monoclonal antibodies in cases where the preliminary polyclonal antibody reaction against the plant protein extract indicated some cross-reactivity. Dr. Alfio Comis (Plant Genomic Centre, University of Adelaide, Australia) performed all the steps involved in raising monoclonal antibodies in mice.

B.7 Total protein extraction from plant tissue

Total protein from plant tissues (1 g of both root tip, representative of dividing and elongating cells, and leaf tip, representative of mature and less metabolically active cells) were extracted as described in section 5.2.12.

B.8 Western analysis to test antibody specificity

Initially, the antigen was dot-blotted onto an Osmonics nitrocellulose membrane and all the probing steps were the same as described in section 5.2.5. At the same time, the pre-bleed serum was used as a negative control against the antigen. A plant protein extract was separated on an SDS-PAGE gel as described in section 5.2.4 and Western analysis was performed as described in section 5.2.5.

B.9 Antibody purification using protein A sepharose

Protein A is derived from a strain of *Staphylococcus aureus*, which binds to the Fc region of immunoglobulins (IgGs) through an interaction with the heavy chain of the antibody. Therefore, protein A immobilised with sepharose is capable of binding to IgG molecules, thus removing the impurities present in animal serum while retaining the IgGs. Here, a protein A sepharose column was attached to a fast performance liquid chromatography (FPLC) instrument and equilibrated with binding buffer (0.1 M Na_2HPO_4 buffer, pH 7.0). The antibody was diluted with the binding buffer (1:4) and the diluted antibody and all other solutions passed through a 0.45 µm filter to avoid clogging the column. The column was loaded with the diluted antibody *via* FPLC. The bound IgGs were eluted from the column with elution buffer (0.1 M citric acid buffer, pH 4.0) and collected in Eppendorf tubes containing 1 M Tris-HCl buffer, pH 9.0 (60 µl) to adjust the pH to 7.0. The column was rinsed with 20% (v/v) ethanol and stored at 4°C for future use.

B.10 Transmission electron microscopy (TEM)

TEM was performed on barley cell suspension sections (cv. Schooner) by Dr. Sarah Wilson (Department of Botany, University of Melbourne).

C. RESULTS

C.1 Heterologous expression of HvGlyT1, HvGlyT2, HvGlyT3 and HvGlyT4

An antigenicity plot was used to determine the most probable antigenic segments of HvGlyT1 (99 amino acid residues), HvGlyT2 (105 amino acid residues) and HvGlyT3 (108 amino acid residues) which met the requirements outlined in B2. For HvGlyT4 (344 amino acid residues), the highly variable region could not be determined and therefore the presumed full-length sequence at the time was amplified. Primers were designed (Table a.1) and the fragments were amplified using Elongase as described in section B.3. The PCR products (Figure a.2) were gel purified, digested and ligated into the pET expression vector. The ligation mixtures were used to transform DH5α *E. coli* cells. Plasmids were extracted from the colonies and the insertions of the fragments into pET3a-HT expression vector were checked by restriction enzyme digest and also *via* DNA sequencing using T7 and T7-terminator primers as described in section 5.2.2. The vectors containing correctly in-frame *HvGlyT1*, *HvGlyT2*, *HvGlyT3* and *HvGlyT4* partial fragments were transformed into BL21 *E. coli* cells for heterologous expression. The expected expressed protein sizes for HvGlyT1-3 and HvGlyT4 were 12-13 kDa and 41 kDa, respectively. Expression fractions were separated on SDS-PAGE gels (Figures a.3 and a.4, Panel A). HvGlyT1 and HvGlyT2 did not express under normal expression conditions, or under conditions modified by changing the concentration of IPTG (0.005, 0.05, 0.5 and 1 mM) and lowering the temperature to 4°C for 24 h after induction. HvGlyT3 was expressed in the soluble fraction (Figure a.3) while HvGlyT4 was located in inclusion bodies as part of the insoluble fraction (Figure a.4, Panel A). Both the soluble (*i.e.* HvGlyT3) and insoluble (*i.e.* HvGlyT4) fractions were passed through a Ni-NTA column and the relative purity of the bound proteins was checked on an SDS-PAGE gel (Figures a.3 and a.4, Panel A). Moreover, in order to make sure that there were no other minor proteins in the Ni-NTA purified fractions, an aliquot of these fractions were separated through RP-HPLC. The profile obtained showed the relative purity of the

Gene	Primer name	Primer sequence
HvGlyT1	ABFG	5′ CATCAACCATATGGCCTTCTCCGGCGAC 3′
	ABRG	5′ GCAGGGCCGCGGCGACGACCCGGTCAC 3′
HvGlyT2	ABF2	5′ CCGATCATCCATATGGTCCTGTTCATCTTC 3′
	ABR2	5′ CACGAGCACCCGCGGCCGCCCCGGCGC 3′
HvGlyT3	ABF3	5′ TCCTGGTCCATATGGGTACAATTGGGCTC 3′
	ABR3	5′ AAGCAGGATCCGCGGCTTGCCGCCCG 3′
HvGlyT4	pETGUT-F1	5′ TGCCTTAATCATATGTTTGCTGCGGAAATA 3′
	pETGUT-R1	5′ GATGGACCGCGGAACTAACCACGGTTTCAGATCTCC 3′

Table a.1 Primers for amplification of *HvGlyT1*, *HvGlyT2*, *HvGlyT3* and *HvGlyT4* partial fragments. The engineered restriction enzyme sites are underlined (CATATG = *Nde*I and CCGCGG = *Sac*II).

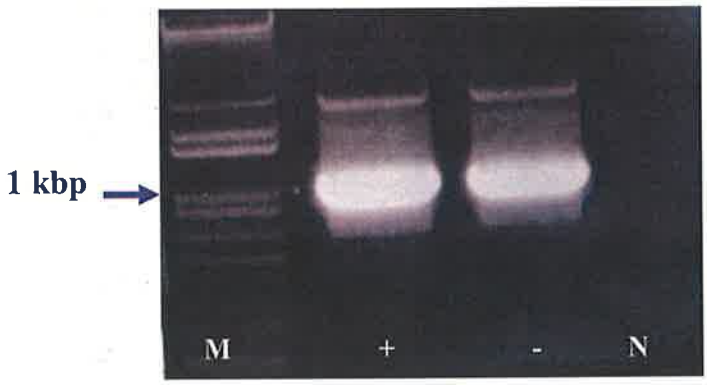

Figure a.2 Agarose gel electrophoresis of the PCR amplified *HvGlyT4* fragment. M = marker, + = presence of DMSO in the PCR, - = absence of DMSO in the PCR, N = negative control

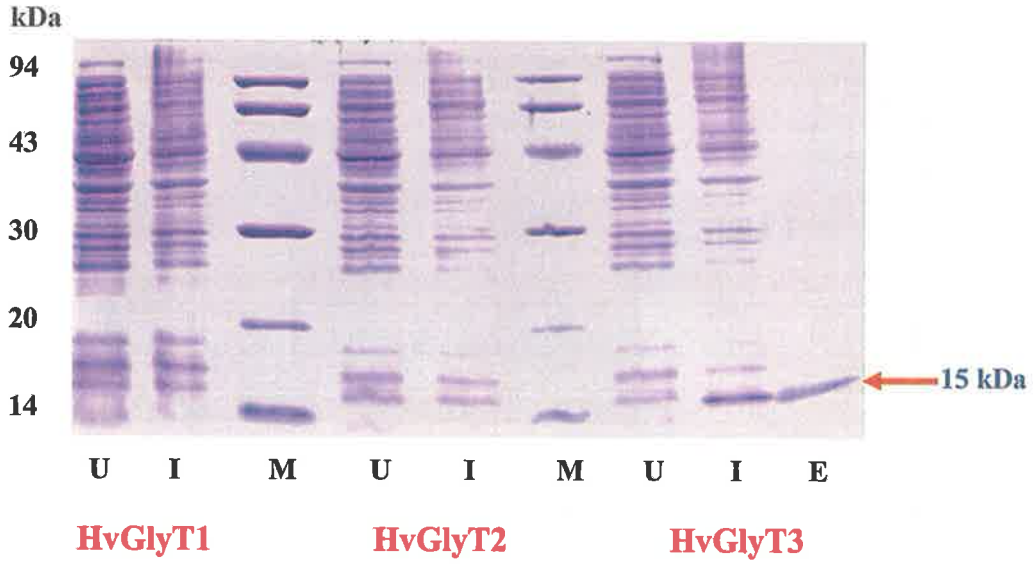

Figure a.3 SDS-PAGE of *E. coli* expression products by BL21 strains transformed with HvGlyT1, HvGlyT2, and HvGlyT3 expression plasmids. No expression was seen for HvGlyT1 and HvGlyT2, but a putative 15 kDa HvGlyT3 protein was expressed and later purified using a Ni-NTA affinity column. U = uninduced, I = induced, M = marker, E = eluate from affinity chromatography. Arrow indicates the expressed and purified protein bands.

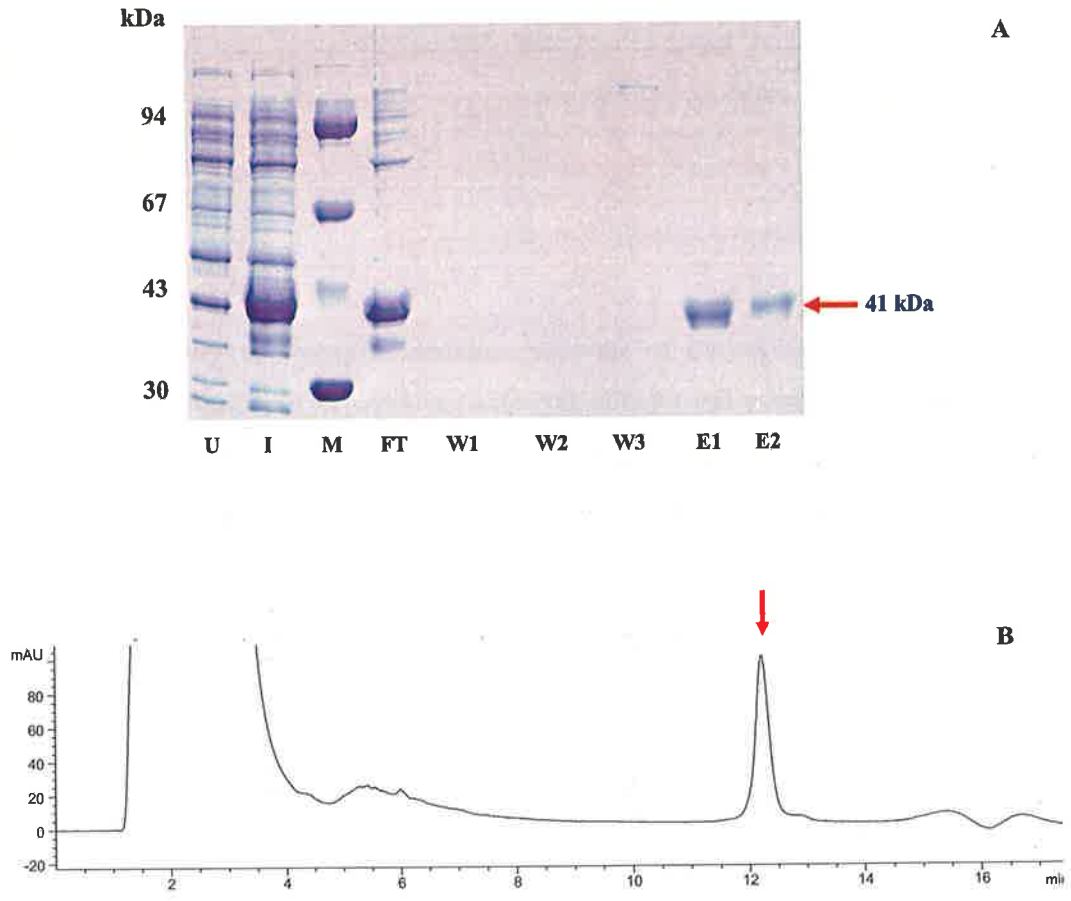

Figure a.4 SDS-PAGE of *HvGlyT4* in *E. coli* strain BL21 and RP-HPLC purification of the elution fraction obtained from the Ni-NTA column containing expressed HvGlyT4. **A**: SDS-PAGE gel, U = uninduced, I = induced, M = protein standard, FT = column flow through, W1-3 = three stepwise washes, E1-2 = two stepwise elutions. Arrow indicates the expressed and purified protein bands. **B**: A sharp clean peak, as indicated by the red arrow, is indicative of the purity of the expressed protein.

expressed protein (Figure a.4, Panel B). The same steps were repeated after scaling up the culture for batch purification of the expressed protein. The pure protein was aliquoted in three tubes of a similar concentration and sent to the IMVS (Adelaide, SA, Australia) for antibody production.

C.2 Antibody production in mouse

Following the failure to produce suitable antigens for HvGlyT1 and HvGlyT2, the peptide sequences (HvGlyT1: Arg-Glu-Iso-Arg-Ser-Asp-Ser-Asp-Pro-Asp-Glu-Gly-Asp-Gln-Cys; HvGlyT2: Arg-Ile-Arg-Ile-Glu-Tyr-Ala-Arg-Arg-Asp-Gly-Asp-Arg-Asp-Cys) were selected, synthesised and used for mouse immunisation. After three injections, the mice were bled to test the specificity of the antibody against both the peptide *via* an ELISA test and root protein extract *via* Western analysis, since this is the tissue where *HvGlyT1* and *HvGlyT2* are most highly transcribed (see Chapter 3). The antibodies showed a strong reaction against the peptides, but failed to recognise a protein band with the predicted size (50 kDa) or bigger in the barley root protein extract, indicating their inadequacy for further use in detecting HvGlyT1 and HvGlyT2.

C.3 Testing the specificity of the antibodies

Polyclonal antibodies for HvGlyT3 and HvGlyT4 were raised in rabbit and purified from blood serum using a protein A sepharose column attached to an FPLC. The relatively pure IgGs containing HvGlyT3 and HvGlyT4 antibodies were used to determine their specificities against both the antigen and barley protein extracts. The antibody raised against the HvGlyT3 antigen recognised itself but not the endogenous protein in plant extracts, even though the transcript data (Chapter 3) showed that *HvGlyT3* is a highly abundant in all tissues examined

Whereas, the HvGlyT4 antibody recognised both the antigen and a single protein (55 kDa) in the barley extracts on the Western membrane (Figure a.5). The size obtained is bigger than the predicted size (41 kDa), and this higher value might be as a result of post translational modifications. Western analysis demonstrated the presence of HvGlyT4 in both protein fractions extracted with or without detergent (10% SDS). When the antibody was used against the HvGlyT3 antigen, no cross-reactivity was observed (Figure a.5).

C.4 Immunocytochemical localisation of HvGlyT4 in barley cell suspension culture

To investigate the membraneous location of the HvGlyT4 protein the purified antibody was used for immunocytochemical staining of sections of a barley cell suspension culture (Figure a.6). The antibody labeled all the Golgi sacs present in a single cell but not specifically a certain cisternae (Figure a.6, Panel A). Furthermore, the antibody recognised minor amounts of protein at the plasmamembrane.

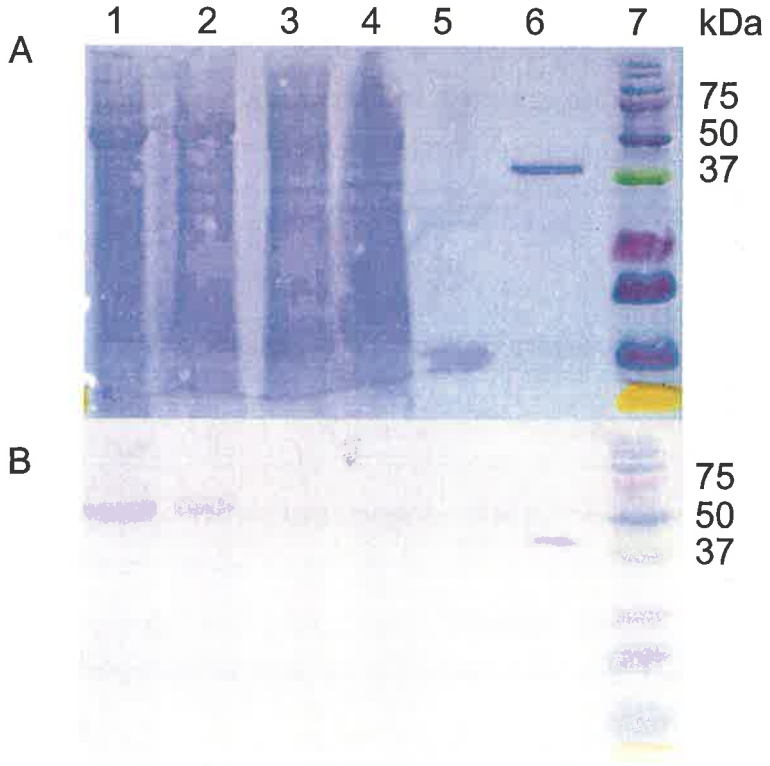

Figure a.5 Western analysis, using the protein A sepharose purified HvGlyT4 antibody against 7 d old barley leaf protein extracts and the HvGlyT3 and HvGlyT4 antigens. **A**: SDS-PAGE gel followed by transferring onto a membrane and staining with DB71 to show total protein. **B**: Western analysis using the HvGlyT4 antibody. Lane 1 = barley leaf tip, Lane 2 = barley leaf tip + 10% SDS, Lane 3 = barley root tip, Lane 4 = barley root tip + 10% SDS, Lane 5 = HvGlyT3 antigen, Lane 6 = HvGlyT4 antigen, Lane 7 = Marker.

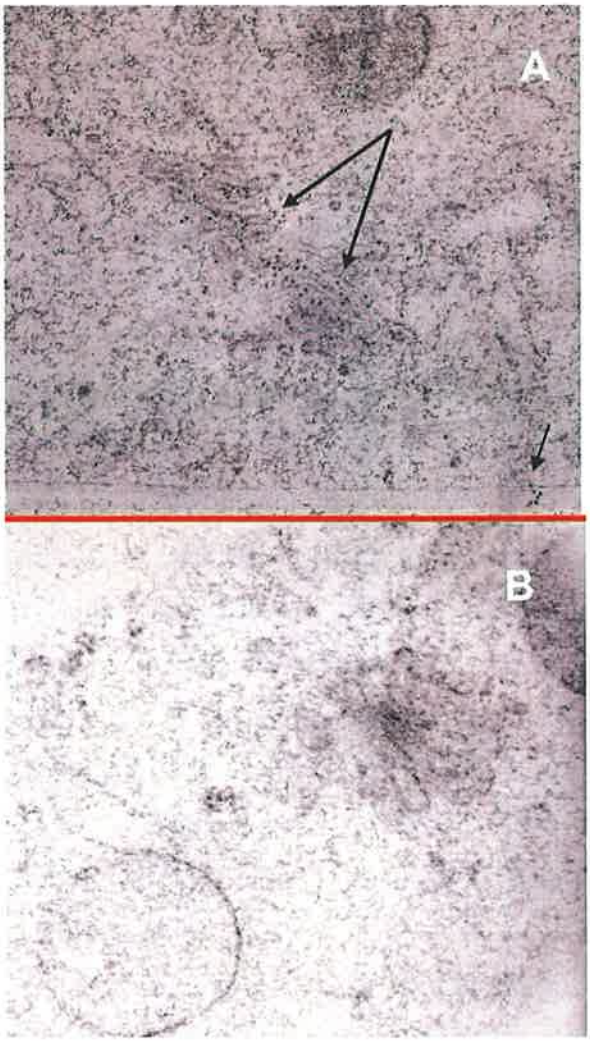

Figure a.6 Electron micrographs of barley cell suspension culture probed with immunogold labeled HvGlyT4 antibody. **A**: The arrows indicate the Golgi stacks and the plasmamembrane, when sections were treated with the HvGlyT4 antibody. **B**: No labeling of the cell section was seen when only the secondary antibody was used as probe.

D. DISCUSSION

To locate proteins and carbohydrates using specific antibodies can provide an informative view of the ongoing events in a cell. This in turn opens new doors in our understanding of the pathways involved in the construction of certain biomolecules and in our case, cell wall polysaccharides. As discussed earlier, there is evidence that the biosynthesis of cell wall polysaccharides, other than cellulose, occurs in Golgi stacks. These data were obtained from the location of the glycosylated products with the use of polysaccharide specific antibodies (Northcote *et al.*, 1989; Moore *et al.*, 1991; Lynch and Staehelin, 1992; Zhang and Staehelin, 1992; Vicre *et al.*, 1998), the biochemical fractionation of the cell compartments followed by the evaluation of the activity of particular glycosyltransferases within each fraction (Sterling *et al.*, 2001; Nunan and Scheller, 2003), developing glycosyltransferase specific antibodies, followed by immunogold localisation of the enzymes within cells and tissues (Dhugga *et al.*, 1997; Kimura *et al.*, 1999; Bolwell, 2000; Gregory *et al.*, 2002) and finally the detection of epitope tagged heterologously expressed glycosyltransferases using epitope-specific antibodies (Follet-Gueye *et al.*, 2003; Pagny *et al.*, 2003). In this Chapter, attempts were focused on generating gene-specific antibodies for the barley glycosyltransferases either by heterologously expressing them in *E. coli* or by using synthetic oligopeptides to develop polyclonal or monoclonal antibodies, respectively.

The results showed that the expression of HvGlyT1 and HvGlyT2 fragments in *E. coli* failed to produce any protein and when selected oligopeptides were used to raise antibodies in mice, the final antisera failed to recognise a specific protein band in barley tissue extracts. In the meantime, successful HvGlyT3 and HvGlyT4 expression in *E. coli* led to the generation of polyclonal antibodies. The HvGlyT3 specific antibody managed to recognise the antigen but did not bind to any components in the barley protein extract, whereas the HvGlyT4 antibody specifically bound to both the antigen and a protein

bigger than the predicted size in barley tissue extracts. The detection of a single protein with higher size may indicate the post translational modification of this enzyme.

The data obtained from Western analysis for HvGlyT4 is consistent with transcript data for this gene (see Chapter 3). As shown earlier, HvGlyT4 is highly abundant in the leaf tip whereas the transcript level in the root tip is much lower (Figure 3.6, Panel E). Furthermore, as discussed earlier (see Chapter 2) the hydropathy plot failed to recognise a defined TMH, which may suggest that HvGlyT4 is a peripheral protein. The TEM results showed that the antibody locates the enzyme predominantly in the Golgi sacks with a minor amount present at the plasma membrane (Figure a.6). This information for HvGlyT4 may suggest its involvement in a secretary pathway in barley, and, given that the major labeling is seen at the Golgi apparatus, these results may indirectly suggest that HvGlyT4 is involved in cell wall biosynthesis.

REFERENCES

Ahluwalia, B., and Fry, S.C. (1986) Barley endosperm cell walls contain a feruloylated arabinoxylan and a non-feruloylated β-glucan. *J Cereal Sci,* **4:** 287-295

Altschul, S., Madden, T., Schaffer, A., Zhang, J., Zhang, Z., Miller, W., and Lipman, D. (1997). Gapped BLAST and PSI-BLAST: a new generation of protein database search programs. *Nucleic Acids Res*, **25:** 3389-3402

Ambros, V., Bartel, B., Bartel, D., Burge, C., Carrington, J., Chen, X., Dreyfuss, G., Eddy, S., Griffiths-Jones, S., Marshall, M., Matzke, M., Ruvkun, G., and Tuschl, T. (2003). A uniform system for microRNA annotation. *RNA*, **9:** 277-279

Andreeva, A., Kutuzov, M., Evans, D., and Hawes, C. (1998). The structure and function of the Golgi apparatus: a hundred years of questions. *Journal of Experimental Botany*, **49:** 1281-1291

***Arabidopsis* Genome Initiative** (2000). Analysis of the genome sequence of the flowering plant *Arabidopsis thaliana*. *Nature*, **408:** 796-815

Arioli, T., Peng, L., Betzner, A., Burn, J., Wittke, W., Herth, W., Camilleri, C., Hofte, H., Plazinski, J., Birch, R., Cork, A., Glover, J., Redmond, J., and Williamson, R. (1998). Molecular analysis of cellulose biosynthesis in *Arabidopsis*. *Science*, **279:** 717-720

Auerbach, D., Galeuchet-Schenk, B., Hottiger, M., and Stagljar, I. (2002). Genetic approaches to the identification of interactions between membrane proteins in yeast. *J Recept Signal Transduct Res*, **22:** 471-481

Azevedo, C., Sadanandom, A., Kitagawa, K., Freialdenhoven, A., Shirasu, K., and Schulze-Lefert, P. (2002). The *RAR1* interactor *SGT1*, an essential component of R gene-triggered disease resistance. *Science*, **295:** 2073-2076

Baca, A.M., and Hol, W.G. (2000). Overcoming codon bias: a method for high-level overexpression of *Plasmodium* and other AT-rich parasite genes in *Escherichia coli*. *Int J Parasitol*, **30:** 113-118

Bacic, A., Du, H., Stone, B.A., and Clarke, A.E. (1996). Arabinogalactan proteins: a family of cell-surface and extracellular matrix plant proteoglycans. *Essays Biochem*, **31:** 91-101

Bacic, A., and Stone, B. (1981). Chemistry and organization of aleurone cell wall components from wheat and barley. *Aust. J. Plant Physiol.*, **8:** 475-495

Bacic, A., and Stone, B. (1981). Isolation and ultrastructureof aleurone cell-walls from wheat and barley. *Aust. J. Plant Physiol.*, **8:** 453-474

Baldwin, T.C., Handford, M.G., Yuseff, M.I., Orellana, A., and Dupree, P. (2001). Identification and characterization of GONST1, a golgi-localized GDP-mannose transporter in *Arabidopsis*. *Plant Cell*, **13:** 2283-2295

Ballance, G., and Manners, D. (1978). Structural analysis and enzymic solubilization of barley endosperm cell walls. *Carbohydrate research*, **61:** 107-118

Baneyx, F. (1999). Recombinant protein expression in *Escherichia coli*. *Curr Opin Biotechnol*, **10:** 411-421

Baneyx, F., and Mujacic, M. (2004). Recombinant protein folding and misfolding in *Escherichia coli*. *Nat Biotechnol*, **22:** 1399-1408

Barakat, A., Carels, N., and Bernardi, G. (1997). The distribution of genes in the genomes of Gramineae. *Proc Natl Acad Sci U S A*, **94:** 6857-6861

Barakat, A., Gallois, P., Raynal, M., Mestre-Ortega, D., Sallaud, C., Guiderdoni, E., Delseny, M., and Bernardi, G. (2000). The distribution of T-DNA in the genomes of transgenic *Arabidopsis* and rice. *FEBS Lett*, **471:** 161-164

Barr, A., Karakousis, A., Lance, R., Logue, S.J., Manning, S., Chalmers, K., Kretschmer, J., Boyd, W., Collins, H., Roumeliotis, S., Coventry, S., Moody, D., Read, B., Poulsen, D., Li, C., Platz, G., Inkerman, P., Panozzo, J., Cullis, B., Smith, A., Lim, P., and Langridge, P. (2003). Mapping and QTL analysis of the barley population Chebec × Harrington. *Australian Journal of Agricultural Research*, **54:** 1125-1130

Bartel, B., and Bartel, D. (2003). MicroRNAs: at the root of plant development? *Plant Physiol*, **132:** 709-717

Bartel, P., Chien, C., Sternglanz, R., and Fields, S. (1993). Elimination of false positives that arise in using the two-hybrid system. *Biotechniques*, **14:** 920-924

Bassham, D.C., and Raikhel, N.V. (2000). Plant cells are not just green yeast. *Plant Physiol*, **122:** 999-1001

Bateman, A., Birney, E., Durbin, R., Eddy, S.R., Finn, R.D., and Sonnhammer, E.L. (1999). Pfam 3.1: 1313 multiple alignments and profile HMMs match the majority of proteins. *Nucleic Acids Res*, **27:** 260-262

Bathgate, G., Palmer, G., and Wilson, G. (1974). The action of endo-B-glucanases on barley and malt B-glucans. *J. Inst. Brew*, **80:** 278-285

Baulcombe, D. (1999). Fast forward genetics based on virus-induced gene silencing. *Curr Opin Plant Biol*, **2:** 109-113

Bencurova, M., Rendic, D., Fabini, G., Kopecky, E., Altmann, F., and Wilson, I. (2003). Expression of eukaryotic glycosyltransferases in the yeast *Pichia pastoris*. *Biochimie*, **85:** 413-422

Bendtsen, J.D., Nielsen, H., von Heijne, G., and Brunak, S. (2004). Improved prediction of signal peptides: SignalP 3.0. *J Mol Biol*, **340:** 783-795

Benfey, P., Ren, L., and Chua, N. (1990). Tissue-specific expression from CaMV 35S enhancer subdomains in early stages of plant development. *EMBO J*, **9:** 1677-1684

Benton, W., and Davis, R. (1977). Screening lambdagt recombinant clones by hybridization to single plaques *in situ*. *Science*, **196:** 180-182

Bernstein, E., Caudy, A., Hammond, S., and Hannon, G. (2001). Role for a bidentate ribonuclease in the initiation step of RNA interference. *Nature*, **409:** 363-366

Birge, R.B., Fajardo, J.E., Reichman, C., Shoelson, S.E., Songyang, Z., Cantley, L.C., and Hanafusa, H. (1993). Identification and characterization of a high-affinity interaction between v-Crk and tyrosine-phosphorylated paxillin in CT10-transformed fibroblasts. *Mol Cell Biol*, **13:** 4648-4656

Block, M., Glick, B., Wilcox, C., Wieland, F., and Rothman, J. (1988). Purification of an N-ethylmaleimide-sensitive protein catalyzing vesicular transport. *Proc Natl Acad Sci U S A*, **82:** 7852-7856

Blum, P., Ory, J., Bauernfeind, J., and Krska, J. (1992). Physiological consequences of DnaK and DnaJ overproduction in *Escherichia coli*. *J Bacteriol*, **174:** 7436-7444

Bolwell, G. (2000). Biosynthesis of plant cell wall polysaccharides. *Trends in Glyoscience and Glycotechnology*, **12:** 143-160

Bonetta, D., Facette, M., Raab, T., and Somerville, C. (2002). Genetic dissection of plant cell-wall biosynthesis. *Biochem Soc Trans*, **30:** 298-301

Bonnal, S., Boutonnet, C., Prado-Lourenco, L., and Vagner, S. (2003). IRESdb: the Internal Ribosome Entry Site database. *Nucleic Acids Res*, **31:** 427-428

Boutet, S., Vazquez, F., Liu, J., Beclin, C., Fagard, M., Gratias, A., Morel, J., Crete, P., Chen, X., and Vaucheret, H. (2003). *Arabidopsis HEN1*: a genetic link between endogenous miRNA controlling development and siRNA controlling transgene silencing and virus resistance. *Curr Biol*, **13:** 84-88

Bouton, S., Leboeuf, E., Mouille, G., Leydecker, M., Talbotec, J., Granier, F., Lahaye, M., Hofte, H., and Truong, H. (2002). *QUASIMODO1* encodes a putative membrane-bound glycosyltransferase required for normal pectin synthesis and cell adhesion in *Arabidopsis*. *Plant Cell*, **14:** 2577-2590

Bracha-Drori, K., Shichrur, K., Katz, A., Oliva, M., Angelovici, R., Yalovsky, S., and Ohad, N. (2004). Detection of protein-protein interactions in plants using bimolecular fluorescence complementation. *Plant J*, **40:** 419-427

Bradford, M. (1976). A rapid and sensitive method for the quantification of microgram quantities of protein utilizing the principle of protein-dye binding. *Anal Biochem*, **72:** 248-254

Braun, P., and LaBaer, J. (2003). High throughput protein production for functional proteomics. *Trends Biotechnol*, **21:** 383-388

Brenner, S., Johnson, M., Bridgham, J., Golda, G., Lloyd, D., Johnson, D., Luo, S., McCurdy, S., Foy, M., Ewan, M., Roth, R., George, D., Eletr, S., Albrecht, G., Vermaas, E., Williams, S., Moon, K., Burcham, T., Pallas, M., DuBridge, R., Kirchner, J., Fearon, K., Mao, J., and Corcoran, K. (2000). Gene expression analysis by massively parallel signature sequencing (MPSS) on microbead arrays. *Nat Biotechnol*, **18:** 630-634

Breton, C., Bettler, E., Joziasse, D., Geremia, R., and Imberty, A. (1998). Sequence-function relationship of prokaryotic and eukaryotic galactosyltransferases. *J. Biochem*, **123:** 1000-1009

Breton, C., Heissigerova, H., Jeanneau, C., Moravcova, J., and Imberty, A. (2002). Comparative aspects of glycosyltransferases. *Biochem Soc Symp*: 23-32

Breton, C., and Imberty, A. (1999). Structure/function studies of glycosyltransferases. *Curr Opin Struct Biol*, **9:** 563-571

Breton, C., Mucha, J., and Jeanneau, C. (2001). Structural and functional features of glycosyltransferases. *Biochimie*, **83:** 713-718

Brett, C.T., and Waldron, K.W. (1996). Physiology and Biochemistry of Plant Cell Walls, Ed Second. Kluwer Academic Publishers, DordrechtPages

Bruckner, K., Perez, L., Clausen, H., and Cohen, S. (2000). Glycosyltransferase activity of fringe modulates Notch-Delta interactions. *Nature,* **406:** 411-415

Bucher, P. (1999). Regulatory elements and expression profiles. *Curr Opin Struct Biol*, **9:** 400-407

Burton, R., Gibeaut, D., Bacic, A., Findlay, K., Roberts, K., Hamilton, A., Baulcombe, D., and Fincher, G. (2000). Virus-induced silencing of a plant cellulose synthase gene. *Plant Cell*, **12:** 691-706

Burton, R., King, B., Shirley, N., Gatford, K., Gooding, P., and Fincher, G. (2003). Functional analysis of the barley *CesA* gene family. *In* 7th International Congress of Plant Molecular Biology, Barcelona, Spain, pp 101

Burton, R., Shirley, N., King, B., Harvey, A., and Fincher, G. (2004). The *CesA* gene family of barley. Quantitative analysis of transcripts reveals two groups of co-expressed genes. *Plant Physiol.*, **134:** 224-236

Busch, C., Hofmann, F., Selzer, J., Munro, S., Jeckel, D., and Aktories, K. (1998). A common motif of eukaryotic glycosyltransferases is essential for the enzyme activity of large clostridial cytotoxins. *J Biol Chem*, **273:** 19566-19572

Bustin, S. (2000). Absolute quantification of mRNA using real-time reverse transcription polymerase chain reaction assays. *J Mol Endocrinol*, **25:** 169-193

Callebaut, I., Labesse, G., Durand, P., Poupon, A., Canard, L., Chomilier, J., Henrissat, B., and Mornon, J. (1997). Deciphering protein sequence information through hydrophobic cluster analysis (HCA): current status and perspectives. *Cell Mol Life Sci*, **53:** 621-645

Camacho-Carvajal, M.M., Wollscheid, B., Aebersold, R., Steimlet, V., and Schamel, W.W.A. (2004). Two-dimensional blue native /SDS gel electrophoresis of multi-protein complexes from whole cellular lysates. *Molecular and Cellular Proteomics*, **3:** 176-182

Campbell, J., Davies, G., Bulone, V., and Henrissat, B. (1997). A classification of nucleotide-diphospho-sugar glycosyltransferases based on amino acid sequence similarities. *Biochem J*, **326:** 929-939

Carafa, A., Duckett, J.G., Knox, J.P., and Ligrone, R. (2005). Ditribution of cell-wall xylans in bryophytes and tracheophytes: new insights into basal interrelationships of land plants. *New Phytologist,* **168**: 231-240

Carol, R.J., and Dolan, L. (2002). Building a hair: tip growth in *Arabidopsis thaliana* root hairs. *Philos Trans R Soc Lond B Biol Sci*, **357:** 815-821

Carpita, N. (1996). Structure and biogenesis of the cell walls of grasses. *Ann. Rev. Plant Physiol. Plant Molec. Biol*, **47:** 445-476

Carpita, N., and Gibeaut, D. (1993). Structural models of primary cell walls in flowering plants: consistency of molecular structure with the physical properties of the walls during growth. *Plant J*, **3:** 1-30

Carpita, N., and McCann, M. (2000). The Cell Wall. *In* Biochemistry & Molecular Biology of Plants, Buchanan, B.B., Gruissem, W., and Jones, R., eds. John Wiley & Sons Inc, pp 52-108

Carrington, J., and Ambros, V. (2003). Role of microRNAs in plant and animal development. *Science*, **301:** 336-338

Charnock, S.J., and Davies, G.J. (1999). Structure f the nucleotide-diphospho-sugar transferase, SpsA from *Bacillus subtilis*, in native and nucleotide complex forms. *Biochemistry*, **38**: 6380-6385

Chenna, R., Sugawara, H., Koike, T., Lopez, R., Gibson, T., Higgins, D., and Thompson, J. (2003). Multiple sequence alignment with the Clustal series of programs. *Nucleic Acids Res*, **31:** 3497-3500

Chien, C., Bartel, P., Sternglanz, R., and Fields, S. (1991). The two-hybrid system: a method to identify and clone genes for proteins that interact with a protein of interest. *Proc Natl Acad Sci U S A*, **88:** 9578-9582

Cho, H.T., and Cosgrove, D.J. (2002). Regulation of root hair initiation and expansin gene expression in *Arabidopsis*. *Plant Cell*, **14:** 3237-3253

Chong, S., Mersha, F.B., Comb, D.G., Scott, M.E., Landry, D., Vence, L.M., Perler, F.B., Benner, J., Kucera, R.B., Hirvonen, C.A., Pelletier, J.J., Paulus, H., and Xu, M.Q. (1997). Single-column purification of free recombinant proteins using a self-cleavable affinity tag derived from a protein splicing element. *Gene*, **192:** 271-281

Clark, J. (1988). Novel non-templated nucleotide addition reactions catalyzed by procaryotic and eucaryotic DNA polymerases. *Nucleic Acids Res*, **16:** 9677-9686

Close, T.J., Wanamaker, S.I., Caldo, R.A., Turner, S.M., Ashlock, D.A., Dickerson, J.A., Wing, R.A., Muehlbauer, G.J., Kleinhofs, A., and Wise, R.P. (2004). A new resource for cereal genomics: 22K barley GeneChip comes of age. *Plant Physiol*, **134:** 960-968

Cobbe, N., and Heck, M.M. (2004). Computer dating for proteins. *Heredity*,

Colley, K. (1997). Golgi localization of glycosyltransferases: more questions than answers. *Glycobiology*, **7:** 1-13

Colley, K., Lee, E., and Paulson, J. (1992). The signal anchor and stem regions of the beta-galactoside alpha 2,6-sialyltransferase may each act to localize the enzyme to the Golgi apparatus. *J Biol Chem*, **267:** 7784-7793

Collins, N., Thordal-Christensen, H., Lipka, V., Bau, S., Kombrink, E., Qiu, J., Huckelhoven, R., Stein, M., Freialdenhoven, A., Somerville, S., and Schulze-Lefert, P. (2003). SNARE-protein-mediated disease resistance at the plant cell wall. *Nature*, **425:** 973-977

Collins, T., Gerday, C., Feller, G. (2005). Xylanses, xylanse families and extermophilic xylanases. *FEMS Microbiology Reviews,* **29**: 3-23

Colosimo, A., Goncz, K.K., Holmes, A.R., Kunzelmann, K., Novelli, G., Malone, R.W., Bennett, M.J., and Gruenert, D.C. (2000). Transfer and expression of foreign genes in mammalian cells. *Biotechniques*, **29:** 314-318, 320-312, 324 passim

Cosgrove, D.J., Li, L.C., Cho, H.T., Hoffmann-Benning, S., Moore, R.C., and Blecker, D. (2002). The growing world of expansins. *Plant Cell Physiol*, **43:** 1436-1444

Coutinho, P., Stam, M., Blanc, E., and Henrissat, B. (2003). Why are there so many carbohydrate-active enzyme-related genes in plants? *Trends Plant Sci*, **8:** 563-565

Coutinho, P.M., Deleury, E., Davies, G.J., and Henrissat, B. (2003). An evolving hierarchical family classification for glycosyltransferases. *J Mol Biol*, **328:** 307-317

Cove, D., Knight, C., and Lamparter, T. (1997). Mosses as model systems. *Trends in Plant Science*, **2:** 99-105

Cove, D.J., and Knight, C.D. (1993). The moss *Physcomitrella patens*, a model system with potential for the study of plant reproduction. *Plant Cell*, **5:** 1483-1488

Creasey, E., Delahay, R., Daniell, S., and Frankel, G. (2003). Yeast two-hybrid system survey of interactions between LEE-encoded proteins of enteropathogenic *Escherichia coli*. *Microbiology*, **149:** 2093-2106

Daly, R., and Hearn, M.T. (2005). Expression of heterologous proteins in *Pichia pastoris*: a useful experimental tool in protein engineering and production. *J Mol Recognit*, **18:** 119-138

Davis, G.D., Elisee, C., Newham, D.M., and Harrison, R.G. (1999). New fusion protein systems designed to give soluble expression in *Escherichia coli*. *Biotechnol Bioeng*, **65:** 382-388

Decker, E.L., and Reski, R. (2004). The moss bioreactor. *Curr Opin Plant Biol*, **7:** 166-170

Delmer, D. (1999). Cellulose biosynthesis: exciting times for a difficult field of study. *Annual Review of Plant Physiology and Plant Molecular Biology*, **50:** 245-276

Dhugga, K. (2001). Building the wall: genes and enzyme complexes for polysaccharide synthases. *Curr Opin Plant Biol*, **4:** 488-493

Dhugga, K., Barreiro, R., Whitten, B., Stecca, K., Hazebroek, J., Randhawa, G., Dolan, M., Kinney, A., Tomes, D., Nichols, S., and Anderson, P. (2004). Guar seed beta-mannan synthase is a member of the cellulose synthase super gene family. *Science*, **303:** 363-366

Dhugga, K., Tiwari, S., and Ray, P. (1997). A reversibly glycosylated polypeptide (RGP1) possibly involved in plant cell wall synthesis: purification, gene cloning, and *trans*-Golgi localization. *Proc Natl Acad Sci U S A*, **94:** 7679-7684

Dhugga, K.S. (2005). Plant Golgi cell wall synthesis: from genes to enzyme activities. *Proc Natl Acad Sci U S A*, **102:** 1815-1816

Dhugga, K.S., and Ray, P.M. (1994). Purification of 1,3-beta-D-glucan synthase activity from pea tissue. Two polypeptides of 55 kDa and 70 kDa copurify with enzyme activity. *Eur J Biochem*, **220:** 943-953

di Guan, C., Li, P., Riggs, P.D., and Inouye, H. (1988). Vectors that facilitate the expression and purification of foreign peptides in *Escherichia coli* by fusion to maltose-binding protein. *Gene*, **67:** 21-30

Diatchenko, L., Lau, Y., Campbell, A., Chenchik, A., Moqadam, F., Huang, B., Lukyanov, S., Lukyanov, K., Gurskaya, N., Sverdlov, E., and Siebert, P. (1996). Suppression subtractive hybridization: a method for generating differentially regulated or tissue-specific cDNA probes and libraries. *Proc Natl Acad Sci U S A*, **93:** 6025-6030

Ding, C., and Cantor, C.R. (2003). A high-throughput gene expression analysis technique using competitive PCR and matrix-assisted laser desorption ionization time-of-flight MS. *Proc Natl Acad Sci U S A*, **100:** 3059-3064

Ding, C., and Cantor, C.R. (2004). Quantitative analysis of nucleic acids--the last few years of progress. *J Biochem Mol Biol*, **37:** 1-10

Doan, N., and Fincher, G. (1988). The A- and B-chains of carboxypeptidase I from germinated barley originate from a single precursor polypeptide. *J Biol Chem*, **263:** 11106-11110

Doblin, M., De Melis, L., Newbigin, E., Bacic, A., and Read, S. (2001). Pollen tubes of *Nicotiana alata* express two genes from different beta-glucan synthase families. *Plant Physiol*, **125:** 2040-2052

Doblin, M., Kurek, I., Jacob-Wilk, D., and Delmer, D. (2002). Cellulose biosynthesis in plants: from genes to rosettes. *Plant Cell Physiol*, **43:** 1407-1420

Donson, J., Fang, Y., Espiritu-Santo, G., Xing, W., Salazar, A., Miyamoto, S., Armendarez, V., and Volkmuth, W. (2002). Comprehensive gene expression analysis by transcript profiling. *Plant Mol Biol*, **48:** 75-97

Driouich, A., Faye, L., and Staehelin, L.A. (1993). The plant Golgi apparatus: a factory for complex polysaccharides and glycoproteins. *Trends Biochem Sci*, **18:** 210-214

Dubessay, P., Pages, M., Delbac, F., Bastien, P., Vivares, C., and Blaineau, C. (2004). Can heterologous gene expression shed (a torch) light on protein function? *Trends Biotechnol*, **22:** 557-559

Eckardt, N. (2003). Cellulose synthesis takes the *CesA* train. *Plant Cell*, **15:** 1685-1688

Eckart, M.R., and Bussineau, C.M. (1996). Quality and authenticity of heterologous proteins synthesized in yeast. *Curr Opin Biotechnol*, **7:** 525-530

Eddy, S. (1996). Hidden Markov models. *Curr Opin Struct Biol*, **6:** 361-365

Edwards, M., Bulpin, P., Dea, I., and Reid, J. (1989). Biosynthesis of legume seed galactomannans *in vitro*. *Planta*, **187:** 67-74

Edwards, M., Choo, T., Dickson, C., Scott, C., Gidley, M., and Reid, J. (2004). The seeds of *Lotus japonicus* lines transformed with sense, antisense, and sense/antisense galactomannan galactosyltransferase constructs have structurally altered galactomannans in their endosperm cell walls. *Plant Physiol*, **134:** 1153-1162

Edwards, M., Dickson, C., Chengappa, S., Sidebottom, C., Gidley, M., and Reid, J. (1999). Molecular characterisation of a membrane-bound galactosyltransferase of plant cell wall matrix polysaccharide biosynthesis. *Plant J*, **19:** 691-697

Egelund, J., Skjot, M., Geshi, N., Ulvskov, P., and Petersen, B.L. (2004). A complementary bioinformatics approach to identify potential plant cell wall glycosyltransferase-encoding genes. *Plant Physiol*, **136:** 2609-2620

Elbein, A.D. (1969). Biosynthesis of a cell wall glucomannan in mung bean seedlings. *J Biol Chem*, **244:** 1608-1616

Elbein, A.D. (1984). Inhibitors of the biosynthesis and processing of *N*-linked oligosaccharides. *CRC Crit. Rev. Biochem*, **16:** 21-49

Endo, Y., and Sawasaki, T. (2004). High-throughput, genome-scale protein production method based on the wheat germ cell-free expression system. *J Struct Funct Genomics*, **5:** 45-57

Faik, A., Bar-Peled, M., DeRocher, A., Zeng, W., Perrin, R., Wilkerson, C., Raikhel, N., and Keegstra, K. (2000). Biochemical characterization and molecular cloning of an alpha-1,2-fucosyltransferase that catalyzes the last step of cell wall xyloglucan biosynthesis in pea. *J Biol Chem*, **275:** 15082-15089

Faik, A., Price, N., Raikhel, N., and Keegstra, K. (2002). An *Arabidopsis* gene encoding an alpha-xylosyltransferase involved in xyloglucan biosynthesis. *Proc Natl Acad Sci U S A*, **28:** 7797-7802

Fashena, S., Serebriiskii, I., and Golemis, E. (2000). The continued evolution of two-hybrid screening approaches in yeast: how to outwit different preys with different baits. *Genes*, **250:** 1-14

Favery, B., Ryan, E., Foreman, J., Linstead, P., Boudonck, K., Steer, M., Shaw, P., and Dolan, L. (2001). *KOJAK* encodes a cellulose synthase-like protein required for root hair cell morphogenesis in *Arabidopsis*. *Genes & Development*, **15:** 79-89

Federico, R., and Angelini, R. (1991). Polyamine catabolism in plants. *In* Biochemistry and physiology of polyamines in plants, Slocum, R., and Flores, H., eds. CRC Press, Boca Raton, FL, pp 41-56

Feinberg, A., and Vogelstein, B. (1983). A technique for radiolabeling DNA restriction endonuclease fragments to high specific activity. *Anal Biochem*, **132:** 6-13

Feingold, D., Neufeld, E., and Hassid, W. (1958). Synthesis of a ß-(1,3)-linked glucan by extracts of *Phaseoulous aureus* seedlings. *J Biol Chem*, **233:** 783-788

Feng, D., and Doolittle, R. (1987). Progressive sequence alignment as a prerequisite to correct phylogenetic trees. *J Mol Evol*, **25:** 351-360

Ferre, F. (1992). Quantitative or semi-quantitative PCR: reality versus myth. *PCR Methods Appl*, **2:** 1-9

Fetchko, M., Auerbach, D., and Stagljar, I. (2003). Yeast genetic methods for the detection of membrane protein interactions: potential use in drug discovery. *BioDrugs*, **17:** 413-424

Fields, S., and Song, O. (1989). A novel genetic system to detect protein-protein interactions. *Nature*, **340:** 245-246

Fincher, G. (1975). Morphology and chemical composition of barley endosperm cell walls. *Journal of Institute of Brewing*, **81:** 116-122

Fincher, G. (1992). Cell wall metabolism in barley. *In* Barley: Biochemistry, Molecular Biology and Biotechnology, Shewry, P., ed, Ed 1st Vol 5. C.A.B International, pp 413-437

Fincher, G., and Stone, B. (2004). Chemistry of nonstarch polysaccharides. *In* Encyclopedia of Grain Science, Wrigley, C., Corke, H., and Walker, C., eds, Ed 1 Vol 1. Elsevier, pp 206-223

Finnegan, E., Wang, M., and Waterhouse, P. (2001). Gene silencing: fleshing out the bones. *Curr Biol*, **11:** R99-R102

Fire, A., Xu, S., Montgomery, M., Kostas, S., Driver, S., and Mello, C. (1998). Potent and specific genetic interference by double-stranded RNA in *Caenorhabditis elegans*. *Nature*, **391:** 806-811

Fitzmaurice, W.P., Holzberg, S., Lindbo, J.A., Padgett, H.S., Palmer, K.E., Wolfe, G.M., and Pogue, G.P. (2002). Epigenetic modification of plants with systemic RNA viruses. *Omics*, **6:** 137-151

Follet-Gueye, M., Pagny, S., Faye, L., Gomord, V., and Driouich, A. (2003). An improved chemical fixation method suitable for immunogold localization of green fluorescent protein in the Golgi apparatus of tobacco Bright Yellow (BY-2) cells. *J Histochem Cytochem*, **51:** 931-940

Formosa, T., Barry, J., Alberts, B.M., and Greenblatt, J. (1991). Using protein affinity chromatography to probe structure of protein machines. *Methods Enzymol*, **208:** 24-45

Forrest, I. (1977). The role of protein in the structure of barley endosperm cell walls. *Biochem Soc Trans*, **5:** 1154-1156

Frank, W., Ratnadewi, D., and Reski, R. (2005). *Physcomitrella patens* is highly tolerant against drought, salt and osmotic stress. *Planta*, **220:** 384-394

Fraser, H.B., Hirsh, A.E., Wall, D.P., and Eisen, M.B. (2004). Coevolution of gene expression among interacting proteins. *Proc Natl Acad Sci U S A*, **101:** 9033-9038

Freeman, W., Walker, S., and Vrana, K. (1999). Quantitative RT-PCR: pitfalls and potential. *Biotechniques*, **26:** 112-125

Frohman, M., Dush, M., and Martin, G. (1988). Rapid production of full-length cDNAs from rare transcripts: amplification using a single gene-specific oligonucleotide primer. *Proc Natl Acad Sci U S A*, **85:** 8998-9002

ccharide-modifying enzymes in the plant cell wall. *Annual gy and Plant Molecular Biology*, **46:** 497-520

rsheim, P., Darvill, A., Hayashi, T., Joseleau, J., Kato, Y., ı, G., McNeil, M., Mort, A., Reid, J., Seitz, H., Selvendran, ite, A.** (1993). An unambiguous nomenclature for xyloglucan *Physiologia Plantarum*, **89:** 1-3

and Charrier, B. (2004). Real-time PCR: what relevance to ; 1445-1454

ıd Turner, S.** (2003). Control of cellulose synthase complex ... developing xylem. *Plant Cell*, **15:** 1740-1748

Gaspar, Y., Johnson, K., McKenna, J., Bacic, A., and Schultz, C. (2001). The complex structures of arabinogalactan-proteins and the journey towards understanding function. *Plant Mol Biol.*, **47:** 161-176

Gastinel, L., Bignon, C., Misra, A., Hindsgaul, O., Shaper, J., and Joziasse, D. (2001). Bovine alpha1,3-galactosyltransferase catalytic domain structure and its relationship with ABO histo-blood group and glycosphingolipid glycosyltransferases. *EMBO J*, **20:** 638-649

Gastinel, L., Cambillau, C., and Bourne, Y. (1999). Crystal structures of the bovine beta-4-galactosyltransferase catalytic domain and its complex with uridine diphosphogalactose. *EMBO J*, **18:** 3546-3557

Geisse, S., Gram, H., Kleuser, B., and Kocher, H.P. (1996). Eukaryotic expression systems: a comparison. *Protein Expr Purif*, **8:** 271-282

Georgiou, G., and Valax, P. (1996). Expression of correctly folded proteins in *Escherichia coli*. *Curr Opin Biotechnol*, **7:** 190-197

Geremia, R., Petroni, E., Ielpi, L., and Henrissat, B. (1996). Towards a classification of glycosyltransferases based on amino acid sequence similarities: prokaryotic alpha-mannosyltransferases. *Biochem J*, **318:** 133-138

Geshi, N. (2003). An alfa xylosyl transferase possibly involved in RG-II biosynthesis. *In* Gordon Cell Wall Conference, USA

Gibeaut, D. (2000). Nucleotide sugars and glycosyltransferases for synthesis of cell wall matrix polysaccharides. *Plant Physiol. Biochem*, **38:** 69-80

Gibeaut, D., and Carpita, N. (1994). Biosynthesis of plant cell wall polysaccharides. *FASEB J*, **8:** 904-915

Gibeaut, D.M., and Carpita, N.C. (1991). Tracing cell wall biogenesis in intact cells and plants. Selective turnover and alteration of soluble and cell wall polysaccharides in grasses. *Plant Physiol*, **97:** 551-561

Gibeaut, D.M., Pauly, M., Bacic, A., and Fincher, G.B. (2005). Changes in cell wall polysaccharides in developing barley (*Hordeum vulgare*) coleoptiles. *Planta*,

Gibson, U.E., Heid, C.A., and Williams, P.M. (1996). A novel method for real time quantitative RT-PCR. *Genome Res*, **6:** 995-1001

Gilliland, G., Perrin, S., Blanchard, K., and Bunn, H. (1990). Analysis of cytokine mRNA and DNA: detection and quantitation by competitive polymerase chain reaction. *Proc Natl Acad Sci U S A*, **87:** 2725-2729

Gleba, Y., Marillonnet, S., and Klimyuk, V. (2004). Engineering viral expression vectors for plants: the 'full virus' and the 'deconstructed virus' strategies. *Curr Opin Plant Biol*, **7:** 182-188

Goff, S., Ricke, D., Lan, T., Presting, G., Wang, R., Dunn, M., Glazebrook, J., Sessions, A., Oeller, P., Varma, H., Hadley, D., Hutchison, D., Martin, C., Katagiri, F., Lange, B., Moughamer, T., Xia, Y., Budworth, P., Zhong, J., Miguel, T., Paszkowski, U., Zhang, S., Colbert, M., Sun, W., Chen, L., Cooper, B., Park, S., Wood, T., Mao, L., Quail, P., Wing, R., Dean, R., Yu, Y., Zharkikh, A., Shen, R., Sahasrabudhe, S., Thomas, A., Cannings, R., Gutin, A., Pruss, D., Reid, J., Tavtigian, S., Mitchell, J., Eldredge, G., Scholl, T., Miller, R., Bhatnagar, S., Adey, N., Rubano, T., Tusneem, N., Robinson, R., Feldhaus, J., Macalma, T., Oliphant, A., and Briggs, S. (2002). A draft sequence of the rice genome (*Oryza sativa* L. ssp. japonica). *Science*, **296:** 92-100

Golemis, E., and Brent, R. (1992). Fused protein domains inhibit DNA binding by LexA. *Mol Cell Biol*, **12:** 3006-3014

Gomord, V., and Faye, L. (2004). Posttranslational modification of therapeutic proteins in plants. *Curr Opin plant Biol*, **7:** 171-181

Gordon, G.W., Berry, G., Liang, X.H., Levine, B., and Herman, B. (1998). Quantitative fluorescence resonance energy transfer measurements using fluorescence microscopy. *Biophys J*, **74:** 2702-2713

Goubet, F., Misrahi, A., Park, S., Zhang, Z., Twell, D., and Dupree, P. (2003). *AtCSLA7*, a cellulose synthase-like putative glycosyltransferase, is important for pollen tube growth and embryogenesis in *Arabidopsis*. *Plant Physiol*, **131:** 547-557

Graham, A., and Newton, C. (1997). PCR, Ed second. Springer VerlagPages

Gregory, A., Smith, C., Kerry, M., Wheatley, E., and Bolwell, G. (2002). Comparative subcellular immunolocation of polypeptides associated with xylan and callose synthases in French bean (*Phaseolus vulgaris*) during secondary wall formation. *Phytochemistry*, **59:** 249-259

Grisebach, H. (1981). Lignins. *In* Secondary plant products, Stumpf, P., and Conn, E., eds, Vol 7. Academic Press, New York, pp 457-478

Grisshammer, R., and Tate, C.G. (1995). Overexpression of integral membrane proteins for structural studies. *Q Rev Biophys*, **28:** 315-422

Grunstein, M., and Hogness, D. (1975). Colony hybridization: a method for the isolation of cloned DNAs that contain a specific gene. *Proc Natl Acad Sci U S A*, **72:** 3961-3965

Gubler, F., and Ashford, A. (1985). Release of ferulic acid esters from barley aleurone. *Aust. J. Plant Physiol.*, **12:** 297-305

Gustafsson, C., Govindarajan, S., and Minshull, J. (2004). Codon bias and heterologous protein expression. *Trends Biotechnol*, **22:** 346-353

Gygi, S., Rochon, Y., Franza, B., and Aebersold, R. (1999). Correlation between protein and mRNA abundance in yeast. *Mol Cell Biol*, **19:** 1720-1730

Hagen, F., Hazes, B., Raffo, R., DeSa, D., and Tabak, L. (1999). Structure-function analysis of the UDP-N-acetyl-D-galactosamine:polypeptide N-acetylgalactosaminyl-transferase. Essential residues lie in a predicted active site cleft resembling a lactose repressor fold. *J Biol Chem*, **274:** 6797-6803

Hagen, F., Wuyckhuyse, B.V., and Tabak, L. (1993). Purification, cloning, and expression of a bovine UDP-GalNAc: polypeptide N-acetyl-galactosaminyltransferase. *J. Biol. Chem*, **268:** 18960-18965

Hake, S. (2003). MicroRNAs: a role in plant development. *Curr Biol*, **13:** R851-852

Hamilton, A., and Baulcombe, D. (1999). A species of small antisense RNA in posttranscriptional gene silencing in plants. *Science*, **286:** 950-952

Hamilton, A., Voinnet, O., Chappell, L., and Baulcombe, D. (2002). Two classes of short interfering RNA in RNA silencing. *EMBO J*, **21:** 4671-4679

Hartley, J.L., Temple, G.F., and Brasch, M.A. (2000). DNA cloning using *in vitro* site-specific recombination. *Genome Res*, **10:** 1788-1795

Hayashi, T. (1989). Xyloglucan in the primary cell wall. *Annu. Rev. Plant Physiol. Plant Mol. Biol.*, **40:** 139-168

Hazen, S., Scott-Craig, J., and Walton, J. (2002). Cellulose synthase-like genes of rice. *Plant Physiol*, **128:** 336-340

Heid, C., Stevens, J., Livak, K., and Williams, P. (1996). Real time quantitative PCR. *Genome Res*, **6:** 986-994

Hellwig, S., Drossard, J., Twyman, R., and Fischer, R. (2004). Plant cell cultures for the production of recombinant proteins. *Nat Biotechnol*, **22:** 1415-1422

Henikoff, S., and Comai, L. (2003). Single-nucleotide mutations for plant functional genomics. *Annu Rev Plant Biol*, **54:** 375-401

Henikoff, S., Till, B., and Comai, L. (2004). TILLING. Traditional mutagenesis meets functional genomics. *Plant Physiol*, **135:** 630-636

Higuchi, R., Dollinger, G., Walsh, P.S., and Griffith, R. (1992). Simultaneous amplification and detection of specific DNA sequences. *Biotechnology (N Y)*, **10:** 413-417

Higuchi, R., Fockler, C., Dollinger, G., and Watson, R. (1993). Kinetic PCR analysis: real-time monitoring of DNA amplification reactions. *Biotechnology (N Y)*, **11:** 1026-1030

Himber, C., Dunoyer, P., Moissiard, G., Ritzenthaler, C., and Voinnet, O. (2003). Transitivity-dependent and -independent cell-to-cell movement of RNA silencing. *EMBO J*, **22:** 4523-4533

Hochuli, E., Dobeli, H., and Schacher, A. (1987). New metal chelate adsorbent selective for proteins and peptides containing neighbouring histidine residues. *J Chromatogr*, **411:** 177-184

Hod, Y. (1992). A simplified ribonuclease protection assay. *Biotechniques*, **13:** 852-854

Holtorf, H., Guitton, M., and Reski, R. (2002). Plant functional genomics. *Naturwissenschaften*, **89:** 235-249

Holzberg, S., Brosio, P., Gross, C., and Pogue, G. (2002). Barley stripe mosaic virus-induced gene silencing in a monocot plant. *Plant J*, **30:** 315-327

Hong, H.Y., Yoo, G.S., and Choi, J.K. (2000). Direct Blue 71 staining of proteins bound to blotting membranes. *Electrophoresis*, **21:** 841-845

Hong, Z., Zhang, Z., Olson, J.M., and Verma, D.P. (2001). A novel UDP-glucose transferase is part of the callose synthase complex and interacts with phragmoplastin at the forming cell plate. *Plant Cell*, **13:** 769-779

Hopp, T.P., and Woods, K.R. (1981). Prediction of protein antigenic determinants from amino acid sequences. *Proc Natl Acad Sci USA*, **86:** 152-156

Horiguchi, G. (2004). RNA silencing in plants: a shortcut to functional analysis. *Differentiation*, **72:** 65-73

Horser, C., Abbott, D., Wesley, S., Smith, N., and Waterhouse, P. (2002). Gene silencing-principles and application. *In* Genetic engineering, Setlow, J., ed, Vol 24. Kluwer Academic/plenum, New York, pp 239-256

Horstmann, V., Huether, C.M., Jost, W., Reski, R., and Decker, E.L. (2004). Quantitative promoter analysis in *Physcomitrella patens*: a set of plant vectors activating gene expression within three orders of magnitude. *BMC Biotechnol*, **4:** 13

Hrmova, M., and Fincher, G. (2001). Structure-function relationships of beta-D-glucan endo- and exohydrolases from higher plants. *Plant Mol Biol*, **47:** 73-91

Hrmova, M., and Fincher, G. (2002). Enzymic Hydrolysis of Cereal (1-3,1-4)-b-Glucans. *In* Handbook of Food Enzymology, Whitaker, J.R., Voragen, A.G.J., and Wong, D.W.S., eds, pp 943-960

Hu, C.D., Chinenov, Y., and Kerppola, T.K. (2002). Visualization of interactions among bZIP and Rel family proteins in living cells using bimolecular fluorescence complementation. *Mol Cell*, **9:** 789-798

Hu, C.D., and Kerppola, T.K. (2003). Simultaneous visualization of multiple protein interactions in living cells using multicolor fluorescence complementation analysis. *Nat Biotechnol*, **21:** 539-545

Hu, J., Kornacker, M., and Hochschild, A. (2000). *Escherichia coli* one- and two-hybrid systems for the analysis and identification of protein-protein interactions. *Methods*, **20:** 80-94

Hubank, M., and Schatz, D. (1994). Identifying differences in mRNA expression by representational difference analysis of cDNA. *Nucleic Acids Res*, **22:** 5640-5648

Hunter, C., and Poethig, R. (2003). miSSING LINKS: miRNAs and plant development. *Curr Opin Genet Dev*, **13:** 372-378

Huth, J.R., Bewley, C.A., Jackson, B.M., Hinnebusch, A.G., Clore, G.M., and Gronenborn, A.M. (1997). Design of an expression system for detecting folded protein domains and mapping macromolecular interactions by NMR. *Protein Sci*, **6:** 2359-2364

Huttermann, A., Mai, C., and Kharazipour, A. (2001). Modification of lignin for the production of new compounded materials. *Appl Microbiol Biotechnol,* **55**: 387-394

Imberty, A., Monier, C., Bettler, E., Morera, S., Freemont, P., Sippl, M., Flockner, H., Ruger, W., and Breton, C. (1999). Fold recognition study of alpha3-galactosyltransferase and molecular modeling of the nucleotide sugar-binding domain. *Glycobiology*, **9:** 713-722

Immink, R.G., Gadella, T.W., Jr., Ferrario, S., Busscher, M., and Angenent, G.C. (2002). Analysis of MADS box protein-protein interactions in living plant cells. *Proc Natl Acad Sci U S A*, **99:** 2416-2421

Inouhe, M., McClellan, M., and Nevins, D. (1997). Developmental regulation of polysaccharide metabolism and growth in the primary cell walls of maize. *Int J Biol Macromol*, **21:** 21-28

Irizarry, R.A., Hobbs, B., Collin, F., Beazer-Barclay, Y.D., Antonellis, K.J., Scherf, U., and Speed, T.P. (2003). Exploration, normalization, and summaries of high density oligonucleotide array probe level data. *Biostatistics*, **4:** 249-264

Islam, A., Shepherd, K., and Sparrow, D. (1981). Isolation and characterization of euplasmic wheat-barley chromosome addition lines. *Heredity*, **46:** 161-174

Iwai, H., Masaoka, N., Ishii, T., and Satoh, S. (2002). A pectin glucuronyltransferase gene is essential for intercellular attachment in the plant meristem. *Proc Natl Acad Sci U S A*, **99:** 16319-16324

Iyer, K., Burkle, L., Auerbach, D., Thaminy, S., Dinkel, M., Engels, K., and Stagljar, I. (2005). Utilizing the split-ubiquitin membrane yeast two-hybrid system to identify protein-protein interactions of integral membrane proteins. *Sci STKE*, **275**

Jacobs, A., Lipka, V., Burton, R., Panstruga, R., Strizhov, N., Schulze-Lefert, P., and Fincher, G. (2003). An *Arabidopsis* callose synthase, *GSL5*, is required for wound and papillary callose formation. *Plant Cell*, **15:** 2503-2513

Jarvis, M. (2003). Chemistry: Cellulose stacks up. *Nature*, **426:** 611-612

Jeong, D., An, S., Kang, H., Moon, S., Han, J., Park, S., Lee, H., An, K., and An, G. (2002). T-DNA insertional mutagenesis for activation tagging in rice. *Plant Physiol*, **130:** 1636-1644

Jones, D.T. (1999). Protein secondary structure prediction based on position-specific scoring matrices. *J Mol Biol*, **292:** 195-202

Jost, W., Link, S., Horstmann, V., Decker, E.L., Reski, R., and Gorr, G. (2005). Isolation and characterisation of three moss-derived beta-tubulin promoters suitable for recombinant expression. *Curr Genet*, **47:** 111-120

Kamath, R., Fraser, A., Dong, Y., Poulin, G., Durbin, R., Gotta, M., Kanapin, A., Le Bot, N., Moreno, S., Sohrmann, M., Welchman, D., Zipperlen, P., and Ahringer, J. (2003). Systematic functional analysis of the *Caenorhabditis elegans* genome using RNAi. *Nature*, **421:** 231-237

Kammerloher, W., Fischer, U., Piechottka, G.P., and Schaffner, A.R. (1994). Water channels in the plant plasma membrane cloned by immunoselection from a mammalian expression system. *Plant J*, **6:** 187-199

Kapust, R.B., and Waugh, D.S. (1999). *Escherichia coli* maltose-binding protein is uncommonly effective at promoting the solubility of polypeptides to which it is fused. *Protein Sci*, **8:** 1668-1674

Karakousis, A., Barr, A., Kretschmer, J., Manning, S., Jefferies, S., Chalmers, K., Islam, A., and Langridge, P. (2003). Mapping and QTL analysis of the barley population Clipper × Sahara. *Australian Journal of Agricultural Research*, **54:** 1137-1140

Keegstra, K., and Raikhel, N. (2001). Plant glycosyltransferases. *Curr Opin Plant Biol*, **4:** 219-224

Kikuchi, N., Kwon, Y., Gotoh, M., and Narimatsu, H. (2003). Comparison of glycosyltransferase families using the profile hidden Markov model. *Biochem Biophys Res Commun*, **310:** 574-579

Kim, U., Birren, B., Slepak, T., Mancino, V., Boysen, C., Kang, H., Simon, M., and Shizuya, H. (1996). Construction and characterization of a human bacterial artificial chromosome library. *Genomics*, **34:** 213-218

Kimura, S., Laosinchai, W., Itoh, T., Cui, X., Linder, C., and Brown, R.J. (1999). Immunogold labeling of rosette terminal cellulose-synthesizing complexes in the vascular plant *vigna angularis*. *Plant Cell*, **11:** 2075-2086

Klahre, U., Crete, P., Leuenberger, S., Iglesias, V., and Meins, F.J. (2002). High molecular weight RNAs and small interfering RNAs induce systemic posttranscriptional gene silencing in plants. *Proc Natl Acad Sci U S A*, **99:** 11981-11986

Kleene, R., and Berger, E.G. (1993). The molecular and cell biology of glycosyltransferases. *Biochim Biophys Acta*, **1154:** 283-325

Kobayashi, M., Matoh, T., and Azuma, J. (1996). Two chains of rhamnogalacturonan II are cross-linked by borate-diol ester bonds in higher plant cell walls. *Plant Physiol*, **110:** 1017-1020

Kohler, F., and Muller, K. (2003). Adaptation of the Ras-recruitment system to the analysis of interactions between membrane-associated proteins. *Nucleic Acids Res*, **31:** e28

Kokubo, A., Kuraishi, S., and Sakurai, N. (1989). Culm strength of barley. *Plant Physiology*, **91:** 876-872

Komarnytsky, S., Gaume, A., Garvey, A., Borisjuk, N., and Raskin, I. (2004). A quick and efficient system for antibiotic-free expression of heterologous genes in tobacco roots. *Plant Cell Rep*, **22:** 765-773

Koprivova, A., Altmann, F., Gorr, G., Kopriva, S., Reski, R., and Decker, E. (2003). N-glycosylation in the moss *Physcomitrella patens* is organised similarly to that in higher plants. *Plant Biol*, **5:** 582-591

Kost, T.A. (1997). Expression systems: Gene expression systems in the genomics era. *Curr Opin Biotechnol*, **8:** 539-541

Kruscal, J. (1964). Multidimentional scaling by optimising goodness of fit to a nonmetric hypothesis. *Psychometrika*, **29:** 1-27

Krysan, P., Young, J., and Sussman, M. (1999). T-DNA as an insertional mutagen in *Arabidopsis*. *Plant Cell*, **11:** 2283-2290

Kudlicka, K., and Brown, R.M. (1997). Cellulose and callose biosynthesis in higher plants (I. solubilization and separation of (1,3)- and (1,4)-beta-glucan synthase activities from mung bean). *Plant Physiol*, **115:** 643-656

Kurland, C., and Gallant, J. (1996). Errors of heterologous protein expression. *Curr Opin Biotechnol*, **7:** 489-493

Kuroyama, H., and Tsumuraya, Y. (2001). A xylosyltransferase that synthesizes beta-(1,4)-xylans in wheat (*Triticum aestivum* L.) seedlings. *Planta*, **213:** 231-240

Lacomme, C., Hrubikova, K., and Hein, I. (2003). Enhancement of virus-induced gene silencing through viral-based production of inverted-repeats. *Plant J*, **34:** 543-553

Laemmli, U. (1970). Cleavage of structural proteins during the assembly of the head of bacteriophage T4. *Nature*, **277:** 680-685

Lai-Kee-Him, J., Chanzy, H., Muller, M., Putaux, J., Imai, T., and Bulone, V. (2002). *In vitro* versus *in vivo* cellulose microfibrils from plant primary wall synthases: structural differences. *J Biol Chem*, **277:** 36931-36939

Lane, B.G. (2000). Oxalate oxidases and differentiating surface structure in wheat: germins. *Biochem J*, **349**: 309-321

Landy, A. (1989). Dynamic, structural, and regulatory aspects of λ site-specific recombination. *Annu. Rev. Biochem.*, **58:** 913-949

Lapierre, C., Pollet, B., Ralet, M.C., and Saulnier, L. (2001). The phenolic fraction of maize bran: evidence for lignin-heteroxylan association. *Phytochemistry*, **57:** 765-772

LaVallie, E.R., DiBlasio, E.A., Kovacic, S., Grant, K.L., Schendel, P.F., and McCoy, J.M. (1993). A thioredoxin gene fusion expression system that circumvents inclusion body formation in the *E. coli* cytoplasm. *Biotechnology (N Y)*, **11:** 187-193

Leavitt, R. (1904). Trichomes of the root in vascular cryptograms and angiosperms. *Proc Boston Soc Nat Hist*, **31:** 273-313

Lee, R.C., Burton, R.A., Hrmova, M., and Fincher, G.B. (2001). Barley arabinoxylan arabinofuranohydrolases: purification, characterization and determination of primary structures from cDNA clones. *Biochem J*, **356:** 181-189

Leemans, J., Shaw, C., Deblaere, R., De Greve, H., Hernalsteens, J., Maes, M., Van Montagu, M., and Schell, J. (1981). Site-specific mutagenesis of *Agrobacterium* Ti plasmids and transfer of genes to plant cells. *Mol Appl Genet*, **1:** 149-164

Li, J., Burton, R., Harvey, A., Hrmova, M., Wardak, A., Stone, B., and Fincher, G. (2003). Biochemical evidence linking a putative callose synthase gene with (1 --> 3)-beta-D-glucan biosynthesis in barley. *Plant Mol Biol*, **53:** 213-225

Li, X., Cordero, I., Caplan, J., Molhoj, M., and Reiter, W. (2004). Molecular analysis of 10 coding regions from *Arabidopsis* that are homologous to the *MUR3* xyloglucan galactosyltransferase. *Plant Physiol*, **134:** 940-950

Li, X., Lassner, M., and Zhang, Y. (2002). Deleteagene: a fast neutron deletion mutagenesis-based gene knockout system for plants. *Comp Funct Genom*, **3:** 158-160

Li, X., and Zhang, Y. (2002). Reverse genetics by fast neutron mutagenesis in higher plants. *Funct Integr Genomics*, **2:** 254-258

Li, Y., Geng, Y., Song, H., Zheng, G., Huan, L., and Qiu, B. (2004). Expression of a human lactoferrin N-lobe in *Nicotiana benthmiana* with potato virus X-based agroinfection. *Biotechnol Lett*, **26:** 953-957

Liang, P., and Pardee, A. (1992). Differential display of eukaryotic messenger RNA by means of the polymerase chain reaction. *Science*, **257:** 967-971

Liepman, A.H., Wilkerson, C.G., and Keegstra, K. (2005). Expression of cellulose synthase-like (*Csl*) genes in insect cells reveals that *CslA* family members encode mannan synthases. *Proc Natl Acad Sci U S A*,

Lima, D.U., Loh, W., and Buckeridge, M.S. (2004). Xyloglucan-cellulose interaction depends on the sidechains and molecular weight of xyloglucan. *Plant Physiol Biochem*, **42:** 389-394

Lind, T., Tufaro, F., McCormick, C., Lindahl, U., and Lidholt, K. (1998). The putative tumor suppressors EXT1 and EXT2 are glycosyltransferases required for the biosynthesis of heparan sulfate. *J Biol Chem*, **273:** 26265-26268

Lipshutz, R., Fodor, S., Gingeras, T., and Lockhart, D. (1999). High density synthetic oligonucleotide arrays. *Nat Genet*, **21:** 20-24

Liu, L., Eriksson, K., and Dean, J. (1995). Localization of hydrogen peroxide production in *Pisum sativum* L. using epi-polarization microscopy to follow cerium perhydroxide deposition. *Plant Physiol*, **107:** 501-506

Llave, C., Kasschau, K., Rector, M., and Carrington, J. (2002a). Endogenous and silencing-associated small RNAs in plants. *Plant Cell*, **14:** 1605-1619

Llave, C., Xie, Z., Kasschau, K.D., and Carrington, J.C. (2002b). . Cleavage of Scarecrow-like mRNA targets directed by a class of *Arabidopsis* miRNA. *Science*, **297:** 2053-2056

Lorimer, G.H. (1996). A quantitative assessment of the role of the chaperonin proteins in protein folding *in vivo*. *Faseb J*, **10:** 5-9

Louvet, O., Doignon, F., and Crouzet, M. (1997). Stable DNA-binding yeast vector allowing high-bait expression for use in the two-hybrid system. *Biotechniques*, **23:** 816-819

Lynch, M.A., and Staehelin, L.A. (1992). Domain-specific and cell type-specific localization of two types of cell wall matrix polysaccharides in the clover root tip. *J Cell Biol*, **118:** 467-479

MacGregor, A., and Fincher, G. (1993). Carbohydrates of the barley grain. *In* Barley Chemistry and Technology, Macgregor, A., and Bhatty, R., eds, pp 73-130

Madson, M., Dunand, C., Li, X., Verma, R., Vanzin, G., Caplan, J., Shoue, D., Carpita, N., and Reiter, W. (2003). The *MUR3* gene of *Arabidopsis* encodes a xyloglucan galactosyltransferase that is evolutionarily related to animal exostosins. *Plant Cell*, **15:** 1662-1670

Makrides, S.C. (1999). Components of vectors for gene transfer and expression in mammalian cells. *Protein Expr Purif*, **17:** 183-202

Malissard, M., Dinter, A., Berger, E., and Hennet, T. (2002). Functional assignment of motifs conserved in beta 1,3-glycosyltransferases. *Eur J Biochem*, **269:** 233-239

Malissard, M., Zeng, S., and Berger, E.G. (1999). The yeast expression system for recombinant glycosyltransferases. *Glycoconj J*, **16:** 125-139

Mallory, A., and Vaucheret, H. (2004). MicroRNAs: something important between the genes. *Curr Opin Plant Biol*, **7:** 120-125

Manly, K., Cudmore, J., RH, and Meer, J. (2001). Map Manager QTX, cross-platform software for genetic mapping. *Mammalian Genome*, **12:** 930-932

Marillonnet, S., Giritch, A., Gils, M., Kandzia, R., Klimyuk, V., and Gleba, Y. (2004). *In planta* engineering of viral RNA replicons: efficient assembly by recombination of DNA modules delivered by *Agrobacterium*. *Proc Natl Acad Sci U S A*, **101:** 6852-6857

Marino, M. (1989). Expression systems for heterologous protein production. *BioPharm*, **2:** 18-33

Matzke, M., Matzke, A., and Kooter, J. (2001). RNA: guiding gene silencing. *Science*, **293:** 1080-1083

McCallum, C., Comai, L., Greene, E., and Henikoff, S. (2000). Targeting induced local lesions IN genomes (TILLING) for plant functional genomics.

McCarroll, L., and King, L.A. (1997). Stable insect cell cultures for recombinant protein production. *Curr Opin Biotechnol*, **8:** 590-594

McGuffin, L., Bryson, K., and Jones, D. (2000). The PSIPRED protein structure prediction server. *Bioinformatics*, **16:** 404-405

McMaugh, S., and Lyon, B. (2003). Real-Time quantitative RT-PCR assay of gene expression in plant roots during fungal pathogenesis. *Biotechniques*, **34:** 982-986

McQueen-Mason, S., Durachko, D., and Cosgrove, D. (1992). Two endogenous proteins that induce cell wall extension in plants. *Plant Cell*, **4:** 1425-1433

Meikle, P., Ng, K., Johnson, E., Hoogenraad, N., and Stone, B. (1991). The beta-glucan synthase from *Lolium multiflorum*. Detergent solubilization, purification using monoclonal antibodies, and photoaffinity labeling with a novel photoreactive pyrimidine analogue of uridine 5'-diphosphoglucose. *J. Biol. Chem*, **266:** 22569-22581

Mette, M., van der Winden, J., Matzke, M., and Matzke, A. (2002). Short RNAs can identify new candidate transposable element families in *Arabidopsis*. *Plant Physiol*, **130:** 6-9

Mlotshwa, S., Voinnet, O., Mette, M., Matzke, M., Vaucheret, H., Ding, S., Pruss, G., and Vance, V. (2002). RNA silencing and the mobile silencing signal. *Plant Cell*, **14:** S289-301

Mohnen, D. (1999). Biosynthesis of pectins and galactomannans. *In* Carbohydrates and Their Derivatives Including Tannins, Cellulose and Related Lignins, Barton, D., Nakanishi, K., and Meth-Cohn, O., eds, Vol 3. Elsevier Science, Amstredam, pp 497-527

Montgomery, R., and Dallman, M. (1997). Semi-quantitative polymerase chain reaction analysis of cytokine and cytokine receptor gene expression during thymic ontogeny. *Cytokine*, **9:** 717-726

Moore, P.J., Swords, K.M., Lynch, M.A., and Staehelin, L.A. (1991). Spatial organization of the assembly pathways of glycoproteins and complex polysaccharides in the Golgi apparatus of plants. *J Cell Biol*, **112:** 589-602

Morrison, T., Weis, J., and Wittwer, C. (1998). Quantification of low-copy transcripts by continuous SYBR Green I monitoring during amplification. *Biotechniques*, **24:** 954-958

Muntz, K., Belozersky, M., Dunaevsky, Y., Schlereth, A., and Tiedemann, J. (2001). Stored proteinases and the initiation of storage protein mobilization in seeds during germination and seedling growth. *J Exp Bot*, **52:** 1741-1752

Murashige, T., and Skoog, F. (1962). A revised medium for rapid growth and bioassays with tobacco cultures. *Physiologia Plantarum*, **15:** 473-497

Murray, E., Lotzer, J., and Eberle, M. (1989). Codon usage in plant genes. *Nucleic Acids Res*, **25:** 477-498

Murray, F., Brettell, R., Matthews, P., Bishop, D., and Jacobsen, J. (2004). Comparison of *Agrobacterium*-mediated transformation of four barley cultivars using the GFP and GUS reporter genes. *Plant Cell Rep*, **22:** 397-402

Napoli, C., Lemieux, C., and Jorgensen, R. (1990). Introduction of a chimeric chalcone synthase gene into petunia results in reversible co-suppression of homologous genes in trans. *Plant Cell*, **2:** 279-289

Needleman, S.B., and Wunsch, C.D. (1970). A general method applicable to the search for similarities in the amino acid sequence of two proteins. *J Mol Biol*, **48:** 443-453

Neumann, U., Brandizzi, F., and Hawes, C. (2003). Protein transport in plant cells: in and out of the Golgi. *Ann Bot*, **92:** 167-180

Nielsen, H., Engelbrecht, J., Brunak, S., and von Heijne, G. (1997). Identification of prokaryotic and eukaryotic signal peptides and prediction of their cleavage sites. *Protein Eng*, **10:** 1-6

Nielsen, H., and Krogh, A. (1998). Prediction of signal peptides and signal anchors by a hidden Markov model. *In* The Sixth International Conference on Intelligent Systems for Molecular Biology (ISMB 6), AAAI Press, Menlo Park, California, pp 122-130

Northcote, D.H., Davey, R., and Lay, J. (1989). Use of antisera to localize callose, xylan and arabinogalactan in the cell-plate, primary and secondary walls of plant cells. *Planta*, **178:** 353-366

Northcote, D.H., and Pickett-Heaps, J.D. (1966). A function of the Golgi apparatus in polysaccharide synthesis and transport in root-cap cells of wheat. *Biochemical J,* **98:** 159-167

Nunan, K., and Scheller, H. (2003). Solubilization of an arabinan arabinosyltransferase activity from mung bean hypocotyls. *Plant Physiol*, **132:** 331-342

O'Neill, M., Ishii, T., Albersheim, P., and Darvill, A. (2004). Rhamnogalacturonan II: structure and function of a borate cross-linked cell wall pectic polysaccharide. *Annu Rev Plant Physiol Plant Mol Biol*, **55:** 109-139

O'Neill, M., and York, W. (2003). The composition and structure of plant primary cell walls. BlackwellPages

Ohtsuki, S., Levine, M., and Cai, H. (1998). Different core promoters possess distinct regulatory activities in the *Drosophila* embryo. *Genes Dev*, **12:** 547-556

Olins, P.O. (1996). Quantity versus authenticity of heterologously produced proteins: an inevitable compromise? *Curr Opin Biotechnol*, **7:** 487-488

Opekarova, M., Robl, I., Grassl, R., and Tanner, W. (1999). Expression of eukaryotic plasma membrane transporter HUP1 from *Chlorella kessleri* in *Escherichia coli*. *FEMS Microbiol Lett*, **174:** 65-72

Opekarova, M., and Tanner, W. (2003). Specific lipid requirements of membrane proteins-a putative bottleneck in heterologous expression. *Biochim Biophys Acta*, **1610:** 11-22

Pagny, S., Bouissonnie, F., Sarkar, M., Follet-Gueye, M., Driouich, A., Schachter, H., Faye, L., and Gomord, V. (2003). Structural requirements for *Arabidopsis* beta1,2-xylosyltransferase activity and targeting to the Golgi. *Plant J*, **33:** 189-203

Palauqui, J., Elmayan, T., Pollien, J., and Vaucheret, H. (1997). Systemic acquired silencing: transgene-specific post-transcriptional silencing is transmitted by grafting from silenced stocks to non-silenced scions. *EMBO J*, **16:** 4738-4745

Parinov, S., Sevugan, M., Ye, D., Yang, W., Kumaran, M., and Sundaresan, V. (1999). Analysis of flanking sequences from dissociation insertion lines: a database for reverse genetics in *Arabidopsis*. *Plant Cell*, **11:** 2263-2270

Park, W., Li, J., Song, R., Messing, J., and Chen, X. (2002). CARPEL FACTORY, a Dicer homolog, and *HEN1*, a novel protein, act in microRNA metabolism in *Arabidopsis thaliana*. *Curr Biol*, **12:** 1484-1495

Parker, R., and Barnes, N. (1999). mRNA: detection by *in Situ* and northern hybridization. *Methods Mol Biol*, **106:** 247-283

Pear, J., Kawagoe, Y., Schreckengost, W., Delmer, D., and Stalker, D. (1996). Higher plants contain homologs of the bacterial *celA* genes encoding the catalytic subunit of cellulose synthase. *Proc Natl Acad Sci USA*, **93:** 1263712642

Pena, M., Ryden, P., Madson, M., Smith, A., and Carpita, N. (2004). The galactose residues of xyloglucan are essential to maintain mechanical strength of the primary cell walls in *Arabidopsis* during growth. *Plant Physiol*, **134:** 443-451

Perlin, A. (1951). Structure of the soluble pentosans of wheat flours. *Cereal Chem.*, **28:** 382-393

Perrin, R. (2001). Cellulose: how many cellulose synthases to make a plant? *Curr Biol*, **11:** R213-216

Perrin, R., DeRocher, A., Bar-Peled, M., Zeng, W., Norambuena, L., Orellana, A., Raikhel, N., and Keegstra, K. (1999). Xyloglucan fucosyltransferase, an enzyme involved in plant cell wall biosynthesis. *Science*, **284:** 1976-1979

Perrin, R., Jia, Z., Wagner, T., O'Neill, M., Sarria, R., York, W., Raikhel, N., and Keegstra, K. (2003). Analysis of xyloglucan fucosylation in *Arabidopsis*. *Plant Physiol*, **132:** 768-778

Perrin, R., Wilkerson, C., and Keegstra, K. (2001). Golgi enzymes that synthesize plant cell wall polysaccharides: finding and evaluating candidates in the genomic era. *Plant Mol Biol*, **47**

Persans, M.W., Nieman, K., and Salt, D.E. (2001). Functional activity and role of cation-efflux family members in Ni hyperaccumulation in *Thlaspi goesingense*. *Proc. Natl. Acad. Sci. U S A*, **98:** 9995-10000

Persson, K., Ly, H., Dieckelmann, M., Wakarchuk, W., Withers, S., and Strynadka, N. (2001). Crystal structure of the retaining galactosyltransferase LgtC from *Neisseria meningitidis* in complex with donor and acceptor sugar analogs. *Nat Struct Biol*, **8:** 166-175

Peugnet, I., Goubet, F., Bruyant-Vannier, M.P., Thoiron, B., Morvan, C., Schols, H.A., and Voragen, A.G. (2001). Solubilization of rhamnogalacturonan I galactosyltransfrases from membranes of a flax cell suspension. *Planta*, **213:** 435-445

Phizicky, E.M., and Fields, S. (1995). Protein-protein interactions: methods for detection and analysis. *Microbiol Rev*, **59:** 94-123

Podrazky, V. (1964). Some charcteristics of cereal gums. *Chem. Ind.*: 712-713

Poirot, O., Suhre, K., Abergel, C., O'Toole, E., and Notredame, C. (2004). 3DCoffee@igs: a web server for combining sequences and structures into a multiple sequence alignment. *Nucleic Acids Res*, **32:** W37-40

Potvin, B., and Stanley, P. (1991). Activation of two new alpha(1,3)fucosyltransferase activities in Chinese hamster ovary cells by 5-azacytidine. *Cell Regul*, **2:** 989-1000

Prashar, Y., and Weissman, S. (1996). Analysis of differential gene expression by display of 3' end restriction fragments of cDNAs. *Proc Natl Acad Sci U S A*, **93:** 6659-6663

Rabouille, C., Hui, N., Hunte, F., Kieckbusch, R., Berger, E., Warren, G., and Nilsson, T. (1995). Mapping the distribution of Golgi enzymes involved in the construction of complex oligosaccharides. *J Cell Sci*, **108**

Raikhel, N., and Chrispeels, M. (2000). Protein sorting and vesicle traffic. *In* Biochemistry & Molecular biology Of Plants, Buchanan, B.B., Gruissem, W., and Jones, R., eds. The American Society of Plant physiologists, pp 160-201

Ramesh, H.P., and Tharanathan, R.N. (2003). Carbohydrates--the renewable raw materials of high biotechnological value. *Crit Rev Biotechnol*, **23:** 149-173

Ramirez-Zavala, B., Mercado-Flores, Y., Hernandez-Rodriguez, C., and Villa-Tanaca, L. (2004). Purification and characterization of a serine carboxypeptidase from *Kluyveromyces marxianus*. *Int J Food Microbiol*, **91:** 245-252

Rappolee, D., Wang, A., Mark, D., and Werb, Z. (1989). Novel method for studying mRNA phenotypes in single or small numbers of cells. *J Cell Biochem*, **39:** 1-11

Reid, J., Edwards, M., Dickson, C., Scott, C., and Gidley, M. (2003). Tobacco transgenic lines that express fenugreek galactomannan galactosyltransferase constitutively have structurally altered galactomannans in their seed endosperm cell walls. *Plant Physiol*, **131:** 1487-1495

Reinhart, B., Weinstein, E., Rhoades, M., Bartel, B., and Bartel, D. (2002). MicroRNAs in plants. *Genes Dev*, **16:** 1616-1626

Reiter, W. (1998). The molecular analysis of cell wall components. *Elsevier Science Ltd.*, **3:** 27-32

Reiter, W. (2002). Biosynthesis and properties of the plant cell wall. *Curr Opin Plant Biol*, **5:** 536-542

Reiter, W., Chapple, C., and Somerville, C. (1997). Mutants of *Arabidopsis thaliana* with altered cell wall polysaccharide composition. *Plant J*, **12:** 335-345

Reski, R., and Cove, D.J. (2004). *Physcomitrella patens*. *Curr Biol*, **14:** R261-262

Rhoades, M., Reinhart, B., Lim, L., Burge, C., Bartel, B., and Bartel, D. (2002). Prediction of plant microRNA targets. *Cell*, **110:** 513-520

Richmond, T. (2000). Higher plant cellulose synthases. *Genome Biol.*, **1:** 1-5

Richmond, T., and Somerville, C. (2000). The cellulose synthase superfamily. *Plant Physiol*, **124:** 495-498

Richmond, T., and Somerville, C. (2001). Integrative approaches to determining Csl function. *Plant Mol Biol*, **47:** 131-143

Ririe, K., Rasmussen, R., and Wittwer, C. (1997). Product differentiation by analysis of DNA melting curves during the polymerase chain reaction. *Anal Biochem*, **245:** 154-160

Robl, I., Grassl, R., Tanner, W., and Opekarova, M. (2000). Properties of a reconstituted eukaryotic hexose/proton symporter solubilized by structurally related non-ionic detergents: specific requirement of phosphatidylcholine for permease stability. *Biochim Biophys Acta*, **1463:** 407-418

Rosen, M.L., Edman, M., Sjostrom, M., and Wieslander, A. (2004). Recognition of fold and sugar linkage for glycosyltransferases by multivariate sequence analysis. *J Biol Chem*, **279:** 38683-38692

Ross, J., Li, Y., Lim, E., and Bowles, D. (2001). Higher plant glycosyltransferases. *Genome Biology*, **2:** R3004.3001-3006

Rost, B., Liu, J., Nair, R., Wrzeszczynski, K.O., and Ofran, Y. (2003). Automatic prediction of protein function. *Cell Mol Life Sci*, **60:** 2637-2650

Roth, J. (1991). Localization of glycosylation sites in the Golgi apparatus using immunolabeling and cytochemistry. *J Electron Microsc Tech*, **17:** 121-131

Ruan, Y., Gilmore, J., and Conner, T. (1998). Towards *Arabidopsis* genome analysis: monitoring expression profiles of 1400 genes using cDNA microarrays. *Plant J*, **15:** 821-833

Ryden, P., Sugimoto-Shirasu, K., Smith, A., Findlay, K., Reiter, W., and McCann, M. (2003). Tensile properties of *Arabidopsis* cell walls depend on both a xyloglucan cross-linked microfibrillar network and rhamnogalacturonan II-borate complexes. *Plant Physiol*, **132:** 1033-1040

Saccomanno, C., Bordonaro, M., Chen, J., and Nordstrom, J. (1992). A faster ribonuclease protection assay. *Biotechniques*, **13:** 846-850

Sadhukhan, R., and Sen, I. (1996). Different glycosylation requirements for the synthesis of enzymatically active angiotensin-converting enzyme in mammalian cells and yeast. *J Biol Chem*, **271:** 6429-6434

Sakurai, N., and Masuda, Y. (1978). Auxin-induced changes in barley coleoptile cell wall composition. *Plant Cell Physiol*, **19:** 1217-1223

Sanger, F., Nicklen, S., and Coulson, A. (1977). DNA sequencing with chain-terminating inhibitors. *Proc Natl Acad Sci U S A*, **74:** 5463-5467

Sargent, T. (1987). Isolation of differentially expressed genes. *Meth Enzymol*, **152:** 423-432

Sawasaki, T., Hasegawa, Y., Morishita, R., Seki, M., Shinozaki, K., and Endo, Y. (2004). Genome-scale, biochemical annotation method based on the wheat germ cell-free protein synthesis system. *Phytochemistry*, **65:** 1549-1555

Sawasaki, T., Ogasawara, T., Morishita, R., and Endo, Y. (2002). A cell-free protein synthesis system for high-throughput proteomics. *Proc Natl Acad Sci U S A*, **99:** 14652-14657

Saxena, I., and Brown, R.J. (2000). Cellulose synthases and related enzymes. *Curr Opin Plant Biol*, **3:** 523-531

Schaefer, D.G., and Zryd, J.P. (1997). Efficient gene targeting in the moss *Physcomitrella patens*. *Plant J.*, **11:** 1195-1206

Schagger, H., Cramer, W.A., and von Jagow, G. (1994). Analysis of molecular masses and oligomeric states of protein complexes by blue native electrophoresis and

isolation of membrane protein complexes by two-dimensional native electrophoresis. *Analytical Biochem,* **217:** 220-230

Scheible, W.R., and Pauly, M. (2004). Glycosyltransferases and cell wall biosynthesis: novel players and insights. *Curr Opin Plant Biol*, **7:** 285-295

Scherer, L., and Rossi, J. (2003). Approaches for the sequence-specific knockdown of mRNA. *Nat Biotechnol*, **21:** 1457-1465

Schiefelbein, J.W. (2000). Constructing a plant cell. The genetic control of root hair development. *Plant Physiol*, **124:** 1525-1531

Schmittgen, T., Zakrajsek, B., Mills, A., Gorn, V., Singer, M., and Reed, M. (2000). Quantitative reverse transcription-polymerase chain reaction to study mRNA decay: comparison of endpoint and real-time methods. *Anal Biochem*, **285:** 194-204

Schnepf, E. (1986). Cellular polarity. *Annu Rev Plant Physiol*, **37:** 23-47

Schünmann, P., Smith, R., Lang, V., Mattews, P., and Chandler, P. (1997). Expression of XET-related genes and its relation to elongation in leaves of barley (*Hordeum vulgare* L.). *Plant, Cell and Environment*, **20:** 1439

Schweizer, P., Pokorny, J., Schulze-Lefert, P., and Dudler, R. (2000). Technical advance. Double-stranded RNA interferes with gene function at the single-cell level in cereals. *Plant J*, **24:** 895-903

Selth, L.A., Randles, J.W., and Rezaian, M.A. (2004). Host responses to transient expression of individual genes encoded by tomato leaf curl virus. *Mol Plant Microbe Interact*, **17:** 27-33

Serebriiskii, I., Estojak, J., Berman, M., and Golemis, E. (2000). Approaches to detecting false positives in yeast two-hybrid systems. *Biotechniques*, **28:** 328-330

Shimkets, R., Lowe, D., Tai, J., Sehl, P., Jin, H., Yang, R., Predki, P., Rothberg, B., Murtha, M., Roth, M., Shenoy, S., Windemuth, A., Simpson, J., Simons, J., Daley, M., Gold, S., McKenna, M., Hillan, K., Went, G., and Rothberg, J. (1999). Gene expression analysis by transcript profiling coupled to a gene database query. *Nat Biotechnol*, **17:** 798-803

Siebert, P., Chenchik, A., Kellogg, D., Lukyanov, K., and Lukyanov, S. (1995). An improved PCR method for walking in uncloned genomic DNA. *Nucleic Acids Res*, **23:** 1087-1088

Simmons, A.D., Musy, M.M., Lopes, C.S., Hwang, L.Y., Yang, Y.P., and Lovett, M. (1999). A direct interaction between EXT proteins and glycosyltransferases is defective in hereditary multiple exostoses. *Hum Mol Genet*, **8:** 2155-2164

Slocum, R., and Furey, M. (1991). Electron-microscopic cytochemical localization of diamine and polyamine oxidases in pea and maize tissues. *Planta*, **183:** 443-450

Smith, B.G., and Harris, P.J. (1999). The polysaccharide composition of Poales cell walls: Poaceae are not unique. *Biochemical Systematics and Ecology*, **27:** 33-53

Smith, C., Watson, C., Bird, C., Ray, J., Schuch, W., and Grierson, D. (1990). Expression of a truncated tomato polygalacturonase gene inhibits expression of the endogenous gene in transgenic plants. *Mol Gen Genet*, **224:** 477-481

Smith, D.B. (2000). Generating fusions to glutathione S-transferase for protein studies. *Methods Enzymol*, **326:** 254-270

Smith, D.B., and Johnson, K.S. (1988). Single-step purification of polypeptides expressed in *Escherichia coli* as fusions with glutathione S-transferase. *Gene*, **67:** 31-40

Smith, N.A., Singh, S.P., Wang, M.B., Stoutjesdijk, P.A., Green, A.G., and Waterhouse, P.M. (2000). Total silencing by intron-spliced hairpin RNAs. *Nature*, **407:** 319-320

Somerville, C., Bauer, S., Brininstool, G., Facette, M., Hamann, T., Milne, J., Osborne, E., Paredez, A., Persson, S., Raab, T., Vorwerk, S., and Youngs, H. (2004). Toward a systems approach to understanding plant cell walls. *Science*, **306:** 2206-2211

Sonnhammer, E., von Heijne, G., and Krogh, A. (1998). A hidden Markov model for predicting transmembrane helices in protein sequences. *Proc Int Conf Intell Syst Mol Biol*, **6:** 175-182

Speulman, E., Metz, P., van Arkel, G., te Lintel Hekkert, B., Stiekema, W., and Pereira, A. (1999). A two-component enhancer-inhibitor transposon mutagenesis system for functional analysis of the *Arabidopsis* genome. *Plant Cell*, **11:** 1853-1866

Spremulli, L. (2000). Protein synthesis, assembly, and degradation. *In* Biochemistry & Molecular biology Of Plants, Buchanan, B.B., Gruissem, W., and Jones, R., eds. The American Society of Plant physiologists, pp 412-454

Srisodsuk, M., Kleman-Leyer, K., Keränen, S., Kirk, T., and Teeri, T. (1998). Modes of action on cotton and bacterial cellulose of a homologous endoglucanase-exoglucanase pair from *Trichoderma reesei*. *Eur J Biochem*, **251:** 885-892

Staehelin, L.A., and Moore, I. (1995). The plant Golgi apparatus: structure, functional organization and trafficking mechanisms. *Annu. Rev. Plant Physiol. Plant Mol. Biol.*, **46:** 261-288

Stagljar, I., Korostensky, C., Johnsson, N., and te Heesen, S. (1998). A genetic system based on split-ubiquitin for the analysis of interactions between membrane proteins in vivo. *Proc Natl Acad Sci U S A*, **95:** 5187-5192

Sterling, J., Quigley, H., Orellana, A., and Mohnen, D. (2001). The catalytic site of the pectin biosynthetic enzyme alpha-1,4-galacturonosyltransferase is located in the lumen of the Golgi. *Plant Physiol*, **127:** 360-371

Strous, G.J., and Berger, E.G. (1982). Biosynthesis, intracellular transport, and release of the Golgi enzyme galactosyltransferase (lactose synthetase A protein) in HeLa cells. *J Biol Chem*, **257:** 7623-7628

Sutcliffe, J., Foye, P., Erlander, M., Hilbush, B., Bodzin, L., Durham, J., and Hasel, K. (2000). TOGA: an automated parsing technology for analyzing expression of nearly all genes. *Proc Natl Acad Sci U S A*, **97:** 1976-1981

Tanaka, K., Murata, K., Yamazaki, M., Onosato, K., Miyao, A., and Hirochika, H. (2003). Three distinct rice cellulose synthase catalytic subunit genes required for cellulose synthesis in the secondary wall. *Plant Physiol*, **133:** 73-83

Tang, G., Reinhart, B., Bartel, D., and Zamore, P. (2003). A biochemical framework for RNA silencing in plants. *Genes Dev*, **17:** 49-63

Tani, H., Chen, X., Nurmberg, P., Grant, J., SantaMaria, M., Chini, A., Gilroy, E., Birch, P., and Loake, G. (2004). Activation tagging in plants: a tool for gene discovery. *Funct Integr Genomics*,

Taylor, N., Howells, R., Huttly, A., Vickers, K., and Turner, S. (2003). Interactions among three distinct CesA proteins essential for cellulose synthesis. *Proc Natl Acad Sci U S A*, **100:** 1450-1455

Taylor, N., Laurie, S., and Turner, S. (2000). Multiple cellulose synthase catalytic subunits are required for cellulose synthesis in *Arabidopsis*. *Plant Cell*, **12:** 2529-2540

Tenllado, F., Llave, C., and Diaz-Ruiz, J. (2004). RNA interference as a new biotechnological tool for the control of virus diseases in plants. *Virus Res*, **102:** 85-96

Terpe, K. (2003). Overview of tag protein fusions: from molecular and biochemical fundamentals to commercial systems. *Appl Microbiol Biotechnol*, **60:** 523-533

Thaminy, S., Miller, J., and Stagljar, I. (2004). The split-ubiquitin membrane-based yeast two-hybrid system. *In* Protein-Protein Interactions, Fu, H., ed, Vol 261. Humana Press, pp 297-312

Thompson, J.D., Higgins, D.G., and Gibson, T.J. (1994). CLUSTAL W: improving the sensitivity of progressive multiple sequence alignment through sequence weighting, position-specific gap penalties and weight matrix choice. *Nucleic Acids Res*, **22:** 4673-4680

Till, B., Reynolds, S., Greene, E., Codomo, C., Enns, L., Johnson, J., Burtner, C., Odden, A., Young, K., Taylor, N., Henikoff, J., Comai, L., and Henikoff, S. (2003). Large-scale discovery of induced point mutations with high-throughput TILLING. *Genome Res*, **13:** 524-530

Tingay, S., McElroy, D., Kalla, R., Fieg, S., Wang, M., Thornton, S., and Brettell, R. (1997). *Agrobacterium tumefaciens*-mediated barley transformation. *The Plant Journal*, **11:** 1369-1376

Turner, A., Bacic, A., Harris, P.J., and Read, S.M. (1998). Membrane fractionation and enrichment of callose synthase from pollen tubes of *Nicotiana alata* Link et Otto. *Planta*, **205:** 380-388

Tyagi, S., and Kramer, F. (1996). Molecular beacons: probes that fluoresce upon hybridization. *Nat Biotechnol*, **14:** 303-308

Van Criekinge, W., and Beyaert, R. (1999). Yeast two-hybrid: state of the art. *Biol Proced Online*, **2:** 1-38

van der Krol, A., Mur, L., Beld, M., Mol, J., and Stuitje, A. (1990). Flavonoid genes in petunia: addition of a limited number of gene copies may lead to a suppression of gene expression. *Plant Cell*, **2:** 291-299

van Vliet, C., Thomas, E., Merino-Trigo, A., Teasdale, R., and Gleeson, P. (2003). Intracellular sorting and transport of proteins. *Prog Biophys Mol Biol*, **83:** 1-45

Vanden Heuvel, J., Tyson, F., and DA, B. (1993). Construction of recombinant RNA templates for use as internal standards in quantitative RT-PCR. *Biotechniques*, **14:** 395-398

Vandesompele, J., De Preter, K., Pattyn, F., Poppe, B., Van Roy, N., De Paepe, A., and Speleman, F. (2002). Accurate normalization of real-time quantitative RT-PCR data by geometric averaging of multiple internal control genes. *Genome Biol.*, **3:** Research0034

Vanzin, G., Madson, M., Carpita, N., Raikhel, N., Keegstra, K., and Reiter, W. (2002). The *mur2* mutant of *Arabidopsis thaliana* lacks fucosylated xyloglucan because of a lesion in fucosyltransferase *AtFUT1*. *Proc Natl Acad Sci U S A*, **99:** 3340-3345

Velculescu, V., Zhang, L., Vogelstein, B., and Kinzler, K. (1995). Serial analysis of gene expression. *Science*, **270:** 484-487

Vergara, C., and Carpita, N. (2001). Beta-D-glycan synthases and the *CesA* gene family: lessons to be learned from the mixed-linkage (1–>3),(1–>4)beta-D-glucan synthase. *Plant Mol Biol*, **47:** 145-160

Vicre, M., Janneau, A., Knox, J.P., and Driouich, A. (1998). Immunolocalization of b(1-4)- and b(1-6)-D-galactan epitopes in the cell wall and Golgi stacks of developing flax root tissues. *Protoplasma*, **203:** 26-34

Vidal, S., Doco, T., Williams, P., Pellerin, P., York, W., O'Neill, M., Glushka, J., Darvill, A., and Albersheim, P. (2000). Structural characterization of the pectic polysaccharide rhamnogalacturonan II: evidence for the backbone location of the aceric acid-containing oligoglycosyl side chain. *Carbohydr Res.*, **326:** 277-294

Vietor, R.J., Hoffmann, R.A., Angelino, S.A., Voragen, A.G., Kamerling, J.P., and Vliegenthart, J.F. (1994). Structures of small oligomers liberated from barley arabinoxylans by endoxylanase from *Aspergillus awamori*. *Carbohydr Res*, **254:** 245-255

Vincken, J.P., de Keizer, A., Beldman, G., and Voragen, A.G. (1995). Fractionation of xyloglucan fragments and their interaction with cellulose. *Plant Physiol*, **108:** 1579-1585

Voinnet, O., Rivas, S., Mestre, P., and Baulcombe, D. (2003). An enhanced transient expression system in plants based on suppression of gene silencing by the p19 protein of tomato bushy stunt virus. *Plant J*, **33:** 949-956

Voinnet, O., Vain, P., Angell, S., and Baulcombe, D. (1998). Systemic spread of sequence-specific transgene RNA degradation in plants is initiated by localized introduction of ectopic promoterless DNA. *Cell*, **95:** 177-187

von Heijne, G. (1983). Patterns of amino acids near signal-sequence cleavage sites. *Eur J Biochem*, **133:** 17-21

von Heijne, G. (1985). Signal sequences. The limits of variation. *J Mol Biol*, **184:** 99-105

Voragen, A., Scholls, H., Marijs, J., Rombouts, F., and Angelino, S. (1987). Non-starch polysaccharides from barley: structural features and break down during malting. *J. Inst. Brew*, **93:** 202-208

Vos, P., Hogers, R., Bleeker, M., Reijans, M., van de Lee, T., Hornes, M., Frijters, A., Pot, J., Peleman, J., and Kuiper, M. (1995). AFLP: a new technique for DNA fingerprinting. *Nucleic Acids Res*, **23:** 4407-4414

Wada, T., Tachibana, T., Shimura, Y., and Okada, K. (1997). Epidermal cell differentiation in *Arabidopsis* determined by a Myb homolog, CPC. *Science*, **277:** 1113-1116

Wagner, B., Hufnagl, K., Radauer, C., Wagner, S., Baier, K., Scheiner, O., Wiedermann, U., and Breiteneder, H. (2004). Expression of the B subunit of the heat-labile enterotoxin of *Escherichia coli* in tobacco mosaic virus-infected *Nicotiana benthamiana* plants and its characterization as mucosal immunogen and adjuvant. *J Immunol Methods*, **287:** 203-215

Walhout, A., and Vidal, M. (1999). A genetic strategy to eliminate self-activator baits prior to high-throughput yeast two-hybrid screens. *Genome Res*, **9:** 1128-1134

Walhout, A.J., Temple, G.F., Brasch, M.A., Hartley, J.L., Lorson, M.A., van den Heuvel, S., and Vidal, M. (2000). GATEWAY recombinational cloning: application to the cloning of large numbers of open reading frames or ORFeomes. *Methods Enzymol*, **328:** 575-592

Walter, M., Chaban, C., Schutze, K., Batistic, O., Weckermann, K., Nake, C., Blazevic, D., Grefen, C., Schumacher, K., Oecking, C., Harter, K., and Kudla, J.

(2004). Visualization of protein interactions in living plant cells using bimolecular fluorescence complementation. *Plant J*, **40:** 428-438

Wan, Y., and Lemaux, P. (1994). Generation of large numbers of independently transformed fertile barley plants. *Plant Physiol*, **104:** 37-48

Wang, A., Doyle, M., and Mark, D. (1989). Quantitation of mRNA by the polymerase chain reaction. *Proc Natl Acad Sci U S A*, **86:** 9717-9721

Wang, M., Abbott, D., Upadhyaya, N., Jacobsen, J., and Waterhouse, P. (2001). *Agrobacterium tumefaciens*-mediated transformation of an elite barley cultivar with virus resistance and reporter genes. *Aust. J. Plant Physiol. 28:149-156*, **28:** 149-156

Wang, T., and Brown, M. (1999). mRNA quantification by real time TaqMan polymerase chain reaction: validation and comparison with RNase protection. *Anal Biochem*, **269:** 198-201

Wang, X., Cnops, G., Vanderhaeghen, R., De Block, S., Van Montagu, M., and Van Lijsebettens, M. (2001). *AtCSLD3*, a cellulose synthase-like gene important for root hair growth in *Arabidopsis*. *Plant Physiol*, **126:** 575-586

Warne, P.H., Viciana, P.R., and Downward, J. (1993). Direct interaction of Ras and the amino-terminal region of Raf-1 *in vitro*. *Nature*, **364:** 352-355

Waterhouse, P., Graham, M., and Wang, M. (1998). Virus resistance and gene silencing in plants can be induced by simultaneous expression of sense and antisense RNA. *Proc Natl Acad Sci U S A*, **95:** 13959-13964

Waterhouse, P., and Helliwell, C. (2003). Exploring plant genomes by RNA-induced gene silencing. *Nat Rev Genet*, **4:** 29-38

Wee, E., Sherrier, D., Prime, T., and Dupree, P. (1998). Targeting of active sialyltransferase to the plant Golgi apparatus. *Plant Cell*, **10:** 1759-1768

Weickert, M.J., Doherty, D.H., Best, E.A., and Olins, P.O. (1996). Optimization of heterologous protein production in *Escherichia coli*. *Curr Opin Biotechnol*, **7:** 494-499

Weigel, D., Ahn, J., Blazquez, M., Borevitz, J., Christensen, S., Fankhauser, C., Ferrandiz, C., Kardailsky, I., Malancharuvil, E., Neff, M., Nguyen, J., Sato, S., Wang, Z., Xia, Y., Dixon, R., Harrison, M., Lamb, C., Yanofsky, M., and Chory, J. (2000). Activation tagging in *Arabidopsis*. *Plant Physiol*, **122:** 1003-1013

Weis, J., Tan, S., Martin, B., and Wittwer, C. (1992). Detection of rare mRNAs *via* quantitative RT-PCR. *Trends Genet*, **8:** 263-264

Welsh, J., Chada, K., Dalal, S., Cheng, R., Ralph, D., and McClelland, M. (1992). Arbitrarily primed PCR fingerprinting of RNA. *Nucleic Acids Res*, **20:** 4965-4970

Wende, G., and Fry, S.C. (1997). *O*-feruloylated, *O*-acetylated oligosaccharides as side-chains of grass xylans. *Phytochemistry*, **44:** 1011-1018

Wenzel, C., Williamson, R., and Wasteneys, G. (2000). Gibberellin-induced changes in growth anisotropy precede gibberellin-dependent changes in cortical microtubule orientation in developing epidermal cells of barley leaves. Kinematic and cytological studies on a gibberellin-responsive dwarf mutant, M489. *Plant Physiol*, **124:** 813-822

Wesley, S., Helliwell, C., Smith, N., Wang, M., Rouse, D., Liu, Q., Gooding, P., Singh, S., Abbott, D., Stoutjesdijk, P., Robinson, S., Gleave, A., Green, A., and Waterhouse, P. (2001). Construct design for efficient, effective and high-throughput gene silencing in plants. *Plant J*, **27:** 581-590

Wesley, S.V., Helliwell, C., Wang, M.B., and Waterhouse, P. (2004). Posttranscriptional gene silencing in plants. *Methods Mol Biol*, **265:** 117-129

Wetzel, R. (1994). Mutations and off-pathway aggregation of proteins. *Trends Biotechnol*, **12:** 193-198

Whitcombe, D., Theaker, J., Guy, S., Brown, T., and Little, S. (1999). Detection of PCR products using self-probing amplicons and fluorescence. *Nat Biotechnol*, **17:** 804-807

Wilhelm, J., and Pingoud, A. (2003). Real-time polymerase chain reaction. *Chembiochem*, **4:** 1120-1128

Wilhelm, J., Pingoud, A., and Hahn, M. (2003). Real-time PCR-based method for the estimation of genome sizes. *Nucleic Acids Res*, **31:** e56 (51-56)

Wilkie, K.C.B. (1979). The hemicelluloses of grasses and cereals. *Adv Carbohydrate Chem Biochem*, **36**: 215-264

Willats, W., McCartney, L., Mackie, W., and Knox, J. (2001). Pectin: cell biology and prospects for functional analysis. *Plant Mol Biol*, **47:** 9-27

Willats, W., McCartney, L., Steele-King, C., Marcus, S., Mort, A., Huisman, M., Van Alebeek, G., Schols, H., Voragen, A., Le Goff, A., Bonnin, E., Thibault, J., and Knox, J. (2004). A xylogalacturonan epitope is specifically associated with plant cell detachment. *Planta*, **218:** 673-681

Wilson, L., and Fry, J. (1986). Extensin-a major cell wall glycoprotein. *Plant Cell Environ*, **9:** 239-260

Winston, W.M., Molodowitch, C., and Hunter, C.P. (2002). Systemic RNAi in *C. elegans* requires the putative transmembrane protein SID-1. *Science*, **295:** 2456-2459

Wittwer, C., Herrmann, M., Moss, A., and Rasmussen, R. (1997). Continuous fluorescence monitoring of rapid cycle DNA amplification. *Biotechniques*, **22:** 134-138

Wittwer, C., Ririe, K., Andrew, R., David, D., Gundry, R., and Balis, U. (1997). The LightCycler: a microvolume multisample fluorimeter with rapid temperature control. *Biotechniques*, **22:** 176-181

Wong, L., Belonogoff, V., Boyd, V., Hunkapiller, N., Casey, P., Liew, S., Lazaruk, K., and Baumhueter, S. (2000). General method for HPLC purification and sequencing of selected dsDNA gene fragments from complex PCRs generated during gene expression profiling. *Biotechniques*, **28:** 776-783

Xiao, H., Wang, Y., Liu, D., Wang, W., Li, X., Zhao, X., Xu, J., Zhai, W., and Zhu, L. (2003). Functional analysis of the rice *AP3* homologue *OsMADS16* by RNA interference. *Plant Mol Biol*, **52:** 957-966

Xie, Z., Johansen, L.K., Gustafson, A.M., Kasschau, K.D., Lellis, A.D., Zilberman, D., Jacobsen, S.E., and Carrington, J.C. (2004). Genetic and functional diversification of small RNA pathways in plants. *PLoS Biol*, **2:** E104

Xu, D., Xu, Y., and Uberbacher, E. (2000). Computational tools for protein modeling. *Curr Protein Pept Sci*, **1:** 1-21

Xu, Z., Vo, L., and Macher, B. (1996). Structure-function analysis of human alpha1,3-fucosyltransferase. Amino acids involved in acceptor substrate specificity. *J Biol Chem*, **271:** 8818-8823

Yoo, B., Kragler, F., Varkonyi-Gasic, E., Haywood, V., Archer-Evans, S., Lee, Y., Lough, T., and Lucas, W. (2004). A systemic small RNA signaling system in plants. *Plant Cell*, **16:** 1979-2000

Young, J., Krysan, P., and Sussman, M. (2001). Efficient screening of *Arabidopsis* T-DNA insertion lines using degenerate primers. *Plant Physiol*, **125:** 513-518

Young, W.W., Jr. (2004). Organization of Golgi glycosyltransferases in membranes: complexity *via* complexes. *J Membr Biol*, **198:** 1-13

Yu, J., Hu, S., Wang, J., Wong, G., Li, S., Liu, B., Deng, Y., Dai, L., Zhou, Y., Zhang, X., Cao, M., Liu, J., Sun, J., Tang, J., Chen, Y., Huang, X., Lin, W., Ye, C., Tong, W., Cong, L., Geng, J., Han, Y., Li, L., Li, W., Hu, G., Huang, X., Li, W., Li, J., Liu, Z., Li, L., Liu, J., Qi, Q., Liu, J., Li, L., Li, T., Wang, X., Lu, H., Wu, T., Zhu, M., Ni, P., Han, H., Dong, W., Ren, X., Feng, X., Cui, P., Li, X., Wang, H., Xu, X., Zhai, W., Xu, Z., Zhang, J., He, S., Zhang, J., Xu, J., Zhang, K., Zheng, X., Dong, J., Zeng, W., Tao, L., Ye, J., Tan, J., Ren, X., Chen, X., He, J., Liu, D., Tian, W., Tian, C., Xia, H., Bao, Q., Li, G., Gao, H., Cao, T., Wang, J., Zhao, W., Li, P., Chen, W., Wang, X., Zhang, Y., Hu, J., Wang, J., Liu, S., Yang, J., Zhang, G., Xiong, Y., Li, Z., Mao, L., Zhou, C., Zhu, Z., Chen, R., Hao, B., Zheng, W., Chen, S., Guo, W., Li, G., Liu, S., Tao, M., Wang, J., Zhu, L., Yuan, L., and Yang, H. (2002). A draft sequence of the rice genome (*Oryza sativa* L. ssp. indica). *Science*, **296:** 79-92

Yu, Y., Tomkins, J., Waugh, R., Frisch, D., Kudrna, D., Kleinhofs, A., Brueggeman, R., Muehlbauer, G., Wise, P., and Wing, R. (2000). A bacterial artificial chromosome library for barley (*Hordeum vulgare* L.) and the identification of clones containing putative resistance genes. *Theoretical and Applied Genetics*, **101:** 1093-1099

Zhang, F., and Staehelin, L.A. (1992). Functional compartmentation of the Golgi apparatus of plant cells. Immunocytochemical analysis of high-pressure frozen - and freeze-substituted *Sycamore Maple* suspension culture cells. *Plant Physiol*, **99:** 1070-1083

Zhang, J. (2003). Overexpression analysis of plant transcription factors. *Curr Opin Plant Biol*, **6:** 430-440

Zhang, Q., Shirley, N., Lahnstein, J., and Fincher, G.B. (in press). Characterisation and expression patterns of UDP-D-glucuronate decarboxylase genes in barley. *Plant Physiol*, **138:** 131-141

Zhang, Z., Kochhar, S., and Grigorov, M. (2003). Exploring the sequence-structure protein landscape in the glycosyltransferase family. *Protein Science*, **12:** 2291-2302

Zhao, D., Ni, W., Feng, B., Han, T., Petrasek, M., and Ma, H. (2003). Members of the *Arabidopsis-SKP1-like* gene family exhibit a variety of expression patterns and may play diverse roles in *Arabidopsis*. *Plant Physiol*, **133:** 203-217